CONTENTS

CONTENTS

Mètodes per a generar superfícies de Bézier triangulars mitjançant minimització de funcionals, EDPs i màscares.

Presentació.

L'objectiu principal d'aquest treball és l'obtenció de diferents tècniques per tal de generar superfícies de Bézier triangulars des del punt de vista d'un dels més antics problemes del disseny geomètric assistit per ordinador: la construcció d'una superfície que interpole unes fronteres donades.

Les superfícies més estudiades dins l'àmbit del disseny geomètric assistit per ordinador (Computer Aided Geometric Design, CAGD) han estat les superfícies de Bézier rectangulars, que foren introduïdes als anys seixanta per Coons i Bézier. El nostre treball, però, està basat en l'estudi de les superfícies de Bézier triangulars, que són la generalització natural de les corbes de Bézier per la següent raó: la definició d'una corba de Bézier es basa en el concepte d'interpolació lineal, que és la combinació convexa de dos punts i, anàlogament, la definició de superfície de Bézier triangular es basa en les coordenades baricèntriques, que són la combinació convexa de tres punts. De fet, les superfícies triangulars van ser introduïdes per Paul de Casteljau a finals dels anys cinquanta, abans que les rectangulars[1], veure [**13**] i [**15**], i va definir aquestes superfícies amb una formulació simètrica en termes de les coordenades baricèntriques respecte a un domini triangular.

La importància del problema que considerem, determinar una superfície donada la seua frontera, és conseqüència dels molts àmbits on té aplicació, com ara el disseny d'objectes, el *fairing* i el *blending* de superfícies.

En l'àmbit del disseny d'objectes la dificultat més gran que es troba a l'hora de crear objectes pràctics amb l'ordinador com a eina és la manca de mètodes que permeten un disseny intuïtiu. Des del punt de vista del dissenyador és extremadament important poder crear objectes reals i manipular-los d'una manera simple. Així, com que gran part de la informació referent a la forma d'un objecte ve donada per la seua frontera, els mètodes per a generar superfícies interpolant una frontera donada i compatibles amb transformacions afins són una bona manera de construir superfícies a partir de pocs paràmetres.

[1]El lector podria preguntar-se per què s'anomenen superfícies de Bézier triangulars si va ser de Casteljau el primer en introduir aquest concepte, i és que mentre el treball de de Casteljau mai fou publicat, el de Bézier sí que va ser difós i és per això que les superfícies triangulars també porten el seu nom, encara que ell mai les va considerar.

Com hem dit abans, hi ha altres problemes importants en CAGD que estan relacionats amb el problema de construir una superfície donada la seua frontera, per exemple el *fairing* i el *blending*.

El problema anomenat *fairing* d'una superfície, que se sol resoldre mitjançant la construcció d'una superfície amb frontera prescrita, consisteix en suavitzar (com el terme anglès indica) aquelles regions d'una superfície on es troben rugositats o altres imperfeccions. Aquestes irregularitats, que normalment es produeixen quan el procés de modelat es fa especificant directament els punts de control i especialment quan es tracta d'un gran nombre de punts, solen detectar-se mitjançant l'anàlisi de les segones derivades o, equivalentment, de la curvatura[2].

Generalment els procediments del *fairing* tracten d'eliminar aquests errors des del punt de vista del disseny variacional. Per a suavitzar una superfície parametritzada, $\overrightarrow{x} : U \to \mathbb{R}^3$, en alguna regió interior, $U_0 \subset U$, s'elegeix una nova superfície, $\overrightarrow{y} : U \to \mathbb{R}^3$, que coincidisca amb $\overrightarrow{x}$ fora de U_0 i que a més minimitze un determinat funcional que mesure la suavitat de la superfície. És a dir, es defineix una nova superfície en U_0 amb frontera prescrita per la superfície inicial.

Els principis variacionals són una bona eina per tal de suavitzar les superfícies obtingudes en el disseny de superfícies de forma lliure, *free form surfaces*. Una superfície variacional restringida és una superfície que minimitza un determinat funcional d'energia sota certes condicions d'interpolació. Aquests mètodes que inclouen la minimització d'un funcional, el qual, en certa manera, mesura la suavitat de la superfície, s'anomenen mètodes de disseny variacional. Els funcionals que es minimitzen depenen, generalment, de propietats locals de la superfície, com ara el vector normal o la curvatura. En l'article [**20**] es desenvolupa un estudi al voltant de quins funcionals permeten suavitzar una superfície eficientment. El modelat de superfícies utilitzant principis variacionals amb restriccions és atractiu perquè el dissenyador no s'ha de molestar en especificar els punts de control directament.

Un altra aplicació important de les superfícies interpolants és la unió de diferents superfícies, anomenada *blending*. Les superfícies que no tenen una topologia trivial necessiten més d'una parametrització per a ser representades. Una superfície *blending*, és una superfície d'unió que connecta suaument dues superfícies al llarg de corbes arbitràries contingudes en les superfícies donades. Les corbes de contacte poden ser fixades per l'usuari o bé obtenir-se per intersecció de les superfícies que s'han d'unir. La superfície nexe que s'obté acompleix certes condicions de continuïtat així com també la continuïtat del vector normal al llarg de les corbes d'unió definides per les dues superfícies base. El procés de *blending* és molt important en el modelat geomètric de superfícies i és molt utilitzat a l'hora de millorar la forma d'un producte.

[2]Donat que la majoria dels nostres mètodes estan relacionats amb la curvatura mitjana es pot esperar que els resultats obtinguts no presenten aquest tipus d'irregularitats.

El problema de generar una superfície donada la seua frontera és, per tant, una qüestió que ha estat estudiada àmpliament amb anterioritat. Una de les solucions més famoses d'aquest problema és la superfície de Coons: donades quatre corbes, la superfície de Coons és una superfície paramètrica definida en el quadrat unitat i que té aquestes corbes com a corbes frontereres. Una generalització de les superfícies interpoladores de Coons són les superfícies de Gordon, que varen ser definides per aquest a finals dels seixanta quan treballava als laboratoris d'investigació de General Motors. A la interpolació mitjançant aquest tipus de superfícies li va donar el nom de "interpolació transfinita."

Pel que fa a la interpolació de corbes amb superfícies triangulars també s'ha desenvolupat una gran quantitat de treball, com es pot veure a Barnhill et al. [**4**], Barnhill i Gregory [**5**], o Nielson [**32**], on els autors defineixen diferents polinomis interpoladors de corbes frontereres. També podem trobar una generalització de la superfície interpoladora de Coons per al cas triangular a l'article [**33**].

Dins l'àmbit del CAGD es poden trobar molts mètodes diferents per tal de generar superfícies que interpolen corbes frontereres o que s'adeqüen a altres tipus de restriccions. En aquest treball nosaltres considerem, mitjançant alguns d'aquests mètodes, el problema de determinar una superfície polinòmica associada a un conjunt de dades inicials, com ara corbes frontereres o algun conjunt de punts de control. Concretament, les tècniques que hem utilitzat es poden classificar en tres categories:

(1) **Minimització de funcionals:** donada la frontera, determinem la superfície que minimitza un funcional entre totes les superfícies polinòmiques amb aquesta frontera. Hem considerat tres funcionals quadràtics: el funcional de Dirichlet, el funcional Biharmònic[3] i el funcional que és minimitzat per la superfície de Coons. A més a més, hem considerat un funcional cúbic, l'associat a les superfícies de curvatura mitjana constant. Com que el nostre estudi es desenvolupa sempre en termes de superfícies de Bézier[4], aquests funcionals, restringits a l'espai dels polinomis, es poden considerar com a funcions que depenen dels punts de control. Per tant, l'extremal d'un funcional, $\mathcal{I}$, entre totes les superfícies triangulars es pot calcular com el mínim d'una funció real

$$\mathcal{P} \to \mathcal{I}\left(\overrightarrow{x}_{\mathcal{P}}\right),$$

sent $\overrightarrow{x}_{\mathcal{P}}$ la superfície de Bézier triangular associada a la xarxa de control $\mathcal{P}$.

(2) **Equacions en derivades parcials (EDPs):** es pot determinar una superfície de Bézier triangular que verifique una equació en derivades parcials donats alguns dels seus punts de control. Quin és el mínim conjunt de punts de control que es pot prescriure depèn de l'equació que s'estudie, i sobre tot de l'ordre d'aquesta. Hi ha alguns treballs previs que tracten aquesta qüestió. En [**30**] i [**31**], es realitza un estudi al voltant de la construcció de superfícies de Bézier rectangulars com a

[3]Aquests funcionals que s'anomenen funcional de Dirichlet i funcional Biharmònic en l'àmbit matemàtic, es coneixen com *stretching energy* and *bending energy* respectivament a la física, l'enginyeria i el CAGD.

[4]Si no s'especifica el contrari quan diem superfície de Bézier ens referim a superfície de Bézier triangular.

solucions de l'equació de Laplace i de l'equació biharmònica. Per un altra banda, en [**6**], s'estudien les solucions en forma de Bézier d'un altra equació, l'equació d'ones. Per al cas de les superfícies de Bézier rectangulars harmòniques calia prescriure dues corbes frontereres per tal de construir la superfície mentre que per a construir superfícies de Bézier rectangulars biharmòniques eren necessàries quatre corbes com a condicions inicials.

És important remarcar en aquest moment que, encara que siga un problema de contorn, el problema biharmònic en el cas rectangular té solució única només amb la prescripció de la frontera de la superfície quan es busquen solucions polinòmiques. Així, no és necessari fixar el valor de les derivades normals al llarg de la frontera. Si no es tractara el cas restringit, es podria esperar que fos necessari prescriure tant la frontera com les derivades normals al llarg d'aquesta per tal que la superfície estigués totalment determinada. El cas és que si es tracta de superfícies de Bézier rectangulars biharmòniques polinòmiques les derivades normals estan determinades per la frontera.

En aquest treball hem considerat les equacions en derivades parcials donades per les equacions d'Euler-Lagrange associades al funcional de Dirichlet i al funcional Biharmònic que són l'equació de Laplace i l'equació biharmònica, i hem determinat en cada cas quins són els punts de control que s'han de conèixer per tal que la superfície estiga totalment determinada per l'EDP. A més a més, hem introduït una equació en derivades parcials de tercer ordre, que no està associada a cap funcional, però que ens permet definir una superfície de Bézier triangular donats els punts de control fronterers. La prescripció de la frontera incrementa el control sobre les superfícies que poden ser dissenyades.

Hem de posar èmfasi que, donat que restringim la minimització dels funcionals a l'espai de les superfícies polinòmiques, el funcionals passen a ser funcions, i no és necessari que un extremal d'aquestes funcions siga solució de l'equació d'Euler-Lagrange associada al funcional. Per tant, la minimització de funcionals ens dona unes solucions que són diferents a les que obtenim com a solució de les equacions d'Euler-Lagrange corresponents.

(3) **Màscares:** un altre mètode per a construir superfícies és mitjançant màscares. Una màscara és un conjunt de coeficients que defineixen cada punt de control d'una superfície de Bézier com a combinació lineal dels seus punts de control veïns. Així, tota la xarxa de control s'obté com a solució d'un sistema lineal. L'ús de màscares té el seu origen en els mètodes numèrics per a discretitzar i resoldre equacions diferencials. Una manera d'obtenir una aproximació de la solució d'una equació diferencial és fent la seua discretització en diferències finites i llavors les solucions discretes poden ser representades mitjançant màscares.

En [**14**], G. Farin i D. Hansford van introduir un nou mètode per a generar xarxes de control basat en un tipus especial de màscares. Les superfícies obtingudes amb aquestes màscares les van anomenar *permanence patches*, superfícies de permanència. La màscara per a superfícies rectangulars la van definir fent una generalització de la superfície discreta de Coons i la màscara per a superfícies triangulars com a extensió de la definició per a rectangulars. El mètode de generació de superfícies donat per aquestes màscares, que permeten la construcció de superfícies de permanència, també es pot interpretar en termes d'EDPs discretitzades com a una combinació de principis variacionals.

En aquest treball hem definit algunes màscares associades als funcionals i a les EDPs que hem estudiat. També hem comparat els nostres resultats amb els obtinguts per a superfícies de permanència en [**14**].

Abans de començar amb una descripció un poc més explícita del nostre treball, farem uns comentaris referents a parametritzacions. El fet és que hi ha una notable diferència entre la simetria dels resultats obtinguts per a superfícies de Bézier rectangulars i la asimetria que s'obté per a superfícies triangulars. Per a superfícies rectangulars hi ha una clara relació entre la xarxa de control rectangular i la parametrització de la superfície. En el cas triangular les coses no són tan senzilles.

L'associació més directa que es pot fer entre les xarxes de control triangulars i les parametritzacions de superfícies de Bézier triangulars és la que s'obté al substituir una de les coordenades baricèntriques per una expressió dependent de les altres dues tenint en compte que $u+v+w=1$. Per exemple, si $\overrightarrow{y}(u,v,w)$ és la superfície en coordenades baricèntriques, llavors treballaríem amb la superfície $\overrightarrow{x}(u,v)=\overrightarrow{y}(u,v,1-u-v)$. A més, si suposem que (u,v) són les coordenades cartesianes, o equivalentment que el triangle utilitzat per a definir les coordenades baricèntriques és el triangle format pels punts $(0,0)$, $(1,0)$ i $(0,1)$, llavors ens trobem amb un seriós inconvenient: es perd la simetria. Fins i tot si la xarxa de control és simètrica ($P_{\sigma(i)\sigma(j)\sigma(k)}=P_{ijk}$ per a qualsevol permutació σ), la superfície de Bézier triangular associada no conserva la simetria.

Malgrat aquesta pèrdua de simetria, nosaltres treballem amb aquestes parametritzacions asimètriques per les següents raons:

(1) Les nostres aproximacions, encara que s'han obtingut mitjançant mètodes asimètrics, semblen ser almenys tan bones com altres deduïdes de mètodes simètrics com ara la construcció de superfícies de permanència o altres mètodes deduïts exigint simetria als resultats.

(2) Per a grau 3, hi ha un important exemple de superfície minimal: la superfície d'Enneper. Aquesta superfície s'obté com a resultat amb els mètodes asimètrics, però en canvi no es pot obtenir mitjançant cap màscara simètrica. Es pot provar que hi ha parts de la superfície d'Enneper per a les quals el punt de control interior no es pot obtenir aplicant cap màscara simètrica als punts fronterers.

(3) Les màscares simètriques es dedueixen exigint algunes característiques a la xarxa de control però, no a la superfície de Bézier associada. Els nostres mètodes es basen directament en les superfícies de Bézier, donat que el que volem és minimitzar algun funcional relacionat directament amb la superfície.

Ara introduirem el nostre treball amb un poc més de detall.

Els tres primers capítols del nostre estudi tracten del disseny de superfícies mitjançant la resolució d'equacions en derivades parcials: obtenim una superfície com a solució d'un problema de contorn determinat. L'any 1989, Bloor i Wilson van anomenar *PDE surfaces* (superfícies EDP) a les superfícies obtingudes amb aquesta tècnica, veure [**8**]. Amb aquest mètode per a generar superfícies, com que la major part de la informació que defineix una superfície la dóna la frontera i afegint a l'EDP condicions de contorn, s'aconsegueix el control de la superfície a partir de pocs paràmetres.

Al **primer capítol** estudiem la manera de generar superfícies de Bézier harmòniques donats alguns dels seus punts de control com a informació inicial. Les superfícies de Bézier harmòniques són superfícies EDP que s'obtenen com a solucions de l'equació $\Delta \overrightarrow{x} = 0$, on Δ denota l'operador harmònic o Laplacià. Les superfícies harmòniques, que tenen relació amb diverses àrees d'aplicació en CAGD, com ara el disseny de superfícies, la suavització de xarxes geomètriques i el *fairing*, estan relacionades, a més a més, amb les superfícies minimals: una superfície paramètrica isoterma és minimal si i només si és harmònica.

Nosaltres hem desenvolupat en aquest capítol dos mètodes diferents per a generar superfícies de Bézier triangulars harmòniques. El primer mètode permet construir una superfície harmònica donada una corba fronterera i el pla tangent al llarg d'aquesta, és a dir, donades dues files de punts de control. Aquest mètode ens ha permès obtenir bons resultats per a graus inferiors però, com que al prescriure dues files de punts de control deixem lliure el tercer vèrtex, en alguns cassos aquest pot divergir de la forma desitjada, com de fet passa al augmentar el grau dels nostres exemples. Aquest problema l'hem pogut solucionar amb el segon mètode que proposem. En lloc de prescriure dues files de punts de control, amb aquest segon mètode s'obté una superfície harmònica prefixant un conjunt de punts el més semblant possible a dues corbes frontereres. D'aquesta manera s'incrementa el control sobre la forma de la superfície obtinguda, donat que els tres vèrtex estan controlats. Les superfícies obtingudes amb aquest mètode s'adapten perfectament a la informació donada per l'usuari.

En blau representem el conjunt de punts de control que, a cadascun dels mètodes, permet determinar totalment una superfície de Bézier harmònica.

Al **segon capítol** donem dos mètodes per a generar superfícies de Bézier triangulars biharmòniques amb alguns dels seus punts de control prefixats. Una superfície biharmònica acompleix l'EDP $\Delta^2 \overrightarrow{x} = 0$, on Δ^2 és l'operador bilaplacià. El terme *thin plate problem* que s'utilitza per a fer referència al problema de contorn biharmònic, es deu a l'analogia d'aquest problema amb el problema físic referent al doblegament d'una fina làmina de metall.

Com hem dit abans, en [**30**] i [**31**] podem trobar un estudi del problema biharmònic per a superfícies de Bézier rectangulars. En aquests articles es va provar que dues corbes frontereres oposades determinen una superfície de Bézier rectangular harmònica i que una superfície de Bézier rectangular biharmònica està totalment determinada per les seues quatre corbes frontereres. D'aquests resultats i dels nostres per a superfícies triangulars, es dedueix que l'ordre de l'EDP determina, d'alguna manera, el nombre de paràmetres que queden lliures.

Efectivament, en aquest capítol hem obtingut dos mètodes per a generar a partir de l'equació biharmònica, que és una EDP quart ordre, superfícies de Bézier biharmòniques donades quatre files de punts de control. En el primer mètode les quatre files de punts de control són una fronterera i les tres files següents, de manera que un dels vèrtex queda lliure, com en el cas harmònic i, per tant, de vegades podem obtenir resultats no desitjats si aquest vèrtex divergeix de la informació inicial. Al segon mètode, es prefixen dues corbes frontereres i els plans tangents al llarg d'aquestes, és a dir, dues files de punts de control fronterers i les seues files veïnes, de manera que els tres vèrtex són informació donada així com les dues corbes frontereres i els plans tangents al llarg d'aquestes, i només resten lliures els punts de control interiors d'una corba fronterera. Per tant, amb aquest mètode augmenta considerablement el control sobre la forma de la superfície dissenyada.

En blau representem el conjunt de punts de control que, a cadascun dels mètodes, permet determinar totalment una superfície de Bézier biharmònica.

Vists els resultats obtinguts per a EDPs de segon i quart ordre és lògic pensar que, donades les corbes frontereres d'una superfície de Bézier triangular, es podria determinar una superfície interpoladora com a solució d'una EDP de tercer ordre.

Així, al **quart capítol**, hem introduït una equació en derivades parcials de tercer ordre i hem donat un mètode per a generar la superfície EDP associada donada la frontera. Així com les quatre corbes frontereres determinen una superfície de Bézier rectangular biharmònica, per al cas triangular les corbes frontereres determinen una superfície solució d'una EDP de tercer ordre. Aquest mètode, que hem anomenat mètode de tercer ordre, fa possible la

creació d'objectes reals basada en la informació provinent de la frontera de l'objecte que es vol dissenyar.

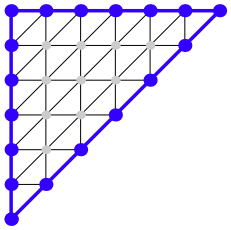

Donats els punts de control fronterers està totalment determinada una superfície de Bézier que satisfà l'EDP de tercer ordre que hem introduït en aquest capítol.

Els dissenyadors treballen, generalment, amb superfícies de baix grau, però, malgrat això, si considerem el problema d'aproximar superfícies harmòniques o biharmòniques mitjançant superfícies polinòmiques, el grau de les superfícies polinòmiques ha d'incrementar-se per tal d'obtenir bones aproximacions. Per tant, hem provat tots els resultats esmentats en general, per a un grau arbitrari.

Abans d'introduir el mètode de tercer ordre al quart capítol, al **tercer capítol** fem un estudi de les superfícies de Coons triangulars. En contret, fem una comparació entre les superfícies de Coons triangulars i les rectangulars.

Hem considerat el problema de trobar un extremal polinòmic del funcional

$$\mathcal{F}(\overrightarrow{x}) = \int_U \|\overrightarrow{x_{uv}}\|^2 du\, dv,$$

entre totes les superfícies rectangulars amb la mateixa frontera. Hem provat que minimitzar aquest funcional és equivalent a resoldre l'EDP $\overrightarrow{x}_{uuvv} = 0$ i que a més a més, la superfície de Coons rectangular és l'única solució d'aquest problema.

D'altra banda, hem demostrat que les superfícies de Coons triangulars no són extremals d'aquest funcional. Llavors, hem estudiat sota quines condicions seria equivalent trobar els extremals de $\mathcal{F}$ entre totes les superfícies triangulars polinòmiques amb la mateixa frontera i resoldre l'EDP $\overrightarrow{x}_{uuvv} = 0$.

En aquest capítol també hem introduït les superfícies de Coons tringulars discretes i hem donat una caracterització de la xarxa de control dels extremals del funcional. Aquesta caracterització ens ha permès desenvolupar dos mètodes més per a generar superfícies de Bézier triangulars donada la seua frontera. El primer mètode consisteix en trobar els extremals del funcional com a solució d'un sistema d'equacions lineals en funció dels punts de control. El segon mètode ens permet generar superfícies de Bézier triangulars mitjançant una màscara deduïda de la caracterització dels extremals cúbics del funcional. Comparant els resultats obtinguts amb aquests mètodes podem dir que s'obtenen formes més ben adaptades a la informació inicial amb el càlcul d'extremals del funcional que mitjançant la màscara associada.

També s'obtenen bons resultats per a la superfície triangular de Coons, però l'ús d'aquesta implica un augment del grau de la superfície.

Al cinquè i al sisè capítols d'aquest treball hem presentat diversos mètodes per generar superfícies de Bézier triangulars donats diferents conjunts de condicions inicials, però en contrast amb els capítols previs, aquests mètodes generen ara superfícies minimals i aproximacions de superfícies minimals.

Al **capítol cinquè** donem alguns mètodes basats en les fórmules de representació de superfícies minimals definides per K. Weierstrass al 1861. Fent ús de la teoria de variable complexa, descrivim la manera de generar superfícies minimals i isotermes a partir de diferents conjunts de condicions inicials, com ara: punts de control, els plans tangents als vèrtex de la superfície o altres tipus de paràmetres.

El primer mètode que descrivim en aquest capítol, permet construir una superfície minimal cúbica donats els tres vèrtex. El segon mètode, permet construir una superfície minimal de grau 7 donats els tres vèrtex i els vectors normals associats. El tercer métode, que és una generalització de l'anterior, permet generar superfícies de grau superior donat un conjunt arbitrari de punts de la superfície i els vectors normals als tres vertex.

A més a més, en aquest capítol hem estudiat la relació entre les superfícies minimals i les corbes complexes minimals. Amb l'objectiu de reduir al màxim el nombre de paràmetres que determinen una superfície minimal, hem obtingut dos mètodes més per a generar superfícies cúbiques minimals i isotermes, un amb 9 graus de llibertat i un altre que només deixa lliures 2 paràmetres.

Dels resultats obtinguts deduïm que al reduir el nombre de paràmetres lliures les superfícies minimals resulten ser massa restrictives. Per a baix grau, per exemple quan representem parts de la superfície d'Enneper, obtenim bons resultats, però trobem que al agmentar el grau les superfícies obtingudes són massa complicades.

D'altra banda, també podem concloure que les superfícies minimals no són adequades per resoldre problemes com el *blending*. La condició $H = 0$ imposa excessives restriccions a una superfície, de manera que no podem esperar trobar una superfície minimal polinòmica donada la seua frontera.

Al **capítol sisè** hem considerat el problema de Plateau-Bézier. Al llarg dels anys el problema de trobar una superfície minimal donada la seua frontera, anomenat problema de Plateau, ha estat àmpliament estudiat. En aquest treball hem considerat aquest problema però restringit, el qual hem anomenat problema de Plateau-Bézier, que consisteix en trobar la superfície de Bézier triangular amb àrea mínima entre totes les superfícies de Bézier triangulars amb una frontera prescrita. Aquest problema fou estudiat amb anterioritat en [**30**] per a superfícies de Bézier rectangulars. En aquest capítol fem un estudi similar al realitzat a l'article citat, però per a superfícies triangulars. Per tal d'obtenir una aproximació de la solució del problema de Plateau, substituïm el funcional de l'àrea pel funcional de Dirichlet. Llavors, comparem les àrees de les superfícies extremals del funcional de Dirichlet

amb les de les superfícies generades mitjançant les màscares definides en [**14**], és a dir, les superfícies de permanència. A més, donem una expressió del funcional de Dirichlet en termes dels punts de control, així el funcional passa a ser una funció dels punts de control. Després, a partir d'aquesta expressió, hem deduït una caracterització de la xarxa de control d'un extremal del funcional.

Les superfícies obtingudes pel mètode de Dirichlet s'adeqüen perfectament a la informació donada per la frontera prescrita, a més a més, com que hem comparat les seues àrees amb les de les superfíces construïdes mitjançant diferents màscares, podem afirmar que amb aquest mètode s'obtenen bones aproximacions polinòmiques de superfícies minimals. Però, com que la condició necessària per a que coincideixin el funcional de l'àrea i el de Dirichlet és la isotermalitat de la superfície, si la frontera prefixada no gaudeix d'aquesta característica, les aproximacions obtingudes mitjançant el mètode de Dirichlet patiran un error de sortida inevitable. Per tal d'evitar aquest inconvenient hem desenvolupat un nou mètode, que anomenem correció del mètode de Dirichlet, amb el qual millorem les aproximacions de Dirichlet.

Finalment, en aquest capítol hem fet un estudi anàleg al realitzat amb el funcional de Dirichlet, però per al funcional biharmònic.

A l'**últim capítol** hem estudiat les superfícies de Bézier triangulars amb curvatura mitjana constant, les superfícies CMC. Aquestes superfícies són extremals del funcional $\mathcal{D}_H(\overrightarrow{x}) = \mathcal{D}(\overrightarrow{x}) + 2\,HV(\overrightarrow{x})$, on $\mathcal{D}(\overrightarrow{x})$ és el funcional de Dirichlet i el funcional $V(\overrightarrow{x})$, que introduirem en aquest capítol, és el que mesura el volum englobat pel con format per totes les l´ínies que uneixen els punts de la superfície, $\overrightarrow{x}\,(u,v)$, amb l'origen. En aquest treball hem considerat aquest funcional restringit a les superfícies de Bézier triangulars i hem obtingut un mètode per a generar aproximacions polinòmiques de superfícies amb curvatura mitjana constant.

Com al capítol sisè, donem ací una caracterització en termes dels punts de control dels extremals de $\mathcal{D}_H$ entre totes les superfícies de Bézier triangulars amb la mateixa frontera. Aquesta caracterització ens permet generar aproximacions polinòmiques a superfícies CMC com a solució d'un sistema quadràtic en funció dels punts de control.

Donada una frontera, es pot trobar una família d'aproximacions polinòmiques a superfícies CMC amb curvatures mitjanes en un determinat interval. Així, la possibilitat de prescriure la curvatura amb aquest mètode es pot interpretar com un grau més de llibertat a l'hora de fer un disseny en comparació amb el mètode de Dirichlet.

Finalment, a l'última secció d'aquest treball hem considerat el problema $\mathcal{C}^1$ i hem introduït un mètode per a generar aproximacions polinòmiques de superfícies amb curvatura mitjana constant donada la seua frontera i els plans tangents al llarg d'aquesta.

Introduction

The broad aim of this work is to develop different techniques to generate triangular Bézier surfaces from the point of view of one of the oldest problems in Computer Aided Geometric Design: the construction of a surface which interpolates given boundary curves.

Computer Aided Geometric Design, CAGD, has focused its study of surfaces mainly on the theory of rectangular surface patches, introduced by Coons and Bézier in the sixties. Nevertheless, our work is based on triangular Bézier surfaces, so let us explain why. Triangular patches are considered a more "natural" generalization of Bézier curves than tensor product patches. This is due to the following fact: The linear interpolation, in the definition of a Bézier curve, is the convex combination of two points, while the barycentric coordinates, used to define a triangular Bézier surface, are the convex combination of three points. In fact, triangular patches were first considered by Paul de Casteljau in the late fifties, before tensor product Bézier surfaces were defined[1], see [**13**] and [**15**]. He defined these patches with a symmetric formulation in terms of barycentric coordinates with respect to a triangular domain.

The importance of the problem of determining a surface given its boundary curves lies in its application in several issues such as object design or fairing and blending of surfaces.

A major difficulty in creating practical objects on the computer stems from to the lack of methods for defining them in an easy intuitive way. From the point of view of a designer it is extremely important to be able to create realistic objects and manipulate them in a simple manner. Thus, since a very important part of the information about the shape of an object comes from its boundary curves, methods to create a surface interpolating those boundaries compatible with affine transformations are a good way of building surfaces from a few parameters.

As we have said, there are other important problems in CAGD related with the problem of building a surface that interpolates given boundaries, such as fairing and blending.

The problem of fairing a surface can also be solved by means of the construction of surfaces with a prescribed boundary. Fairing consists in smoothing those regions of a surface with wrinkles or other flaws. These irregularities, that are often produced when the process of modeling is done by specifying directly the control points, especially when the surface is

[1]The reader could wonder why they are called triangular Bézier surfaces when it was de Casteljau who first introduced the concept. The fact is that whereas de Casteljau's work was never published, that of Bézier was, and this accounts for the fact that triangular Bézier surfaces bear Bézier's name although he never considered them.

determined by a large number of points, are mainly detected thanks to second-order analysis o equivalently to curvature analysis[2].

Fairing procedures typically aim at removing noise from data points from the variational design point of view. For fairing a parametrized surface, $\overrightarrow{x} : U \to \mathbb{R}^3$, in some inner region, $U_0 \subset U$, a new surface, $\overrightarrow{y} : U \to \mathbb{R}^3$, is chosen that coincides with $\overrightarrow{x}$ outside of U_0 and also minimizes some fairness functional. That is, a new patch is defined on U_0 with its boundary prescribed by the initial surface.

Variational principles have become quite useful for fairing purposes in the design of free form surfaces. A constrained variational surface is a surface that minimizes some energy functional under certain interpolation constraints. These methods involving the minimizing of a functional, which measures the fairness of a surface, are called variational design. The functionals typically depend on local properties of the surface, such as the normal vector and curvature. In [**20**], a study of some fairness functionals that allows efficient fairing is presented. Modeling surfaces using constrained variational principles is attractive, because the designer is not bothered by the precise representation of the surface by means of control points.

Another important application of interpolant surfaces is blending. Surfaces with non trivial topology need more than one patch to be represented. A blending surface is a surface that smoothly connects given surfaces along arbitrary curves on each surface. The contact curves are either user-defined or obtained by offset surface intersection. The blending surface usually ensures positional and normal vector continuity along the contact curves on the two base surfaces within a given accuracy. Blending is very important in geometric modeling and it is widely used to improve aesthetics and reduce stress concentrations of a product.

A lot of research has been conducted on the problem of determining a surface given its boundary. A popular polynomial solution to the problem is the bilinearly blended Coons patch: Given four boundary curves, the Coons patch is a parametric surface, defined over the unit square, which has these four curves as boundary curves. Indeed, this problem is under-specified because there are an infinite number of surfaces that can interpolate any four given boundary curves. A generalization of Coons patches interpolating a rectangular network of curves are Gordon surfaces, which were developed in the late 1960s when Gordon was working for the General Motors Research labs. He coined the term "transfinite interpolation" for this kind of surfaces.

As regards polynomial interpolation to boundary data on triangles, some previous work has also been carried out. See Barnhill et al. [**4**], Barnhill and Gregory [**5**], or Nielson [**32**], where the authors derived different polynomials interpolating boundary data. Moreover, a particular triangular Coons patch can be found in [**33**].

The literature offers many different methods that have been used for surface construction by interpolating boundary curves or fitting to some other kind of constraints. In this work we address the problem of determining a polynomial surface described by a set of initial data,

[2]Since most of our method are related to the mean curvature we can expect to avoid these irregular shapes.

such as the boundary curves or some of their control points, with some of these techniques. The generation methods we have studied can be classified in three categories:

(1) **Functional minimization:** Given the boundary curves, we determine the surface that minimizes some functional among all the polynomial surfaces with that given boundary. We have considered three quadratic functionals: the Dirichlet functional, the Biharmonic functional[3] and the functional that the Coons patch minimizes. Moreover, we have considered a cubic functional, the CMC-functional. We conduct our study in terms of Bézier surfaces[4], and these functionals, restricted to the space of polynomials, turn into functions of the control points. Thus, the extremal of a functional $\mathcal{I}$ among all triangular Bézier surfaces can be computed as the minimum of the real function

$$\mathcal{P} \to \mathcal{I}\left(\overrightarrow{x}_{\mathcal{P}}\right),$$

$\overrightarrow{x}_{\mathcal{P}}$ being the triangular Bézier patch associated to the control net $\mathcal{P}$.

(2) **PDE surfaces:** A triangular Bézier surface satisfying a partial differential equation can be determined given some of its control points. The minimum set of prescribed control points depends on the PDE under study, mainly on the order of the PDE. Previous work on this subject was performed in [**30**] and [**31**]. The cited papers study the generation of rectangular Bézier surfaces satisfying the Laplace equation as well as the biharmonic equation. Moreover, an analogous study about the Bézier solutions of the wave equation can be found in [**6**]. In the case of harmonic Bézier surfaces two boundary conditions were required to construct the surface while for biharmonic Bézier surfaces four boundary curves were needed as initial data. It is important to highlight the fact that although boundary-value problems are considered, if polynomial solutions are sought, the problem has a unique solution only by prescribing the boundary and no normal derivatives along it are required. One would expect biharmonic surfaces unconstrained to be a polynomial to be defined not only by the boundaries but also by the boundary cross-slopes; but the fact is that, if polynomial surfaces are required, the cross-slopes are determined by the boundary.

Here we have considered the PDE defined by the Euler-Lagrange equations associated to the Dirichlet functional and to the Biharmonic functional which are the Laplace and the biharmonic equation, and we have computed in each case which points on the control net must be known to have a surface uniquely determined by the PDE. Moreover we have introduced a third-order PDE, which is not associated to any functional, that enables us to define a triangular Bézier surface given the border control points. The prescription of the boundary increases the control over the shapes that can be designed.

[3]These functionals, which are called the Dirichlet and the Biharmonic functionals in the mathematical literature, are known as stretching energy and bending energy, respectively, in the physical, engineering or CAGD literature.

[4]Unless otherwise stated Bézier surface means triangular Bézier surface along this introduction.

Let us emphatically remark that, since we restrict the minimization of a functional to the space of polynomial surfaces the functional is now just a function, and an extremal of this function is not forced to fulfill the Euler-Lagrange equation associated to the functional. Therefore functional minimization offers us solutions that are different to those we get as a solution of its Euler-Lagrange PDE.

(3) **Masks:** Another way of building surfaces is by means of masks. A mask is a set of coefficients that define any control point of a Bézier surface in terms of its neighboring control points. Thus, the whole control net is obtained as a solution of a linear system. The use of masks has its origin in numerical methods to discretize and solve differential equations. One way of obtaining an approximated solution to a differential equation is by performing its finite difference discretization, and then the discrete solutions can be represented by masks.

In [**14**], G. Farin and D. Hansford present a new class of control net generation schemes based on a special kind of masks that they call permanence patches. A mask for rectangular patches is defined as a generalization of the discrete Coons patch and the analogous mask for triangular surfaces is an extension of their definition for the rectangular case. These masks, which allow the construction of permanence patches, can also be considered in terms of discretized PDEs as a blend of variational principles.

Here we have defined some masks associated to the functionals and to the PDEs that we have studied, and we have also discussed our results in comparison with those corresponding to permanence patches obtained through the masks defined in [**14**].

Before starting an explicit description of our work, we would like to make a comment concerning parametrizations. There is a difference between the symmetry of the results obtained for rectangular Bézier surfaces and the asymmetry of triangular surfaces. For usual Bézier surfaces, there is a very clear association between rectangular control nets and parametrizations of a Bézier surface. In the case of triangular Bézier surfaces, things are not so easy. The most direct association between triangular control nets and parametrizations of triangular Bézier surfaces is the one obtained after the substitution of one of the barycentric coordinates by an expression depending on the other two bearing in mind the relation $u + v + w = 1$. For example, if $\overrightarrow{y}(u, v, w)$ is the patch in barycentric coordinates, then we shall work with the patch $\overrightarrow{x}(u, v) = \overrightarrow{y}(u, v, 1 - u - v)$. Moreover, if we suppose now that (u, v) are Cartesian coordinates or, equivalently, that the triangle used to define the barycentric coordinates is the non-equilateral one whose vertices are $(0, 0)$, $(1, 0)$ and $(0, 1)$, then this association has a serious drawback, namely, the breakdown of symmetry. Even if the control net is symmetric ($P_{\sigma(i)\sigma(j)\sigma(k)} = P_{ijk}$ for any permutation σ), the Bézier triangular surface does not preserve the symmetry.

Nevertheless, we have followed this non-symmetric approach due to the following facts:

(1) Our approximations, despite the use of non-symmetric methods, seem to be at least as good as other results deduced from symmetric methods, such as the construction of permanence patches or other methods that are deduced forcing symmetry.
(2) For degree 3, there is a well-known minimal surface, Enneper's surface. The use of asymmetric methods allows us to obtain this surface as a result but this is no longer true for any symmetric mask. It can be shown that there are pieces of the Enneper surface for which the interior control point cannot be obtained by applying a symmetric mask to the exterior control points.
(3) Symmetric masks are deduced after some arguments on the control net, but not on the Bézier surface. Our methods are based directly on the Bézier surface when we want to minimize some functional directly related with the surface.

Let us introduce our work with a little more detail.

Our approach in the first three chapters regards surface design by solving Partial Differential Equations (PDEs): we create a surface as a solution to an appropriately chosen boundary-value problem. In 1989, Bloor and Wilson gave this type of surface modeling techniques the name "PDE surfaces", see [**8**]. Since most information defining a surface comes from its boundary curves, adding some boundary conditions to the PDE allows the PDE-based method to generate and control the surface shape through very few parameters.

In the **first chapter** we study the way to generate harmonic surfaces given some of their control points as initial data. Harmonic surfaces are the PDE surfaces obtained as a solution of the equation $\Delta \overrightarrow{x} = 0$, where Δ denotes the harmonic operator otherwise known as the Laplacian. Harmonic surfaces, which have found their way into various application areas of CAGD such as surface design, geometric mesh smoothing and fairing, are moreover related to surfaces minimizing the area: an isothermal parametric surface is minimal if and only if it is harmonic.

In the **second chapter** we give two different methods to generate biharmonic triangular Bézier surfaces with some of their control points prescribed. A biharmonic surface satisfies the PDE $\Delta^2 \overrightarrow{x} = 0$, where Δ^2 is the bilaplacian operator. The term "thin plate problem", which is used to refer to the biharmonic boundary problem, comes from the physical analogy involving the bending of a thin sheet of metal.

As we said before, for tensor-product Bézier surfaces an analogous study of harmonic and biharmonic surfaces was previously conducted in [**30**] and [**31**]. In these papers it was proved that two opposite boundary curves of an harmonic Bézier rectangular patch determine the surface and that any biharmonic rectangular Bézier surface is fully determined by the boundary control points, that is, four boundary curves. From these results and from our analogous findings for triangular Bézier surfaces, it can be deduced that the order of the PDE somehow determines the number of parameters that are free. Therefore, it is natural to think that, given the boundary curves of a triangular patch, an interpolating surface would be totally determined as a solution of a third-order PDE.

In this way, in the **fourth chapter**, we introduce a third order PDE and we give a method to generate the associated PDE surface from a prescribed boundary. Since the boundary curves determine the whole of a biharmonic surface in the rectangular case, in the triangular case the boundary control points determine a surface associated to a third-order PDE. This method, which we call the third-order method, makes it possible to create the geometry of realistic objects based upon the surface information at the boundaries of the object to be designed.

Before introducing the third-order method in chapter four, we present a study about triangular Coons patches in the **third chapter**. More specifically we have compared triangular Coons patches with rectangular Coons patches.

Here, we have considered the problem of finding a polynomial extremal of the functional

$$\mathcal{F}(\overrightarrow{x}) = \int_U \|\overrightarrow{x_{uv}}\|^2 du\, dv,$$

among all rectangular patches with the same boundary. We have proved that this is equivalent to solve the PDE $\overrightarrow{x}_{uuvv} = 0$, and that, in addition, the Coons rectangular patch is a solution.

On the other hand, we have seen that triangular Coons patches are not extremals of this functional. We then studied the conditions under which it would be equivalent to finding an extremal of $\mathcal{F}$ among all polynomial triangular patches with a prescribed boundary and to solving the PDE $\overrightarrow{x}_{uuvv} = 0$.

Moreover, we defined the Triangular Discrete Coons patch and we gave a characterization of the control net of a triangular Bézier extremal of the functional $\mathcal{F}$. This characterization allowed us to develop two methods to generate triangular patches given the boundary curves. The first method is to find the extremals of the functional as a solution of a linear system of the control points. The second method enables us to build a Bézier triangle by means of a mask deduced from the characterization of cubical extremals.

In general, we know designers usually only deal with low degree surfaces but, anyway, if we think about the problem of approximating arbitrary harmonic or biharmonic surfaces by polynomial surfaces then it is known that the degree of polynomial surfaces must increase in order to get good approximations. Therefore we have proved all our related results in general, for an arbitrary degree.

In the fifth and the sixth chapters of this work we also give different methods to generate Bézier triangles given some different kinds of initial data but, in contrast to the previous chapters, we generate minimal surfaces and polynomial approximations to minimal surfaces.

In **chapter five** we give some methods to generate minimal surfaces based on the representation formulas obtained by K. Weierstrass in 1861. Making use of the theory of complex analysis, we describe the way to build minimal and isothermal surfaces starting out from several sets of initial conditions such as control points, the tangent planes at the surface vertices or other kind of parameters.

Moreover, we study the relation between minimal surfaces and minimal complex curves and we deduce from this study two more methods to generate cubical minimal isothermal surfaces.

In **chapter six**, we have considered the Plateau-Bézier problem. Over the years it has been studied the general problem of determining the shape of the minimal surface constrained by a given boundary, which is known as Plateau's Problem. Here, we have considered a restricted problem, the Plateau-Bézier problem, which consists in finding the Bézier surface with minimal area from among all Bézier surfaces with a prescribed boundary. This problem was previously discussed in [**30**] for rectangular Bézier patches. In this chapter we provide an analogous discussion. We give an approximation to the solution of the Plateau problem obtained by replacing the area functional with the Dirichlet functional, for triangular Bézier surfaces. Then we make some comparisons between Dirichlet extremals and Bézier surfaces obtained by the use of the masks defined in [**14**], that is, the permanence patches. We also provide an expression of the Dirichlet functional in terms of the control points of a triangular Bézier surface, and then the functional translates into a function of the control points. Afterwards, from this expression we derive a characterization of the triangular control net of an extremal of this functional. In addition, an analogous study to the one described above for the Dirichlet functional but in this case concerning the Biharmonic functional is also included in this chapter.

In the **last chapter** we study constant mean curvature triangular Bézier surfaces. CMC-surfaces are extremals of the functional $\mathcal{D}_H(\overrightarrow{x}) = \mathcal{D}(\overrightarrow{x}) + 2\,HV(\overrightarrow{x})$, where $\mathcal{D}(\overrightarrow{x})$ is the Dirichlet functional and the functional $V(\overrightarrow{x})$, that we introduce in this chapter, is the functional that measures the algebraic volume enclosed in the cone segment consisting of all lines joining points $\overrightarrow{x}\,(u,v)$ on the surface with the origin.

Here we consider this functional over triangular Bézier patches and we obtain a method to generate polynomial approximations to constant mean curvature surfaces.

As we did in chapter six, we give a characterization, in terms of control points, of an extremal of $\mathcal{D}_H$ among all Bézier triangles with the same border. This characterization of the Bézier extremals of $\mathcal{D}_H$ allows us to compute the polynomial approximations to CMC-surfaces as a solution of a quadratic system of the control points.

For a given boundary it can be found a family of polynomial approximations to CMC-surfaces with curvatures in a particular interval. Therefore, the prescription of the curvature in this method can be seen as an additional degree of freedom.

At the end of each chapter we will present a discussion about the work done. We will explain our conclusions deduced from the results we have obtained in relation to the problems under consideration.

CHAPTER 1

Constructing triangular Bézier surfaces using linear PDEs:

Harmonic surfaces

In this chapter we present some results related with harmonic triangular Bézier surfaces, that is, those Bézier triangles verifying $\Delta \overrightarrow{x} = 0$ where $\Delta = \left(\frac{\partial^2}{\partial u^2} + \frac{\partial^2}{\partial v^2}\right)$. The harmonic operator, otherwise known as the Laplacian operator, has been widely used in many application areas such as physics. It is associated with a wide range of physical problems, for example gravity, electromagnetism and fluid flows.

Moreover, as is well known, harmonic surfaces are related to minimal surfaces. The relation is as follows: given a parametric surface patch $\overrightarrow{x}(u, v)$ satisfying the isothermality condition, i.e.,

$$< \overrightarrow{x}_u, \overrightarrow{x}_u >=< \overrightarrow{x}_v, \overrightarrow{x}_v > \quad \text{and} \quad < \overrightarrow{x}_u, \overrightarrow{x}_v >= 0$$

where $\overrightarrow{x}_u$ and $\overrightarrow{x}_v$ are the first derivatives with respect to u and v and $<,>$ is the dot product, then the surface it represents is minimal, in the sense of minimal area, if and only if it is harmonic. Let us remark that the harmonicity of a surface is a characteristic that depends on the parametrization.

The main result from the theory of minimal surfaces states that, under certain conditions, given the boundary there is a unique minimal surface prescribed by that boundary. In [**29**] it was proved that the harmonicity condition, for rectangular Bézier patches, and the knowledge of two opposite boundary curves determine the whole of the surface. Here we will present a similar study of harmonic Bézier surfaces, (as it was done in paper [**29**]), but instead of rectangular Bézier patches we will deal with Bézier triangles.

Triangular Bézier surfaces have an advantage over rectangular Bézier surfaces when dealing with derivatives. Let us illustrate it with an example: Given a polynomial $u^n v^n$, as a tensor-product Bézier surface coordinate function, its degree is (n, n), while if it is considered as a triangular Bézier coordinate function its degree would be $2n$. Then if we take derivatives, for example, if we consider the Laplacian, $\Delta(u^n v^n) = u^{n-2}v^n + u^n v^{n-2}$, in terms of rectangular patches its degree is still (n, n), but it decreases to $2n-2$ in terms of triangular Bézier surfaces. Therefore we can consider that triangular Bézier patches are better adapted to PDE problems.

First of all let us recall some definitions and basic properties related with Bézier surfaces.

1. Triangular Bézier Surfaces

Consider a triangle with vertices A, B, C and a fourth point P, all in $\mathbb{R}^3$. Then, it is always possible to write P as a barycentric combination of A, B, C

$$P = uA + vB + wC \quad \text{requiring that} \quad u + v + w = 1.$$

The coefficients $\mathbf{u} = (u, v, w)$ are called *barycentric coordinates* of P with respect to A, B, C.

To build a triangular Bézier surface of degree n we have to repeat the barycentric interpolation in the same way we repeat the bilinear interpolation in the de Casteljau algorithm for constructing a Bézier surface, see [**21**]. The control net for a triangular Bézier surface of degree n consists of $\frac{(n+1)(n+2)}{2}$ points arranged in a triangular grid. As an example, we can see the following triangular control net which shows the case of degree 4:

$$\begin{array}{c} P_{400}\ P_{310}\ P_{220}\ P_{130}\ P_{040} \\ P_{301}\ P_{211}\ P_{121}\ P_{031} \\ P_{202}\ P_{112}\ P_{022} \\ P_{103}\ P_{013} \\ P_{004} \end{array} \tag{1}$$

We will denote each point of the triangular control net by P_I where $I = (i, j, k)$ and $|I| = i + j + k$.

In the same way that a rectangular Bézier surface admits two equivalent definitions, the one from the de Casteljau algorithm and the one with univariate Bernstein polynomials, a triangular Bézier surface can be defined in both equivalent ways. A triangular Bézier surface in terms of the trivariate Bernstein polynomials :

Definition 1.1. *The trivariate Bernstein polynomial of degree n is defined as*

$$B_I^n(\mathbf{u}) = \binom{n}{I} u^i\, v^j\, w^k = \frac{n!}{i!j!k!}\, u^i\, v^j\, w^k \quad \text{if} \quad |I| = n,$$

otherwise $B_I^n(\mathbf{u}) = 0$.

Although these Bernstein polynomials look trivariate, they are not, since the barycentric coordinates verify the relation $u + v + w = 1$.

We will denote by $\mathcal{R}$ the region $\mathcal{R} = \{\mathbf{u} = (u, v, w) \in \mathbb{R}^3 / u+v+w = 1 \text{ and } u, v, w \geq 0\}$ and by T the region $T = \{(u, v) \in \mathbb{R}^2 : 0 \leq u, 0 \leq v, u + v \leq 1\}$.

The following lemmas will introduce us to some of the properties of Bernstein polynomials.

LEMMA 1.2. *The product of a pair of Bernstein polynomials is given by:*

$$B_I^n(\mathbf{u}) \cdot B_J^m(\mathbf{u}) = \frac{\binom{n}{I}\binom{m}{J}}{\binom{n+m}{I+J}} B_{I+J}^{n+m}(\mathbf{u}) \qquad \text{where} \quad |I| = n,\ |J| = m. \tag{2}$$

LEMMA 1.3. *The partial derivatives of Bernstein polynomials are given by:*

$$\frac{\partial}{\partial u} B_I^n(\mathbf{u}) = n\,(B_{I-e_1}^{n-1}(\mathbf{u}) - B_{I-e_3}^{n-1}(\mathbf{u}))$$

$$\frac{\partial}{\partial v} B_I^n(\mathbf{u}) = n\,(B_{I-e_2}^{n-1}(\mathbf{u}) - B_{I-e_3}^{n-1}(\mathbf{u})),$$

where we have denoted $e_1 = (1,0,0)$, $e_2 = (0,1,0)$, $e_3 = (0,0,1)$.

LEMMA 1.4. *The integral of a Bernstein polynomial over the triangle* T *is given by*

$$\int_T B_I^n(u,v,1-u-v)\; dv\, du \;=\; \frac{1}{(n+1)(n+2)} \qquad \text{for all} \quad I; \quad |I| = n. \tag{3}$$

Proof: Taking into account that for $k = 0$ we have that $j = n - i$ we get:

$$\begin{aligned} \textstyle\int_T B_{(i,j,0)}^n(u,v,1-u-v)\; dv\, du &= \int_0^1 \int_0^{1-u} B_{(i,j,0)}^n(u,v,1-u-v)\; dv\, du \\ &= \int_0^1 \int_0^{1-u} \tbinom{n}{I} u^i\, v^{n-i}\; dv\, du \\ &= \int_0^1 \tbinom{n}{I} u^i\, \tfrac{(1-u)^{n-i+1}}{n-i+1}\, du \\ &= \int_0^1 \tfrac{1}{n+1} B_i^{n+1}(u)\, du \;=\; \tfrac{1}{(n+1)(n+2)}, \end{aligned} \tag{4}$$

where $B_i^{n+1}(u)$ is the univariate Bernstein polynomial.

Now, integrating by parts, we get the equality:

$$\int_0^{1-u} B_{(i,j+1,k-1)}^n(u,v,1-u-v)\; dv = \int_0^{1-u} B_{(i,j,k)}^n(u,v,1-u-v)\; dv. \tag{5}$$

and therefore, by successive application of (5) to the previous computation (4), we get the desired result.

■

DEFINITION 1.5. *Given a triangular control net in* $\mathbb{R}^3$, $\mathcal{P} = \{P_I\}_{|I|=n}$, *the triangular Bézier surface of degree* n *associated to a control net* $\mathcal{P}$, $\overrightarrow{x} : T \longrightarrow \mathbb{R}^3$ *is given by:*

$$\overrightarrow{x}(\mathbf{u}) = \sum_{|I|=n} P_I B_I^n(\mathbf{u}).$$

LEMMA 1.6. *The partial m-th derivatives of a triangular Bézier patch, $\overrightarrow{x}$, are given by the following formulas*

$$\begin{aligned}\frac{\partial^m \overrightarrow{x}}{\partial u^m}(u,v) &= \frac{n!}{(n-m)!}\sum_{|I|=n-m}\Delta^{m,0}P_I B_I^{(n-m)}(u,v),\\ \frac{\partial^m \overrightarrow{x}}{\partial v^m}(u,v) &= \frac{n!}{(n-m)!}\sum_{|I|=n-m}\Delta^{0,m}P_I B_I^{(n-m)}(u,v).\end{aligned} \tag{6}$$

where we have introduced the notation

$$\begin{aligned}\Delta^{l,m}P_{i,j,k} &= \Delta^{l-1,m}\Delta^{1,0}P_{i,j,k} = \Delta^{l-1,m}\left(P_{i+1,j,k}-P_{i,j,k+1}\right),\\ \Delta^{l,m}P_{i,j,k} &= \Delta^{l,m-1}\Delta^{0,1}P_{i,j,k} = \Delta^{l,m-1}\left(P_{i,j+1,k}-P_{i,j,k+1}\right).\end{aligned} \tag{7}$$

Proof: First we will compute partial derivatives with respect to u.

$$\begin{aligned}\frac{\partial \overrightarrow{x}}{\partial u}(u,v) &= \frac{\partial}{\partial u}\Big(\sum_{|I|=n}P_I B_I^n(u,v)\Big) = \sum_{|I|=n}P_I\frac{\partial}{\partial u}B_I^n(u,v)\\ &= n\sum_{|I|=n}P_I\big(B_{I-e_1}^{n-1}(u,v)-B_{I-e_3}^{n-1}(u,v)\big)\\ &= n\Big(\sum_{|I|=n}P_I B_{I-e_1}^{n-1}(u,v)-\sum_{|I|=n}P_I B_{I-e_3}^{n-1}(u,v)\Big)\\ &= n\sum_{|I|=n-1}(P_{I+e_1}-P_{I+e_3})B_I^{n-1}(u,v)\\ &= n\sum_{|I|=n-1}(P_{i+1,j,k}-P_{i,j,k+1})B_I^{n-1}(u,v)\\ &= n\sum_{|I|=n-1}\Delta^{1,0}P_I B_I^{n-1}(u,v).\end{aligned}$$

So

$$\frac{\partial \overrightarrow{x}}{\partial u}(u,v) = n\sum_{|I|=n-1}(P_{i+1,j,k}-P_{i,j,k+1})B_I^{n-1}(u,v) = n\sum_{|I|=n-1}\Delta^{1,0}P_I B_I^{n-1}(u,v). \tag{8}$$

and analogously,

$$\frac{\partial \overrightarrow{x}}{\partial v}(u,v) = n\sum_{|I|=n-1}(P_{i,j+1,k}-P_{i,j,k+1})B_I^{n-1}(u,v) = n\sum_{|I|=n-1}\Delta^{0,1}P_I B_I^{n-1}(u,v). \tag{9}$$

After taking derivatives repeatedly we get the m-th derivative with respect to u,

$$\begin{aligned}
\frac{\partial^m \overrightarrow{x}}{\partial u^m}(u,v) &= n\frac{\partial^{m-1}}{\partial u^{m-1}} \sum_{|I|=n-1} \Delta^{1,0} P_I B_I^{n-1}(u,v) \\
&= n(n-1)\frac{\partial^{m-2}}{\partial u^{m-2}} \sum_{|I|=n-2} \Delta^{1,0}(\Delta^{1,0} P_I) B_I^{n-2}(u,v) \\
&= n(n-1)\frac{\partial^{m-2}}{\partial u^{m-2}} \sum_{|I|=n-2} \Delta^{2,0} P_I B_I^{n-2}(u,v) \\
&= \frac{n!}{(n-m+1)!}\frac{\partial}{\partial u} \sum_{|I|=n-m+1} \Delta^{m-1,0} P_I B_I^{(n-m+1)}(u,v) \\
&= \frac{n!}{(n-m)!} \sum_{|I|=n-m} \Delta^{m,0} P_I B_I^{(n-m)}(u,v).
\end{aligned}$$

An analogous computation gives the m-th derivative with respect to v.

■

2. The harmonic condition

In this section we will study the harmonic operator, that is, the Laplacian, acting on a triangular Bézier surface in an analogous way to [**29**]. First of all, we will compute its expression in terms of the control points of a Bézier triangle and afterwards, in Theorem 1.9 and Theorem 1.18, we will discuss how a harmonic Bézier surface is totally determined by the knowledge of some of its control points.

Some authors have previously carried out some similar work related with the Laplacian operator, (see [**14**]), but from a discrete point of view. They have described the relations between the control points of a Bézier surface satisfying the discrete Laplacian condition instead of establishing the relations between points in the control net of a harmonic surface. That is what we have done. We have obtained some discrete conditions but not by using the discrete operator.

First of all, as we said before, we seek the conditions that the function $\overrightarrow{x}$ must fulfill in order to be harmonic, that is, we compute the Laplacian of the Bézier patch. We do this in terms of the control points, that is, we obtain the conditions that the control net of a triangular Bézier surface must satisfy in order to be associated to a harmonic surface:

$$\Delta \overrightarrow{x}\,(\mathbf{u}) = \left(\frac{\partial^2}{\partial u^2} + \frac{\partial^2}{\partial v^2}\right) \overrightarrow{x}\,(\mathbf{u}) = \left(\frac{\partial^2}{\partial u^2} + \frac{\partial^2}{\partial v^2}\right) \sum_{|I|=n} P_I\, B_I^n\,(\mathbf{u})$$

then bearing in mind the previously computed derivative of a Bézier surface, Equation (6), we have

$$
\begin{aligned}
=&n\,(n-1)\left(\sum_{|I|=n-2}\Delta^{2,0}P_I B_I^{n-2}(\mathbf{u})+\sum_{|I|=n-2}\Delta^{0,2}P_I B_I^{n-2}(\mathbf{u})\right)\\
=&n\,(n-1)\sum_{|I|=n-2}\left(\Delta^{1,0}\left(P_{I+e_1}-P_{I+e_3}\right)+\Delta^{0,1}\left(P_{I+e_2}-P_{I+e_3}\right)\right)B_I^{n-2}(\mathbf{u})\\
=&n\,(n-1)\sum_{|I|=n-2}\left(P_{I+2e_1}+P_{I+2e_2}+2P_{I+2e_3}-2\left(P_{I+e_1+e_3}+P_{I+e_2+e_3}\right)\right)B_I^{n-2}(\mathbf{u}).
\end{aligned}
$$

Thus, the Laplacian of a triangular Bézier surface can be seen as a triangular Bézier patch of degree $n-2$ with associated control points

$$
Q_I=n\,(n-1)\left(P_{I+2e_1}+P_{I+2e_2}+2P_{I+2e_3}-2\left(P_{I+e_1+e_3}+P_{I+e_2+e_3}\right)\right)\quad\text{for}\quad|I|=n-2.
$$

Let us recall that in the rectangular Bézier case there is no reduction of degree if the Laplacian is computed, but here there is a decrease of total degree.

Due to the fact that $\{B_I^{n-2}(\mathbf{u})\}_{|I|=n-2}$ is a basis, we get that $\overrightarrow{x}$ is harmonic iff $Q_I=0$ for all $|I|=n-2$.

PROPOSITION 1.7. *The triangular Bézier surface associated to a control net $\{P_I\}_{|I|=n}$ is harmonic, i.e., satisfies $\Delta\overrightarrow{x}=0$, if and only if*

$$
0=P_{I+2e_1}+P_{I+2e_2}+2P_{I+2e_3}-2\left(P_{I+e_1+e_3}+P_{I+e_2+e_3}\right)\qquad\textit{for}\quad|I|=n-2. \tag{10}
$$

REMARK 1.8. *The previous equation, Equation (10), can be rewritten as:*

$$
0=P_{k+2,l,n-k-l-2}+P_{k,l+2,n-k-l-2}+2P_{k,l,n-k-l}-2\left(P_{k+1,l,n-k-l-1}+P_{k,l+1,n-k-l-1}\right) \tag{11}
$$

$\forall k,l\geq 0$, or equivalently as $0=\left(\Delta^{2,0}+\Delta^{0,2}\right)P_{k,l,n-k-l}$, where $\Delta^{2,0}$ and $\Delta^{0,2}$ are the usual difference operators defined in Equation (7).

At this point we can state that the harmonic condition implies that some of the control points of a triangular Bézier surface can be expressed as a linear combination of the other control points. In the following sections we will study this dependence relation between control points at harmonic control nets of an arbitrary dimension, but, first of all, we will study the low dimensional cases, $n=2$ and $n=3$.

For the quadratic case the harmonic condition, which has been translated into a linear system given by Equation (10) for $|I|=n-2$, is reduced to a unique equation. So, in this case we obtain that two lines of border control points determine a family of harmonic Bézier control triangles. On the other hand, for the cubic case, the linear system consists of three equations which allow us to determine, given two lines of border control points, a harmonic triangular Bézier surface. Let us explain these results.

2.1. The quadratic case. For $n = 2$ a quadratic triangular Bézier surface is defined by the following triangular control net:

$$\mathcal{P} \equiv \begin{array}{ccc} P_{002} & P_{011} & P_{020} \\ P_{101} & P_{110} & \\ P_{200} & & \end{array}$$

If the patch associated to a quadratic triangular Bézier surface is harmonic, then Equation (11) gives us the condition:

$$P_{200} + P_{020} - 2\,(P_{101} + P_{011}) + 2P_{002} = 0.$$

From this equation we can express one of the control points in terms of the other five, for example:

$$P_{101} = \frac{1}{2}(P_{200} + P_{020} - 2\,P_{011} + 2P_{002}).$$

The equation above can be written by way of a "kind" of mask:

$$P_{101} = \frac{1}{2} \quad \times \quad \begin{array}{ccc} 2 & -2 & 1 \\ & \star & 0 \\ & 1 & \end{array}$$

Note that, according to this, given two rows of border control points (five points), the sixth point is fully determined by the harmonic condition. Moreover, given four points of the triangular control net we obtain a family of harmonic quadratic surfaces since the condition for the Laplacian does not depend on the control point P_{110}.

2.2. The cubic case. For $n = 3$ the cubic triangular surface is associated to the following triangular control net:

$$\mathcal{P} \equiv \begin{array}{cccc} P_{003} & P_{012} & P_{021} & P_{030} \\ P_{102} & P_{111} & P_{120} & \\ P_{201} & P_{210} & & \\ P_{300} & & & \end{array} \tag{12}$$

The equations that a cubic triangular Bézier surface must satisfy in order to be harmonic are the following:

$$\begin{cases} P_{300} + P_{120} - 2\left(P_{201} + P_{111}\right) + 2P_{102} = 0, \\ P_{210} + P_{030} - 2\left(P_{111} + P_{021}\right) + 2P_{012} = 0, \\ P_{201} + P_{021} - 2\left(P_{102} + P_{012}\right) + 2P_{003} = 0. \end{cases}$$

From these equations it is possible to express three control points in terms of the other seven, since we have obtained that the null space of the coefficient matrix is of dimension seven. Therefore it is possible to choose two lines of border control points of a triangular control net as free variables, and then the other three points are fully determined by the harmonic condition:

$$P_{102} = \frac{-1}{2} \times \begin{array}{ccccc} -4 & & 6 & & -4 \\ & \star & & 0 & \\ & & 0 & & 1 \\ & & & -1 & \end{array} \qquad P_{111} = \frac{-1}{2} \times \begin{array}{ccccc} 0 & & -2 & & 2 \\ & 0 & & \star & \\ & & 0 & & -1 \\ & & & 0 & \end{array}$$

$$P_{201} = \begin{array}{ccccc} 2 & & -4 & & 3 \\ & 0 & & 0 & \\ & & \star & & -1 \\ & & & 1 & \end{array}$$

3. Constructing triangular Bézier surfaces from a boundary curve and the normal derivative along it

Now, after studying the first two low dimensional cases, and seeing that the harmonic condition determines some control points in terms of border control points, we will try to extend this result to triangular Bézier surfaces in general. But for greater dimensions we will find that this result has a variation. We will prove in section 5 that from $n = 4$ onwards, two rows of border control points do not give enough information to determine all the other control points. Therefore, instead of taking two border lines of control points as known points, we will consider two different variations of the set of points that are considered as known points.

The first variation, which we will study in this section, comes from the following usual boundary value problem:

$$\Delta \overrightarrow{x}\,(u,v) = 0, \qquad \begin{cases} \overrightarrow{x}\,(0,v) = \alpha\,(v) \\ \overrightarrow{x}_{\,u}\,(0,v) = \beta\,(v)\,. \end{cases}$$

We consider the linear PDE given by the harmonic operator with Cauchy boundary conditions. The value of the solution along a border curve, $\overrightarrow{x}\,(0,v)$, and its transversal partial derivative, $\overrightarrow{x}_{\,u}\,(0,v)$, which determines the tangent plane to the surface along this border curve, are the conditions which are specified. It is known that in general a solution to this problem can be uniquely determined, the point is that here we will determine a polynomial solution. In terms of triangular Bézier surfaces, the problem is: Given the first

two rows of control points we determine the associated harmonic surface. This will be the first result we will prove in this section (Theorem 1.9).

The second variation of the set of known points, which we will study in section 5, is as follows. In the rectangular case it holds that two rows of border control points fully determine the associated harmonic chart, see [**29**], but unfortunately this is no longer true for the triangular case. Therefore we will consider as known points a set of control points which is as similar as possible to a set of border points: We consider two border lines of control points with the exception of some of them, which are replaced by their neighboring interior control points. The choice of the neighboring points to replace the excluded border points comes from the fact that they are closer to the frontier, so they can give better information about the desired shape of the surface.

The following Theorem will show that a harmonic triangular Bézier surface can be determined from its first two rows of control points in the control net.

THEOREM 1.9. *Let* $\overrightarrow{x}(u,v) = \sum_{|I|=n} P_I B_I^n(u,v)$ *be a harmonic triangular Bézier surface with control net* $\{P_I\}_{|I|=n}$*, then the control points* $P_{i,j,k}$ *with* $i \neq 0, 1$ *are totally determined by the first two rows of the control net* $\{P_{0,j,n-j}\}_{j=0}^{n}$ *and* $\{P_{1,j,n-j}\}_{j=0}^{n-1}$.

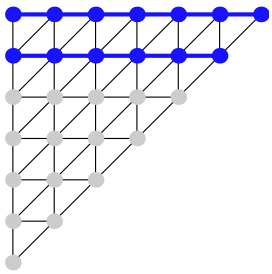

FIGURE 1. An schematic grid of control points. The blue dots are known and the gray would be obtained by asking for harmonicity.

Proof: The harmonicity condition (11) allows us to establish some relations between control points, so if we consider the set of equations associated for any pair of indices k, l, we get a system of linear equations where the points at the first two rows are considered as known points and the rest of the control points are the variables. Then our goal is to ensure that the system always has a solution. So, in order to do that, we split the system into a number of subsystems and then we prove the solvability of them.

The following scheme shows a triangular control net of degree n written in such a way that, at our convenience, it allows us to talk about columns:

$$
\begin{array}{ccccccccccc}
\mathbf{P_{0,0,n}} & \mathbf{P_{0,1,n-1}} & \mathbf{P_{0,2,n-2}} & \cdots & \mathbf{P_{0,n-5,5}} & \mathbf{P_{0,n-4,4}} & \mathbf{P_{0,n-3,3}} & \mathbf{P_{0,n-2,2}} & \mathbf{P_{0,n-1,1}} & \mathbf{P_{0,n,0}} \\
\mathbf{P_{1,0,n-1}} & \mathbf{P_{1,1,n-2}} & \mathbf{P_{1,2,n-3}} & \cdots & \mathbf{P_{1,n-5,4}} & \mathbf{P_{1,n-4,3}} & \mathbf{P_{1,n-3,2}} & \mathbf{P_{1,n-2,1}} & \mathbf{P_{1,n-1,0}} & \\
P_{2,0,n-2} & P_{2,1,n-3} & P_{2,2,n-4} & \cdots & P_{2,n-5,3} & P_{2,n-4,2} & P_{2,n-3,1} & P_{2,n-2,0} & & \\
P_{3,0,n-3} & P_{3,1,n-4} & P_{3,2,n-5} & \cdots & P_{3,n-5,2} & P_{3,n-4,1} & P_{3,n-3,0} & & & \\
P_{4,0,n-4} & P_{4,1,n-5} & P_{4,2,n-6} & \cdots & P_{4,n-5,1} & P_{4,n-4,0} & & & & \\
P_{5,0,n-5} & P_{5,1,n-6} & P_{5,2,n-7} & \cdots & P_{5,n-5,0} & & & & & \\
\vdots & \vdots & \vdots & & & & & & & \\
P_{n-3,0,3} & P_{n-3,1,2} & P_{n-3,2,1} & & & & & & & \\
P_{n-2,0,2} & P_{n-2,1,1} & P_{n-2,2,0} & & & & & & & \\
P_{n-1,0,1} & P_{n-1,1,0} & & & & & & & & \\
P_{n,0,0} & & & & & & & & &
\end{array}
\tag{13}
$$

Bearing in mind this scheme, and starting from the right corner we have that in the first and second column there are no unknown points: In the first column from the right, the nth column, we find $P_{0,n,0}$, which is assumed to be known, and the same happens with the following column, the column $n-1$, where we have $P_{0,n-1,1}$ and $P_{1,n-1,0}$.

On decreasing the column index, in column $n-2$, the first unknown point, $P_{2,n-2,0}$, appears, but Equation (11) with $k=0, l=n-2$:

$$2P_{0,n-2,2} - 2(P_{1,n-2,1} + P_{0,n-1,1}) + P_{2,n-2,0} + P_{0,n,0} = 0,$$

determines it. This would be the first subsystem we solve, and it allows us to obtain the point $P_{2,n-2,0}$ in terms of control points at the first two rows. In next step we consider the relations for $k=0, l=n-3$ and $k=1, l=n-3$:

$$\begin{cases} 2P_{0,n-3,3} - 2(P_{1,n-3,2} + P_{0,n-2,2}) + P_{2,n-3,1} + P_{0,n-1,1} = 0 \\ 2P_{1,n-3,2} - 2(P_{2,n-3,1} + P_{1,n-2,1}) + P_{3,n-3,0} + P_{1,n-1,0} = 0. \end{cases}$$

We have two equations and two unknown points, $P_{2,n-3,1}$ and $P_{3,n-3,0}$, which are also determined in terms of control points of the first and second rows. We have solved the second subsystem.

Now, if we follow this process column by column, we can observe that in each column we have a subsystem of linear equations which has an associated triangular coefficient matrix with negative-sloping diagonals defined by:

$$a_{i,i} = 1, \quad a_{i+1,i} = -2, \quad a_{i+2,i} = 2.$$

This is a triangular matrix whose determinant is equal to one when we take the points $\{P_{i,j,n-i-j}\}_{i=2,j=0}^{n,n-i}$ as variables. So we can ensure the solvability of each system associated in any column.

At this point we have that, for degree n, the linear system has a solution since it can be split into $n-2$ determined compatible subsystems. Therefore, we have that a harmonic control net can be obtained only in terms of control points in the first two rows, that is, if we look for a harmonic patch the whole control net is totally determined if the first and the second row in the control net are known.

■

Let us remark that the coefficient matrix in the previous proof is a particular case of Toeplitz pentadiagonal matrix, a kind of matrices we will study in the following section.

The following figures show, for degree $n = 4$ and $n = 6$, some harmonic surfaces obtained by means of Theorem 1.9. The first two rows of control points in the control net are prescribed.

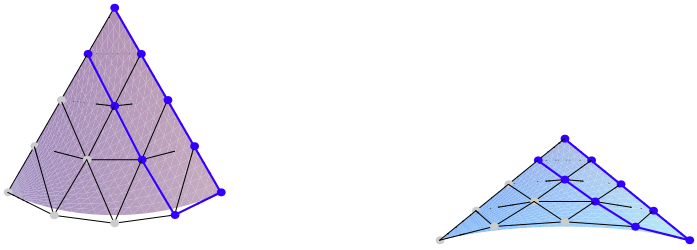

FIGURE 2. Two views of the harmonic surface, similar to a piece of a cone, determined by a set of control points placed along two parallel straight lines.

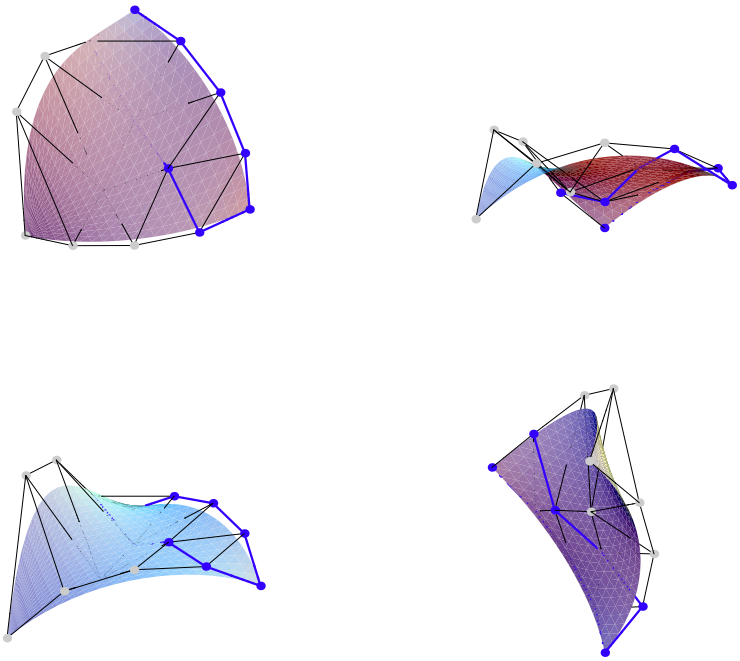

FIGURE 3. Four different points of view of the harmonic surface obtained with Theorem 1.9 when the set of fixed control points were on two "parallel" circular arcs.

The following figures show the previous harmonic surfaces but now for degree $n = 6$. Here it can be observed that for some higher degree examples, the first and the second line of control points do not give enough control over the shape of the generated harmonic surface.

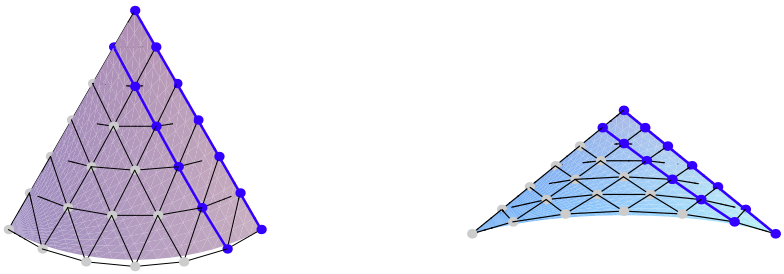

FIGURE 4. Two views of the harmonic surface, similar to a piece of cone as before but for $n = 6$, determined by a set of control points placed along two parallel straight lines.

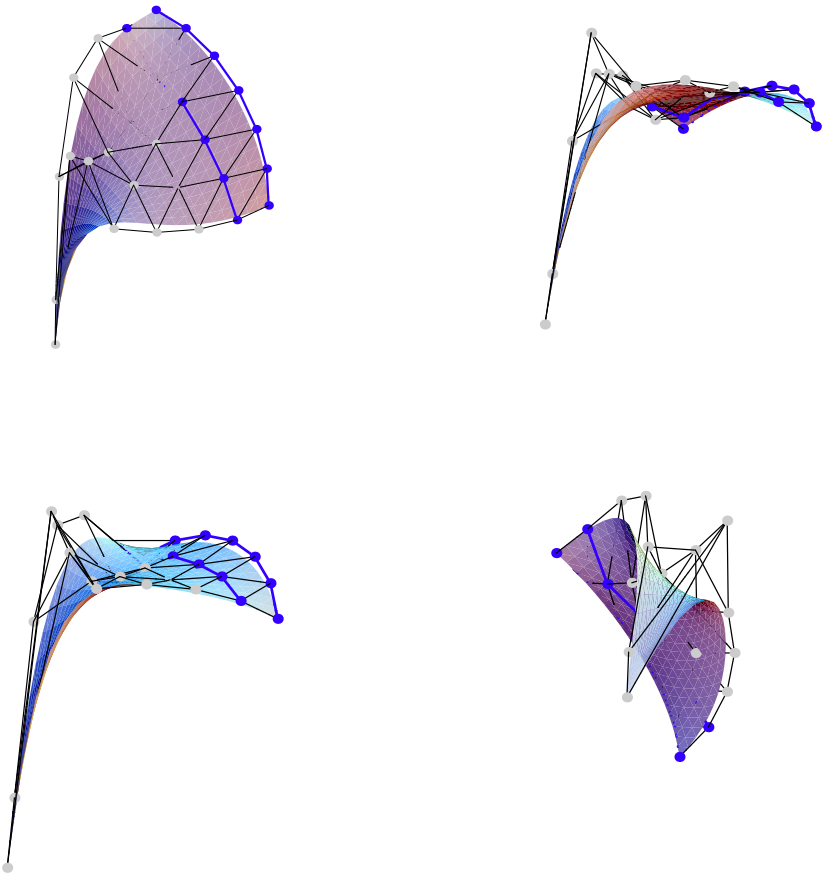

FIGURE 5. These are four views of the harmonic surface obtained with Theorem 1.9 when the set of fixed control points were in two "parallel" circular arcs. On comparing these figures with the corresponding figures shown for $n = 4$ it can be seen that for this higher degree the first and the second line of control points do not give much control over the shape of the harmonic surface that is determined.

4. Some Toeplitz matrices and their determinants

As we have seen in the previous section, the proof of the existence of a solution to the problem of determining a PDE surface when some of its control points are prescribed is reduced in order to check the solvability of some linear systems. In this section we will prove some results that will be useful for these purposes.

DEFINITION 1.10. *A $(2k+1)-$banded matrix, M, is a matrix that fulfilles*

$$m_{i,j} = 0 \quad \textit{if} \quad |i-j| > k.$$

Hence a 3-banded matrix is said to be tridiagonal, a 4-banded matrix is said to be tetradiagonal and a 5-banded is a pentadiagonal matrix or quindiagonal matrix.

DEFINITION 1.11. *Given $2n-1$ numbers a_k, where $k = -n+1, ..., -1, 0, 1, ..., n-1$, a Toeplitz matrix is defined as a matrix which has constant values along negative-sloping diagonals, i.e., a matrix of the form*

$$\begin{pmatrix} a_0 & a_{-1} & a_{-2} & \cdots & a_{-n+1} \\ a_1 & a_0 & a_{-1} & \ddots & \vdots \\ a_2 & a_1 & a_0 & \ddots & a_{-2} \\ \vdots & \ddots & \ddots & \ddots & a_{-1} \\ a_{n-1} & \cdots & a_2 & a_1 & a_0 \end{pmatrix}. \tag{14}$$

Therefore if a $(2k+1)-$banded matrix has constant values along its diagonals it is said to be a Toeplitz matrix defined by $2k+1$ scalars.

A $n \times n$ pentadiagonal Toeplitz matrix, which we will denote by $M_n^{(a,b,c,d,e)}$, is a matrix defined by five scalars located at the entries

$$m_{i-2,i} = a, \quad m_{i-1,i} = b, \quad m_{i,i} = c, \quad m_{i+1,i} = d, \quad m_{i+1,i} = e,$$

that is,

$$M_n^{(a,b,c,d,e)} = \begin{pmatrix} c & d & e & 0 & \cdots & 0 & 0 & 0 & 0 & 0 & 0 \\ b & c & d & e & 0 & \cdots & 0 & 0 & 0 & 0 & 0 \\ a & b & c & d & e & 0 & \cdots & 0 & 0 & 0 & 0 \\ 0 & a & b & c & d & e & 0 & \cdots & 0 & 0 & 0 \\ 0 & 0 & a & b & c & d & e & 0 & \cdots & 0 & 0 \\ \vdots & \vdots & \ddots & \ddots & \ddots & \ddots & \ddots & \ddots & \ddots & \vdots & \vdots \\ 0 & 0 & \cdots & 0 & a & b & c & d & e & 0 & 0 \\ 0 & 0 & 0 & \cdots & 0 & a & b & c & d & e & 0 \\ 0 & 0 & 0 & 0 & \cdots & 0 & a & b & c & d & e \\ 0 & 0 & 0 & 0 & 0 & \cdots & 0 & a & b & c & d \\ 0 & 0 & 0 & 0 & 0 & 0 & \cdots & 0 & a & b & c \end{pmatrix}. \tag{15}$$

LEMMA 1.12. *The determinant, D_n, of the n-dimensional Toeplitz penta-diagonal matrix, $M_n^{(a,b,c,d,e)}$, defined in Equation (15), can be computed by the following recursive formula:*

(16)

$$D_n = cD_{n-1}+(ae-bd)D_{n-2}+(b^2e+ad^2-2aec)D_{n-3}+ae(ae-bd)D_{n-4}+a^2e^2cD_{n-5}-a^3e^3D_{n-6}$$

Proof:

We compute this determinant by performing expansion by minors, and we start by the first column:

$$D_n = a\begin{vmatrix} d & e & 0 & 0 & \cdots & 0 \\ c & d & e & 0 & \cdots & 0 \\ \hline a & b & & & & \\ 0 & a & & & & \\ 0 & 0 & & & & \\ \vdots & \vdots & & M_{n-3}^{(a,b,c,d,e)} & & \\ 0 & 0 & & & & \end{vmatrix} - b\begin{vmatrix} d & e & 0 & 0 & \cdots & 0 \\ \hline b & & & & & \\ a & & & & & \\ 0 & & & & & \\ 0 & & & & & \\ \vdots & & & M_{n-2}^{(a,b,c,d,e)} & & \\ 0 & & & & & \end{vmatrix} + cD_{n-1}$$

and again by the first columns we get:

$$D_n = a^2\begin{vmatrix} e & 0 & 0 & 0 & \cdots & 0 \\ d & e & 0 & 0 & \cdots & 0 \\ \hline a & b & & & & \\ 0 & a & & & & \\ 0 & 0 & & & & \\ \vdots & \vdots & & M_{n-4}^{(a,b,c,d,e)} & & \\ 0 & 0 & & & & \end{vmatrix} - ac\begin{vmatrix} e & 0 & 0 & 0 & \cdots & 0 \\ \hline b & & & & & \\ a & & & & & \\ 0 & & & & & \\ 0 & & & & & \\ \vdots & & & M_{n-3}^{(a,b,c,d,e)} & & \\ 0 & & & & & \end{vmatrix}$$

$$+ad\begin{vmatrix} d & e & 0 & 0 & \cdots & 0 \\ \hline b & & & & & \\ a & & & & & \\ 0 & & & & & \\ 0 & & & & & \\ \vdots & & & M_{n-3}^{(a,b,c,d,e)} & & \\ 0 & & & & & \end{vmatrix} - ba\begin{vmatrix} e & 0 & 0 & 0 & \cdots & 0 \\ c & d & e & 0 & \cdots & 0 \\ \hline a & b & & & & \\ 0 & a & & & & \\ 0 & 0 & & & & \\ \vdots & \vdots & & M_{n-4}^{(a,b,c,d,e)} & & \\ 0 & 0 & & & & \end{vmatrix}$$

$$+b^2\begin{vmatrix} e & 0 & 0 & 0 & \cdots & 0 \\ \hline b & & & & & \\ a & & & & & \\ 0 & & & & & \\ 0 & & & & & \\ \vdots & & & M_{n-3}^{(a,b,c,d,e)} & & \\ 0 & & & & & \end{vmatrix} - bdD_{n-2} + cD_{n-1},$$

that is,

$$D_n = a^2e^2D_{n-4} - aceD_{n-3} + ad\begin{vmatrix} d & e & 0 & 0 & \cdots & 0 \\ b & & & & & \\ a & & & & & \\ 0 & & & & & \\ 0 & & & M_{n-3}^{(a,b,c,d,e)} & & \\ \vdots & & & & & \\ 0 & & & & & \end{vmatrix} - bae\begin{vmatrix} d & e & 0 & \cdots & 0 \\ b & & & & \\ a & & & & \\ 0 & & & & \\ \vdots & & M_{n-4}^{(a,b,c,d,e)} & & \\ 0 & & & & \end{vmatrix}$$

$$+b^2eD_{n-3} - bdD_{n-2} + cD_{n-1}$$

where we have only rewritten the determinants including the row $(e, 0, ..., 0)$.

Now, we develop the first of the remaining determinants performing expansion by minors again and, on the other hand, we denote the second determinant by B_{n-3} since its dimension is $(n-3) \times (n-3)$:

$$D_n = a^2e^2D_{n-4} - aceD_{n-3} + a^2d\begin{vmatrix} e & 0 & 0 & 0 & \cdots & 0 \\ c & d & e & 0 & \cdots & 0 \\ a & b & & & & \\ 0 & a & & & & \\ 0 & 0 & & M_{n-5}^{(a,b,c,d,e)} & & \\ \vdots & \vdots & & & & \\ 0 & 0 & & & & \end{vmatrix} + adb\begin{vmatrix} e & 0 & 0 & 0 & \cdots & 0 \\ b & & & & & \\ a & & & & & \\ 0 & & & & & \\ 0 & & & & & \\ \vdots & & & M_{n-4}^{(a,b,c,d,e)} & & \\ 0 & & & & & \end{vmatrix}$$

$$+ad^2D_{n-3} - baeB_{n-3} + b^2eD_{n-3} - bdD_{n-2} + cD_{n-1} = a^2e^2D_{n-4} - aceD_{n-3}$$

$$+a^2de\begin{vmatrix} d & e & 0 & \cdots & 0 \\ b & & & & \\ a & & & & \\ 0 & & M_{n-5}^{(a,b,c,d,e)} & & \\ \vdots & & & & \\ 0 & & & & \end{vmatrix} + adbeD_{n-4} + ad^2D_{n-3} - baeB_{n-2} + b^2eD_{n-3} - bdD_{n-2} + cD_{n-1}$$

We denote the determinant that is still not computed by B_{n-4} since it is a $(n-4) \times (n-4)$ determinant with the same structure as B_{n-3}. Then we have:

$$D_n = a^2e^2D_{n-4} - aceD_{n-3} + a^2deB_{n-3} + adbeD_{n-4} + ad^2D_{n-3} - baeB_{n-2} + b^2eD_{n-3} - bdD_{n-2} + cD_{n-1}$$

Now, in order to get a recurrence formula, we would have to get an expression in terms of some D_i for the determinants denoted by B_{n-2} and B_{n-3}. To this end, we compute D_{n-2}:

$$D_{n-2} = a\begin{vmatrix} d & e & 0 & 0 & 0 & \cdots & 0 \\ c & d & e & 0 & 0 & \cdots & 0 \\ a & b & & & & & \\ 0 & a & & & & & \\ 0 & 0 & & & M_{n-4}^{(a,b,c,d,e)} & & \\ \vdots & \vdots & & & & & \\ 0 & 0 & & & & & \end{vmatrix} - b\begin{vmatrix} d & e & 0 & 0 & 0 & \cdots & 0 \\ b & & & & & & \\ a & & & & & & \\ 0 & & & & & & \\ 0 & & & & M_{n-3}^{(a,b,c,d,e)} & & \\ \vdots & & & & & & \\ 0 & & & & & & \end{vmatrix} + cD_{n-3}$$

$$D_{n-2} = a^2 \left|\begin{array}{cc|ccc} e & 0 & 0 & 0 & \cdots & 0 \\ d & e & 0 & 0 & \cdots & 0 \\ \hline a & b & & & & \\ 0 & a & & & & \\ 0 & 0 & & & & \\ \vdots & & & M_{n-6}^{(a,b,c,d,e)} & & \\ 0 & 0 & & & & \end{array}\right| - ac \left|\begin{array}{c|cccc} e & 0 & 0 & 0 & \cdots & 0 \\ \hline b & & & & & \\ a & & & & & \\ 0 & & & & & \\ 0 & & & & & \\ \vdots & & & M_{n-5}^{(a,b,c,d,e)} & & \\ 0 & & & & & \end{array}\right|$$

$$+ad \left|\begin{array}{c|cccc} d & e & 0 & 0 & \cdots & 0 \\ \hline b & & & & & \\ a & & & & & \\ 0 & & & & & \\ 0 & & & & & \\ \vdots & & & M_{n-5}^{(a,b,c,d,e)} & & \\ 0 & & & & & \end{array}\right| - bB_{n-2} + cD_{n-3}$$

$$= a^2e^2D_{n-6} - aceD_{n-4} + adB_{n-3} - bB_{n-2} + cD_{n-3}.$$

Then we have:

$$-aeD_{n-2} = -a^3e^3D_{n-6} + a^2e^2cD_{n-4} - a^2edB_{n-3} + aebB_{n-2} - aecD_{n-3},$$

that is,

$$a^2deB_{n-3} - baeB_{n-2} = aeD_{n-2} - a^3e^3D_{n-6} + a^2e^2cD_{n-5} - aecD_{n-3}.$$

Therefore:

$$D_n = cD_{n-1} + (ae - bd)D_{n-2} + (b^2e + ad^2 - 2aec)D_{n-3} + ae(ae - bd)D_{n-4} + a^2e^2cD_{n-5} - a^3e^3D_{n-6}$$

■

Let us consider separately tridiagonal and tetradiagonal Toeplitz matrices although they are particular cases of pentadiagonal Toeplitz matrices.

A $n \times n$ tridiagonal Toeplitz matrix, which we will denote by $M_n^{(a,b,c)}$, is defined by three scalars which are located at the entries

$$m_{i-1,i} = a, \quad m_{i,i} = b, \quad m_{i+1,i} = c$$

which are the only non-null entries in the matrix, that is,

$$M_n^{(a,b,c)} = \begin{pmatrix} b & c & 0 & \cdots & 0 \\ a & b & c & \ddots & \vdots \\ 0 & a & b & \ddots & 0 \\ \vdots & \ddots & \ddots & \ddots & c \\ 0 & \cdots & 0 & a & b \end{pmatrix}. \tag{17}$$

COROLLARY 1.13. *The determinant, D_n, of the n-dimensional Toeplitz tridiagonal matrix, $M_n^{(a,b,c)}$, defined in Equation (17), can be computed by the following recursive formula:*

$$D_n = bD_{n-1} - acD_{n-2}.$$

Proof: It follows from Lemma 1.12 since a tridiagonal matrix is a pentadiagonal matrix with the the entries

$$m_{i-2,i} = 0, \quad m_{i-1,i} = a, \quad m_{i,i} = b, \quad m_{i+1,i} = c, \quad m_{i+1,i} = 0,$$

that is, $M_n^{(a,b,c)} = M_n^{(0,a,b,c,0)}$.

■

LEMMA 1.14. *The determinant of a Toeplitz tridiagonal matrix $M_n^{(a,b,c)}$ is given by the general term*

$$D_n = \frac{1}{2^{n+1}} \frac{\left(b + \sqrt{b^2 - 4ac}\right)^{n+1} - \left(b - \sqrt{b^2 - 4ac}\right)^{n+1}}{\sqrt{b^2 - 4ac}}.$$

REMARK 1.15. *The determinant D_n is a real number. Although $\sqrt{b^2 - 4ac}$ could be a complex number, D_n is real since $D_n = \bar{D_n}$.*

Proof: From Corollary 13 we have the following recursive formula

$$D_n = bD_{n-1} - acD_{n-2}.$$

Then, following the usual method to find the general term of a recursively defined sequence, we consider the solution $D_n = \lambda^n$, and we get the equation:

$$\lambda^n = b\lambda^{n-1} - ac\lambda^{n-2},$$

which is equivalent to

$$\lambda^2 - b\lambda + ac = 0.$$

We solve this equation by obtaining the roots:

$$\lambda = \frac{b \pm \sqrt{b^2 - 4ac}}{2},$$

which could be real or complex.

At this point we must distinguish two cases:

The case $b^2 - 4ac = 0$ which implies an unique solution with multiplicity two, and the case $b^2 - 4ac \neq 0$ which implies two different solutions with multiplicity one.

If $b^2 - 4ac = 0$ then $\lambda = \frac{b}{2}$ with multiplicity 2, so we have to consider the nth term:

$$D_n = \left(\frac{b}{2}\right)^n (A + Bn)$$

with the initial conditions: $D_1 = b$ and $D_2 = b^2 - ac$. Therefore we find the coefficients

$$A = \frac{4ac}{b^2}, \qquad B = 2 - \frac{4ac}{b^2},$$

and then we have

$$D_n = \frac{b^{n-2}}{2^{n-1}}\left(-2ac\,(n-1) + b^2 n\right) \quad \text{if} \quad b^2 - 4ac = 0.$$

If $b^2 - 4ac \neq 0$ the nth term of the sequence is given by:

$$D_n = A\left(\frac{b + \sqrt{b^2 - 4ac}}{2}\right)^n + B\left(\frac{b - \sqrt{b^2 - 4ac}}{2}\right)^n,$$

also with the initial conditions: $D_1 = b$ and $D_2 = b^2 - ac$. So we compute the coefficients

$$A = \frac{1}{2}\left(1 + \frac{b}{\sqrt{b^2 - 4ac}}\right), \quad B = \frac{1}{2}\left(1 - \frac{b}{\sqrt{b^2 - 4ac}}\right)$$

and therefore we conclude that

$$D_n = \frac{1}{2^{n+1}} \frac{\left(b + \sqrt{b^2 - 4ac}\right)^{n+1} - \left(b - \sqrt{b^2 - 4ac}\right)^{n+1}}{\sqrt{b^2 - 4ac}} \quad \text{if} \quad b^2 - 4ac \neq 0.$$

■

A tetradiagonal Toeplitz matrix, which we will denote by $M_n^{(a,b,c,d)}$, is defined by four scalars which are located at the entries

$$m_{i-1,i} = a, \quad m_{i,i} = b, \quad m_{i+1,i} = c, \quad m_{i+2,i} = d$$

which are the only non-null entries in the matrix, that is,

$$M_n^{(a,b,c,d)} = \begin{pmatrix} b & c & d & 0 & \cdots & 0 & 0 & 0 \\ a & b & c & d & 0 & \cdots & 0 & 0 \\ 0 & a & b & c & d & 0 & \cdots & 0 \\ \vdots & \ddots & \ddots & \ddots & \ddots & \ddots & \ddots & \vdots \\ 0 & \cdots & 0 & a & b & c & d & 0 \\ 0 & 0 & \cdots & 0 & a & b & c & d \\ 0 & 0 & 0 & \cdots & 0 & a & b & c \\ 0 & 0 & 0 & 0 & \cdots & 0 & a & b \end{pmatrix}. \tag{18}$$

Corollary 1.16. *The determinant, D_n, of the n-dimensional Toeplitz tetradiagonal matrix, $M_n^{(a,b,c,d)}$, defined in (18), can be computed by the following recursive formula:*

$$D_n = bD_{n-1} - acD_{n-2} + a^2 dD_{n-3}, \tag{19}$$

Proof: It follows from Lemma 1.12 since a tetradiagonal matrix is a pentadiagonal matrix with the the entries

$$m_{i-2,i} = 0, \quad m_{i-1,i} = a, \quad m_{i,i} = b, \quad m_{i+1,i} = c, \quad m_{i+1,i} = d,$$

that is, $M_n^{(a,b,c,d)} = M_n^{(0,a,b,c,d)}$.

■

The determinant of a Toeplitz tridiagonal matrix can be represented by a second-order recursive formula, and therefore its general term can be obtained after computing the solutions of a quadratic equation.

On the other hand, the determinant of a Toeplitz tetradiagonal matrix is represented by a third-order recursive formula, as we have seen in the previous corollary. Hence, its general term could also be computed in terms of the solutions of a third-degree equation. But we do not give it here because it is defined by a large expression.

However, the determinant of a Toeplitz pentadiagonal matrix is provided by our sixth-order recursive formula or by Sweet's fifth-order formula, see [**41**]. Therefore, since it is impossible to compute in general the roots of a degree 5 or 6 polynomial equation in a single variable, a formula cannot be given for the corresponding general terms.

4.1. Comparison with other recursive relations for the Determinant of a Pentadiagonal Matrix. Since pentadiagonal matrices occur frequently in boundary value problems involving fourth-order derivatives, there are some results in the literature which approach the problem of computing their determinant in order to develop a good method for determining their eigenvalues. With this aim a recursive equation relating leading principal minors for pentadiagonal matrices was developed in [**41**]. The result is the following:

THEOREM 1.17. [**41**] *Given a pentadiagonal matrix, not necessarily Toplitz matrix,* $S = \{s_{i,j}\}_{i,j=0}^{n}$, *where it is assumed that*

$$\begin{aligned} s_{i,j} &= 0 \qquad if \quad |i-j| > 2 \\ s_{i,j} &\neq 0 \qquad if \quad |i-j| = 1, \end{aligned}$$

defining the quantities

$$\begin{array}{ll} a_i = s_{i,i} & i = 1, 2, ..., n-1, n-2, n \\ b_i = s_{i,i+1}s_{i+1,i} & i = 1, 2, ..., n-2, n-1 \\ \beta_i = s_{i,i+2}s_{i+2,i} & i = 1, 2, ..., n-2 \\ c_i = s_{i,i+1}s_{i+1,i+2}s_{i+2,i} & i = 1, 2, ..., n-2 \\ c_i^t = s_{i+1,i}s_{i+2,i+1}s_{i,i+2} & i = 1, 2, ..., n-2 \end{array}$$

the following algorithm allows the computation of the determinant $D_n = |S|$*:*

Set $D_{-1} = 0$, $D_0 = 1$, $D_1 = a_1$, $D_2 = a_1a_2 - b_1$, $\epsilon_{-1} = e_{-1} = 0$, $D_{-1} = 0$, *and compute*

$$\begin{aligned}\delta_{k-2} &= a_{k-1}D_{k-3} - \beta_{k-3}D_{k-4},\\ \epsilon_{k-3} &= D_{k-3} - \frac{c^t_{k-3}}{b_{k-2}}e_{k-4},\\ e_{k-3} &= D_{k-3} - \frac{c_{k-3}}{b_{k-2}}\epsilon_{k-4}.\end{aligned} \tag{20}$$

Then

$$D_k = a_kD_{k-1} - b_{k-1}D_{k-2} - \beta_{k-2}\delta_{k-2} + c_{k-2}\epsilon_{k-3} + c^t_{k-2}e_{k-3} \tag{21}$$

for $k = 3, 4, ..., n$.

Moreover, in the same reference a 6-term recursive relation for the determinant of a particular pentadiagonal matrix can also be found. The recursive rule holds for cyclically symmetric matrices, i.e., such that $c_i = c^t_i$, for $i = 1, 2, ..., n-2$. If S is cyclically symmetric then

$$\begin{aligned}D_k = &\left(a_k - \frac{c_{k-2}}{b_{k-2}}\right)D_{k-1} - \left(b_{k-1} - \frac{a_{k-1}c_{k-2}}{b_{k-2}}\right)D_{k-2} - \left(\beta_{k-2}a_{k-1} - c_{k-2}\right)D_{k-3}\\ &+ \beta_{k-3}\left(\beta_{k-2} - \frac{a_{k-1}c_{k-2}}{b_{k-2}}\right)D_{k-4} + \left(\frac{\beta_{k-3}\beta_{k-4} - c_{k-2}}{b_{k-2}}\right)D_{k-5}.\end{aligned} \tag{22}$$

If S is a symmetric matrix, then it is cyclically symmetric, so (22) holds for symmetric matrices.

In the next chapter we will need to prove the nonsingularity of a concrete Toeplitz pentadiagonal matrix. Let us remark now that this matrix, that will be studied in Theorem 1.3, is cyclically symmetric, since $c_i = c^t_i = 64$. Therefore the 6-term recursive relation given in Equation (22), which in this particular case is:

$$D_k = 6D_{k-1} - 16D_{k-2} + 32D_{k-3} - 48D_{k-4} + 32D_{k-5},$$

could be used, in Theorem 1.3, in order to prove that the Toeplitz pentadiagonal matrix under study is non singular. Nevertheless we will do it using our recursive relation, in Equation (16), which is given for this particular matrix in Equation (24). In fact, both recursive relations have the same general nth-term.

The reason why we choose to use our formula, Equation (16), in the mentioned proof, even when Sweet's formula has the benefit being 6-term recursive instead of 7-term, is is as follows: The 7-term recursive formula, Equation (16), we give in Lemma 1.12 holds for the general case of Toeplitz pentadiagonal matrices, including both non symmetric and non cyclically symmetric matrices.

Therefore while the determinant of *any* Toeplitz pentadiagonal matrix could be computed by means of the 7-term recursive formula given in Equation (24), the simpler 6-term formula (22) only holds for cyclically symmetric matrices, so for any other kind of pentadiagonal

matrix the general algorithm, given in Equation (21), should be the only way to compute the determinant proposed in [**41**].

This algorithm holds in general, but it has the problem of its complexity due to the recursivity of the coefficients ϵ_k and e_k, in Equation (20). In fact, in the cited article R. A. Sweet states that a 7-term recursive relation may be derived for a non cyclically symmetric matrix. This relation would eliminate the factors ϵ_k and e_k, but he did not put it forward since he thought it was too complicated.

5. Constructing triangular Bézier surfaces from what are almost two boundary curves

Now, as we have said previously, we will perform another choice of the subset of control points, which we assume to be prescribed, in order to build the associated harmonic surface. The set of fixed control points, from which we will determine the associated harmonic Bézier triangle, should describe as much as possible the shape of the surface that will be obtained. Because of this, an appropriate choice would be two rows of border control points describing two of the border curves of the surface. But for this case the harmonic condition do not determine a triangular Bézier surface. An incompatible system is obtained if we consider two lines of border control points as preset information and the rest of control points as variables.

We will therefore consider a similar set of control points as known points, since they will also provide information about the shape of the border curves of the desired surface. We will consider two border lines of control points with the exception of some of them which will be replaced by their neighboring control points. The choice of using neighboring points to substitute the excluded border points stems from the fact that they are closer to the boundary, so they can give better information about the desired shape of the surface.

The following theorem allows us to state that, given some border control points and a few interior control points the harmonic condition univocally determines the surface.

THEOREM 1.18. *Let $\overrightarrow{x}(u,v) = \sum_{|I|=n} P_I B_I^n(u,v)$ be a harmonic triangular Bézier surface with control net $\{P_I\}_{|I|=n}$. Then, given the border points in the first row $\{P_{0,n-i,i}\}_{i=0}^n$, the points in the diagonal border row $\{P_{i,n-i,0}\}_{i=0}^n$ with $i \neq 4k$ and including the corresponding neighboring points $\{P_{i-1,n-i,1}\}$ when $i = 4k$, the harmonic triangular control net is totally determined.*

Proof: The proof of this result is analogous to the previous proof of Theorem 1.9. As before, we will prove the solvability of the linear system obtained by considering the harmonicity condition (11), for any pair k, l, but now looking for a solution in terms of the border points in the rows $\{P_{0,j,n-j}\}_{j=0}^n$ and $\{P_{i,n-i,0}\}_{i=0}^n$, in addition to some points $\{P_{i-1,n-i,1}\}$ for the values $i = 4k$, which we suppose are known. As before, we split the linear system in subsystems.

Bearing scheme (13) in mind, and starting from the right corner, we have that there are no unknown points in either the nth column or the column that follows it, $n-1$.

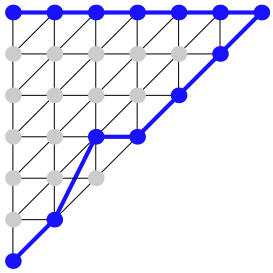

FIGURE 6. Compare this schematic grid of control points with the one corresponding to Theorem 1.9 in Figure 9. The blue dots are known and the gray would be obtained by asking for harmonicity.

When we consider the $n-2$ column, the unknown point is $P_{1,n-2,1}$, and Equation (11) with $k=0, l=n-2$:

$$2\,P_{0,n-2,2} - 2\,(P_{1,n-2,1} + P_{0,n-1,1}) + P_{2,n-2,0} + P_{0,n,0} = 0,$$

determines it. This equation is the first subsystem we consider.

The second subsystem appears when we consider the $n-3$ column, that is, the harmonicity condition for $k=0, l=n-3$ and $k=1, l=n-3$:

$$\begin{cases} 2\,P_{0,n-3,3} - 2\,(P_{1,n-3,2} + P_{0,n-2,2}) + P_{2,n-3,1} + P_{0,n-1,1} = 0 \\ 2\,P_{1,n-3,2} - 2\,(P_{2,n-3,1} + P_{1,n-2,1}) + P_{3,n-3,0} + P_{1,n-1,0} = 0. \end{cases}$$

At this step we have two unknown points, $P_{1,n-3,2}$ and $P_{2,n-3,1}$, which are also determined by the equations above in terms of some of the prescribed control points.

One column forward something different happens, namely, we find an incompatible system. At the $n-4$ column, corresponding to the indexes $k=0, l=n-4$; $k=1, l=n-4$ and $k=2, l=n-4$ we have the equations:

$$\begin{cases} 2\,P_{0,n-4,4} - 2\,(P_{1,n-4,3} + P_{0,n-3,3}) + P_{2,n-4,2} + P_{0,n-2,2} = 0, \\ 2\,P_{1,n-4,3} - 2\,(P_{2,n-4,2} + P_{1,n-3,2}) + P_{3,n-4,1} + P_{1,n-2,1} = 0, \\ 2\,P_{2,n-4,2} - 2\,(P_{3,n-4,1} + P_{2,n-3,1}) + P_{4,n-4,0} + P_{2,n-2,0} = 0. \end{cases}$$

Since we consider the control points in column $n-4$: $P_{1,n-4,3}$, $P_{2,n-4,2}$ and $P_{3,n-4,1}$, to be variables, the coefficient matrix is a tridiagonal Toeplitz matrix, $M_3^{(2,-2,1)}$, which has null determinant:

$$D_3 = \det M_3^{(2,-2,1)} = \begin{vmatrix} -2 & 1 & 0 \\ 2 & -2 & 1 \\ 0 & 2 & -2 \end{vmatrix} = 0.$$

Therefore, the subsystem corresponding to column $n-4$, has no solution.

If we continue this process by columns, we can observe that, in each column, we find a subsystem of linear equations which has an associated coefficient matrix that is a Toeplitz

tridiagonal matrix, $M_m^{(2,-2,1)}$. With this notation let us consider the determinant of order m:

$$D_m = \det M_m^{(2,-2,1)} = \begin{vmatrix} -2 & 1 & 0 & 0 & 0 & \cdots & 0 \\ 2 & -2 & 1 & 0 & 0 & \cdots & 0 \\ 0 & 2 & -2 & 1 & 0 & \cdots & 0 \\ 0 & 0 & 2 & -2 & 1 & \cdots & \vdots \\ 0 & 0 & 0 & 2 & -2 & \ddots & 0 \\ \vdots & \vdots & \vdots & \ddots & \ddots & \ddots & 1 \\ 0 & 0 & 0 & ... & 0 & 2 & -2 \end{vmatrix}.$$

From Corollary 13 we have a recursive rule to compute this determinant. For our convenience we perform some transformations of this recursive rule

$$\begin{aligned} D_m &= -2D_{m-1} - 2D_{m-2} = -2\left(-2D_{m-2} - 2D_{m-3}\right) - 2\left(-2D_{m-3} - 2D_{m-4}\right) \\ &= 4D_{m-2} + 8D_{m-3} + 4D_{m-4} = 4\left(-2D_{m-3} - 2D_{m-4}\right) + 8D_{m-3} + 4D_{m-4} = -4D_{m-4}. \end{aligned}$$

Therefore we can say $D_m = -4D_{m-4}$, where the first four determinants are $D_1 = -2$, $D_2 = 2$, $D_3 = 0$ and $D_4 = -4$, so we will find some null determinants since $D_3 = 0$. At each value $m = 3 + 4k$ we will find an incompatible system which will turn into a determined compatible system by considering a different set of unknown points in the corresponding columns. That is, if we were dealing with the column $n - i$ and it had $m = 3 + 4k$ variables then we would consider the border point, $P_{i,n-i,0}$, as a variable and instead we would suppose its neighboring point, $P_{i-1,n-i,1}$, to be known.

Taking into account the previous variation of the set of variables, the corresponding coefficient matrix is now given by:

$$N_{3+4k} = \begin{pmatrix} -2 & 1 & 0 & 0 & 0 & \cdots & 0 \\ 2 & -2 & 1 & 0 & 0 & \cdots & 0 \\ 0 & 2 & -2 & 1 & 0 & \cdots & 0 \\ 0 & 0 & 2 & -2 & 1 & \ddots & \vdots \\ \vdots & \vdots & \vdots & \ddots & \ddots & \ddots & 0 \\ 0 & 0 & 0 & 0 & 2 & -2 & 0 \\ 0 & 0 & 0 & ... & 0 & 2 & 1 \end{pmatrix}.$$

where it can be observed that the last column contains $P_{i,n-i,0}$ coefficients. This point is only involved in the last equation so it implies the values in this column to be $(0, ..., 0, 1)^T$.

Thus, if we compute its determinant using expansion by minors, in particular through the last column, we find that $|N_{3+4k}| = |M_{3+4k-1}| = D_{4k+2}$ which is not null, as we have already said.

Therefore, we can now state that we will find a compatible determinate subsystem for each column, and from this we can ensure the solvability of the global linear system. Therefore a

control net can be determined in order to get a harmonic chart in terms of the border points in the first row $\{P_{0,n-i,0}\}_{i=0}^{n}$, the points in the diagonal border row $\{P_{i,n-i,0}\}_{i=0}^{n}$ excluding the points with $i = 4k$, and, instead, including the points $\{P_{4k-1,n-4k,1}\}$.

■

The following figures show, for $n = 4$, some harmonic surfaces obtained through Theorem 1.18 when the blue points are given.

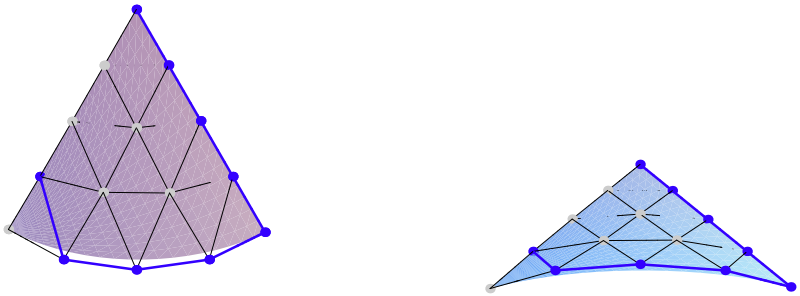

FIGURE 7. Two views of a harmonic surface of degree $n = 4$, similar to a cone, determined by a set of control points placed, with the exception of one of them, on a straight line and in a circular arc.

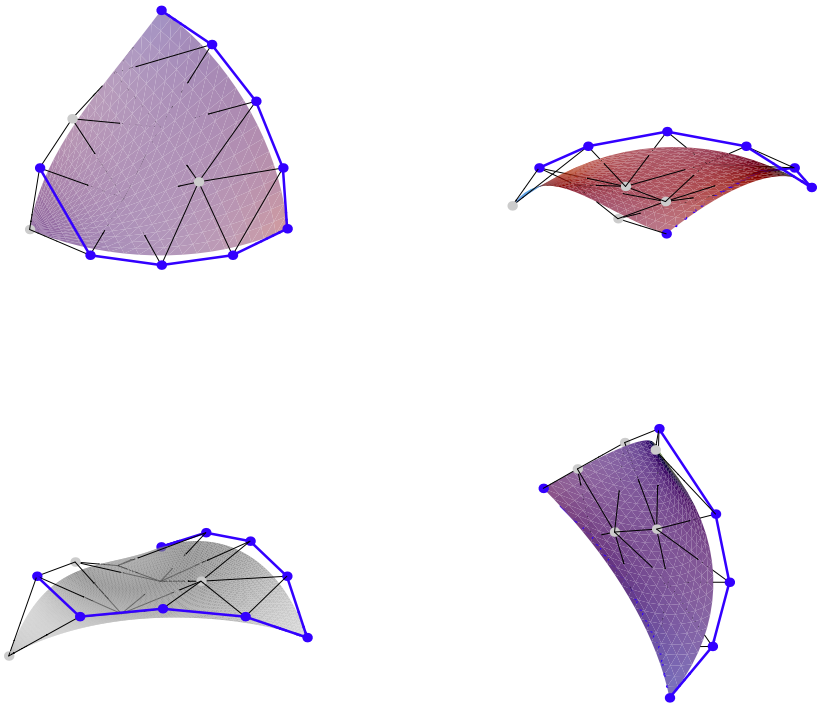

FIGURE 8. Four different points of view of a triangular Bézier surface looking like a piece of a sphere. The known control points in blue are equally spaced on two circular arcs.

The following figures show, for $n = 6$, some harmonic surfaces obtained through Theorem 1.18 when the blue points are given. These examples will show how Theorem 1.18 provides us with a better control of the shape of the harmonic surface than Theorem 1.9. This improvement is obtained because in Theorem 1.18 the prescribed data are border control points which give more information on the desired shape of the surface.

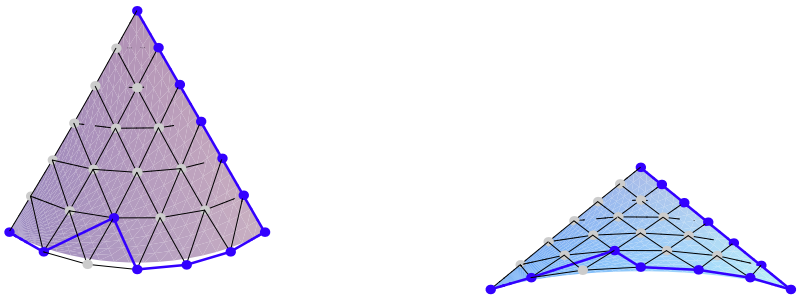

FIGURE 9. Two views of the harmonic surface, similar to a piece of cone, determined by a set of control points placed, with the exception of one of them, along a straight line and along a circular arc.

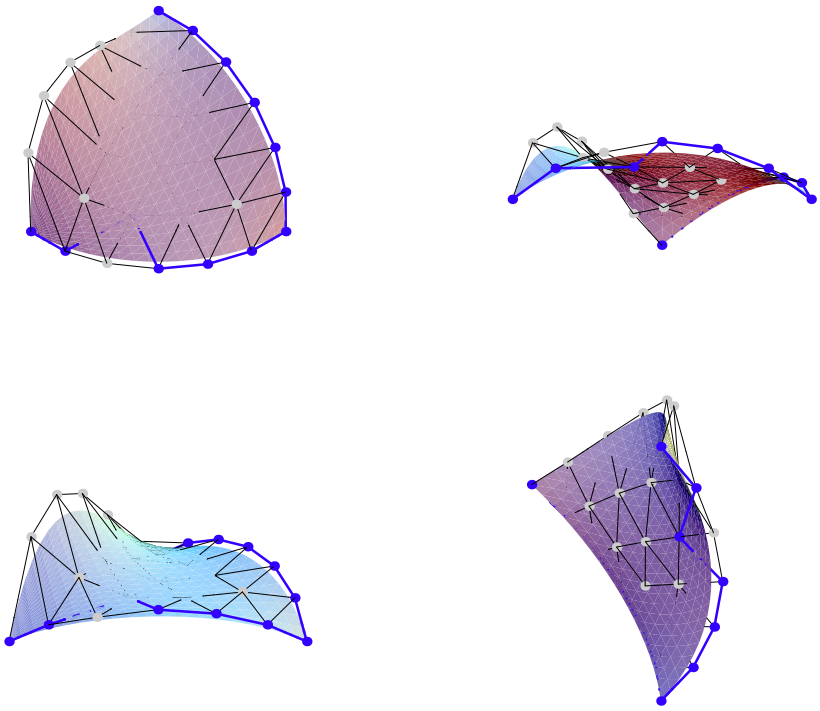

FIGURE 10. Four different points of view of a triangular surface looking like a piece of a sphere. The known control points are equally spaced on two circular arcs. It can be seen that the control over the shape of the surface is improved if we compare with the corresponding example for Theorem 1.9, in Figure 3.

6. Conclusions

In this chapter we have given two different methods for generating harmonic surfaces from a prescribed set of control points.

In our first method, in Theorem 1.9, the prescription of a boundary curve and the tangent plane along it, that is, two rows of control points, gave us good results for low degrees but we ran into some trouble when the degree of the Bézier surface was increased. Since one of the corners of the surface is out of control it could diverge from the desired shape.

In Theorem 1.18 we propose a second method in order to solve this lack of control. Instead of prescribing two parallel rows of control points we prescribed a set of control points that were as similar as possible to prescribing two boundary curves. This gave us better control over the shapes obtained. The surfaces we obtained by this method provided an appropriate description of the behavior of the initial information.

The Laplace equation is a second-order PDE and we find that a harmonic surface is totally determined after the prescription of two lines of control points. Increasing the PDE order would enable us to prescribe a bigger set of control points and therefore to gain better control over the surface, although it would reduce degrees of freedom. So, in the next chapter we will study the biharmonic equation, a fourth-order PDE.

CHAPTER 2

Constructing triangular Bézier surfaces using linear PDEs: Biharmonic surfaces

In this chapter we present some results concerning with biharmonic triangular Bézier surfaces, that is, those Bézier triangles verifying $\Delta^2 \overrightarrow{x} = 0$, where Δ^2 is the biharmonic operator also known as the bilaplacian. There are many mathematical and engineering approaches to solve the biharmonic problem in a rectangle, and a extensive description of the long history of this classical problem can be found in [**27**].

The biharmonic equation is associated with a great variety of physical problems such as tension in elastic membranes and the study of stress and strain in physical structures. There are many mechanical problems concerning the bending of a thin elastic clamped rectangular plate, and they can all be formulated in terms of a two-dimensional biharmonic equation with prescribed values of the function and its normal derivative at the boundary. Hence, the biharmonic boundary problem is also known as the thin plate problem.

From a geometric design point of view, which is our field of interest, this operator has found its way into various areas of application, such as surface design, geometric mesh, smoothing and fairing. From this background let us refer to Bloor and Wilson's PDE method for intuitive shape generation, based on the solution of the biharmonic PDE with appropriately chosen boundary conditions, see [**7**], [**42**] and [**43**]. We also take note of the work by Schneider and Kobbelt and others on geometric mesh fairing, see [**25**], [**38**] and [**39**], where the properties of the bilaplacian operator are used to fair triangular meshes.

As we have said previously, a fundamental result from the theory of minimal surfaces states that, under certain conditions, given the boundary, there is a unique minimal surface prescribed by that boundary. It is noteworthy that a similar result for rectangular Bézier surfaces can be found in [**31**], where it is shown that the knowledge of the boundary of a biharmonic Bézier rectangle fully determines the entire surface. Therefore, our first idea is to study whether the biharmonic condition implies that the interior control points of a triangular Bézier surface can be expressed as a linear combination of boundary control points, as happens in the rectangular case. We will see how things change for triangular Bézier patches.

1. The biharmonic condition

Following a similar path to that taken in the harmonic case, we look for the conditions that the control points of a triangular Bézier surface must fulfill in order to be associated to

a biharmonic patch. Thus, let us compute the bilaplacian of the parametrization:

$$\Delta^2 \overrightarrow{x}(\mathbf{u}) = \left(\frac{\partial^2}{\partial u^2} + \frac{\partial^2}{\partial v^2}\right)^2 \overrightarrow{x}(\mathbf{u}) = \left(\frac{\partial^4}{\partial u^4} + 2\frac{\partial^4}{\partial u^2 v^2} + \frac{\partial^4}{\partial v^4}\right) \sum_{|I|=n} P_I B_I^n(\mathbf{u})$$

$$= n(n-1)(n-2)(n-3) \sum_{|I|=n-4} \left(\Delta^{4,0} P_I + 2\Delta^{2,2} P_I + \Delta^{0,4} P_I\right) B_I^{n-4}(\mathbf{u})$$

$$= \sum_{|I|=n-4} Q_I B_I^{n-4}(\mathbf{u})$$

where

$$\begin{aligned} Q_I = \frac{n!}{(n-4)!}(&P_{I+4e_1} - 4P_{I+3e_1+e_3} + 8P_{I+2e_1+2e_3} - 8P_{I+e_1+3e_3} + 4P_{I+4e_3} \\ &+2P_{I+2e_1+2e_2} - 4P_{I+e_1+2e_2+e_3} + 8P_{I+2e_2+2e_3} - 4P_{I+2e_1+e_2+e_3} \\ &+8P_{I+e_1+e_2+2e_3} - 8P_{I+e_2+3e_3} - 4P_{I+3e_2+e_3} + P_{I+4e_2}). \end{aligned}$$

It can be seen that $\Delta^2 \overrightarrow{x}(\mathbf{u})$ is also a Bézier surface with control points $\{Q_I\}_{|I|=n-4}$, thus, as in the harmonic case and due to the fact that $\{B_I^{n-4}(\mathbf{u})\}_{|I|=n-4}$ is a basis, we get that $\overrightarrow{x}$ is a biharmonic chart iff $Q_I = 0$ for all $|I| = n-4$. Moreover,

REMARK 2.1. *Equivalently, a triangular Bézier patch is biharmonic iff its associated control net verifies:*

$$0 = (\Delta^{4,0} + 2\Delta^{2,2} + \Delta^{0,4}) P_{k,l,n-k-l},$$

that is, if and only if

$$\begin{aligned} 0 =& P_{k+4,l,n-k-l-4} - 4P_{k+3,l,n-k-l-3} + 8P_{k+2,l,n-k-l-2} - 8P_{k+1,l,n-k-l-1} \\ &+ 4P_{k,l,n-k-l} + 2P_{k+2,l+2,n-k-l-4} - 4P_{k+1,l+2,n-k-l-3} + 8P_{k,l+2,n-k-l-2} \\ &- 4P_{k+2,l+1,n-k-l-3} + 8P_{k+1,l+1,n-k-l-2} - 8P_{k,l+1,n-k-l-1} - 4P_{k,l+3,n-k-l-3} \\ &+ P_{k,l+4,n-k-l-4} \qquad \forall k, l \geq 0. \end{aligned} \tag{23}$$

2. Constructing triangular Bézier surfaces from four lines of control points

There exist different representations of general solutions to the biharmonic equation, here we will determine a polynomial solution of this problem. The following result states that a biharmonic triangular Bézier surface is completely determined by the first four rows of control points starting from one side.

THEOREM 2.2. *Let $\overrightarrow{x}(u,v) = \sum_{|I|=n} P_I B_I^n(u,v)$ be a biharmonic triangular Bézier surface of degree $n \geq 4$ with control net $\{P_I\}_{|I|=n}$, then the whole control net is determined by the first four rows of control points $\{P_{i,j,n-i-j}\}_{j=0}^n$ where $i = 0,1,2,3$.*

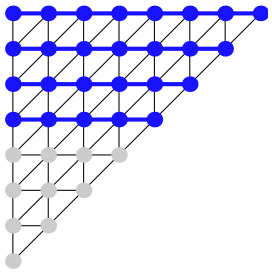

FIGURE 1. As in the harmonic case we show a schematic grid of control points where the blue are known and the gray would be obtained by asking the chart to be biharmonic.

Proof: The proof of this result is analogous to the previous proofs of Theorems 2.9 and 2.18. We will prove the solvability of the linear system that is obtained when the biharmonic condition, in Equation (23), is considered for all k, l. As before, we will prove that the system has a solution by splitting it into some solvable subsystems of linear equations. Any linear subsystem includes some control points in the first four rows which are known by hypothesis, and some of the other control points in the control net, which are the variables.

So, having scheme (13) in mind again, and starting from the right corner column, as we did before, we have that now we do not find any unknown points in the first four columns. It is in the fifth column from the right, that is for $k = 0, l = n - 4$, that we find the first unknown point, $P_{4,n-4,0}$. Then the biharmonic condition, given in Equation (23):

$$\begin{aligned} 0 =& P_{4,n-4,0} - 4P_{3,n-4,1} + 8P_{2,n-4,2} - 8P_{1,n-4,3} + 4P_{0,n-4,4} + 2P_{2,n-2,0} \\ & -4P_{1,n-2,1} + 8P_{0,n-2,n+2} - 4P_{2,n-3,1} + 8P_{1,n-3,2} - 8P_{0,n-3,3} - 4P_{0,n-1,1} + P_{0,n,0}, \end{aligned}$$

determines it.

Next we would consider the relations for $k = 0, l = n-5$ and $k = 1, l = n-5$. As before, both equations determine univocally, in terms of points in the first four rows, the pair of unknown points in this step which are $P_{4,n-5,1}$ and $P_{5,n-5,0}$.

Therefore, if we continue this process by columns, we have that, taking as variables the points $\{P_{i,j,n-i-j}\}_{i=4,j=0}^{n,n-i}$, the corresponding system of linear equations in each column has a coefficient matrix associated to it defined by:

$$a_{i,i} = 1, \quad a_{i+1,i} = -4, \quad a_{i+2,i} = 8 \quad a_{i+3,i} = -8 \quad a_{i+4,i} = 4.$$

This is a triangular matrix with 1 in the diagonal so its determinant is equal to one.

Therefore, a biharmonic control net can be totally determined by the first four rows of the control net.

■

The following figures show some biharmonic surfaces obtained by means of Theorem 2.2.

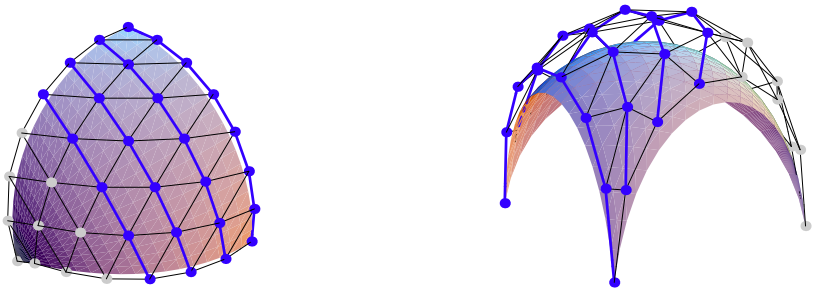

FIGURE 2. A pair of biharmonic Bézier triangles obtained by Theorem 2.2. By hypothesis the four lines of blue points are known and the grey points are determined by the biharmonicity condition (23). Notice that "good" results are obtained. The shapes seem to be desirable from a designer point of view. As stated by Farin and Hansford in [**14**], "good" refers to the traditional designers' paradigm that the interior of a surface should not have different shape characteristics to those implied by the boundary curves.

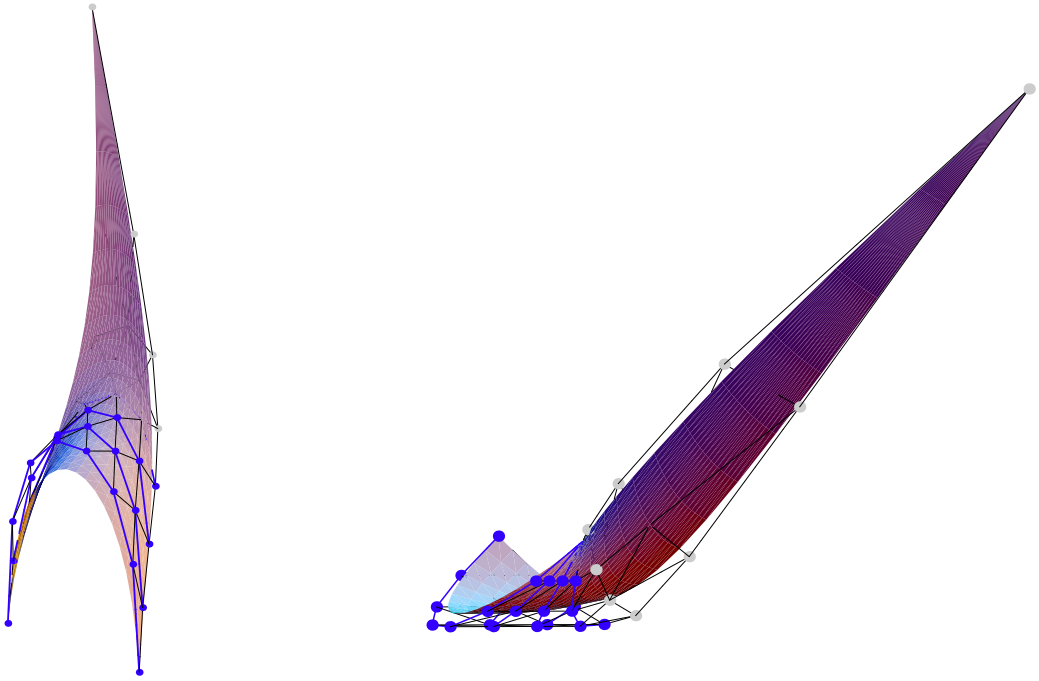

FIGURE 3. Two more biharmonic Bézier surfaces obtained by Theorem 2.2. As can be seen, some initial conditions, the four lines of control points chosen as known points, do not give good shapes. Here, one of the three corners of the surface is not under control, in the next section we will give a solution to this problem.

3. Constructing triangular Bézier surfaces from two boundary curves and the normal derivatives along them

Now, in a similar way to the harmonic case, we will consider the boundary value problem:

$$\Delta^2 \overrightarrow{x}(u,v) = 0 \qquad \begin{cases} \overrightarrow{x}(0,v) = \alpha(v) \\ \overrightarrow{x}_u(0,v) = \beta(v) \end{cases} \qquad \begin{cases} \overrightarrow{x}(1-v,v) = \gamma(v) \\ \overrightarrow{x}_u(1-v,v) = \delta(v). \end{cases}$$

So, we will consider the PDE given by the biharmonic operator with Cauchy boundary conditions. We prescribe the value of the solution along two border curves, $\overrightarrow{x}(0,v)$ and $\overrightarrow{x}(1-v,v)$, and its partial derivatives, $\overrightarrow{x}_u(0,v)$ and $\overrightarrow{x}_u(1-v,v)$, which fix the tangent planes to the surface along the given border curves. This problem can be written, as before, in terms of control points of a Bézier surface: Find the biharmonic surface completely determined by a pair of border lines of control points and its corresponding neighboring lines on the triangular grid. This is what we prove in the following theorem.

THEOREM 2.3. *Let $\overrightarrow{x}(u,v) = \sum_{|I|=n} P_I B_I^n(u,v)$ be a biharmonic triangular Bézier surface with control net $\{P_I\}_{|I|=n}$, then given the points in the first and second rows ($\{P_{0,n-i,0}\}_{i=0}^{n}$ and $\{P_{1,n-i,0}\}_{i=0}^{n-1}$), and the points in the diagonal border row $\{P_{i,n-i,0}\}_{i=0}^{n}$ and its neighbor row $\{P_{i,n-i-1,1}\}_{i=0}^{n}$, the whole biharmonic triangular control net is totally determined.*

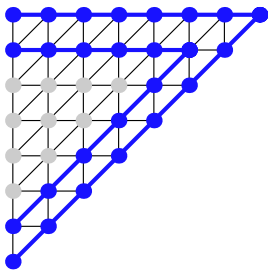

FIGURE 4. The schematic grid of control points corresponding with Theorem 2.3.

Proof: As we did in Theorem 2.2, we consider the linear system given by the set of conditions that a control net must fulfill in order to be associated to a biharmonic chart. Thus, this system is composed of the biharmonicity condition (23) for all pair of indexes k, l. In order to prove the existence of a biharmonic solution of the system, having scheme (13) in mind again, we consider the corresponding subsystem for each column. Then we find that the coefficient matrices corresponding to each subsystem are the Toeplitz pentadiagonal matrices:

$$M_n^{(4,-8,8,-4,1)}.$$

Then, from Lemma 1.12 we have that the determinant of this matrix can be defined by the recursive formula:

$$D_n = 8D_{n-1} - 28D_{n-2} + 64D_{n-3} - 112D_{n-4} + 128D_{n-5} - 64D_{n-6}. \tag{24}$$

We will compute the general term of the sequence $\{D_n\}_{n=0}^{\infty}$. Following the well known method to obtain the nth term of recursive equations we must solve the equation:

$$\lambda^6 - 8\lambda^5 + 28\lambda^4 - 64\lambda^3 + 112\lambda^2 - 128\lambda + 64 = (\lambda - 2)^4 \left(\lambda^2 + 4\right) = 0$$

obtaining three different solutions:

$$\lambda_1 = 2, \quad \text{with multiplicity } 4, \quad \lambda_2 = 2\mathbf{i} \quad \text{and} \quad \lambda_3 = -2\mathbf{i}.$$

Therefore, the general term of the sequence is given by the formula:

$$D_n = 2^n \left(A + Bn + Cn^2 + Dn^3 + E\mathbf{i}^n + F(-\mathbf{i})^n\right),$$

and we would finally obtain the coefficients by considering the initial conditions:

$$D_1 = 2^3 \quad D_2 = 2^5 \quad D_3 = 3 \cdot 2^5 \quad D_4 = 17 \cdot 2^4 \quad D_5 = 3 \cdot 2^8 \quad D_6 = 2^{11}.$$

Therefore

$$D_n = 2^n \left(\frac{3}{2} + 2n + \frac{1}{2}n^2 - \frac{1}{4}\left(\mathbf{i}^n + (-\mathbf{i})^n\right)\right) = 2^{(n-1)}(3 + 4n + n^2 - \cos(\frac{n\pi}{2}))$$

$$D_n \geq 2^{(n-1)}(2 + 4n + n^2) \geq 0.$$

And the system has unique solution.

■

REMARK 2.4. *An analogous result could be stated to build a biharmonic surface constrained by a similar configuration of prescribed control points. For example, we could prescribe the lines of border control points* $\{P_{0,i,n-i}\}_{i=0}^{n}$ *and* $\{P_{i,0,n-i}\}_{i=0}^{n}$*, and their respective neighboring lines of points on the control net. The proof of this result would be analogous to the previous one, that is, instead of considering the subsystem of linear equations associated to each column of control points, the system associated to each diagonal line should be considered, see scheme (13).*

The following figures show some biharmonic surfaces obtained by means of Theorem 2.3

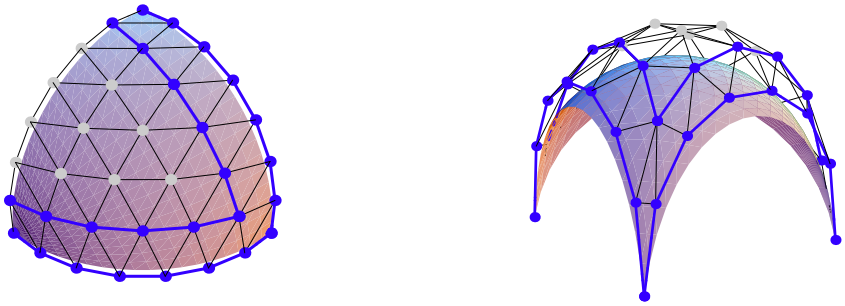

FIGURE 5. A pair of biharmonic Bézier triangles obtained by Theorem 2.3. By hypothesis the four lines of blue points are known and the grey points are determined by the biharmonicity condition (23). It can be seen that, as in the analogous examples for Theorem 2.2, good shapes are obtained.

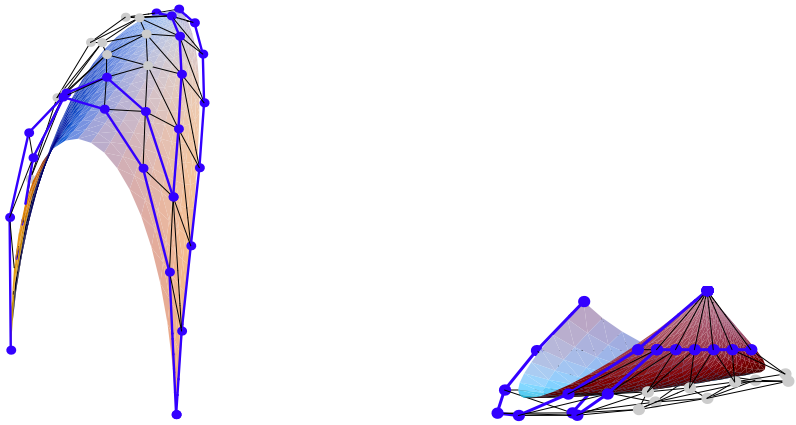

FIGURE 6. Here we have two more biharmonic surfaces obtained by means of Theorem 2.3. Now we can observe the improvement in the shapes obtained in comparison to Figure 2.

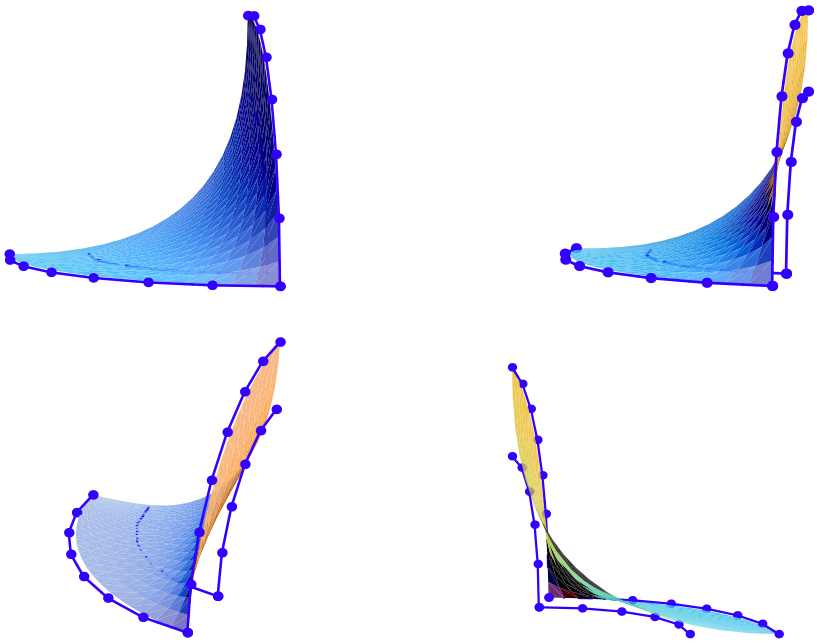

FIGURE 7. Four different points of view of the biharmonic surface obtained thanks to Theorem 2.3. The set of known control points, in blue, are located along two concentric and parallel circular arcs contained in two orthogonal planes.

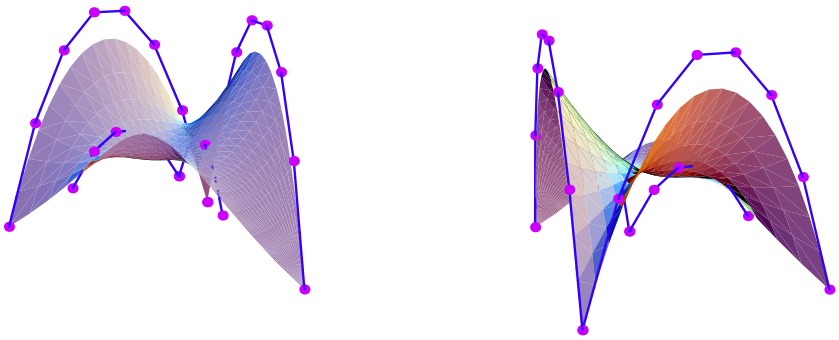

FIGURE 8. Two views of a biharmonic surface obtained by Theorem 2.3. The set of known control points, in blue, are located along four parabolas.

4. Conclusions

For rectangular Bézier surfaces it was proved in [**31**] that the knowledge of the boundary of a biharmonic Bézier rectangle fully determines the entire surface. Here we have conducted an analogous study of the biharmonic equation and we have obtained that, in general, this is not true for triangular Bézier patches.

In this chapter we have given two methods with which to generate biharmonic surfaces. We have seen that when a fourth-order PDE, as the biharmonic equation, is considered, four lines of control points must be known in order to ensure that a biharmonic surface is totally

determined. So, the set of boundary control points (just three lines) does not give us enough information to determine a biharmonic surface.

In the first method, Theorem 2.2, we have described the way to generate a biharmonic surface given the first four rows of control points. The prescription of these rows left one corner of the control net free, and, as happened before with the harmonic condition, it can sometimes produce unwanted shapes.

Our second method, in Theorem 2.3, increased the control over the surface shape. The prescription of two boundary curves and the tangent planes along them improved our results. If the first and the second row and the points in the diagonal border row and their neighbors are prescribed, only the central control points of one of the boundary curves are free. Note that the three vertices and the tangent planes on them are now prescribed and the boundary curves are almost under control. As a consequence better results are obtained with this method.

CHAPTER 3

Coons patches

One of the oldest surface problems in CAGD is the following: given the boundary curves, find the parametric surface $\overrightarrow{x}$ with these as boundary curves with no other restriction. A popular solution of this problem is the Coons patch.

Before we present our study about triangular Coons patches, let us describe the more conventional rectangular Coons patch and its properties.

1. Background on Coons rectangular patches

Coons first described this type of interpolant in [**10**]. It is assumed that four boundary curves are given, which it is convenient to think of as coming from a surface denoted $\overrightarrow{x_0}$, and so the notation $\overrightarrow{x_0}(u,0)$, $\overrightarrow{x_0}(u,1)$, $\overrightarrow{x_0}(0,v)$ and $\overrightarrow{x_0}(1,v)$ is used to represent these boundary curves. The bilinearly blended Coons patch that interpolates to the given boundary curves is defined by:

$$\overrightarrow{x}(u,v) = (1-u)\,\overrightarrow{x_0}(0,v) + u\,\overrightarrow{x_0}(1,v) + (1-v)\,\overrightarrow{x_0}(u,0) + v\,\overrightarrow{x_0}(u,1)$$
$$- \begin{pmatrix} 1-u & u \end{pmatrix} \begin{pmatrix} \overrightarrow{x_0}(0,0) & \overrightarrow{x_0}(0,1) \\ \overrightarrow{x_0}(1,0) & \overrightarrow{x_0}(1,1) \end{pmatrix} \begin{pmatrix} 1-v \\ v \end{pmatrix}.$$

The Coons rectangular patch interpolates four boundary curves and in addition is an extremal of the functional

$$\mathcal{F}(\overrightarrow{x}) = \int_U \|\overrightarrow{x_{uv}}\|^2 du\, dv,$$

where $U = [0,1] \times [0,1]$, over all patches, $\overrightarrow{x} \in \mathcal{C}^\infty[u,v]$, with a prescribed boundary. The Coons patch was described in [**32**] as the unique interpolant that minimizes the functional $\mathcal{F}(\overrightarrow{x})$.

In general if a surface, $\overrightarrow{x}$, is an extremal of a functional, then it satisfies the associated Euler-Lagrange equation, which, for this functional, is the PDE

$$\overrightarrow{x}_{uuvv} = 0. \tag{25}$$

Therefore the Coons patch can be considered as a PDE surface, since it is a solution of the equation above.

In some of the following chapters we will address the problem of finding extremals of different quadratic functionals. But we will consider a restricted problem, namely that of finding the polynomial patch that minimizes a functional among all polynomial patches with the same boundary. Then, let us remark that an extremal of a functional on the restricted

space of polynomials, $\mathbb{R}_n[u,v]$, must not necessarily satisfy the associated Euler-Lagrange equation but a kind of weak version of it as we will show later.

Now we will study the special situation that is given for the restricted problem of finding an extremal of the functional $\mathcal{F}(\overrightarrow{x})$ in the space of polynomials. In the following theorem, Theorem 3.5, we will show that, for this case, a polynomial patch is an extremal if and only if it is a solution of the PDE (25). That is, the weak version of the Euler-Lagrange equation is equivalent to it.

Let us recall the definition of the shifted Legendre polynomials and to state two lemmas which will be needed in order to prove Theorem 3.5.

DEFINITION 3.1. *An explicit expression of the shifted Legendre polynomials is given by*

$$L_n(t) = (-1)^n \sum_{k=0}^{n} \binom{n}{k}\binom{n+k}{k}(-t)^k.$$

The first few are

$$L_0(t) = 1,$$
$$L_1(t) = 2t - 1,$$
$$L_2(t) = 6t^2 - 6t + 1,$$
$$L_3(t) = 20t^3 - 30t^2 + 12t - 1.$$

The shifted Legendre polynomials, see [**2**], are a set of functions that are analogous to the Legendre polynomials, but defined on the interval $[0,1]$. They obey the orthogonality relationship with respect to the usual scalar product of square integrable functions on $[0,1]$

$$\int_0^1 L_m(t)L_n(t)\,dt = \frac{1}{2n+1}\delta_{mn}. \tag{26}$$

Now, let us recall the fundamental lemma of calculus of variations because it has a statement similar to our following lemma, which is of interest to us.

LEMMA 3.2. *If M is continuous and $\int_a^b M(x)h(x)dx = 0$ for all infinitely differentiable $h(x)$, then $M(x) = 0$ on the open interval (a,b).*

So, let us study what happens if the product under the integral sign includes all the Bernstein polynomials at the basis of the degree n polynomials.

LEMMA 3.3. *Let P be a degree n polynomial, then the equality*

$$\int_0^1 P(t)\,B_i^n(t)\,dt = 0 \quad \textit{is true for all} \quad i = 0,...,n \tag{27}$$

if and only if $P(t) = 0$.

Proof: Bernstein polynomials are a basis of the degree n polynomials, so we take a polynomial $Q(t) = \sum_{i=0}^{n} c_i B_i^n(t)$, and rewrite conditions (27). They are equivalent to

$$\int_0^1 P(t)\, Q(t)\, dt = 0 \qquad \forall Q \in \mathbb{R}_n[t].$$

Now, if we consider the basis of the shifted Legendre polynomials, described in Definition 3.1, which have the property

$$\int_0^1 L_m(t) L_n(t)\, dt = \frac{1}{2n+1}\delta_{mn},$$

we can express $Q(t) = \sum_{k=0}^{n} c_k L_k(t)$, and then Equation (27) is equivalent to

$$0 = \int_0^1 P(t)\, L_k(t)\, dt \quad \forall k = 0, ..., n.$$

Finally, if we consider $P(t) = \sum_{j=0}^{n} A_j L_j(t)$, we have that for all k:

$$0 = \int_0^1 P(t) L_k(t)\, dt = \frac{1}{2k+1} A_k \Leftrightarrow A_k = 0 \Rightarrow P(t) = 0.$$

■

In an analogous way to the previous lemmas, we now consider the product of a polynomial of degree $n-2$ by another one of degree n but null at the extremes of the interval of integration.

LEMMA 3.4. *Let us consider the vectorial subspace $V_n \subseteq \mathbb{R}_n[t]$ defined by*

$$V_n = \{P \in \mathbb{R}_n[t] : P(0) = 0 \ \text{ and } \ P(1) = 0\}.$$

Given a polynomial $y \in \mathbb{R}_{n-2}[t]$, if $\int_0^1 y(t)P(t)\, dt = 0$ for all $P \in V_n$ then $y = 0$. In other words,

$$V_n^{\perp} \cap \mathbb{R}_{n-2}[t] = \{0\},$$

where $V_n^{\perp}$ denotes the orthogonal complement of V_n.

Proof: In order to prove this result we will express the polynomials y and P on the basis of shifted Legendre polynomials, $P(t) = \sum_{i=0}^{n} A_i L_i(t)$ and $y(t) = \sum_{j=0}^{n-2} B_j L_j(t)$.

First of all let us note that any $P \in V_n$ is defined by a set of coefficients $\{A_i\}_{i=0}^{n}$ with the following constraints

$$0 = P(0) = \sum_{i=0}^{n} A_i L_i(0) = \sum_{i=0}^{n} (-1)^i A_i$$

$$0 = P(1) = \sum_{i=0}^{n} A_i L_i(1) = \sum_{i=0}^{n} A_i.$$

Then we have that for any $P \in V_n$

$$0 = \int_0^1 y(t)P(t)\,dt = \int_0^1 \sum_{i=0}^{n}\sum_{j=0}^{n-2} B_j A_i L_i(t) L_j(t)\,dt = \sum_{j=0}^{n-2} \frac{1}{2j+1} B_j A_j, \tag{28}$$

where the orthogonality condition (26) has been applied.

Since P is an arbitrary polynomial on V_n, we can consider a family of polynomials P_j and make a free choice of $n-2$ of its coefficients.

Let us consider $P_j = \sum_{i=0}^{n} A_i^j L_i(t)$ with

$$A_i^j = \begin{cases} 1 & i = j \\ 0 & i \neq j \end{cases} \qquad \text{for} \quad i = 0, ..., n-2,$$

with the coefficients A_{n-1}^j and A_n^j, determined for any P_j by the constraints

$$\left.\begin{array}{c} (-1)^j + (-1)^{n-1} A_{n-1} + (-1)^n A_n = 0 \\ 1 + A_{n-1} + A_n = 0 \end{array}\right\},$$

which imply

$$A_{n-1}^j = \frac{-1 + (-1)^{j-n}}{2}, \qquad A_n^j = \frac{-1 - (-1)^{j-n}}{2}.$$

Now, if we consider Equation (28), for any P_j we obtain that $B_j = 0$, for $j = 0, ..., n-2$. Therefore $y = 0$.

■

The following theorem proves that a polynomial surface is an extremal of the functional $\mathcal{F}$ among all polynomial surfaces with the same boundary if and only if it is a PDE surface associated to the equation $\overrightarrow{x}_{uuvv} = 0$.

THEOREM 3.5. *A polynomial patch, $\overrightarrow{x} \in \mathbb{R}_n[u,v]$, satisfies $\overrightarrow{x}_{uuvv} = 0$ iff it is an extremal of the functional*

$$\mathcal{F}(\overrightarrow{y}) = \int_U \|\overrightarrow{y_{uv}}\|^2 du\,dv \qquad \overrightarrow{y} \in \mathbb{R}_n[u,v],$$

among all polynomial patches with a given boundary.

Proof: First we will see that if $\overrightarrow{x} \in \mathbb{R}_n[u,v]$ satisfies $\overrightarrow{x}_{uuvv} = 0$, then it is an extremal of the functional $\mathcal{F}(\overrightarrow{x})$ among all patches with a prescribed boundary.

The patch $\overrightarrow{x}$ would be an extremal of the functional $\mathcal{F}(\overrightarrow{x})$ among all patches with the same boundary if and only if

$$\frac{d}{dt}\Big|_{t=0} \mathcal{F}(\overrightarrow{x} + t\overrightarrow{y}) = 0,$$

for any $\overrightarrow{y} \in \mathbb{R}_n[u,v]$ null along its border. So let us compute this derivative

$$\frac{d}{dt}\Big|_{t=0} \mathcal{F}\left(\overrightarrow{x}+t\,\overrightarrow{y}\right) = \frac{d}{dt}\Big|_{t=0} \int_R < \overrightarrow{x}_{uv} + t\,\overrightarrow{y}_{uv},\, \overrightarrow{x}_{uv} + t\,\overrightarrow{y}_{uv} > \, du\,dv$$
$$= 2\int_R < \overrightarrow{x}_{uv},\, \overrightarrow{y}_{uv} > \, du\,dv.$$

Since the polynomial patch $\overrightarrow{y}$ is null along its boundary, all its border control points are zero when we consider its Bézier form. This implies that there are some Bernstein polynomials which are not involved in its Bézier expression:

$$\overrightarrow{y}\left(u,v\right) = \sum_{i,j=1}^{n-1} Q_{ij} B_i^n\left(u\right) B_j^n\left(v\right).$$

Therefore, at this point, we have that $\overrightarrow{x}$ is an extremal of $\mathcal{F}\left(\overrightarrow{x}\right)$ if and only if

$$0 = \int_R < \overrightarrow{x}_{uv}, \left(B_i^n\left(u\right) B_j^n\left(v\right)\right)_{uv} e_a > \, du\,dv, \qquad i,j = 1,...,n-1$$

where e_a, $a \in \{1,2,3\}$ denotes the a-th vector of the canonical basis.

Let us consider the following integration by parts

$$\int_R \frac{d}{dv} < \overrightarrow{x}_{uv}, \left(B_i^n\left(u\right) B_j^n\left(v\right) e_a\right)_u > \, du\,dv = \int_R < \overrightarrow{x}_{uvv}, \left(B_i^n\left(u\right) B_j^n\left(v\right) e_a\right)_u > \, du\,dv$$
$$+ \int_R < \overrightarrow{x}_{uv}, \left(B_i^n\left(u\right) B_j^n\left(v\right) e_a\right)_{uv} > \, du\,dv,$$

then we have

$$\int_R < \overrightarrow{x}_{uv}, \left(B_i^n\left(u\right) B_j^n\left(v\right) e_a\right)_{uv} > \, du\,dv = \int_0^1 < \overrightarrow{x}_{uv}, \left(B_i^n\left(u\right)\right)_u B_j^n\left(v\right) e_a > \Big]_{v=0}^{v=1} du$$
$$- \int_R < \overrightarrow{x}_{uvv}, \left(B_i^n\left(u\right) B_j^n\left(v\right) e_a\right)_u > \, du\,dv.$$

Bearing in mind that $B_j^n\left(0\right)$ and $B_j^n\left(1\right)$ are zero for $i = 1,...,n-1$ we have

$$\int_R < \overrightarrow{x}_{uv}, \left(B_i^n\left(u\right) B_j^n\left(v\right) e_a\right)_{uv} > \, du\,dv = -\int_R < \overrightarrow{x}_{uvv}, \left(B_i^n\left(u\right) B_j^n\left(v\right) e_a\right)_u > \, du\,dv.$$

Now applying that

$$\int_R \frac{d}{du} < \overrightarrow{x}_{uvv}, B_i^n\left(u\right) B_j^n\left(v\right) e_a > \, du\,dv = \int_R < \overrightarrow{x}_{uuvv}, B_i^n\left(u\right) B_j^n\left(v\right) e_a > \, du\,dv$$
$$+ \int_R < \overrightarrow{x}_{uvv}, \left(B_i^n\left(u\right) B_j^n\left(v\right) e_a\right)_u > \, du\,dv,$$

we have that

$$\int_R < \overrightarrow{x}_{uv}, \left(B_i^n(u)\, B_j^n(v)\, e_a\right)_{uv} > \, du\, dv =$$

$$= -\int_R \frac{d}{du} < \overrightarrow{x}_{uvv}, B_i^n(u)\, B_j^n(v)\, e_a > \, du\, dv + \int_R < \overrightarrow{x}_{uuvv}, B_i^n(u)\, B_j^n(v)\, e_a > \, du\, dv$$

$$= -\int_0^1 < \overrightarrow{x}_{uvv}, B_i^n(u)\, B_j^n(v)\, e_a > \Big]_{u=0}^{u=1} dv + \int_R < \overrightarrow{x}_{uuvv}, B_i^n(u)\, B_j^n(v)\, e_a > \, du\, dv.$$

Then, after evaluating the Bernstein polynomials as before, it is obtained that $\overrightarrow{x}$ is an extremal of $\mathcal{F}(\overrightarrow{x})$ if and only if

$$\int_R < \overrightarrow{x}_{uv}, \left(B_i^n(u)\, B_j^n(v)\, e_a\right)_{uv} > \, du\, dv = \int_R < \overrightarrow{x}_{uuvv}, B_i^n(u)\, B_j^n(v)\, e_a > \, du\, dv = 0.$$

Therefore a chart $\overrightarrow{x}$ such that $\overrightarrow{x}_{uuvv} = 0$ is an extremal for a prescribed border of the functional $\mathcal{F}(\overrightarrow{x})$.

Now, in order to prove the reciprocal, we only have to apply Lemma 3.4. If a chart $\overrightarrow{x}$ is an extremal with a prescribed boundary of the functional $\mathcal{F}(\overrightarrow{x})$, then, as we have previously seen, it satisfies

$$0 = \int_R < \overrightarrow{x}_{uuvv}, B_i^n(u)\, B_j^n(v)\, e_a > \, du\, dv \qquad \text{for} \quad i, j = 1, ..., n-1 \tag{29}$$

Then, since the Bernstein polynomials $\{B_i^n(t)\}_{i=1}^{n-1}$ are a basis of the vector subspace V_n defined in Lemma 3.4, and $\int_0^1 < \overrightarrow{x}_{uuvv}, B_i^n(u)\, e_a > \, du$ is a polynomial of degree $n-2$ in v, applying this lemma we have:

$$0 = \int_0^1 < \overrightarrow{x}_{uuvv}, e_a > \, B_i^n(u)\, du, \quad \text{for} \quad i = 1, ..., n-1.$$

Analogously, applying Lemma 3.4 again, we have that since $< \overrightarrow{x}_{uuvv}, e_a > \in \mathbb{R}_{n-2}[u]$, then it is zero for $a \in \{1, 2, 3\}$, that is, $\overrightarrow{x}_{uuvv} = 0$.

■

REMARK 3.6. *Equation (29) gives the weak version of the Euler-Lagrange equation associated to the functional $\mathcal{F}$, which we mentioned before.*

An extremal of the functional among all the polynomial patches with a prescribed boundary must fulfill

$$0 = \int_R < \overrightarrow{x}_{uuvv}, B_i^n(u)\, B_j^n(v)\, e_a > \, du\, dv \qquad \textit{for} \quad i, j = 1, ..., n-1.$$

But, thanks to Lemma 3.4 we can also ensure that, for the case of this functional, it implies that $\overrightarrow{x}_{uuvv} = 0$.

COROLLARY 3.7. *The Coons patch is an extremal in* $\mathbb{R}_n[u,v]$ *of the functional* $\mathcal{F}(\overrightarrow{x})$ *among all patches with a prescribed boundary.*

Proof:
The Coons patch satisfies the PDE $\overrightarrow{x}_{uuvv} = 0$ since $\overrightarrow{x}_{uu}$ is linear with respect to v.

■

Some work related with rectangular Coons patches was carried out in [**14**] by Farin and Hansford. While the boundary curves $\overrightarrow{x_0}(u,0)$, $\overrightarrow{x_0}(u,1)$, $\overrightarrow{x_0}(0,v)$ and $\overrightarrow{x_0}(1,v)$ may be totally arbitrary, in the early days the boundary curves were considered as discretized curves with many points on them. In fact, in [**14**] these boundary polygons are treated as Bézier border control points and a discrete version of the Coons patch is given. The interior control points $P_{i,j}$ are defined in terms of boundary points by the discrete Coons patch:

$$\begin{aligned} P_{i,j} = &\left(1-\frac{i}{m}\right)P_{0,j} + \frac{i}{m}P_{m,j} + \left(1-\frac{j}{m}\right)P_{i,0} + \frac{j}{n}P_{i,n} \\ &- \begin{pmatrix} 1-\frac{i}{m} & \frac{i}{m} \end{pmatrix} \begin{pmatrix} P_{0,0} & P_{0,n} \\ P_{m,0} & P_{m,n} \end{pmatrix} \begin{pmatrix} 1-\frac{j}{n} \\ \frac{j}{n} \end{pmatrix}. \end{aligned} \tag{30}$$

for $0 < i < m$ and $0 < j < n$. These control points define the discrete Coons patch which is the same patch as if Coons interpolation was applied to the Bézier curves associated to the boundary polygons.

The discrete Coons patch also minimizes the discrete version of the functional $\mathcal{F}$, in Equation (1). In fact, the discrete Coons patch is a PDE Bézier surface satisfying the discrete version of $\overrightarrow{x}_{uuvv} = 0$.

2. Triangular Coons patches

Now after introducing all these topics for rectangular surfaces, let us come back to triangular patches. The triangular Coons patch we will define first appeared in [**32**]. Similar to the rectangular Coons patch we consider the border curves $\overrightarrow{x_0}(u,0)$, $\overrightarrow{x_0}(0,v)$ and $\overrightarrow{x_0}(u,1-u)$, (or $\overrightarrow{x_0}(1-v,v)$), to denote the boundary curves and define the patch as

$$\begin{aligned} \overrightarrow{x}(u,v) = &(1-u-v)\left(\overrightarrow{x_0}(u,0) + \overrightarrow{x_0}(0,v) - \overrightarrow{x_0}(0,0)\right) \\ &+ v\left(\overrightarrow{x_0}(0,u+v) + \overrightarrow{x_0}(u,1-u) - \overrightarrow{x_0}(0,1)\right) \\ &+ u\left(\overrightarrow{x_0}(u+v,0) + \overrightarrow{x_0}(1-v,v) - \overrightarrow{x_0}(1,0)\right), \end{aligned} \tag{31}$$

or analogously, in barycentric coordinates,

$$\begin{aligned} \overrightarrow{x}(u,v,w) = &w\left(\overrightarrow{x_0}(u,0,1-u) + \overrightarrow{x_0}(0,v,1-v) - \overrightarrow{x_0}(0,0,1)\right) \\ &+ v\left(\overrightarrow{x_0}(0,1-w,w) + \overrightarrow{x_0}(u,1-u,0) - \overrightarrow{x_0}(0,1,0)\right) \\ &+ u\left(\overrightarrow{x_0}(1-w,0,w) + \overrightarrow{x_0}(1-v,v,0) - \overrightarrow{x_0}(1,0,0)\right), \end{aligned}$$

with $u+v+w=1$.

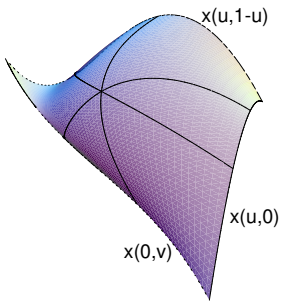

FIGURE 1. A representation of a triangular Coons patch defined in Equation (31) for prescribed boundary data.

Some differences with respect to the rectangular Coons patch must be pointed out. First let us remark that if we consider the border curves $\overrightarrow{x_0}(u,0)$, $\overrightarrow{x_0}(0,v)$ and $\overrightarrow{x_0}(u,1-u)$ or $\overrightarrow{x_0}(1-v,v)$ to be polynomial curves of degree n, then the associated triangular Coons patch is a degree $n+1$ polynomial surface. This increase in degree does not happen in the rectangular case.

Moreover in the comparison between the rectangular and the triangular Coons patch we find that, since the triangular patch is not linear in both variables, then $\overrightarrow{x}_{uuvv} \neq 0$.

Now, analogously to what was done in [**14**] for rectangular patches, we have obtained the discrete version of the triangular Coons patch.

DEFINITION 3.8. *The interior points $P_{i,j,k}$ with $i+j+k=n+1$, of the Triangular Discrete Coons patch are defined by*

$$\begin{aligned} P_{i,j,k} = & \frac{k}{n+1}\left(P_{i,0,n-i}+P_{0,j,n-j}-P_{0,0,n}\right) \\ & +\frac{j}{n+1}\left(P_{0,n-k,k}+P_{i,n-i,0}-P_{0,n,0}\right) \\ & +\frac{i}{n+1}\left(P_{n-k,0,k}+P_{n-j,j,0}-P_{n,0,0}\right). \end{aligned} \tag{32}$$

The triangular Bézier surface with the previous interior control points coincides with the triangular Coons patch that would be obtained from the Bézier curves associated to the boundary control points.

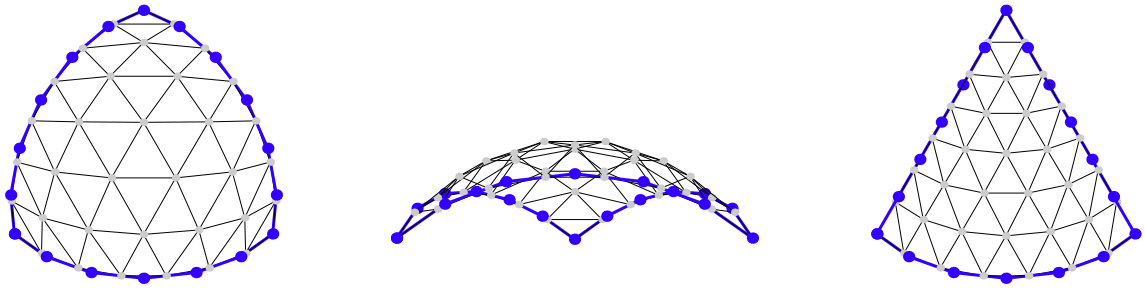

FIGURE 2. Two discrete triangular Coons patches. The first two figures are two views of the same control net and a second example is shown in the third figure.

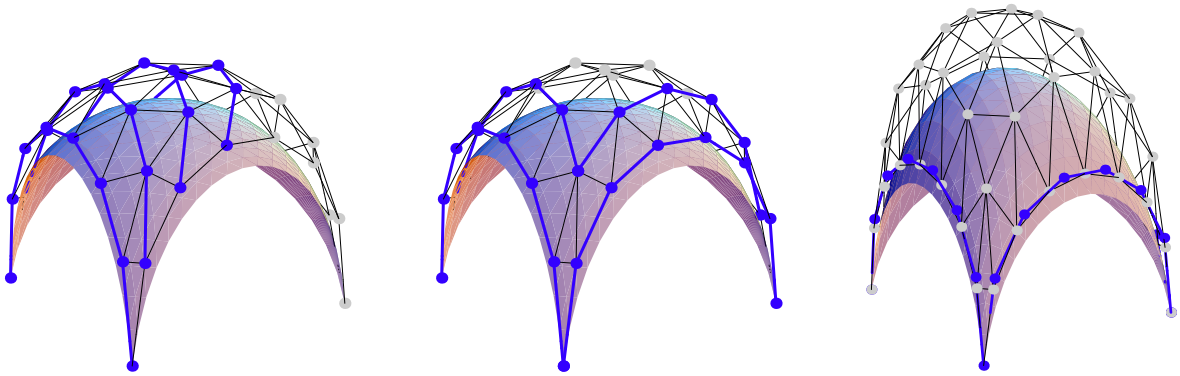

FIGURE 3. Three similar triangular Bézier surfaces. The first is obtained by Theorem 2.2 and the second by Theorem 2.3. The third surface is a triangular Coons patch and therefore its degree increases for an analogous set of given data. It can be seen that in the first two cases better shapes are obtained than for the Coons case.

In the following proposition we give a formula to express the functional of a Bézier triangular patch

$$\mathcal{F}(\overrightarrow{x}) = \int_T \|\overrightarrow{x_{uv}}\|^2 du\, dv, \tag{33}$$

defined now in the triangle, T, in terms of the control points, $P_I = (x_I^1, x_I^2, x_I^3)$.

PROPOSITION 3.9. *The functional, $\mathcal{F}(\overrightarrow{x})$, of a triangular Bézier surface can be expressed by the formula*

$$\mathcal{F}(\overrightarrow{x}) = \sum_{a=1}^{3} \sum_{|I_0|=n} \sum_{|I_1|=n} C_{I_0 I_1} x_{I_0}^a x_{I_1}^a \tag{34}$$

with

$$C_{I_0I_1} = 2n\,(2n-1)\,\frac{\binom{n}{I_0}\binom{n}{I_1}}{\binom{2n}{I_0+I_1}}\Big(\frac{1}{2}\left(b_{12}^{12}+b_{13}^{13}+b_{23}^{23}+b_{33}^{33}\right)-b_{12}^{13}-b_{12}^{23}+b_{12}^{33}+b_{13}^{23}-b_{13}^{33}-b_{23}^{33}\Big), \tag{35}$$

where the coefficients b_{rs}^{tl} *satisfy the symmetry relation* $b_{rs}^{tl}=b_{sr}^{tl}=b_{rs}^{lt}=b_{sr}^{lt}$, *and are defined by*

$$b_{rs}^{tl}=\begin{cases}\frac{I_0^rI_0^sI_1^tI_1^r+I_1^rI_1^sI_0^tI_0^r}{(I_0^r+I_1^r)(I_0^s+I_1^s)(I_0^t+I_1^t)(I_0^r+I_1^r-1)} & r=l\\ \frac{I_0^rI_0^sI_1^t(I_1^t-1)+I_1^rI_1^sI_0^t(I_0^t-1)}{(I_0^r+I_1^r)(I_0^s+I_1^s)(I_0^t+I_1^t)(I_0^t+I_1^t-1)} & t=l\\ \frac{2\,I_0^rI_0^sI_1^rI_1^r}{(I_0^r+I_1^r)(I_0^r+I_1^r-1)(I_0^s+I_1^s)(I_0^s+I_1^s-1)} & r=t,s=l\\ \frac{2\,I_0^r(I_0^r-1)I_1^t(I_1^t-1)}{(I_0^r+I_1^r)(I_0^r+I_1^r-1)(I_0^t+I_1^t)(I_0^t+I_1^t-1)} & r=s,t=l\\ \frac{I_0^rI_0^sI_1^r(I_1^r-1)+I_1^rI_1^sI_0^r(I_0^r-1)}{(I_0^r+I_1^r)(I_0^s+I_1^s)(I_0^r+I_1^r-1)(I_0^t+I_1^t-2)} & r=t=l\\ \frac{2\,I_0^r(I_0^r-1)I_1^r(I_1^r-1)}{(I_0^r+I_1^r)(I_0^r+I_1^r-1)(I_0^r+I_1^r-2)(I_0^r+I_1^r-3)} & r=s=t=l.\end{cases} \tag{36}$$

Proof: The functional is a second-order functional and, therefore, in order to obtain the coefficients $C_{I_0I_1}$ we compute its second derivative:

$$\frac{\partial^2\mathcal{F}(\overrightarrow{x})}{\partial x_{I_0}^a\partial x_{I_1}^a}=\frac{\partial^2}{\partial x_{I_0}^a\partial x_{I_1}^a}\sum_{\bar a=1}^{3}\sum_{|I|=n}\sum_{|J|=n}C_{IJ}x_I^{\bar a}x_J^{\bar a}=\frac{\partial}{\partial x_{I_1}^a}\sum_{|J|=n}2C_{I_0J}x_J^a=2\,C_{I_0I_1}.$$

We compute the first derivative

$$\frac{\partial\mathcal{F}(\overrightarrow{x})}{\partial x_{I_0}^a}=\int_{\mathcal{T}}\frac{\partial}{\partial x_{I_0}^a}\|\overrightarrow{x_{uv}}\|^2du\,dv=\int_{\mathcal{T}}2\;<\frac{\partial\overrightarrow{x}_{uv}}{\partial x_{I_0}^a},\overrightarrow{x}_{uv}>du\,dv=\int_{\mathcal{T}}2\;<(B_{I_0}^n)_{uv},\overrightarrow{x}_{uv}>du\,dv,$$

and then the second

$$\begin{aligned}\frac{\partial^2\mathcal{F}(\overrightarrow{x})}{\partial x_{I_0}^a\partial x_{I_1}^a}=&2\int_{\mathcal{T}}<(B_{I_0}^n)_{uv},\frac{\partial\overrightarrow{x}_{uv}}{\partial x_{I_1}^a}>du\,dv=2\int_{\mathcal{T}}<(B_{I_0}^n)_{uv},(B_{I_1}^n)_{uv}>du\,dv\\ =&2\int_{\mathcal{T}}n^2(n-1^2)\left(B_{I_0-e_1-e_2}^n-B_{I_0-e_1-e_3}^n-B_{I_0-e_2-e_3}^n+B_{I_0-2e_3}^n\right)\\ &\left(B_{I_1-e_1-e_2}^n-B_{I_1-e_1-e_3}^n-B_{I_1-e_2-e_3}^n+B_{I_1-2e_3}^n\right)dudv\\ =&2n\,(2n-1)\,\frac{\binom{n}{I_0}\binom{n}{I_1}}{\binom{2n}{I_0+I_1}}\Big(\frac{1}{2}\left(b_{12}^{12}+b_{13}^{13}+b_{23}^{23}+b_{33}^{33}\right)-b_{12}^{13}-b_{12}^{23}+b_{12}^{33}+b_{13}^{23}-b_{13}^{33}-b_{23}^{33}\Big),\end{aligned}$$

where we have computed the integral of the Bernstein polynomials with the formula given in Lemma 1.4

$$\int_{\mathcal{T}} B^{2n-2}_{I_0+I_1}(u,v)\,dudv = \frac{1}{(3n-2)(3n-3)},$$

and we have performed some simplifications like the following:

$$\begin{aligned}
&\int_{\mathcal{T}} B^{n-1}_{I_0-e_1-e_2}B^{n-1}_{I_1-e_1-e_3} + B^{n-1}_{I_1-e_1-e_2}B^{n-1}_{I_0-e_1-e_3}\,dudv = \\
&= \int_{\mathcal{T}} \frac{\binom{n-2}{I_0-e_1-e_2}\binom{n-2}{I_1-e_1-e_3} + \binom{n-2}{I_1-e_1-e_2}\binom{n-2}{I_0-e_1-e_3}}{\binom{2n-4}{I_0+I_1-2e_1-e_2-e_3}} B^{2n-4}_{I_0+I_1-2e_1-e_2-e_3}\,dudv \\
&= \frac{2n(2n-1)}{n^2(n-1^2)}\frac{\binom{n}{I_0}\binom{n}{I_1}}{\binom{2n}{I_0+I_1}}\frac{I_0^1I_0^2I_1^1I_1^3 + I_0^1I_0^3I_1^1I_1^2}{(I_0^1+I_1^1)(I_0^2+I_1^2)(I_0^1+I_1^1-1)(I_0^3+I_1^3)} \\
&= \frac{2n(2n-1)}{n^2(n-1^2)}\frac{\binom{n}{I_0}\binom{n}{I_1}}{\binom{2n}{I_0+I_1}} b_{12}^{13}.
\end{aligned}$$

Therefore

$$C_{I_0I_1} = 2n(2n-1)\frac{\binom{n}{I_0}\binom{n}{I_1}}{\binom{2n}{I_0+I_1}}\Big(\frac{1}{2}\left(b_{12}^{12}+b_{13}^{13}+b_{23}^{23}+b_{33}^{33}\right) - b_{12}^{13} - b_{12}^{23} + b_{12}^{33} + b_{13}^{23} - b_{13}^{33} - b_{23}^{33}\Big)$$

where b_{rs}^{tl} are defined in Equation (36) .

■

Let us remark that the formula we give in Equation (34) translates the functional, $\mathcal{F}$, into a function of the control points, $\mathcal{F}(\overrightarrow{x}) = \sum_{a=1}^{3}\sum_{|I_0|=n}\sum_{|I_1|=n} C_{I_0I_1}x^a_{I_0}x^a_{I_1}$. In the following proposition we compute the gradient of the functional with respect to the coordinates of a control point $P_{I_0} = \left(x^1_{I_0}, x^2_{I_0}, x^3_{I_0}\right)$. This will enable us to obtain an extremal of the functional among all Bézier surfaces with the same border as a solution of a linear system.

PROPOSITION 3.10. *A triangular control net, $\mathcal{P} = \{P_I\}_{|I|=n}$, is an extremal of the functional, $\mathcal{F}$, among all triangular Bézier surfaces with a prescribed boundary if and only if:*

$$\sum_{|J|=n} C_{I_0J}P_J = 0 \quad \textit{for all} \quad |I_0 = (I_0^1, I_0^2, I_0^3)| = n \quad \textit{with} \quad I_0^1, I_0^2, I_0^3 > 0, \tag{37}$$

where C_{IJ} are the coefficients defined in Equation (35).

Proof: The gradient of the functional with respect to the coordinates of an interior control point $P_{I_0} = \left(x^1_{I_0}, x^2_{I_0}, x^3_{I_0}\right)$ is given by

$$\frac{\partial \mathcal{F}(\overrightarrow{x})}{\partial P_{I_0}} = \left(\frac{\partial \mathcal{F}(\overrightarrow{x})}{\partial x^1_{I_0}}, \frac{\partial \mathcal{F}(\overrightarrow{x})}{\partial x^2_{I_0}}, \frac{\partial \mathcal{F}(\overrightarrow{x})}{\partial x^3_{I_0}} \right) = 2 \left(\sum_{|J|=n} C_{I_0 J} x^1_J, \sum_{|J|=n} C_{I_0 J} x^2_J, \sum_{|J|=n} C_{I_0 J} x^3_J \right)$$
$$= 2 \sum_{|J|=n} C_{I_0 J} P_J.$$

■

Equivalently, a triangular control net, $\mathcal{P} = \{P_I\}_{|I|=n}$, is an extremal among all control nets with prescribed border control points if and only if

$$0 = \sum_{|I|=n} \frac{\binom{n}{I}}{\binom{2n}{I_0+I}} \left(\frac{1}{2} \left(b^{12}_{12} + b^{13}_{13} + b^{23}_{23} + b^{33}_{33} \right) - b^{13}_{12} - b^{23}_{12} + b^{33}_{12} + b^{23}_{13} - b^{33}_{13} - b^{33}_{23} \right) P_I$$

for all $|I_0 = (I^1_0, I^2_0, I^3_0)| = n$ with $I^1_0, I^2_0, I^3_0 > 0$, with the coefficients b^{tl}_{rs} given in Equation (36).

In particular we give this result for the case $n = 3$.

PROPOSITION 3.11. *A triangular control net of degree 3, $\mathcal{P} = \{P_I\}_{|I|=3}$, is an extremal of the functional, $\mathcal{F}(\mathcal{P})$, among all triangular control nets with a prescribed boundary if and only if*

$$P_{111} = \frac{1}{2} \left(P_{012} - P_{021} + P_{102} + P_{120} - P_{201} + P_{210} \right).$$

From the condition obtained in Proposition 11, given the exterior control points, we can generate the whole triangular net by solving a linear system where the equations are:

$$2P_{i,j,k} = P_{i-1,j,k+1} - P_{i-1,j+1,k} + P_{i,j-1,k+1} + P_{i,j+1,k-1} - P_{i+1,j-1,k} + P_{i+1,j,k-1}$$

$P_{i,j,k}$ being a interior control point. This equation can be expressed by the following mask:

$$P_{i,j,k} = \frac{1}{2} \times \begin{array}{ccccc} & 0 & 1 & -1 & 0 \\ & 1 & & \star & 1 \\ & & -1 & 1 & \\ & & 0 & & \end{array} \tag{38}$$

The following figures show some examples of the triangular Bézier surfaces obtained, given a boundary, by means of three different methods: Coons interpolation, minimization of the functional $\mathcal{F}$ and with the use of the mask defined in Equation (38).

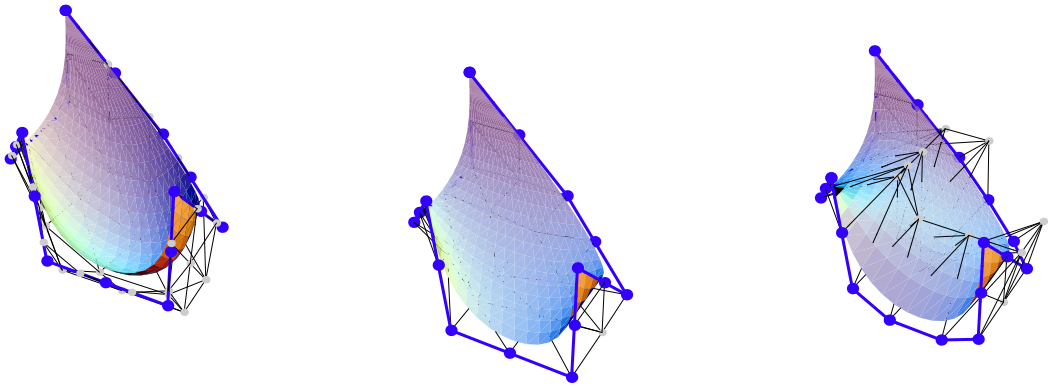

FIGURE 4. Three Bézier surfaces with the same border. On the left the triangular Coons patch. The one in the middle is a Bézier extremal of the functional $\mathcal{F}$. The figure on the right is obtained by means of the mask in Equation (38).

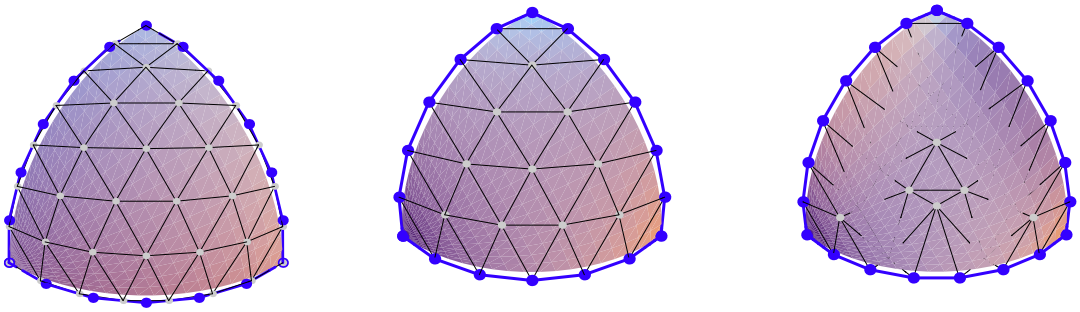

FIGURE 5. Three more examples of Bézier triangles, the triangular Coons patch, the Bézier extremal of $\mathcal{F}$ in the middle and the Bézier surface built with the mask (38).

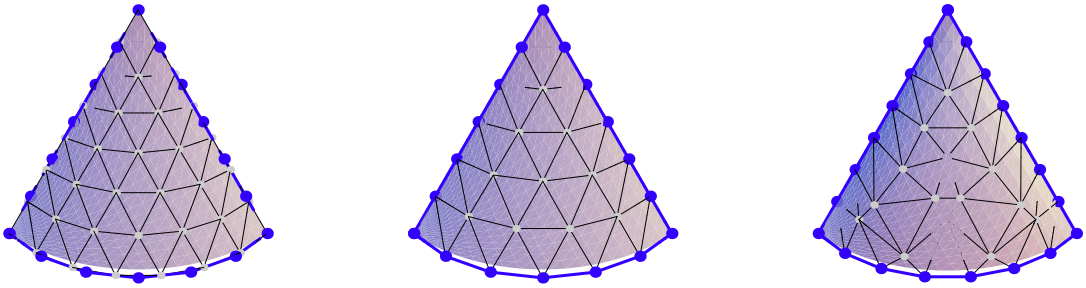

FIGURE 6. As before, the Coons patch, the polynomial extremal of $\mathcal{F}$ in the middle and in the right another surface with the same boundary but obtained thanks to the associated mask.

From the previous figures it can be seen that the control nets obtained by means of the mask, in Equation (38), derived from the functional $\mathcal{F}$ are quite irregular in comparison with the nets obtained as extremals of the functional.

Now, let us remark that in contrast to the rectangular case, the Triangular Coons patch is not an extremal of the functional $\mathcal{F}$. We will prove that for the triangular case, being an extremal of such a functional is not equivalent to satisfying the associated Euler-Lagrange equation, as was true for the rectangular Coons patch. The following Theorem will show that an extremal of the functional, described in Equation (33), would coincide with the solution of its associated Euler-Lagrange equation, $\overrightarrow{x}_{uuvv} = 0$, only under certain conditions on the control points.

The following lemmas, Lemma 3.12 and Lemma 3.15, are analogous to Lemma 3.3 and Lemma 3.4 for bivariate polynomials. They will be needed in order to prove our next theorem and some other results we will prove later on.

In the proof of the following lemma we will make use of the dual basis of bivariate Bernstein polynomials defined in [**22**]. The set of polynomials $\{C_I^n\}_{|I|=n}$ of total degree n is called the dual basis of the Berstein basis $\{B_I^n\}_{|I|=n}$ if

$$\int_T B_I^n(u,v)\, C_I^n(u,v)\, du\, dv = \delta_I^J.$$

LEMMA 3.12. *Let $\overrightarrow{y}$ be a degree n bivariate polynomial, then the equality*

$$\int_{\mathcal{T}} \overrightarrow{y}(u,v)\; B_I^n(u,v)\; dudv = 0 \quad \textit{holds for all} \quad |I| = n \tag{39}$$

if and only if $\overrightarrow{y} = 0$.

Proof: Let us consider the expression of $\overrightarrow{y}$ in terms of the dual basis of Bernstein polynomials defined in [**22**], $y = \sum_{|J|=n} A_J C_J^n$, then

$$0 = \int_{\mathcal{T}} \overrightarrow{y}(u,v)\; B_I^n(u,v)\; dudv = \int_{\mathcal{T}} \sum_{|J|=n} A_J C_J^n(u,v)\; B_I^n(u,v)\; dudv = \sum_{|J|=n} A_J\, \delta_{I,J} = A_I$$

for all $|I| = n$. Therefore $\overrightarrow{y} = 0$.

■

The proof of the next lemma, Lemma 3.15, is based on a method by T. Lyche and K. Scherer for the computation of the eigenvalues of the Gram matrix of the s-variate triangular Bernstein basis of degree n, see [**26**]. In order to prove our next result we needed to show that a special matrix, M, which is similar to the Gram matrix, was a non-singular matrix. So let us recall the definition of the Gram matrix of the bivariate triangular Bernstein basis.

DEFINITION 3.13. *The Gram matrix, G, of the bivariate triangular Bernstein basis of degree n is defined by*

$$G = (< B_I^n, B_J^n >)_{|I|,|J|=n} = \left(\int_T B_I^n(u,v), B_J^n(u,v)\, du\, dv \right)_{|I|,|J|=n}.$$

This is a matrix of order $\binom{n+2}{2}$ and for both rows and columns the following linear ordering is used: If $I^1 < J^1$ then $I < J$, and for $I^1 = J^1$ then the second component must be compared, if $I^1 = J^1$ and $I^2 < J^2$ then $I < J$.

As an example, for $n = 2$, the indexes of the basis would be taken in the order

$$(0,0,2), (0,1,1), (0,2,0), (1,0,1), (1,1,0), (2,0,0).$$

We will need the following lemma in order to prove Lemma 3.15. This was proved in [**26**] for multivariate Bernstein polynomials, and here we rewrite it for the bivariate case.

LEMMA 3.14. *([**26**] Lemma 2.1.) Let us denote $I = \{i, j, n-i-j\}$, then*

(1) $\frac{n!}{(n-k-l)!}\, u^k v^l = \sum_{|I|=n} \frac{i!j!}{(i-k)!(j-l)!} B_I^n(u,v) \quad for \quad k+l \leq n.$

(2) $\int_T u^k v^l B_I^n(u,v) du\, dv = \frac{(k+i)!(l+j)!n!}{i!j!(n+2+k+l)!} \quad for \quad k+l \leq n.$

LEMMA 3.15. *Let us consider the vectorial subspace $V \subseteq \mathbb{R}_n[u,v]$ defined by*

$$V = \{P \in \mathbb{R}_n[u,v] : P(u,0) = P(0,v) = P(u,1-u) = 0\}.$$

Given a polynomial $y \in \mathbb{R}_{n-3}[u,v]$, if

$$\int_T y(u,v)\, P(u,v)\; du\, dv = 0$$

for all $P \in V$, then $y = 0$. In other words

$$V^\perp \cap \mathbb{R}_{n-3}[t] = \{0\},$$

where $V^\perp$ denotes the orthogonal complement of V.

Proof: The Bézier form of a polynomial $P \in V$, null along the border of the parameter domain, only involves the interior Bernstein polynomials

$$P(u,v) = \sum_{|I|=n} a_I\, B_I^n(u,v) \quad \text{with} \quad I^1, I^2, I^3 \neq 0.$$

Therefore, if $\int_T y\, P du\, dv = 0$, we have that for all $|I| = n$ with $I^1, I^2, I^3 \neq 0$

$$0 = \int_T y(u,v)\, B_I^n(u,v)\; du\, dv = \sum_{|J|=n-3} P_J \int_T B_J^{n-3}(u,v) B_I^n(u,v)\; du\, dv. \tag{40}$$

Our goal is to prove that $P_J = 0$ for all $|J| = n-3$. Equivalently we will see that the previous homogeneous linear system with the coefficient matrix

$$M = \left(< B_I^n, B_J^{n-3} >\right) = \left(\int_T B_I^n(u,v) B_J^{n-3}(u,v)\, du\, dv\right)_{\substack{|I|=n,\ I^1,I^2,I^3\neq 0,\\ |J|=n-3}}$$

has a unique solution. This is a square matrix of order $\binom{n-1}{2}$.

In order to prove that matrix M is non-singular we will compute its eigenvalues.

We consider polynomials Q_m (to be determined) of the special form

$$Q_m = \sum_{k=0}^{|m|} \sum_{l=0}^{|m|-k} q_{m,k,l} u^k v^l \quad \text{with} \quad m = (m_1, m_2) \in \mathbb{Z}^2 \quad \text{and} \quad 0 \leq |m| \leq n-3, \tag{41}$$

where

$$q_{m,m} = 1 \quad \text{and} \quad q_{m,k,l} = 0 \quad \text{for} \quad k+l = |m| \quad \text{and} \quad (k,l) \neq m.$$

Note that Q_m is a polynomial of degree $|m|$ and that its only monomial of total degree $|m|$ is $u^{m_1} v^{m_2}$.

Let $d_m = (d_{m,I})$ be the vector of coefficients of Q_m on the Bernstein basis, so

$$Q_m = \sum_{|I|=n-3} d_{m,I} B_I^{n-3}(u,v), \quad \text{with} \quad |m| \leq n-3 \quad \text{and} \quad I = (i,j,n-3-i-j).$$

We will determine the coefficients $q_{m,k,l}$ for fixed m so that d_m is an eigenvector of M. The idea is to express both d_m and $M\, d_m$ in terms of the $q_{m,k,l}$ and use the eigenvalue/eigenvector relation $M\, d_m = \lambda_m\, d_m$ to determine the values of λ_m. Consider first the vector d_m. Inserting (1) from Lemma 3.14 into Equation (41) we can express each $d_{m,I}$ in the form

$$d_{m,I} = \sum_{k=0}^{|m|} \sum_{l=0}^{|m|-k} q_{m,k,l} \frac{(n-3-k-l)!\, i!\, j!}{(n-3)!\,(i-k)!\,(j-l)!} = \sum_{k=0}^{|m|} \sum_{l=0}^{|m|-k} q_{m,k,l} \sum_{s=0}^{k} \sum_{t=0}^{l} \beta_{k,l}^{s,t} i^s j^t, \tag{42}$$

for some constants $\beta_{k,l}^{s,t}$ independent of I, in particular

$$\beta_{k,l}^{k,l} = \frac{(n-3-k-l)!}{(n-3)!}.$$

Let us consider the Ith component of $M\, d_m$

$$(M\, d_m)_I = \sum_{|J|=n-3} < B_{I+\mathbf{1}}^n, B_J^{n-3} > \, d_{m,J} =< B_{I+\mathbf{1}}^n, Q_m >= \sum_{k=0}^{|m|} \sum_{l=0}^{|m|-k} q_{m,k,l} < B_{I+\mathbf{1}}^n, u^k v^l >,$$

where we have denoted $\mathbf{1} = (1,1,1)$. In a similar manner to before, using (2) from Lemma 3.14, we can write it in the form

(43)
$$(M\, d_m)_I = \sum_{k=0}^{|m|} \sum_{l=0}^{|m|-k} q_{m,k,l} \frac{(k+i+1)!(l+j+1)!n!}{(i+1)!(j+1)!(n+2+k+l)!} = \sum_{k=0}^{|m|} \sum_{l=0}^{|m|-k} q_{m,k,l} \sum_{s=0}^{k} \sum_{t=0}^{l} \alpha_{k,l}^{s,t} i^s j^t$$

where the $\alpha_{k,l}^{s,t}$ are independent of I, in particular

$$\alpha_{k,l}^{k,l} = \frac{n!}{(n+2+k+l)!}.$$

Switching the order of summation in Equation (42) and Equation (43) we have $M\, d_m = \lambda_m\, d_m$ if and only if

$$0 = \sum_{s=0}^{|m|} \sum_{t=0}^{|m|-s} \left(\sum_{k=s}^{|m|} \sum_{l=t}^{|m|-k} (\alpha_{k,l}^{s,t} - \lambda_m \beta_{k,l}^{s,t})\, q_{m,k,l} \right) i^s j^t, \quad \forall |I| = n-3.$$

We see that this holds for all such I if and only if

$$0 = \sum_{k=s}^{|m|} \sum_{l=t}^{|m|-k} (\alpha_{k,l}^{s,t} - \lambda_m \beta_{k,l}^{s,t})\, q_{m,k,l} \quad \text{for all} \quad s,t \quad \text{such that} \quad s+t \le |m|. \tag{44}$$

Choosing $(s,t) = m$ in this equation, since $q_{m,m} = 1$ we obtain the eigenvalues

$$\lambda_m = \frac{\alpha_m^m}{\beta_m^m} = \frac{n!(n-3)!}{(n+2+|m|)!(n-3-|m|)!} = \frac{(n-3)\cdots(n-3-|m|+1)}{(n+|m|+2)\cdots(n+1)} \quad \text{for} \quad |m| \le n-3.$$

Therefore, since all the eigenvalues are positive we can ensure that matrix M is non-singular and there exists a unique solution of the linear system in Equation (40): $P_J = 0$ for all $|J| = n-3$. That is, $y = 0$.

■

REMARK 3.16. *Let us remark that matrix M has only $n-2$ different eigenvalues because if $|r| = |m|$ then $\lambda_r = \lambda_m$, for all $|m| \le n-3$.*

Now we can explain the conditions under which there is an equivalence between finding the extremals of the functional $\mathcal{F}$ and computing the PDE surfaces satisfying its Euler-Lagrange equation.

THEOREM 3.17. *A polynomial patch $\overrightarrow{x} \in \mathbb{R}_n[u,v]$ that satisfies $\overrightarrow{x}_{uv}(u,1-u) = 0$ is a solution of the PDE $\overrightarrow{x}_{uuvv} = 0$ iff it is an extremal of the functional*

$$\mathcal{F}(\overrightarrow{x}) = \int_T \|\overrightarrow{x_{uv}}\|^2 du\, dv$$

among all polynomial patches with the same prescribed border.

Proof: This proof is analogous to the proof of Theorem 3.5 for rectangular patches.

A polynomial patch $\overrightarrow{x}$ would be an extremal of the functional $\mathcal{F}(\overrightarrow{x})$ among all polynomial patches with a prescribed boundary if and only if for any $\overrightarrow{y} \in \mathbb{R}_n[u,v]$, null along the border of T,

$$\overrightarrow{y}(u,v) = \sum_{|I|=n} Q_I B_I^n(u,v), \quad |I| = |\{i,j,k\}| = n \quad \text{with} \quad i,j,k \neq 0,$$

the following equality holds

$$0 = \frac{d}{dt}\Big|_{t=0} \mathcal{F}(\overrightarrow{x} + t\overrightarrow{y}) = 2\int_T < \overrightarrow{x}_{uv}, \overrightarrow{y}_{uv} > du\, dv.$$

Equivalently, we have that $\overrightarrow{x}$ is an extremal of $\mathcal{F}(\overrightarrow{x})$ if and only if

$$0 = \int_T < \overrightarrow{x}_{uv}, (B_I^n(u,v))_{uv} e_a > du\, dv,$$

where e_a, $a \in \{1,2,3\}$, denotes the a-th vector of the canonical basis and $|I| = |\{i,j,k\}| = n$ with $i,j,k \neq 0$.

Let us consider the following integration by parts

$$\int_T \frac{d}{dv} < \overrightarrow{x}_{uv}, (B_I^n(u,v))_u e_a > du\, dv = \int_T < \overrightarrow{x}_{uvv}, (B_I^n(u,v))_u e_a > du\, dv + \int_T < \overrightarrow{x}_{uv}, (B_I^n(u,v))_{uv} e_a > du\, dv,$$

then we have

$$\int_T < \overrightarrow{x}_{uv}, (B_I^n(u,v))_{uv} e_a > du\, dv = \int_0^1 < \overrightarrow{x}_{uv}, n\left(B_{I-e_1}^{n-1}(u,v) - B_{I-e_3}^{n-1}(u,v)\right) e_a > \Big]_{v=0}^{v=1-u} du - \int_T < \overrightarrow{x}_{uvv}, (B_I^n(u,v))_u e_a > du\, dv.$$

Now, bearing in mind that $B_{I-e_1}^{n-1}(u,1-u) = 0$ for $k \neq 0$, $B_{I-e_1}^{n-1}(u,0) = B_{I-e_3}^{n-1}(u,0) = 0$ for $j \neq 0$ and that $B_{I-e_3}^{n-1}(u,1-u) = B_i^{n-1}(u)$ if $k = 1$, we have

$$\int_T < \overrightarrow{x}_{uv}, (B_I^n(u,v))_{uv} e_a > du\, dv = -\int_0^1 < \overrightarrow{x}_{uv}(u,1-u), B_i^{n-1}(u) e_a > du - \int_T < \overrightarrow{x}_{uvv}, (B_I^n(u,v))_u e_a > du\, dv.$$

Now if we consider the integral

$$\int_T \frac{d}{du} < \overrightarrow{x}_{uvv}, B_I^n(u,v)\, e_a > \, du\, dv = \int_T < \overrightarrow{x}_{uuvv}, B_I^n(u,v)\, e_a > \, du\, dv + \int_T < \overrightarrow{x}_{uvv}, \left(B_I^n(u,v)\right)_u e_a >, \, du\, dv,$$

we have

$$\int_T < \overrightarrow{x}_{uvv}, \left(B_I^n(u,v)\right)_u e_a > \, du\, dv = \int_0^1 < \overrightarrow{x}_{uvv}, B_I^n(u,v)\, e_a > \Big]_{u=0}^{u=1-v} dv - \int_T < \overrightarrow{x}_{uuvv}, B_I^n(u,v)\, e_a > \, du\, dv.$$

Then, after evaluating the Bernstein polynomials, $B_I^n(1-v,v) = B_I^n(0,v) = 0$ for $i,k \neq 0$, it is obtained that $\overrightarrow{x}$ is an extremal of $\mathcal{F}(\overrightarrow{x})$ if and only if

$$\int_T < \overrightarrow{x}_{uv}, \left(B_I^n(u,v)\right)_{uv} e_a > \, du\, dv = \int_T < \overrightarrow{x}_{uuvv}, B_I^n(u,v)\, e_a > \, du\, dv - \int_0^1 < \overrightarrow{x}_{uv}(u,1-u), B_i^{n-1}(u)\, e_a > \, du = 0. \tag{45}$$

Therefore if $\overrightarrow{x}$ is a polynomial patch satisfying $\overrightarrow{x}_{uuvv} = 0$ and such that $\overrightarrow{x}_{uv}(u,1-u) = 0$ then it is an extremal for a prescribed border of the functional $\mathcal{F}(\overrightarrow{x})$.

Now let us show the reciprocal. If we suppose that $\overrightarrow{x}$ is an extremal of the functional $\mathcal{F}(\overrightarrow{x})$ among all polynomial patches with a prescribed boundary, then, from Equation (45), it satisfies

$$0 = \int_T < \overrightarrow{x}_{uuvv}, B_I^n(u,v)\, e_a > \, du\, dv \quad \text{for} \quad |I| = n \quad \text{with} \quad i,j,k \neq 0.$$

The polynomial patch $\overrightarrow{x}_{uuvv}$ is a triangular Bézier surface of total degree $n-4$, so if we consider its degree elevation, then we can ensure that $\overrightarrow{x}_{uuvv} = 0$ from Lemma 3.15.

■

REMARK 3.18. *The condition* $\overrightarrow{x}_{uv}(u,1-u) = 0$ *is needed in the triangular case since this term does not vanish here as it happened for the rectangular case. It can be written in terms of the control points as follows:*

$$\overrightarrow{x}_{uv}(u,1-u) = \sum_{|I|=n-2} \Delta^{11} P_I B_I^{n-2}(u,1-u) = \sum_{i=0}^{n-2} \Delta^{11} P_{i,n-2-i,0} B_i^{n-2}(u).$$

Then $\overrightarrow{x}_{uv}(u,1-u) = 0$ *if and only if* $\Delta^{11} P_{i,n-2-i,0} = 0$ *for* $i = 0,...,n-2$, *or equivalently iff*

$$P_{i+1,n-1-i,0} - P_{i,n-1-i,1} - P_{i+1,n-2-i,1} + P_{i,n-2-i,2} = 0 \quad \textit{for} \quad i = 0,...,n-2.$$

3. Masks and triangular permanence patches

In general a condition that relates some control points can be written by means of a mask only if (considering a 3×3 triangular grid),

$$P_{i-1,j-1,k+2}\ P_{i-1,j,k+1}\ P_{i-1,j+1,k}\ P_{i-1,j+2,k-1}$$
$$P_{i,j-1,k+1}\ P_{i,j,k}\ P_{i,j+1,k-1}$$
$$P_{i+1,j-1,k}\ P_{i+1,j,k-1}$$
$$P_{i+2,j-1,k-1}$$

this condition relates the points on the grid in such a way, that the interior point can be expressed in terms of the boundary control points. The mask is then considered to be a stencil for the central point.

When we considered quadratic harmonic surfaces, in section 2.1 of the first chapter, we wrote a "kind" of mask. The inverted commas were there to show that it is not really a mask, because the harmonic condition for quadratic surfaces only relates the control points in a $n = 2$ grid. If we consider the $n = 3$ grid, as we did for the cubic case, in section 2.2 of the same chapter, then the harmonic condition does not relate all the control points in a 3×3 triangular grid. In fact, the interior point could be written in terms of the border control points only after solving a linear system of three equations.

On the other hand, if we consider the biharmonic condition we find that it relates the control points in a 4×4 triangular grid, so a mask cannot really be used. If the following scheme is considered:

$$P_{i-2,j-1,k+3}\ P_{i-2,j,k+2}\ P_{i-2,j+1,k+1}\ P_{i-2,j+2,k}\ P_{i-2,j+3,k-1}$$
$$P_{i-1,j-1,k+2}\ P_{i-1,j,k+1}\ P_{i+1,j+1,k}\ P_{i-1,j+2,k-1}$$
$$P_{i,j-1,k+1}\ P_{i,j,k}\ P_{i,j+1,k-1}$$
$$P_{i+1,j-1,k}\ P_{i+1,j,k-1}$$
$$P_{i+2,j-1,k-1}$$

the following arrangement of coefficients is an easy way to show the coefficient that multiplies each control point and allows us to see which points from the control net are related by the biharmonic condition in Equation (23):

$$\begin{array}{ccccccccc} 4 & & -8 & & 8 & & -4 & & 1 \\ & -8 & & 8 & & -4 & & 0 & \\ & & 8 & & -4 & & 2 & & \\ & & & -4 & & 0 & & & \\ & & & & 1 & & & & \end{array}.$$

Therefore as we have said earlier a mask could not be used to describe the biharmonicity of a patch.

In the following chapter we will present a method, which we will call the third-order method, that will enable us to determine the interior control points in terms of the boundary

points. Therefore, when we consider it on a 3×3 grid of control points we obtain an expression of the interior control point in terms of its nine neighbors, so it can be written using a mask.

Some previous work related to masks can be found in [**14**]. The rectangular Coons patch, as well as the associated discrete Coons patch, satisfies a **Permanence Principle**: *Let two points (u_0, v_0) and (u_1, v_1) define a rectangle R in the domain U of the Coons patch. The four boundaries of this subpatch will map onto four curves on the Coons patch. The Coons patch for those four boundary curves is the original Coons patch restricted to the rectangle R.*

Moreover, as we said before, the rectangular Coons patch is a PDE surface satisfying $\overrightarrow{x}_{uuvv} = 0$ and the discrete version of this partial differential equation is verified exactly by the discrete Coons patch. Farin and Hansford, in the previously cited paper, [**14**], deduced the following rectangular mask from this discrete PDE.

$$P_{i,j} = \frac{1}{4} \times \begin{array}{ccc} -1 & 2 & -1 \\ 2 & \star & 2 \\ -1 & 2 & -1 \end{array}$$

Later we will give an explanation of how they did it. After introducing this mask for the Coons patch, which as we said satisfies the permanence principle, the authors generalized it by defining what they called permanence patches: A permanence patch is obtained from a control net

$$P_{i,j} = \begin{array}{ccc} \alpha & \beta & \alpha \\ \beta & \star & \beta \\ \alpha & \beta & \alpha \end{array}$$

with $4\alpha + 4\beta = 1$.

This kind of mask suggests the possibility of different choices for α and β, so in this sense Farin and Hansford, show how some choices of these values give different masks which are also the discrete form of a PDE, as the discrete version of the Euler-Lagrange PDE $\overrightarrow{x}_{uuvv} = 0$, gave the first rectangular mask $\alpha = \frac{-1}{4}$.

Moreover Farin and Hansford extended the permanence patches concept to the triangular case just by considering the analogous triangular mask.

Given a mask of the form

$$P_{i,j,k} = \begin{array}{ccccccc} & & \alpha & & \beta & & \alpha \\ & \beta & & \star & & \beta & \\ & & \beta & & \beta & & \\ & & & \alpha & & & \end{array} \tag{46}$$

with $3\alpha + 6\beta = 1$ the triangular patch formed with such a control net is called a triangular permanence patch.

Now, let us come back to rectangular patches and show how the $\alpha = \frac{-1}{4}$ mask was deduced from the Euler-Lagrange PDE $\overrightarrow{x}_{uuvv} = 0$.

The discrete version of $\overrightarrow{x}_{uuvv} = 0$ is given by $\Delta^{2,2}P_{i,j} = 0$, where

$$\begin{aligned}\Delta^{1,0}P_{i,j} &= P_{i+1,j} - P_{i,j}\\ \Delta^{0,1}P_{i,j} &= P_{i,j+1} - P_{i,j}.\end{aligned}$$

Then

$$0 = \Delta^{2,2}P_{i,j} = P_{i+2,j+2} - 2P_{i+2,j+1} - 2P_{i+1,j+2} + 4P_{i+1,j+1} - 2P_{i+1,j} - 2P_{i,j+1} + P_{i+2,j} + P_{i,j+2} + P_{i,j}$$

gives

(47)

$$P_{i,j} = \frac{-1}{4}\left(P_{i+1,j+1} - 2P_{i+1,j} - 2P_{i,j+1} - 2P_{i,j-1} - 2P_{i-1,j} + P_{i+1,j-1} + P_{i-1,j+1} + P_{i-1,j-1}\right)$$

that is the rectangular mask $\alpha = \frac{-1}{4}$.

This mask could also be deduced as a consequence of the permanence principle. Let us show this. We will determine for which value of α and β, with $4\alpha + 4\beta = 1$, a permanence patch satisfies the permanence principle.

This principle implies that the control point $P_{i,j}$ can be obtained with the discrete Coons formula, Equation (30), from the boundary control points on a $n \times m$ grid or instead one can apply this formula to any 3×3 grid included in the global grid,

$$\begin{matrix} P_{i-1,j-1} & P_{i-1,j} & P_{i-1,j+1} \\ P_{i,j-1} & P_{i,j} & P_{i,j+1} \\ P_{i+1,j-1} & P_{i+1,j} & P_{i+1,j+1} \end{matrix}.$$

Therefore if we consider that any point in the equation

$$P_{i,j} = \alpha\left(P_{i+1,j+1} + P_{i+1,j-1} + P_{i-1,j-1} + P_{i-1,j+1}\right) + \beta\left(P_{i+1,j} + P_{i,j+1} + P_{i,j-1} + P_{i-1,j}\right),$$

can be written in terms of the boundary control points, as we said by means of Equation (30), it leads us to the value $\alpha = \frac{-1}{4}$.

The permanence principle is not verified by triangular Coons patches so the previous reasoning cannot be followed in order to obtain a mask describing the Coons triangle. Anyway we will introduce a mask, which generates a permanence patch, since it is of the kind defined in Equation (46), and which is related to the triangular Coons patch.

We will consider the triangular control net of a triangular Coons patch of degree 3, instead of the general case of degree n,

$$P_{003} \quad P_{012} \quad P_{021} \quad P_{030}$$

$$P_{102} \quad P_{111} \quad P_{120}$$

$$P_{201} \quad P_{210}$$

$$P_{300}$$

The interior control point, P_{111}, is defined, by Equation (32), in terms of the boundary control points of a grid of degree 2. Moreover, the boundary control points on the degree 3 control net are the control points of the degree elevation of degree 2 border curves.

Then if we consider that any interior or border control point in the equation

$$P_{111} = \alpha\,(P_{003} + P_{030} + P_{300}) + \beta\,(P_{012} + P_{021} + P_{102} + P_{201} + P_{120} + P_{210})$$

can be written, thanks to Equation (32), in terms of control points of a degree 2 control net, we find that equality is only attained for the values $\alpha = \frac{-2}{3}$ and $\beta = \frac{1}{2}$.

Therefore the triangular permanence patch for $\alpha = \frac{-2}{3}$ gives the triangular Coons patch of degree 3, although in general a mask cannot be used to obtain a Coons triangle of degree n.

Let us remark that all schemes whose construction satisfies a variational principle share the permanence principle property, see [**14**]. In the following chapter we will present a method to obtain triangular Bézier PDE surfaces as a solution of a third-order partial differential equation. Then we will show that these surfaces satisfy the permanence principle under some special conditions in the chosen triangular subdomain.

Some other special triangular permanence patches are described in [**14**]. The authors show how some values of α give a permanence patch satisfying a PDE. One choice, related to a PDE that is strongly linked with our work, is the mask corresponding to the value $\alpha = 0$, which is the discrete form of the Laplace PDE

$$\overrightarrow{x}_{uu} + \overrightarrow{x}_{vv} = 0.$$

If we assume that we are applying the harmonic operator $\Delta\overrightarrow{x} = 0$ to a given function $\overrightarrow{x} : \mathcal{R} \to \mathbb{R}^3$, where

$$\mathcal{R} = \{\mathbf{u} \ = (u, v, w) \in \mathbb{R}^3 / u + v + w = 1 \ \text{ and } \ u, v, w \geq 0\},$$

then we could discretely represent this by denoting a node in the triangle finite difference mesh by the integers i, j, k with mesh spacing h so that the coordinates are $u = ih$, $v = jh$ and $w = kh$.

Therefore the discrete representation of the harmonic operator is given by:

$$\begin{aligned} 0 = &\frac{\overrightarrow{x}_{i+1,j,k-1} - 2\overrightarrow{x}_{i,j,k} + \overrightarrow{x}_{i-1,j,k+1}}{h^2} + \frac{\overrightarrow{x}_{i,j+1,k-1} - 2\overrightarrow{x}_{i,j,k} + \overrightarrow{x}_{i,j-1,k+1}}{h^2} \\ &+ \frac{\overrightarrow{x}_{i+1,j-1,k} - 2\overrightarrow{x}_{i,j,k} + \overrightarrow{x}_{i-1,j+1,k}}{h^2}, \end{aligned}$$

that is,

$$\overrightarrow{x}_{i,j,k} = \frac{1}{6}\left(\overrightarrow{x}_{i+1,j,k-1} + \overrightarrow{x}_{i-1,j,k+1} + \overrightarrow{x}_{i,j+1,k-1} + \overrightarrow{x}_{i,j-1,k+1} + \overrightarrow{x}_{i+1,j-1,k} + \overrightarrow{x}_{i-1,j+1,k}\right),$$

which can be diagrammatically represented by the following harmonic mask:

$$P_{i,j,k} = \frac{1}{6} \times \begin{array}{ccccc} & 0 & 1 & 1 & 0 \\ & 1 & \star & 1 & \\ & & 1 & 1 & \\ & & 0 & & \end{array}.$$

Moreover, it is shown in [**14**] that the mask (46) can be described as a blend of a corner twist minimizing mask (the value $\alpha = -1/3$ corresponds to the corner twist minimizer) and a Laplace mask:

$$P_{i,j,k} = \frac{1}{6} \left(e \times \begin{array}{ccccc} & -2 & 2 & 2 & -2 \\ & 2 & \star & 2 & \\ & & 2 & 2 & \\ & & -2 & & \end{array} + (1-e) \times \begin{array}{ccccc} & 0 & 1 & 1 & 0 \\ & 1 & \star & 1 & \\ & & 1 & 1 & \\ & & 0 & & \end{array} \right)$$

Then it can be seen the relation $\alpha = \frac{-e}{3}$:

$$P_{i,j,k} = \frac{1}{6} \times \begin{array}{ccccc} & -2e & 1+e & 1+e & -2e \\ & 1+e & \star & 1+e & \\ & & 1+e & 1+e & \\ & & -2e & & \end{array}.$$

These Farin-Hansford masks will be studied and compared with some others in the chapters that follow.

4. Conclusions

In previous chapters we have described some different surface generation methods that start out from a prescribed set of control points. But, since the best information about the desired shape of a surface comes from its boundary, here we have conducted a study of one of the most important solutions to the problem of finding a surface interpolating boundary curves: triangular Coons patches in comparison with rectangular Coons patches.

We have seen that the problem of finding a polynomial extremal of the functional

$$\mathcal{F}(\overrightarrow{x}) = \int_U \|\overrightarrow{x_{uv}}\|^2 du\, dv,$$

among all rectangular patches with the same boundary is equivalent to solving the PDE $\overrightarrow{x}_{uuvv} = 0$ and, moreover, that the Coons rectangular patch is a solution. But, we have seen that triangular Coons patches are not extremals of this functional.

Therefore, we have studied the conditions under which it would be equivalent to find an extremal of $\mathcal{F}$ among all polynomial triangular patches with a prescribed boundary and to solve the PDE $\overrightarrow{x}_{uuvv} = 0$.

Moreover, we have characterized the control net of a triangular Bézier extremal of the functional $\mathcal{F}$. From this characterization we have developed two methods to generate triangular patches given the boundary curves. The first method is to find the extremals of the functional as a solution of a linear system of the control points. The second method makes

it possible to build a Bézier triangle by means of a mask deduced from the characterization of cubical extremals.

On the other hand, we have defined the Triangular Discrete Coons patch and we have compared the shapes of the surfaces obtained by these three surface generation methods. We have observed that better results are obtained for the extremals of the functional and for the triangular Coons patch, but the Coons patch implies an increase of degree. We also compared Coons patches' results with our results about biharmonic surfaces described in the previous chapter.

CHAPTER 4

Constructing triangular Bézier surfaces using linear PDEs:

The third-order method

In the previous chapters our goal was to determine the triangular Bézier patch by verifying the harmonic or the biharmonic condition for a prescribed set of control points, which were previously fixed. We saw that, given two lines of control points, a triangular Bézier surface is totally determined by the harmonic condition, $\Delta \overrightarrow{x} = 0$, which a second-order equation PDE: $\Delta \overrightarrow{x} = \overrightarrow{x}_{uu} + \overrightarrow{x}_{vv}$. The pair of lines of control points were the first and the second row at Theorem 1.9, and two border lines (with the substitution of some of them by a neighboring point) in Theorem 1.18. In the biharmonic case we were able to determine a biharmonic triangular Bézier patch given four lines of control points. It should be noted that the biharmonic condition is a fourth-degree partial differential equation.

Therefore, it is natural to think about our next goal: Given all the border control points (three lines), to determine an associated Bézier surface that will fulfill a third-order condition. This can be achived if we consider third-order PDEs.

1. The third-order PDE

Since there is no natural third-order PDE, let us consider a general linear third-order operator with constant coefficients:

$$R\left(\overrightarrow{x}\right) = \alpha \overrightarrow{x}_{uuu} + \beta \overrightarrow{x}_{uuv} + \gamma \overrightarrow{x}_{vvu} + \delta \overrightarrow{x}_{vvv}.$$

and the corresponding third-order PDE: $R\left(\overrightarrow{x}\right) = 0$.

Let $\overrightarrow{x}$ be a triangular Bézier surface. The third order PDE

$$\alpha \overrightarrow{x}_{uuu} + \beta \overrightarrow{x}_{uuv} + \gamma \overrightarrow{x}_{vvu} + \delta \overrightarrow{x}_{vvv} = 0, \tag{48}$$

in terms of control points is

$$\begin{aligned} 0 =& \left(\alpha \frac{\partial^3}{\partial u^3} + \beta \frac{\partial^3}{\partial u^2 v} + \gamma \frac{\partial^3}{\partial v^2 u} + \delta \frac{\partial^3}{\partial v^3}\right) \overrightarrow{x}\left(\mathbf{u}\right) \\ =& n\left(n-1\right)\left(n-2\right) \sum_{|I|=n-3} \left(\alpha \Delta^{3,0} P_I + \beta \Delta^{2,1} P_I + \gamma \Delta^{1,2} P_I + \delta \Delta^{0,3} P_I\right) B_I^{n-3}\left(\mathbf{u}\right) \end{aligned}$$

$$
\begin{aligned}
=&\frac{n!}{(n-3)!}\sum_{|I|=n-3}[\alpha\left(P_{I+3e_1}-3P_{I+2e_1+e_3}+3P_{I+e_1+2e_3}-P_{I+3e_3}\right)\\
&+\beta\left(P_{I+2e_1+e_2}-P_{I+2e_1+e_3}-2P_{I+e_1+e_2+e_3}+2P_{I+e_1+2e_3}+P_{I+e_2+2e_3}-P_{I+3e_3}\right)\\
&+\gamma\left(P_{I+e_1+2e_2}+P_{I+e_1+2e_3}-2P_{I+e_1+e_2+e_3}+2P_{I+e_2+2e_3}-P_{I+2e_2+e_3}-P_{I+3e_3}\right)\\
&+\delta\left(P_{I+3e_2}-3P_{I+2e_2+e_3}+3P_{I+e_2+2e_3}-P_{I+3e_3}\right)]B_I^{n-3}\left(\mathbf{u}\right)\\
=&\sum_{|I|=n-3}Q_I\,B_I^{n-3}\left(\mathbf{u}\right).
\end{aligned}
$$

Hence $R\left(\overrightarrow{x}\right)=0$ if and only if $Q_I=0$ for all $|I|=n-3$, i.e., if and only if

$$
\begin{aligned}
0=&\left(-\alpha-\beta-\gamma-\delta\right)P_{i-1,j-1,k+2}+\left(\beta+2\gamma+3\delta\right)P_{i-1,j,k+1}+\left(-\gamma-3\delta\right)P_{i-1,j+1,k}\\
&+\delta P_{i-1,j+2,k-1}+\left(3\alpha+2\beta+\gamma\right)P_{i,j-1,k+1}-2\left(\beta+\gamma\right)P_{i,j,k}+\gamma P_{i,j+1,k-1}\\
&+\left(-3\alpha-\beta\right)P_{i+1,j-1,k}+\beta P_{i+1,j,k-1}+\alpha P_{i+2,j-1,k-1},
\end{aligned}
\tag{49}
$$

for all $|I|=n-3$.

2. Mask formulation

Let us consider the control points according to the following scheme,

$$
\begin{array}{c}
P_{i-1,j-1,k+2}\ P_{i-1,j,k+1}\ P_{i-1,j+1,k}\ P_{i-1,j+2,k-1}\\
P_{i,j-1,k+1}\ P_{i,j,k}\ P_{i,j+1,k-1}\\
P_{i+1,j-1,k}\ P_{i+1,j,k-1}\\
P_{i+2,j-1,k-1}.
\end{array}
$$

If the boundary of the previous grid was known, then the interior point, $P_{i,j,k}$, could be determined by

$$
\begin{aligned}
P_{i,j,k}=\frac{1}{2\left(\beta+\gamma\right)}\big(&\left(-\alpha-\beta-\gamma-\delta\right)P_{i-1,j-1,k+2}+\left(\beta+2\gamma+3\delta\right)P_{i-1,j,k+1}\\
&+\left(-\gamma-3\delta\right)P_{i-1,j+1,k}+\delta P_{i-1,j+2,k-1}+\left(3\alpha+2\beta+\gamma\right)P_{i,j-1,k+1}\\
&+\gamma P_{i,j+1,k-1}+\left(-3\alpha-\beta\right)P_{i+1,j-1,k}+\beta P_{i+1,j,k-1}+\alpha P_{i+2,j-1,k-1}\big),
\end{aligned}
\tag{50}
$$

for all $|I|=n$.

A better way of writing this is to use a mask:

$$
P_{i,j,k}=\frac{1}{2\left(\beta+\gamma\right)}\times
\begin{array}{ccccc}
-\alpha-\beta-\gamma-\delta & & \beta+2\gamma+3\delta & -\gamma-3\delta & \delta\\
& 3\alpha+2\beta+\gamma & \star & \gamma & \\
& & -3\alpha-\beta & \beta & \\
& & & \alpha &
\end{array}
\tag{51}
$$

This mask suggests the possibility of having different choices for the parameters α, β, γ and δ which could also be reduced to only three parameters, since the general third-order PDE, Equation (48), could be divided by any of them.

In the following sections we will discuss the choice of the values of α, β, γ and δ.

But before going onto particular cases let us now state the permanence principle fulfilled by triangular patches obtained by the third-order method.

3. The permanence principle

The triangular patches that are obtained as a solution of a third order PDE, such as Equation (48), do not satisfy the permanence principle for all triangular subpatches but only for those defined on isosceles right triangles.

LEMMA 4.1. *Let us consider a triangular patch with a prescribed boundary defined on the triangular domain*

$$T = \{(u, v) \in \mathbb{R}^2 : 0 \leq u, 0 \leq v, u + v \leq 1\}$$

satisfying the general linear third-order PDE

$$\alpha \overrightarrow{x}_{uuu} + \beta \overrightarrow{x}_{uuv} + \gamma \overrightarrow{x}_{uvv} + \delta \overrightarrow{x}_{vvv} = 0,$$

where two of the four coefficients $\alpha, \beta, \gamma, \delta$, are other than zero.

Let two points (u_0, v_1) and (u_1, v_0), with $u_0 < u_1$ and $v_0 < v_1$, define a right triangle T_1 in the domain T of a triangular patch.

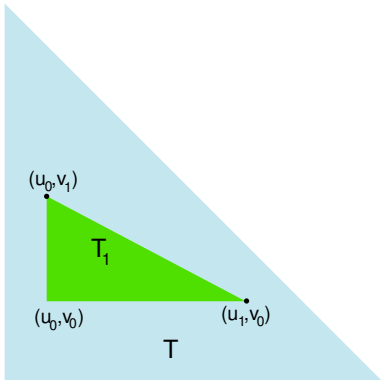

FIGURE 1. Two points determine a right triangle hypotenuse.

The three boundaries of this subdomain will map onto three curves on the solution triangular patch. Thus the triangular patch that is obtained by the third-order method by prescribing those three boundary curves is the original solution triangular patch restricted to the right triangle T_1 if and only if it is an isosceles triangle.

Proof: Let $\overrightarrow{x}(u, v)$, $u, v \in T$ be a solution with a prescribed boundary of a third-order PDE

$$\alpha \overrightarrow{x}_{uuu} + \beta \overrightarrow{x}_{uuv} + \gamma \overrightarrow{x}_{uvv} + \delta \overrightarrow{x}_{vvv} = 0,$$

where two of the four coefficients $\alpha, \beta, \gamma, \delta$, are different from zero.

Let us consider the patch

$$\overrightarrow{y}(u,v) = \overrightarrow{x}(u_0 + u(u_1 - u_0), v_0 + v(v_1 - v_0)) \quad u, v \in T$$

which is the restriction of $\overrightarrow{x}(u,v)$ on the triangle T_1.

Then if we compute the partial derivatives of $\overrightarrow{y}$ what we obtain is:

$$\begin{aligned}
&(\alpha \overrightarrow{y}_{uuu} + \beta \overrightarrow{y}_{uuv} + \gamma \overrightarrow{y}_{uvv} + \delta \overrightarrow{y}_{vvv})(u,v) = \\
&= \big(\alpha (u_1 - u_0)^3 \overrightarrow{x}_{uuu} + \beta (u_1 - u_0)^2 (v_1 - v_0) \overrightarrow{x}_{uuv} + \gamma (u_1 - u_0)(v_1 - v_0)^2 \overrightarrow{x}_{uvv} \\
&\quad + \delta (v_1 - v_0)^3 \overrightarrow{x}_{vvv}\big)(u_0 + u(u_1 - u_0), v_0 + v(v_1 - v_0)).
\end{aligned}$$

In general, this expression does not vanish except when $(u_1 - u_0) = (v_1 - v_0)$, that is, only for triangular subpatches defined on isosceles right triangles.

■

REMARK 4.2. *Here we have only considered subtriangles on T determined by points (u_0, v_1) and (u_1, v_0) with $u_0 < u_1$ and $v_0 < v_1$. The previous lemma could be performed for the rest of cases analogously by just a different change of variable.*

4. The symmetric mask

From the multiple choices of the parameters $\alpha, \beta, \gamma, \delta$, in this section we will study the symmetric cases of the mask in Equation (51). We can distinguish two levels of symmetry, strong and weak symmetry.

Weak symmetry: These are the conditions that the coefficients α, β, γ and δ must fulfill for the mask in Equation (51) to be a symmetric mask

$$\left.\begin{aligned}
-\alpha - \beta - \gamma - \delta = \delta = \alpha \\
3\alpha + 2\beta + \gamma = \beta = -\gamma - 3\delta \\
\beta + 2\gamma + 3\delta = \gamma = -3\alpha - \beta
\end{aligned}\right\}.$$

This implies $\alpha = \delta = -\frac{\beta+\gamma}{3}$, so this is the symmetric case:

$$P_{i,j,k} = \begin{array}{ccccc}
-\frac{1}{6} & & \frac{\gamma}{2(\beta+\gamma)} & & \frac{\beta}{2(\beta+\gamma)} & & -\frac{1}{6} \\
& \frac{\beta}{2(\beta+\gamma)} & & \star & & \frac{\gamma}{2(\beta+\gamma)} & \\
& & \frac{\gamma}{2(\beta+\gamma)} & & \frac{\beta}{2(\beta+\gamma)} & & \\
& & & -\frac{1}{6} & & &
\end{array}. \tag{52}$$

The corresponding operator is

$$S_{\beta,\gamma}(\overrightarrow{x}) = -\frac{1}{6}\overrightarrow{x}_{uuu} + \frac{1}{2(\beta+\gamma)}(\beta \overrightarrow{x}_{uuv} + \gamma \overrightarrow{x}_{uvv}) - \frac{1}{6}\overrightarrow{x}_{vvv}.$$

Strong symmetry: If there are only two different coefficients, one for the vertices and another for the rest of the positions on the mask, then we can talk of strong symmetry. A particular and special case of the symmetric mask in Equation (52) is obtained when $\beta = \gamma$. The third-order operator is

$$S(\overrightarrow{x}) = -\frac{1}{6}\overrightarrow{x}_{uuu} + \frac{1}{4}\left(\overrightarrow{x}_{uuv} + \overrightarrow{x}_{uvv}\right) - \frac{1}{6}\overrightarrow{x}_{vvv},$$

hence the associated PDE $S(\overrightarrow{x}) = 0$ does not depend on β and so the associated mask is given by

$$P_{i,j,k} = \begin{array}{ccccc} -\frac{1}{6} & & \frac{1}{4} & & \frac{1}{4} & & -\frac{1}{6} \\ & \frac{1}{4} & & & & \frac{1}{4} & \\ & & \frac{1}{4} & \star & \frac{1}{4} & & \\ & & & -\frac{1}{6} & & & \end{array}, \tag{53}$$

which turns into a Farin-Hansford mask, see [**14**], defined in Equation (46) with $\alpha = \frac{-1}{6}$. Therefore, the PDE surfaces formed with this mask are also triangular permanence patches. In fact, a special case of permanence patch which has quadratic precision.

The triangular permanence patches resulting from $\alpha = \frac{-1}{6}$ enjoy a quadratic precision property, see [**14**], in the sense that: Given a quadratic discrete patch **Q**, we degree elevate it to an arbitrary degree n, resulting in a patch **EQ**, then the patch obtained with the symmetric mask for given boundaries results in a patch **PEQ** satisfying **PEQ=EQ**

Now we will present a discussion about the existence of a triangular Bézier solution of the third-order PDE $S(\overrightarrow{x}) = 0$.

5. About the existence of solutions

In this section we will see how a triangular PDE Bézier surface satisfying

$$-\frac{1}{6}\overrightarrow{x}_{uuu} + \frac{1}{4}\left(\overrightarrow{x}_{uuv} + \overrightarrow{x}_{uvv}\right) - \frac{1}{6}\overrightarrow{x}_{vvv} = 0 \tag{54}$$

can be determined from a prescribed border.

If this problem is considered in terms of Bézier control points then a solution of the previous PDE must satisfy the following system of linear equations

$$\begin{aligned} P_{i,j,k} = &-\frac{1}{6}\left(P_{i+2,j-1,k-1} + P_{i-1,j+2,k-1} + P_{i-1,j-1,k+2}\right) \\ &+\frac{1}{4}\left(P_{i-1,j,k+1} + P_{i-1,j+1,k} + P_{i,j-1,k+1} + P_{i,j+1,k-1} + P_{i+1,j-1,k} + P_{i+1,j,k-1}\right). \end{aligned} \tag{55}$$

These equations can be described, as we said before, by the mask in Equation (53). That is, each equation in the system, shows how every interior control point can be represented as a linear combination of its triangular neighboring control points, that is: $P_i = \sum_{j \in N_i} \lambda_{ij} P_j$, where N_i denotes the 9 neighboring control points of an interior control point P_i.

This kind of systems was studied extensively in [**18**], where a very interesting method to discuss the existence of solution when the coefficients, λ_{ij}, are a partition of unity was obtained. In the following proposition we describe the weak sufficient condition, which was derived in the cited paper, for the solvability of this kind of linear systems.

PROPOSITION 4.3. *Let the set of weights λ_{ij} be a partition of unity. Then, the linear system of n equations*

$$P_i = \sum_{j \in N_i} \lambda_{ij} P_j, \qquad i = 0, ..., n,$$

has unique solution. These equations require that each interior control point, P_i for $i = 0, ..., n$, be some convex combination of its neighbors, P_j with $j \in N_i$. Thus P_i will be contained in the convex hull of its neighbors.

This result turns out to be a very useful tool in order to discuss the existence of solutions of linear systems derived from masks, both in the rectangular and the triangular case, but with the restriction of having positive weights such that $\sum_{j \in N_i} \lambda_{ij} = 1$. This restriction of having coefficients being a partition of unity is not fulfilled in our case. Although we have that $\sum_{j \in N_i} \lambda_{ij} = 1$, even for our most general mask, in Equation (51), we find that in all particular cases negative weights appear. Therefore, this method cannot be used to discuss the solvability of our problem. Moreover, it is not possible to do a variation of the proof of this result for masks with negative weights since it is based on the convex hull concept, where positive numbers are needed.

The existence of solutions to this kind of problem is not studied by many authors, the reasoning being the following. When we consider a surface generation method which allows us to obtain a patch with a prescribed boundary as a solution of a linear system, if given the boundary curves, it was found that the associated system was incompatible, then a slight change of the boundary curves would probably turn the system into a compatible one.

On the other hand, there are many other authors, such as Floater and Reimers in [**18**], who show their interest on discussing the existence of solutions to these problems using different and interesting techniques.

The existence of solutions also lies within our field of interest. In order to prove our results easily, at the moment we will work with the usual basis of polynomials instead of with the Bernstein basis.

Let $\overrightarrow{x}$ be a polynomial function of degree $n \geq 3$ in terms of the usual basis of polynomials:

$$\overrightarrow{x}\,(u, v) = \sum_{k,l=0}^{n} \frac{a_{k,l}}{k!l!} u^k v^l.$$

Since the total degree is supposed to be n, then $k + l \leq n$, and there are some null coefficients:

$$a_{k,l} = 0 \qquad \text{if} \qquad k + l > n.$$

Moreover, if the polynomial, $\overrightarrow{x}$, satisfies the third-order PDE, $S(\overrightarrow{x}) = 0$, this condition can be translated into a system of linear equations in terms of the coefficients $\{a_{k,l}\}_{k,l=0}^{n}$

$$-\frac{1}{6}a_{k+3,l} + \frac{1}{4}\left(a_{k+2,l+1} + a_{k+1,l+2}\right) - \frac{1}{6}a_{k,l+3} = 0, \qquad k,l = 0,...,n \tag{56}$$

with the convention $a_{k,l} = 0$ if $k + l > n$.

The following triangular scheme shows that $a_{k,l} = 0$ if $k + l > n$ and that the coefficients at the diagonal lines, see the boxed coefficients, fulfill the requirement that $k + l = r$ for $r = 0, ..., n$.

$$\begin{array}{ccccccccc}
a_{0,0} & a_{0,1} & a_{0,2} & a_{0,3} & a_{0,4} & \cdots & \boxed{a_{0,r}} & \cdots & a_{0,n} \\
a_{1,0} & a_{1,1} & a_{1,2} & a_{1,3} & \cdots & \boxed{a_{1,r-1}} & \cdots & a_{1,n-1} & \\
a_{2,0} & a_{2,1} & a_{2,2} & \cdots & \boxed{a_{2,r-2}} & \cdots & a_{2,n-2} & & \\
a_{3,0} & a_{3,1} & \cdots & \boxed{a_{3,r-3}} & & & & & \\
\vdots & \vdots & & & & & & & \\
a_{r-1,0} & \boxed{a_{r-1,1}} & \cdots & a_{r-1,n-r+1} & & & & & \\
\boxed{a_{r,0}} & \cdots & a_{r,n-r} & & & & & & \\
\vdots & & & & & & & & \\
a_{n,0} & & & & & & & &
\end{array}$$

FIGURE 2. Scheme of coefficients

In the following lemma we prove that the knowledge of the first three lines of coefficients of a polynomial satisfying $S(\overrightarrow{x}) = 0$, determines all of them.

LEMMA 4.4. *Let*

$$\overrightarrow{x}(u,v) = \sum_{k,l=0}^{n} \frac{a_{k,l}}{k!l!} u^k v^l$$

be a polynomial function of degree $n \geq 3$ verifying the third-order PDE, $S(\overrightarrow{x}) = 0$, then, the coefficients $\{a_{k,l}\}_{k=3,l=0}^{n}$ are totally determined by $\{a_{0,l}, a_{1,l}, a_{2,l}\}_{l=0}^{n}$.

Proof:

We have seen above that the third-order PDE, $S(\overrightarrow{x}) = 0$, can be translated into a system of linear equations given in Equation (56). So, first of all, let us consider the coefficients $\{a_{3,l}\}_{l=0}^{n}$. We find that each of these coefficients is determined by the trio $\{a_{0,l+3}, a_{1,l+2}, a_{2,l+1}\}_{l=0}^{n}$.

Analogously, any coefficient $a_{k,l}$ with $k > 2$ can be related with $\{a_{k-3,l+3}, a_{k-2,l+2}, a_{k-1,l+1}\}$ and so on until the second subindex is greater than n.

■

Now in order to ensure the solvability of the linear system given in Equation (56), we will split it into $n-2$ subsystems. Each of them relates the coefficients in a diagonal with $k+l=r$ for $r=3,...,n$.

$$
\begin{aligned}
-\frac{1}{6}a_{r,0}+\frac{1}{4}\left(a_{r-1,1}+a_{r-2,2}\right)-\frac{1}{6}a_{r-3,3}&=0\\
-\frac{1}{6}a_{r-1,1}+\frac{1}{4}(a_{r-2,2}+a_{r-3,3})-\frac{1}{6}a_{r-4,4}&=0\\
-\frac{1}{6}a_{r-2,2}+\frac{1}{4}(a_{r-3,3}+a_{r-4,4})-\frac{1}{6}a_{r-5,5}&=0\\
\cdots&\\
-\frac{1}{6}a_{3,r-3}+\frac{1}{4}\left(a_{2,r-2}+a_{1,r-1}\right)-\frac{1}{6}a_{0,r}&=0.
\end{aligned}
\tag{57}
$$

In the following lemma we will see that, for all $r\geq 3$, knowledge of the coefficients $a_{r,0}$, $a_{1,r-1}$ and $a_{0,r}$ determines all the coefficients in the diagonal r.

LEMMA 4.5. *Let $r\geq 3$. If the coefficients $a_{r,0}$, $a_{1,r-1}$ and $a_{0,r}$ are known, then the linear system given in Equation (56) for all k,l such that $k+l=r$ and involving coefficients with non negative subindexes, ($r-2$ equations), and with the unknowns $\{a_{k,l}\}$ with $k+l=r$, $k>1$ and $l>0$, has a unique solution.*

Proof:

Let us consider the linear subsystem in Equation (57). Let us recall that $a_{r,0}$, $a_{1,r-1}$ and $a_{0,r}$ are assumed to be known, so the associated coefficient matrix is the Toeplitz tetradiagonal matrix, $M_{r-2}^{\left(-\frac{1}{6},\frac{1}{4},\frac{1}{4},-\frac{1}{6}\right)}$. Therefore, its determinant, given in Corollary 1.16, is

$$
D_n=\frac{1}{3^{n+2}2^{2n}}\left(2^{2n+3}+2^{n+1}\left(-1\right)^n-1\right),
\tag{58}
$$

which does not vanish for $n\in\mathbb{N}$.

Therefore, there exists a unique solution of the system given in Equation (57).

■

REMARK 4.6. *The linear subsystems in Lemma 4.5 can be represented as the matrix equation:*

$$
M_{r-2}^{(a,b,b,a)}.\begin{pmatrix} a_{r-1,1}\\ a_{r-2,2}\\ a_{r-3,3}\\ \vdots\\ a_{3,r-3}\\ a_{2,r-2}\end{pmatrix}=\begin{pmatrix} -aa_{r,0}\\ 0\\ \vdots\\ 0\\ -ba_{1,r-1}\\ -ba_{1,r-1}+aa_{0,r}\end{pmatrix},
$$

where $a = \frac{-1}{6}$ *and* $b = \frac{1}{4}$.

At this point we have that the first column and the first two lines of coefficients determine the whole of the coefficients of a polynomial that fulfills $S(\overrightarrow{x}) = 0$.

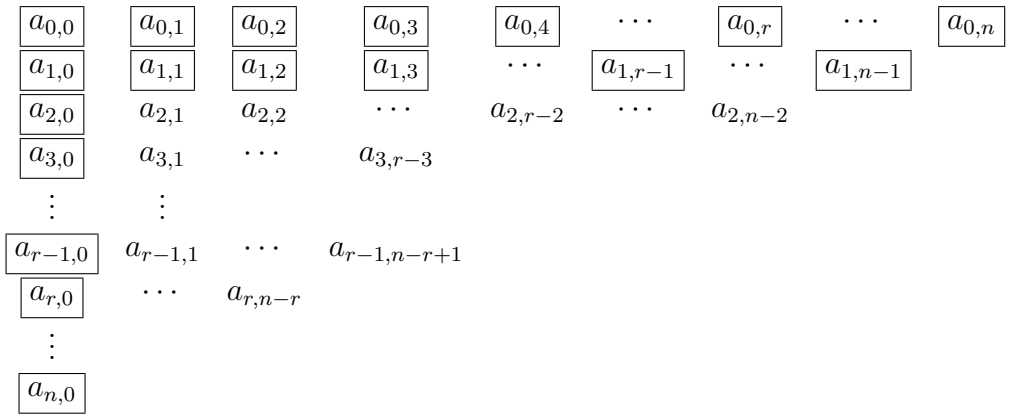

FIGURE 3. The boxed coefficients determine all of the others.

Let us denote the unique solution of each subsystem, given by Equation (57), in terms of $a_{r,0}$, $a_{1,r-1}$ and $a_{0,r}$, as follows

$$a_{k,r-k} = c^k_{r,0}a_{r,0} + c^k_{1,r-1}a_{1,r-1} + c^k_{0,r}a_{0,r} \tag{59}$$

for $k = 2, ..., r-1$. Moreover, if we define

$$\begin{aligned} c^r_{r,0} &= 1, \quad c^r_{1,r-1} = 0, \quad c^r_{0,r} = 0, \\ c^1_{r,0} &= 0, \quad c^1_{1,r-1} = 1, \quad c^1_{0,r} = 0, \\ c^0_{r,0} &= 0, \quad c^0_{1,r-1} = 0, \quad c^0_{0,r} = 1, \end{aligned}$$

we can extend our notation in Equation (59) for $k = 0, ..., r$.

In the following lemma we will compute the coefficients $c^k_{r,0}$, $c^k_{1,r-1}$ and $c^k_{0,r}$ for $k = 2, ..., r-1$. That is, we will give an explicit solution of the subsystems for $r = 3, ..., n$, in terms of $a_{r,0}$, $a_{1,r-1}$ and $a_{0,r}$.

LEMMA 4.7. *The coefficients* $c^k_{r,0}$, $c^k_{1,r-1}$ *and* $c^k_{0,r}$, *which appear in the expression of* $a_{k,r-k}$ *in terms of* $a_{r,0}$, $a_{1,r-1}$ *and* $a_{0,r}$ *given in Equation (59), can be computed by the following*

formulas

$$
\begin{aligned}
c_{r0}^{k} &= \frac{-a}{\det M_{r-2}^{(a,b,b,a)}}\,(-1)^{r-k+1}\,A_{1,r-k},\\
c_{1r-1}^{k} &= \frac{1}{\det M_{r-2}^{(a,b,b,a)}}\left(-a\,(-1)^{2r-3-k}\,A_{r-3,r-k} - b\,(-1)^{2r-2-k}\,A_{r-2,r-k}\right),\\
c_{0r}^{k} &= \frac{-a}{\det M_{r-2}^{(a,b,b,a)}}\,(-1)^{2r-2-k}\,A_{r-2,r-k},
\end{aligned}
\tag{60}
$$

where $a = \frac{-1}{6}$, $b = \frac{1}{4}$, *and* $A_{i,j}$ *denotes the so-called minors of the matrix, obtained by taking the determinant after removing the i-th row and j-th column of the matrix* $M_{r-2}^{(a,b,b,a)}$.

Proof: We will compute the solution of the linear system given in Equation (57) by using Cramer's rule:

$$
a_{k,r-k} = \frac{1}{\det M_{r-2}^{\left(-\frac{1}{6},\frac{1}{4},\frac{1}{4},-\frac{1}{6}\right)}}
\begin{vmatrix}
b & b & a & 0 & \cdots & -a\,a_{r0} & 0 & 0\\
a & b & b & a & 0 & 0 & 0 & 0\\
0 & a & b & b & a & \vdots & \cdots & 0\\
\vdots & \ddots & \ddots & \ddots & \ddots & 0 & \ddots & \vdots\\
0 & \cdots & \ddots & \ddots & b & \vdots & \ddots & 0\\
0 & 0 & \cdots & \ddots & a & \vdots & b & a\\
0 & 0 & 0 & \cdots & 0 & -a\,a_{1r-1} & b & b\\
0 & 0 & 0 & \cdots & 0 & -b\,a_{1r-1} - a\,a_{0,r} & a & b
\end{vmatrix}_{(r-2)\times(r-2)}
$$

$$
\uparrow
$$

$$
(r-k)
$$

$$
column
$$

$$
\begin{aligned}
= \frac{1}{\det M_{r-2}^{\left(-\frac{1}{6},\frac{1}{4},\frac{1}{4},-\frac{1}{6}\right)}}\Big(&-a\,a_{r0}\,(-1)^{1+r-k}\,A_{1,r-k} - a\,a_{1r-1}\,(-1)^{r-3+r-k}\,A_{r-3,r-k}\\
&+ (-b\,a_{1r-1} - a\,a_{0r})\,(-1)^{r-2+r-k}\,A_{r-2,r-k}\Big).
\end{aligned}
$$

■

In the following two lemmas we will give a recursive formula and the general term of a specific determinant which will appear in the proof of the next theorem, Theorem 4.12.

LEMMA 4.8. *The determinant, d_n, of the matrix $m_n^{(a,b,c,d)}$ defined by*

$$m_n^{(a,b,c,d)} = \begin{pmatrix} b & c & d & 0 & \cdots & 0 & 0 & 0 \\ a & b & c & d & 0 & \cdots & 0 & 0 \\ 0 & a & b & c & d & 0 & \cdots & 0 \\ \vdots & \ddots & \ddots & \ddots & \ddots & \ddots & \ddots & \vdots \\ 0 & \cdots & 0 & a & b & c & d & 0 \\ 0 & 0 & \cdots & 0 & a & b & c & d \\ 0 & 0 & 0 & \cdots & 0 & a & b & c \\ -1 & 1 & \cdots & \cdots & \cdots & (-1)^n & & \end{pmatrix} \tag{61}$$

can be determined by the following non-homogeneous recursive equation where $D_n = |M_n^{(a,b,c,d)}|$

$$d_n + c\,d_{n-1} + db\,d_{n-2} + ad^2\,d_{n-3} = (-1)^n\ D_{n-1} + ad\ (-1)^{n-1}\,D_{n-3}. \tag{62}$$

Proof: We compute this determinant doing expansion by minors. We start by the last column:

$$d_n = (-1)^n D_{n-1} + c(-1)^{2n-1} d_{n-1} + d(-1)^{2n-2} \left|\begin{array}{ccc|cc} & & & 0 & 0 \\ & & & \vdots & \vdots \\ & M_{n-3}^{(a,b,c,d)} & & & \\ & & & 0 & 0 \\ & & & d & 0 \\ & & & c & d \\ \hline 0 & \cdots & 0 & a & b \\ -1 & 1 & \cdots & \cdots & (-1)^{n-1} \end{array}\right|$$

$$= (-1)^n D_{n-1} + c(-1)^{2n-1} d_{n-1} + d(-1)^{n-1} \left|\begin{array}{ccc|c} & & & 0 \\ & & & \vdots \\ & M_{n-3}^{(a,b,c,d)} & & 0 \\ & & & d \\ & & & c \\ \hline 0 & \cdots & 0 & a \\ -1 & 1 & \cdots & (-1)^{n-1} \end{array}\right|$$

$$+ db(-1)^{2n-3} d_{n-2} + d^2(-1)^{2n-4} \left|\begin{array}{ccc|cc} & & & 0 & 0 \\ & & & \vdots & \vdots \\ & M_{n-4}^{(a,b,c,d)} & & 0 & 0 \\ & & & d & 0 \\ & & & c & d \\ \hline 0 & \cdots & 0 & 0 & a \\ -1 & 1 & \cdots & \cdots & (-1)^{n-1} \end{array}\right|$$

$$= (-1)^n\,D_{n-1} - c\,d_{n-1} + ad(-1)^{n-1}\,D_{n-3} - db\,d_{n-2} - ad^2\,d_{n-3}.$$

■

Now we compute the corresponding n-term of this determinant in our particular case.

LEMMA 4.9. *The determinant of the matrix* $m_n^{(\frac{-1}{6},\frac{1}{4},\frac{1}{4},\frac{-1}{6})}$, *which can be obtained by the recursive formula given in Equation (62), has the following n-term*

$$d_n = \frac{4}{3^{n+3}}\left(4\left(2\,(-1)^n - \left(\frac{-1}{4}\right)^n - \frac{1}{2^n}\right) + 3\left(\frac{-1}{4}\right)^n\left(-1+4^{n+1}\right)n\right).$$

Proof: The non-homogeneous recursive rule which defines the determinant, d_n, of the matrix $m_n^{(\frac{-1}{6},\frac{1}{4},\frac{1}{4},\frac{-1}{6})}$ is

$$d_n + \frac{1}{4}\,d_{n-1} - \frac{1}{24}\,d_{n-2} - \frac{1}{216}\,d_{n-3} = f(n) \tag{63}$$

where, bearing in mind that D_n is defined by Equation (58), we have that

$$f(n) = (-1)^n D_{n-1} + \frac{1}{36}(-1)^{n-1} D_{n-3} = 2\left(\frac{-1}{3}\right)^n + 4\left(\frac{-1}{12}\right)^n.$$

We will find the solution of this recurrence equation as the sum $d_n = d_n^h + d_n^p$, where d_n^h is the solution of the corresponding homogeneous equation and d_n^p is a particular solution of Equation (63).

Following the usual method, we obtain the solution of the homogeneous equation:

$$d_n^h = A\left(\frac{-1}{3}\right)^n + B\left(\frac{-1}{12}\right)^n + C\left(\frac{1}{6}\right)^n.$$

Now we must find a single solution of the full recurrence

$$d_n + \frac{1}{4}\,d_{n-1} - \frac{1}{24}\,d_{n-2} - \frac{1}{216}\,d_{n-3} = f(n),$$

but we will obtain it as the sum of a pair of particular solutions of the equations

$$d_n + \frac{1}{4}\,d_{n-1} - \frac{1}{24}\,d_{n-2} - \frac{1}{216}\,d_{n-3} = 2\left(\frac{-1}{3}\right)^n$$

$$d_n + \frac{1}{4}\,d_{n-1} - \frac{1}{24}\,d_{n-2} - \frac{1}{216}\,d_{n-3} = 4\left(\frac{-1}{12}\right)^n.$$

Since $\frac{-1}{3}$ and $\frac{-1}{12}$ are solutions of the homogeneous characteristic equation it is obvious that the particular solutions we seek can not be of the form

$$k_1\left(\frac{-1}{3}\right)^n \text{ and } \quad k_2\left(\frac{-1}{12}\right)^n.$$

Therefore, we guess that the solutions are of the form

$$k_1\,2n\left(\frac{-1}{3}\right)^n \text{ and } \quad k_2\,4n\left(\frac{-1}{12}\right)^n,$$

respectively. Substituting this values into the corresponding recurrence equations gives us that $k_1 = \frac{8}{9}$ and $k_2 = \frac{-1}{9}$, then

$$d_n^p = \frac{16}{9} n \left(\frac{-1}{3}\right)^n - \frac{-4}{9} n \left(\frac{-1}{12}\right)^n,$$

is a particular solution of Equation (63).

The general term is given by

$$d_n = A \left(\frac{-1}{3}\right)^n + B \left(\frac{-1}{12}\right)^n + C \left(\frac{1}{6}\right)^n + \frac{16}{9} n \left(\frac{-1}{3}\right)^n - \frac{-4}{9} n \left(\frac{-1}{12}\right)^n,$$

and we finally determine the coefficients $A = B = \frac{-16}{27}$ and $C = \frac{32}{27}$ by applying the initial conditions $d_1 = -1, d_2 = \frac{1}{2}$ and $d_3 = \frac{-35}{144}$. Therefore,

$$d_n = \frac{4}{3^{n+3}} \left(4 \left(2\,(-1)^n - \left(\frac{-1}{4}\right)^n - \frac{1}{2^n}\right) + 3 \left(\frac{-1}{4}\right)^n \left(-1 + 4^{n+1}\right) n\right).$$

■

REMARK 4.10. *We must remark that the determinant, d_n, of the matrix $m_n^{(\frac{-1}{6}, \frac{1}{4}, \frac{1}{4}, \frac{-1}{6})}$ does not vanish for any value of n.*

If n is even, then

$$\begin{aligned} d_n =& \frac{4}{3^{n+3}} \left(4 \left(2 - \frac{1}{2^{2n}} - \frac{1}{2^n}\right) + \frac{3}{2^{2n}} \left(-1 + 4^{n+1}\right) n\right) \\ =& \frac{4}{3^{n+3}} \left(8 + 12n - \frac{4 + 3n}{2^{2n}} - \frac{4}{2^n}\right) \\ =& \frac{4}{3^{n+3}} \left(8 + 12n - \frac{4 + 3n + 4 \cdot 2^n}{2^{2n}}\right). \end{aligned}$$

Since $\frac{4+3n+4\cdot 2^n}{2^{2n}} > 0$, we have that for any natural value of n

$$d_n > \frac{4}{3^{n+3}} (8 + 12n) > 0.$$

On the other hand, if n is odd, then

$$\begin{aligned} d_n =& \frac{4}{3^{n+3}} \left(4 \left(-2 + \frac{1}{2^{2n}} - \frac{1}{2^n}\right) - \frac{3}{2^{2n}} \left(-1 + 4^{n+1}\right) n\right) \\ =& \frac{4}{3^{n+3}} \left(-8 - 12n + \frac{4 + 3n}{2^{2n}} - \frac{4}{2^n}\right) \\ =& \frac{4}{3^{n+3}} \left(-8 - 12n + \frac{4 + 3n - 4 \cdot 2^n}{2^{2n}}\right). \end{aligned}$$

Then, bearing in mind again that $\frac{4+3n-4\cdot 2^n}{2^{2n}} < 0$, *we have that for* $n \in \mathbb{N}$

$$d_n < \frac{4}{3^{n+3}}\,(-8-12n) < 0.$$

Therefore we can conclude that $d_n \neq 0$ *for any natural value of* n.

REMARK 4.11. *Since* $\lim_{n\to\infty} d_n = 0$, *the explicit computation of this determinant for high degrees could involve problems of precision.*

Now, let us come back to the Bézier form. The following theorem, which is the main result in this chapter, shows that a PDE surface satisfying

$$-\frac{1}{6}\overrightarrow{x}_{uuu} + \frac{1}{4}\,(\overrightarrow{x}_{uuv} + \overrightarrow{x}_{uvv}) - \frac{1}{6}\overrightarrow{x}_{vvv} = 0$$

can be determined from a prescribed boundary.

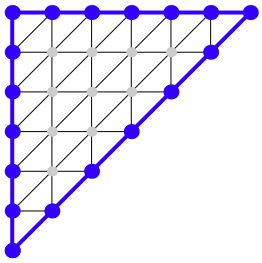

FIGURE 4. Given the boundary control points, i.e. the blue dots, the whole control net is determined by the third-order PDE associated to the symmetric mask.

THEOREM 4.12. *Let* $\overrightarrow{x}(u,v) = \sum_{|I|=n} P_I B_I^n(u,v)$ *be a triangular Bézier surface satisfying the third-order PDE* $S\,(\overrightarrow{x}) = 0$. *Then all the interior control points are determined by the boundary control points,* $P_{i,n-i,0}$, $P_{i,0,n-i}$ *and* $P_{0,i,n-i}$.

Proof: Let us write the Bézier chart in the usual basis of polynomials

$$\overrightarrow{x}(u,v)=\sum_{k,l=0}^{n}a_{k,l}u^{k}v^{l}.$$

Note that the factorial terms in the statement of Lemma 4.4 are now included in the coefficients $a_{k,l}$, and that $a_{k,l}=0$ if $k+l>n$ for a degree n chart.

The boundary control points determine the three boundary curves $\overrightarrow{x}(u,0)$, $\overrightarrow{x}(0,v)$ and $\overrightarrow{x}(u,1-u)$.

The first boundary curve is

$$\overrightarrow{x}(u,0)=\sum_{i=0}^{n}P_{i,0,n-i}B_{i}^{n}(u)=\sum_{i=0}^{n}\sum_{k=i}^{n}(-1)^{k-i}\binom{n}{k}\binom{k}{i}P_{i,0,n-i}u^{k}=\sum_{k=0}^{n}a_{k,0}u^{k}.$$

Therefore the coefficients $\{a_{k,0}\}_{k=0}^{n}$ can be determined from the boundary control points $\{P_{i,0,n-i}\}_{i=0}^{n}$ by

$$a_{k,0}=\sum_{i=0}^{k}(-1)^{k-i}\binom{n}{k}\binom{k}{i}P_{i,0,n-i}\qquad\text{for}\quad k=0,...,n.$$

Analogously, the second boundary curve is

$$\overrightarrow{x}(0,v)=\sum_{i=0}^{n}P_{0,i,n-i}B_{i}^{n}(v)=\sum_{i=0}^{n}\sum_{l=i}^{n}(-1)^{l-i}\binom{n}{l}\binom{l}{i}P_{0,i,n-i}v^{l}=\sum_{l=0}^{n}a_{0,l}v^{l},$$

so the coefficients $\{a_{0,l}\}_{l=0}^{n}$ can be determined from the boundary control points $\{P_{0,i,n-i}\}_{i=0}^{n}$ by the formula

$$a_{0,l}=\sum_{i=0}^{l}(-1)^{l-i}\binom{n}{l}\binom{l}{i}P_{0,i,n-i}\qquad\text{for}\quad l=0,...,n.$$

The third boundary curve, which is determined by the boundary points $\{P_{i,n-i,0}\}_{i=0}^{n}$, is

$$\overrightarrow{x}(u,1-u)=\sum_{i=0}^{n}P_{i,n-i,0}B_{i}^{n}(u)=\sum_{i=0}^{n}\sum_{r=i}^{n}(-1)^{r-i}\binom{n}{r}\binom{r}{i}P_{i,n-i,0}u^{r}=\sum_{r=0}^{n}b_{r}u^{r},\tag{64}$$

where we have denoted by b_r the coefficient of u^r for $r=0,...,n$ in terms of the boundary points:

$$b_{r}=\sum_{i=0}^{r}(-1)^{r-i}\binom{n}{r}\binom{r}{i}P_{i,n-i,0}\qquad\text{for}\quad r=0,...,n.\tag{65}$$

On the other hand if we consider the expression of this third boundary curve in terms of the usual basis, then we have the equation

$$\overrightarrow{x}(u,1-u)=\sum_{k,l=0}^{n}a_{k,l}u^k(1-u)^l=\sum_{k,l=0}^{n}\sum_{r=k}^{k+l}a_{k,l}\,(-1)^{r-k}\binom{l}{k+l-r}u^r. \tag{66}$$

Now if we consider the coefficient of u^r for $r=0,...,n$ in both expressions, (64) and (66), of the curve $\overrightarrow{x}(u,1-u)$ we find that

$$b_r=\sum_{k=0}^{r}\sum_{l=r-k}^{n}(-1)^{r-k}\binom{l}{k+l-r}a_{k,l}\qquad\text{for}\quad r=0,...,n. \tag{67}$$

Let us recall that since $\overrightarrow{x}$ satisfies $S(\overrightarrow{x})=0$, the coefficients $\{a_{k,l}\}$ are zero for $k+l>n$, that is, for $l>n-k$. Therefore, the index l in Equation (67) runs only until $n-k$. Now let us rewrite Equation (67). For $r=0,...,n$ we find

$$b_r=\sum_{k=0}^{r}\sum_{l=r-k}^{n-k}(-1)^{r-k}\binom{l}{k+l-r}a_{k,l}. \tag{68}$$

Later in this proof, we will see that the coefficients in the row of coefficients, $\{a_{1,l}\}_{l=0}^{n-1}$, can be determined from the boundary control points. But, for the time being, we have that the coefficients b_r for $r=0,...,n$ can be written from the boundary points $\{P_{i,n-i,0}\}_{i=0}^{n}$. Then, let us consider Equation (68) for $r=n$

$$b_n=\sum_{k=0}^{n}(-1)^{n-k}\,a_{k,n-k}.$$

From Lemma 4.5, for the case $r=n$, the coefficients $\{a_{k,n-k}\}_{k=0}^{n}$ can be written in terms of $a_{1,n-1}$, $a_{n,0}$ and $a_{0,n}$, then

$$b_n=\sum_{k=0}^{n}(-1)^{n-k}\left(c_{n,0}^{k}a_{n,0}+c_{1,n-1}^{k}a_{1,n-1}+c_{0,n}^{k}a_{0,n}\right)$$

which implies

$$b_n-\sum_{k=0}^{n}(-1)^{n-k}\left(c_{n,0}^{k}a_{n,0}+c_{0,n}^{k}a_{0,n}\right)=\sum_{k=0}^{n}(-1)^{n-k}\,c_{1,n-1}^{k}a_{1,n-1}.$$

Therefore, if $\sum_{k=0}^{n}(-1)^{n-k}\,c_{1,n-1}^{k}$ did not vanish, then $a_{1,n-1}$ could be computed in terms of the border control points, since, as we said before, the coefficients $a_{n,0}$, $a_{0,n}$ and b_n, are determined by boundary control points. Then, by applying Lemma 4.5, all the coefficients $a_{k,l}$ with $k+l=n$ would be determined in terms of $a_{n,0}$, $a_{0,n}$ and $a_{1,n-1}$.

$$\begin{array}{cccccc}
a_{0,0} & a_{0,1} & a_{0,2} & a_{0,3} & a_{0,4} & \boxed{a_{0,5}} \\
a_{1,0} & a_{1,1} & a_{1,2} & a_{1,3} & \boxed{a_{1,4}} & \\
a_{2,0} & a_{2,1} & a_{2,2} & \boxed{a_{2,3}} & & \\
a_{3,0} & a_{3,1} & \boxed{a_{3,2}} & & & \\
a_{4,0} & \boxed{a_{4,1}} & & & & \\
\boxed{a_{5,0}} & & & & &
\end{array}$$

FIGURE 5. In the first step, for $r = n$ we determine the boxed coefficients.

$$\begin{array}{cccccc}
a_{0,0} & a_{0,1} & a_{0,2} & a_{0,3} & \boxed{a_{0,4}} & a_{0,5} \\
a_{1,0} & a_{1,1} & a_{1,2} & \boxed{a_{1,3}} & a_{1,4} & \\
a_{2,0} & a_{2,1} & \boxed{a_{2,2}} & a_{2,3} & & \\
a_{3,0} & \boxed{a_{3,1}} & a_{3,2} & & & \\
\boxed{a_{4,0}} & a_{4,1} & & & & \\
a_{5,0} & & & & &
\end{array}$$

FIGURE 6. In the second step, for $r = n - 1$ we determine the boxed coefficients.

Now in order to determine the rest of coefficients $a_{k,l}$ with $k + l = r$ for $r = 0, ..., n - 1$, we would repeat this reasoning for any r. In general, we have

$$b_r - \sum_{k=0}^{r} \sum_{l=r-k+1}^{n-k} (-1)^{r-k} \binom{l}{k+l-r} a_{k,l} = \sum_{k=0}^{r} (-1)^{r-k} a_{k,r-k}$$

and again from Lemma 4.5,

$$b_r - \sum_{k=0}^{r} \sum_{l=r+1-k}^{n-k} (-1)^{r-k} \binom{l}{k+l-r} a_{k,l} - \sum_{k=0}^{r} (-1)^{r-k} \left(c_{r,0}^{k} a_{r,0} + c_{0,r}^{k} a_{0,r}\right) =$$

$$= \sum_{k=0}^{r} (-1)^{r-k} c_{1,r-1}^{k} a_{1,r-1}.$$

Then, as before, if $\sum_{k=0}^{r} (-1)^{r-k} c_{1,r-1}^{k}$ did not vanish, $a_{1,r-1}$, could be determined.

In the previous equation an expression of $a_{1,r-1}$ this is given in terms of the border control points that define $a_{0,r}$, $a_{r,0}$ and b_r, and also depending on the coefficients $a_{k,l}$ with $k + l > r$. At this point, these coefficients would be known, also in terms of boundary control points, since we start this scheme of computation from $r = n$ until $r = 0$.

Therefore we must prove that for $r = 0, ..., n$

$$\sum_{k=0}^{r} (-1)^{r-k} c_{1,r-1}^{k} \neq 0.$$

Bearing in mind the value of $c_{1,r-1}^{k}$ that was given in Lemma 4.7, for $a = \frac{-1}{6}$ and $b = \frac{1}{4}$, we have

$$\sum_{k=0}^{r} (-1)^{r-k} c_{1,r-1}^{k} = (-1)^{r-1} + \sum_{k=2}^{r-1} (-1)^{r-k} c_{1,r-1}^{k} =$$

$$= (-1)^{r-1} + \sum_{k=2}^{r-1} \frac{(-1)^{r-k}}{\det M_{r-2}^{(a,b,b,a)}} \left(-a\,(-1)^{2r-3-k} A_{r-3,r-k} - b\,(-1)^{2r-2-k} A_{r-2,r-k} \right)$$

$$= (-1)^{r-1} \left(1 + \sum_{k=2}^{r-1} \frac{1}{\det M_{r-2}^{(a,b,b,a)}} \left(-aA_{r-3,r-k} + bA_{r-2,r-k} \right) \right)$$

Therefore our goal is to prove

$$M_{r-2}^{(a,b,b,a)} + \sum_{k=2}^{r-1} \left(-aA_{r-3,r-k} + bA_{r-2,r-k} \right) \neq 0.$$

$$M_{r-2}^{(a,b,b,a)} + \sum_{k=2}^{r-1} \left(-aA_{r-3,r-k} + bA_{r-2,r-k} \right) = M_{r-2}^{(a,b,b,a)} +$$

$$+ \sum_{k=2}^{r-1} \frac{-a}{(-1)^{2n-3-k}} \begin{vmatrix} b & b & a & 0 & 0 & 0 & \cdots & 0 \\ a & b & b & a & 0 & \vdots & \ddots & \vdots \\ 0 & a & b & b & a & \vdots & 0 & \cdots & 0 \\ \vdots & \ddots & \ddots & \ddots & \ddots & \vdots & \ddots & \ddots & \vdots \\ 0 & \cdots & 0 & a & \vdots & b & a & 0 \\ 0 & 0 & \cdots & 0 & 0 & b & b & a \\ 0 & \cdots & \cdots & 0 & 1 & 0 & \cdots & 0 \\ 0 & 0 & 0 & \cdots & 0 & 0 & a & b \end{vmatrix} + \frac{b}{(-1)^{2n-2-k}} \begin{vmatrix} b & b & a & 0 & 0 & 0 & \cdots & 0 \\ a & b & b & a & 0 & \vdots & \ddots & \vdots \\ 0 & a & b & b & a & \vdots & 0 & \cdots & 0 \\ \vdots & \ddots & \ddots & \ddots & \ddots & \vdots & \ddots & \ddots & \vdots \\ 0 & \cdots & 0 & a & \vdots & b & a & 0 \\ 0 & 0 & \cdots & 0 & \vdots & b & b & a \\ 0 & 0 & 0 & \cdots & 0 & a & b & b \\ 0 & 0 & \cdots & 0 & 1 & 0 & \cdots & 0 \end{vmatrix}$$

$$= M_{r-2}^{(a,b,b,a)} + (-1)^{n} a \begin{vmatrix} b & b & a & 0 & \cdots & 0 & 0 & 0 \\ a & b & b & a & 0 & \cdots & 0 & 0 \\ 0 & a & b & b & a & 0 & \cdots & 0 \\ \vdots & \ddots & \ddots & \ddots & \ddots & \ddots & \ddots & \vdots \\ 0 & \cdots & 0 & a & b & b & a & 0 \\ 0 & 0 & \cdots & 0 & a & b & b & a \\ -1 & 1 & \cdots & \cdots & \cdots & & (-1)^{n-2} & \\ 0 & 0 & 0 & 0 & \cdots & 0 & a & b \end{vmatrix} + (-1)^{n} b\, d_{n-2}$$

where d_{n-2} denotes the determinant of the matrix $m_{n-2}^{(a,b,c,d)}$ defined in Equation (61). Now we will compute the other determinant using expansion by minors

$$M_{r-2}^{(a,b,b,a)} + \sum_{k=2}^{r-1} \left(-aA_{r-3,r-k} + bA_{r-2,r-k}\right) = M_{r-2}^{(a,b,b,a)} + (-1)^n \, ab \, d_{n-3}$$

$$-a(-1)^{2n-2} \begin{vmatrix} b & b & a & 0 & \cdots & 0 & 0 \\ a & b & b & a & 0 & \cdots & 0 \\ 0 & a & b & b & a & \ddots & \vdots \\ \vdots & \ddots & \ddots & \ddots & \ddots & \ddots & 0 \\ 0 & \cdots & 0 & a & b & b & a \\ 0 & 0 & \cdots & 0 & a & b & b \\ 0 & 0 & 0 & 0 & \cdots & 0 & a \end{vmatrix} + a^2 (-1)^n \begin{vmatrix} b & b & a & 0 & \cdots & 0 & 0 \\ a & b & b & a & 0 & \cdots & 0 \\ 0 & a & b & b & a & \ddots & \vdots \\ \vdots & \ddots & \ddots & \ddots & \ddots & \ddots & 0 \\ 0 & \cdots & 0 & a & b & b & a \\ -1 & 1 & \cdots & \cdots & & (-1)^{n-3} & \\ 0 & 0 & 0 & 0 & \cdots & 0 & a \end{vmatrix}$$

$$= M_{r-2}^{(a,b,b,a)} + (-1)^n \, ab \, d_{n-3} - a^2 M_{r-4}^{(a,b,b,a)} + a^3 (-1)^n \, d_{n-4} + (-1)^n \, b \, d_{n-2}$$

$$= (-1)^{n-1} \left(-b \, d_{n-2} - ab \, d_{n-3} - a^3 \, d_{n-4} + (-1)^{n-1} \, M_{r-2}^{(a,b,b,a)} + (-1)^{n-2} \, a^2 M_{r-4}^{(a,b,b,a)} \right)$$

$$= (-1)^{n-1} \, d_{n-1}.$$

Then, since $d_n \neq 0$ for all n, from Lemma 4.9, where its general n-th term was given, we can finally state that the whole control net of a triangular Bézier surface satisfying $S\left(\overrightarrow{x}\right) = 0$ is determined if its boundary is prescribed.

■

The following figures will allow us to compare the results obtained by the third-order method to the results obtained in the previous chapters for harmonic and biharmonic surfaces.

First, for $n = 6$ we can compare the third-order method results with the harmonic surfaces obtained in the first chapter by means of Theorem 1.9 and Theorem 1.18. As before we show the grid of control points where the blue are known and the gray are obtained by asking the chart to satisfy a PDE.

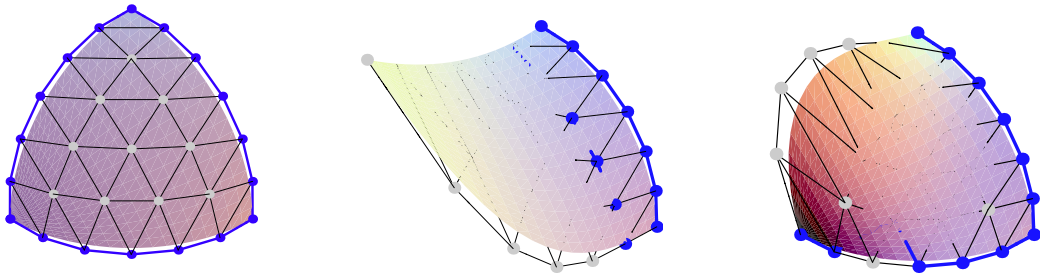

FIGURE 7. Three triangular Bézier surfaces similar to a piece of a sphere. The figure on the left satisfies the third-order PDE corresponding to the symmetric mask and it is obtained for a prescribed border. The others are harmonic Bézier surfaces obtained thanks to Theorem 1.9 and Theorem 1.18 respectively.

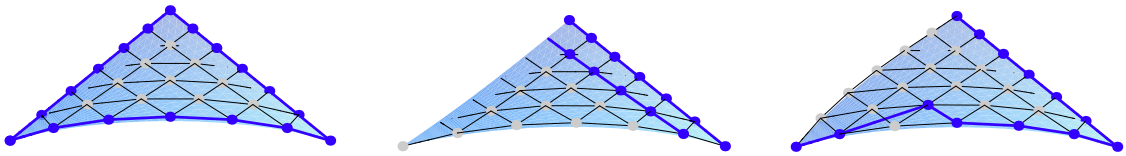

FIGURE 8. Three triangular Bézier surfaces similar to a piece of a cone. As before, the figure on the left satisfies the third-order PDE corresponding to the symmetric mask and the other two surfaces are harmonic surfaces obtained by means of Theorem 1.9 and Theorem 1.18 respectively.

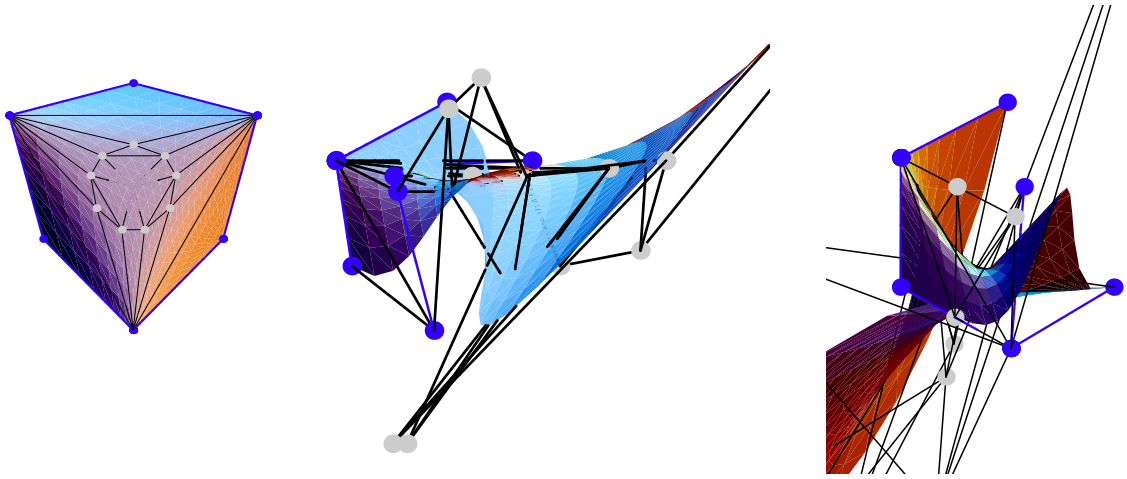

FIGURE 9. These surfaces are approximations to the minimal Schwarz surface which has its boundary curves along some of the edges of a cube. The figure on the left is generated by the third-order method and the other two surfaces are harmonic surfaces obtained by means of Theorem 1.9 and Theorem 1.18 respectively. It can be observed that good results are only obtained when the boundary is prescribed.

The following figures show some surfaces of degree $n = 7$ which will allow us to compare the results obtained for biharmonic surfaces in the second chapter with the PDE surfaces obtained by means of the third-order method, in particular thanks to the symmetric mask.

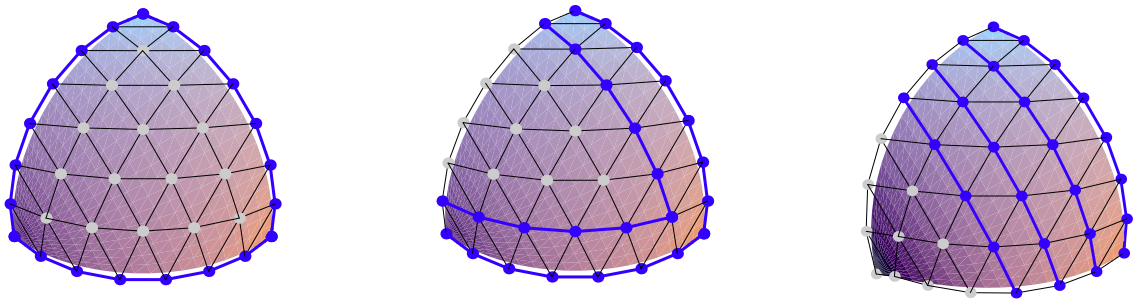

FIGURE 10. Again we can compare our results with triangular Bézier surfaces looking like a piece of a sphere. The figure on the left satisfies the third-order PDE corresponding to the symmetric mask. The other surfaces are biharmonic Bézier surfaces obtained thanks to Theorem 2.2 and Theorem 2.3 respectively.

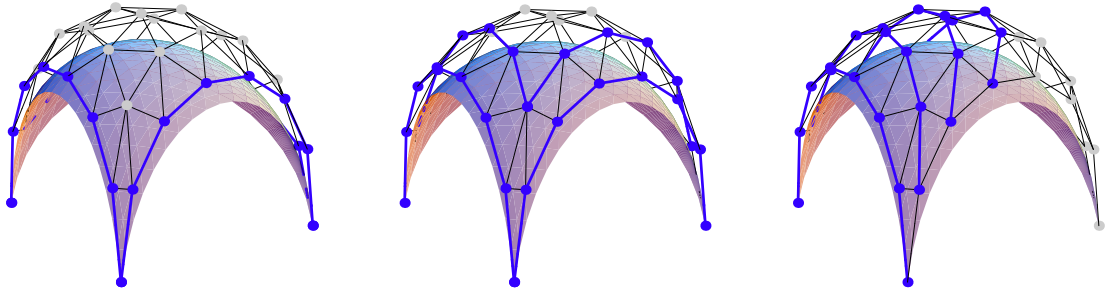

FIGURE 11. The figure on the left satisfies the third-order PDE corresponding to the symmetric mask. The other surfaces are biharmonic Bézier surfaces obtained thanks to Theorem 2.2 and Theorem 2.3 respectively. The three surface generation methods give good shapes for this example.

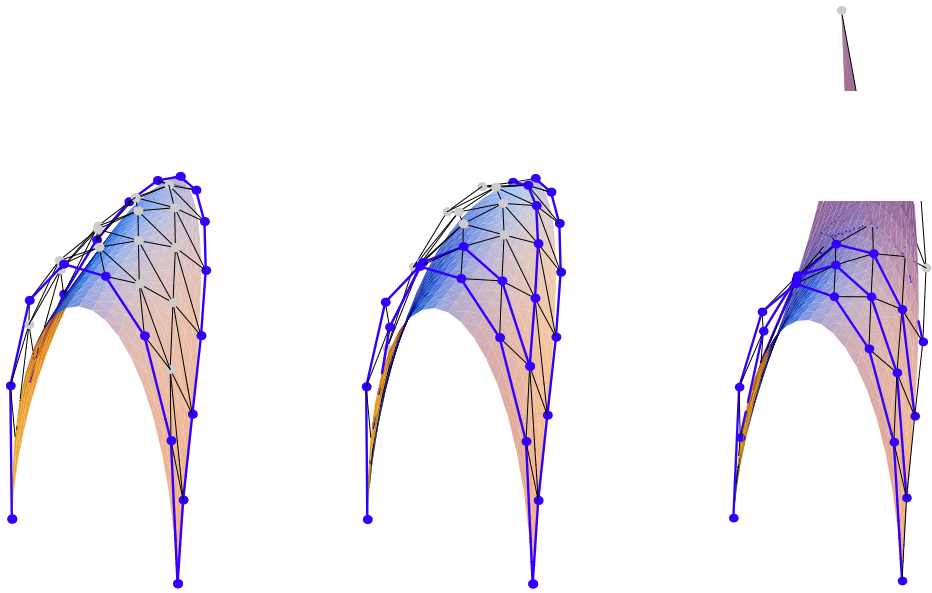

FIGURE 12. The figure on the left satisfies the third-order PDE corresponding to the symmetric mask. The other surfaces are biharmonic Bézier surfaces obtained thanks to Theorem 2.2 and Theorem 2.3 respectively. The control of the boundary curves prevents the loss of control we suffered in the third figure.

6. Conclusions

In the first and the second chapters we deduced different methods to generate triangular Bézier PDE surfaces for a prescribed set of control points. But these sets of prescribed information could not be the boundary control points. Finally, in this chapter we obtain a method to generate triangular Bézier PDE surfaces with a prescribed boundary.

As we said before, given two lines of control points the associated harmonic surface can be determined, and analogously, given four lines of control points a biharmonic surface can also be determined. The harmonic and the biharmonic equations are of second and fourth-order

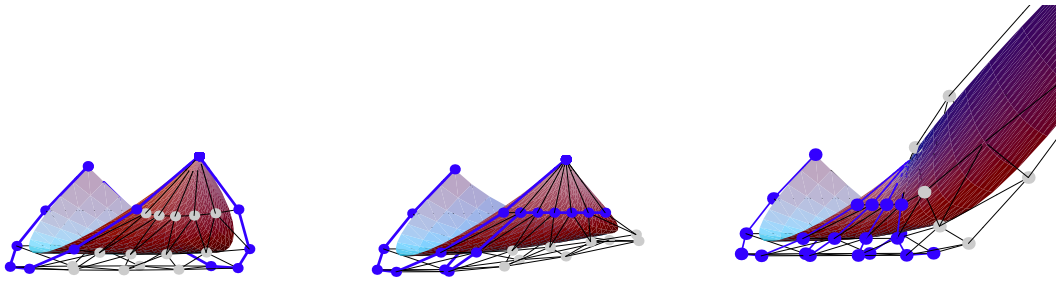

FIGURE 13. The figure on the left satisfies the third-order PDE corresponding to the symmetric mask. The other surfaces are biharmonic Bézier surfaces obtained thanks to Theorem 2.2 and Theorem 2.3 respectively. As before, the prescription of the boundary curves prevents the loss of control we suffered in the third figure.

respectively, then as is to be expected, the boundary curves of a triangular Bézier surface, that is, three lines of control points, determine a surface satisfying a third-order PDE.

Here we have defined a general third-order PDE with constant coefficients and we have deduced that its associated PDE surfaces could be obtained by means of a mask. In particular, we have asked that mask for a symmetry property the result being that the associated PDE surface is in addition a permanence patch.

We have compared the results we obtained with this approach, which we have called the third-order method, with our previous results for harmonic and biharmonic surfaces, and it can be seen that, as could be expected, control of the whole boundary gives better control over the shape of a surface. The surfaces we have obtained with the third-order method are perfectly adapted to the shape traced by the boundary.

CHAPTER 5

The Weierstrass representation for minimal Bézier surfaces

The CAGD problem of building a surface that interpolates given boundary curves reminds one of the most important problems in calculus of variations: to find the minimal surface with a prescribed boundary. The study of surfaces minimizing area with a prescribed boundary, the Plateau problem, has been and still is a major topic in differential geometry.

The construction of surfaces subject to certain constraints such us minimizing area, curvature or other geometric properties, has also been studied from the point of view of graphics. In the case of the area of a surface, the interest comes from the fact that in some real problems, minimal area means minimal cost of the material used to build the surface.

Minimal surfaces admitting a Bézier form have been previously studied in [**12**]. In the cited paper the authors study minimal tensor-product Bézier surfaces and the properties that the associated control net must satisfy. Moreover, they show that in the bicubical case all non-trivial minimal surfaces are, up to an affine transformation, pieces of Enneper's surface.

In this chapter we will describe some methods related with the complex function theory that are used for the study of minimal surfaces, see [**11**]. We will show some methods which will allow us to generate minimal and isothermal triangular Bézier surfaces starting out from different sets of initial conditions that must be satisfied.

First, for the cubical case, a method to build up a minimal surface is given with the prescription of the three vertices.

After that, we suppose that, in addition to the vertices, the tangent planes at these corner points are prescribed, and we show how to obtain a minimal surface of degree 7. Additionally, a similar method for obtaining a minimal surface with prescribed tangent planes at the corner points is also given, but by fixing a free set of points of the surface instead of only the three corners.

Finally, we will study the relations between minimal curves and minimal surfaces. This will enable us to deduce two more methods for the generation of cubical minimal surfaces with prescription of a different kind of initial conditions. Instead of prescribing some control points and some tangent planes to the surface, cubical minimal surfaces can also be determined giving some complex and real parameters.

The first two sections are background.

1. Minimal Surfaces

The study of minimal and constant mean curvature surfaces on three-dimensional Euclidean space has always been one of the most important problems of differential geometry and nowadays it is still one of the most active fields of interest.

Minimal surfaces are surfaces with the least area for given boundary conditions. The study of minimal surfaces began with Lagrange, who addressed the calculus of variations problem of finding a minimal surface of a boundary with specified constraints, later known as Plateau's problem. This study made it possible to establish the Euler-Lagrange differential equation

$$\left(1+h_v^2\right)h_{uu}-2h_uh_{uv}+\left(1+h_u^2\right)h_{vv}=0 \tag{69}$$

which characterizes minimal surfaces that are parametrized as $\overrightarrow{x}=(u,v,h\,(u,v))$.

In 1776 Meusnier found the first non-trivial examples of surfaces satisfying Equation (69), the catenoid and the helicoid. Moreover he gave a geometric interpretation to this equation by introducing the concept of mean curvature. Minimal surfaces were then characterized as the surfaces with null mean curvature.

In 1865 an important boost was given to the theory of minimal surfaces thanks to Schwarz, who obtained the solution of the Plateau problem for a quadrilateral border. This work was based on the representation formulas obtained by Weierstrass in 1861. Similar representation formulas were obtained in 1864 by Enneper, which enabled him to find the minimal surface known nowadays as the Enneper surface. Other representation formulas were introduced by important mathematicians such as Weingarten (1863), Riemann (1866), Peterson (1866) and Beltrami (1868).

We will now introduce some general concepts which are very useful for the study of minimal surfaces.

DEFINITION 5.1. *A chart $\overrightarrow{x}:U\longrightarrow S$ of a surface is said to be isothermal if $E=G, F=0$, being E,F,G the coefficients of the first fundamental form associated to the chart $\overrightarrow{x}$.*

Equivalently, a chart $\overrightarrow{x}:U\longrightarrow S$ of a surface is said to be isothermal if the map $\overrightarrow{x}$ is a conformal map, i.e., if the angles between curves in the surface are equal to the angles between the corresponding curves in the coordinate open subset U.

The following property is a consequence of the minimization of area but it is usually taken as definition of minimal surfaces.

DEFINITION 5.2. *A surface S is minimal if its mean curvature vanishes.*

Equivalently, a different definition of minimal surface can be as follows: S is a minimal surface iff for each point $p\in S$ one can chose a neighborhood, U_p, which has minimal area among other patches V having the same boundary as U_p.

DEFINITION 5.3. *A function, f, with continuous second partial derivatives is said to be harmonic if and only if $\Delta\overrightarrow{f}=0$, where Δ is the usual Laplacian operator.*

DEFINITION 5.4. *A chart $\overrightarrow{x}$ is said to be harmonic if and only if its coordinate functions are harmonic.*

PROPOSITION 5.5. *If a chart, $\overrightarrow{x} : U \to S$, of a surface, S, is isothermal, then $\overrightarrow{x}(U)$ is minimal if and only if the chart is harmonic, i.e., $\Delta \overrightarrow{x} = 0$.*

It is well known that this relation between the mean curvature and the chart, is due to the fact that any isothermal map satisfies

$$\overrightarrow{x}_{uu} + \overrightarrow{x}_{vv} = 2\lambda^2 H \overrightarrow{N}$$

where $\lambda = E = G$ and $\overrightarrow{N}$ is the unitary normal vector to the surface associated to the chart. As a consequence of Proposition 5.5 the study of harmonic maps is an important step forward within the context of minimal surfaces.

EXAMPLE 5.1. *The first non-trivial example of minimal surface with polynomial coordinate functions is Enneper's surface (Figure 1), $\overrightarrow{x} : \mathbb{R}^2 \longrightarrow \mathbb{R}^3$ defined by*

$$\overrightarrow{x}(u,v) := (u - \frac{u^3}{3} + uv^2, v - \frac{v^3}{3} + vu^2, u^2 - v^2). \tag{70}$$

This surface can be expressed in barycentric coordinates as (see [**19**]*):*

$$\overrightarrow{x}(u,v,w) = (\frac{2u^3}{3} + 2u^2v + uv^2 + 2u^2w + 2uvw + 2uw^2,$$
$$2u^2v + 2uv^2 + \frac{2v^3}{3} + 2uvw + 2v^2w + vw^2, u^3 + u^2v - uv^2 - v^3 + u^2w - v^2w).$$

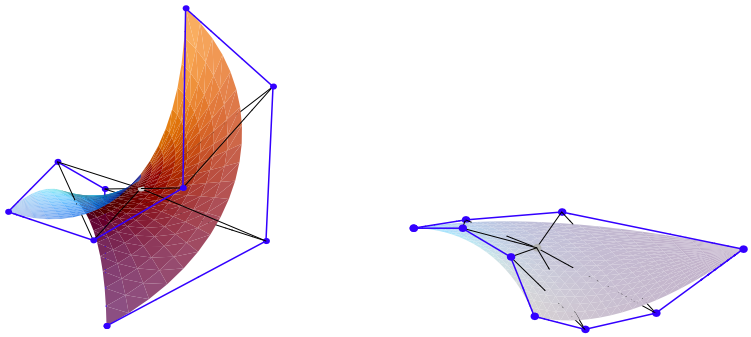

FIGURE 1. Two pieces of Enneper's surface plotted as triangular Bézier patches with their control nets. In particular, these are the reparametrizations $x(1-u-v, v)$ and $x(u+1, v-1)$ respectively.

These are the control nets of the Bézier triangles shown above,

$$\mathcal{E}_1 \equiv \begin{array}{c} (\frac{2}{3},0,1)\ (\frac{2}{3},\frac{2}{3},\frac{1}{3})\ (\frac{2}{3},\frac{2}{3},-\frac{1}{3})\ (0,\frac{2}{3},-1) \\ (\frac{2}{3},0,\frac{1}{3})\ (\frac{1}{3},\frac{1}{3},0)\ (0,\frac{1}{3},0) \\ (\frac{1}{3},0,0)\ (0,\frac{2}{3},-\frac{1}{3}) \\ (0,0,0) \end{array} \qquad \mathcal{E}_2 \equiv \begin{array}{c} (\frac{-4}{3},\frac{14}{3},3)\ (\frac{2}{3},\frac{-10}{3},1)\ (\frac{-10}{3},\frac{2}{3},-1)\ (\frac{14}{3},\frac{-4}{3},-3) \\ (\frac{-10}{3},\frac{2}{3},-1)\ (\frac{5}{3},\frac{5}{3},0)\ (\frac{2}{3},\frac{-10}{3},1) \\ (\frac{2}{3},\frac{-1}{3},-2)\ (\frac{-1}{3},\frac{2}{3},2) \\ (\frac{5}{3},\frac{5}{3},0) \end{array}$$

2. The Weierstrass representation

The usual way of working with complex techniques is to change the real parameters u, v to the equivalent pair of complex variables $z, \overline{z}$:

$$z = u + \mathbf{i}v \qquad \overline{z} = u - \mathbf{i}v.$$

The use of these complex coordinates $z, \overline{z}$ could lead us to some confusion if we think of $\overline{z}$ as being determined by z, which is true when we start from u, v. But, otherwise, we can use $z, \overline{z}$ as abstract coordinates for $\mathbb{R}^2 = \mathbb{C}$, even when they are complex-valued, and later define u, v by means of

$$u = \frac{z+\overline{z}}{2} \qquad v = \frac{z-\overline{z}}{2\mathbf{i}}. \tag{71}$$

Now it is important to introduce the following operators:

$$\frac{\partial}{\partial z} = \frac{1}{2}\left(\frac{\partial}{\partial u} - \mathbf{i}\frac{\partial}{\partial v}\right) \qquad \frac{\partial}{\partial \overline{z}} = \frac{1}{2}\left(\frac{\partial}{\partial u} + \mathbf{i}\frac{\partial}{\partial v}\right),$$

to define the complex derivative of a local parametrization.

Definition 5.6. *The complex derivative of a local parametrization* $\overrightarrow{x} : U \longrightarrow \mathbb{R}^n$ *is defined as*

$$\frac{\partial \overrightarrow{x}}{\partial z}(z) = \frac{1}{2}\left(\overrightarrow{x}_u - \mathbf{i}\,\overrightarrow{x}_v\right)(u,v), \qquad \textit{where} \quad z = u + \mathbf{i}v.$$

Equivalently we can denote the complex derivative as

$$\frac{\partial \overrightarrow{x}}{\partial z} = \phi\left(\overrightarrow{x}\right) = \left(\phi_1\left(\overrightarrow{x}\right), ..., \phi_n\left(\overrightarrow{x}\right)\right) = \frac{1}{2}\left(\frac{\partial x_1}{\partial u} - \mathbf{i}\frac{\partial x_1}{\partial v}, ..., \frac{\partial x_n}{\partial u} - \mathbf{i}\frac{\partial x_n}{\partial v}\right).$$

The following lemma and the next theorem were stated in [**11**]. This lemma gives some relations between the complex derivative of a local parametrization and the coefficients of its first fundamental form.

Lemma 5.7. *([**11**] Lemma 23.7.) The complex derivative of a local parametrization verifies the following identities:*

$$\sum_{k=1}^{n} \phi_k\left(\overrightarrow{x}\right)^2 = \frac{1}{4}\left(\overrightarrow{x}_u \cdot \overrightarrow{x}_u - \overrightarrow{x}_v \cdot \overrightarrow{x}_v - 2\mathbf{i}\,\overrightarrow{x}_u \cdot \overrightarrow{x}_v\right) = \frac{1}{4}\left(E - G - 2\mathbf{i}F\right),$$

$$\sum_{k=1}^{n} |\phi_k(\overrightarrow{x})|^2 = \frac{1}{4}(\overrightarrow{x}_u \cdot \overrightarrow{x}_u + \overrightarrow{x}_v \cdot \overrightarrow{x}_v) = \frac{1}{4}(E+G),$$

where E, F and G are the coefficients of the First Fundamental Form.

In the following theorem, which can also be found in [**11**], it is proved that a minimal and isothermal local parametrization gives rise to a n-tuple of analytic functions such that the sum of its squares is equal to zero. This description of such a parametrization allows the use of important theorems from complex analysis.

THEOREM 5.8. *([**11**] Lemma 23.8.) Let $\overrightarrow{x} : U \longrightarrow \mathbb{R}^n$ be a local parametrization. Then:*

(1) *$\overrightarrow{x}$ is harmonic if and only if its complex derivative, $\phi(\overrightarrow{x}) = \frac{\partial \overrightarrow{x}}{\partial z}$, is analytic.*

(2) *$\overrightarrow{x}$ is isothermal if and only if*

$$\sum_{k=1}^{n} \phi_k(\overrightarrow{x})^2 = 0. \tag{72}$$

(3) *If $\overrightarrow{x}$ is isothermal, $\overrightarrow{x}$ is regular if and only if*

$$\sum_{k=1}^{n} |\phi_k(\overrightarrow{x})|^2 \neq 0. \tag{73}$$

Conversely, let U be simply connected, and $\phi_1, ..., \phi_n : U \longrightarrow \mathbb{C}^n$ analytic functions satisfying:

$$\sum_{k=1}^{n} \phi_k(\overrightarrow{x})^2 = 0 \quad \textit{and} \quad \sum_{k=1}^{n} |\phi_k(\overrightarrow{x})|^2 \neq 0, \tag{74}$$

then, there is a local parametrization $\overrightarrow{x} : U \longrightarrow \mathbb{R}^n$ which is minimal, isothermal and regular and such that $\Phi = (\phi_1, ..., \phi_n)$ is the complex derivative of $\overrightarrow{x}$.

Proof: Although this proof is known we include it here in order to clarify these concepts.

(1) The Cauchy-Riemann equations of $\phi(\overrightarrow{x}) = \frac{\partial \overrightarrow{x}}{\partial z}$ are given by

$$\overrightarrow{x}_{uu} + \overrightarrow{x}_{vv} = 0$$
$$\overrightarrow{x}_{uv} - \overrightarrow{x}_{vu} = 0,$$

that is, the Cauchy-Riemann equations of the complex derivative of a local parametrization are only satisfied if the chart is harmonic and its mixed partial derivatives are equal.

Conversely a harmonic parametrization has continuous second partial derivatives and therefore, in addition to satisfying $\overrightarrow{x}_{uu} + \overrightarrow{x}_{vv} = 0$, its mixed partial derivatives are also equal, $\overrightarrow{x}_{uv} = \overrightarrow{x}_{vu}$. This implies that $\frac{\partial \overrightarrow{x}}{\partial z}$ satisfies the Cauchy-Riemann equations and so it is analytic.

(2) From Lemma 5.7 we have

$$\sum_{k=1}^{n} \phi_k \left(\overrightarrow{x}\right)^2 = \frac{1}{4}\left(E - G - 2\mathbf{i}F\right).$$

Therefore we have $\sum_{k=1}^{n} \phi_k \left(\overrightarrow{x}\right)^2 = 0$ if and only if $E = G$ and $F = 0$, that is for isothermal charts.

(3) Its deduced from Lemma 5.7 since $\sum_{k=1}^{n} |\phi_k \left(\overrightarrow{x}\right)|^2 = \frac{1}{4}\left(E + G\right)$.

Now we will prove the last statement. The chart $\overrightarrow{x}$ is isothermal and regular as a consequence of the previous items, so in order to prove that it is harmonic we must suppose that

$$\overrightarrow{x} = \mathrm{Re} \int \left(\phi_1 \left(z\right), ..., \phi_n \left(z\right)\right) \, dz$$

and

$$\overrightarrow{y} = \mathrm{Im} \int \left(\phi_1 \left(z\right), ..., \phi_n \left(z\right)\right) \, dz.$$

If we denote

$$\psi \left(z\right) = \int \left(\phi_1 \left(z\right), ..., \phi_n \left(z\right)\right) \, dz$$

then the parametrizations $\overrightarrow{x}$ and $\overrightarrow{y}$ are the real and the imaginary part of an n-tuple of analytic functions $\psi_i \left(z\right)$. Therefore these functions satisfy the Cauchy-Riemann equations:

$$\mathrm{Re}\, \psi_i \left(z\right)_u = \mathrm{Im}\, \psi_i \left(z\right)_v \qquad \mathrm{Re}\, \psi_i \left(z\right)_v = -\mathrm{Im}\, \psi_i \left(z\right)_u$$

that is,

$$x_u^i = y_v^i \qquad x_v^i = y_u^i.$$

Then

$$x_{uu}^i + x_{vv}^i = y_{uv}^i - y_{vu}^i = 0,$$

and therefore $\overrightarrow{x}$ is harmonic.

■

Theorem 5.8, which was stated in [**11**], gave a relation between minimal and isothermal local parametrizations and an n-tuple $\Phi = (\phi_1, ..., \phi_n)$ satisfying certain conditions, (74). Now we will introduce the concept of minimal curve taking these conditions as a definition.

Definition 5.9. *Let U be an open subset on $\mathbb{C}$. A minimal curve is defined as an analytic function $\psi : U \longrightarrow \mathbb{C}$ such that*

$$\psi'(z) \cdot \psi'(z) = 0 \quad \textit{for all } z \in U.$$

Moreover if the equality

$$\psi'(z) \cdot \overline{\psi'(z)} \neq 0$$

is satisfied for all $z \in U$, then ψ is said to be a regular minimal curve.

LEMMA 5.10. *([**11**] Lemma 23.11.) There is a one-to-one map between minimal curves and complex derivatives of minimal and isothermal local parametrizations.*

REMARK 5.11. *It is deduced from Theorem 8 that a minimal and isothermal local parametrization has an associated a minimal curve which is called its complexification: Given a minimal and isothermal local parametrization $\overrightarrow{x} : U \longrightarrow \mathbb{R}^n$, if we consider $\overrightarrow{x}(z)$ with $z = u + \mathbf{i}v$ we find that it is a minimal curve since*

$$\overrightarrow{x}'(z) \,.\, \overrightarrow{x}'(z) = \sum_{k=1}^{n} \phi_k \left(\overrightarrow{x}\right)^2 = 0.$$

Conversely, given a minimal curve $\psi : U \longrightarrow \mathbb{C}^n$ we can define a minimal and isothermal local parametrization $\overrightarrow{x} : U \longrightarrow \mathbb{R}^n$ by

$$\overrightarrow{x}(u, v) = Re(\psi(u + \mathbf{i}v)). \tag{75}$$

Therefore, a minimal curve can be seen as a generalization of a minimal and isothermal local parametrization.

LEMMA 5.12. *([**11**]) The real and the imaginary part of an analytic function are both harmonic functions and they are called harmonic conjugated.*

DEFINITION 5.13. *Let $\overrightarrow{x}, \overrightarrow{y} : U \longrightarrow \mathbb{R}^n$ be local parametrizations on the open set $U \subseteq \mathbb{R}^2$.*

It is said that $\overrightarrow{x}$ and $\overrightarrow{y}$ satisfy the Cauchy-Riemann equations if

$$\overrightarrow{x}_u = \overrightarrow{y}_v \qquad and \qquad \overrightarrow{x}_v = \overrightarrow{y}_u.$$

LEMMA 5.14. *([**11**] Lemma 23.4.) If $\overrightarrow{x}, \overrightarrow{y} : U \longrightarrow \mathbb{R}^n$ satisfy the Cauchy-Riemann equations, then they are both harmonic and it is said that $\overrightarrow{x}$ and $\overrightarrow{y}$ are harmonic conjugated.*

As was said in Lemma 5.12, the real and the imaginary part of an analytic function are harmonic conjugated. So from this relation between analytic and harmonic conjugated functions it follows to define an analogous of analytic function related with a pair of harmonic conjugated local parametrizations.

DEFINITION 5.15. *The complexification of a pair $\overrightarrow{x}, \overrightarrow{y} : U \longrightarrow \mathbb{R}^n$ of minimal and isothermal local parametrizations is the map $\overrightarrow{x} + \mathbf{i}\overrightarrow{y} : U \longrightarrow \mathbb{C}^n$.*

LEMMA 5.16. *([**11**] Lemma 23.10.) The complexification $\overrightarrow{x} + \mathbf{i}\overrightarrow{y} : U \longrightarrow \mathbb{C}^n$, of a pair of minimal conjugated parametrizations $\overrightarrow{x}, \overrightarrow{y} : U \longrightarrow \mathbb{R}^n$ is an analytic function. Moreover*

$$\frac{d}{dz}\left(\overrightarrow{x} + \mathbf{i}\overrightarrow{y}\right) = 2\frac{\partial \overrightarrow{x}}{\partial z}.$$

DEFINITION 5.17. *A complex function $f : \mathbb{C} \longrightarrow \mathbb{C}$ is said to be meromorphic iff its only singular points are its poles.*

The following definition will introduce the Weierstrass parametrization to determine minimal surfaces. The Weierstrass formula is another surface generation method: A minimal surface can be determined by a pair of complex functions f and g.

DEFINITION 5.18. *Let $f(z)$ and $g(z)$ be a pair of meromorphic functions defined in a region U on the complex plane $\mathbb{C}$. Let us fix $z_0 \in U$ and then define*

$$\begin{cases} x_1(z) = Re\,(\int_{z_0}^{z} \frac{f(w)}{2}(1-g(w)^2)dw), \\ x_2(z) = Re\,(\int_{z_0}^{z} \frac{\mathbf{i}f(w)}{2}(1+g(w)^2)dw), \\ x_3(z) = Re\,(\int_{z_0}^{z} f(w)g(w)dw). \end{cases}$$

and

$$\begin{cases} y_1(z) = Im\,(\int_{z_0}^{z} \frac{f(w)}{2}(1-g(w)^2)dw), \\ y_2(z) = Im\,(\int_{z_0}^{z} \frac{\mathbf{i}f(w)}{2}(1+g(w)^2)dw), \\ y_3(z) = Im\,(\int_{z_0}^{z} f(w)g(w)dw). \end{cases}$$

where $z = u + \mathbf{i}v$.

Then the Weierstrass local parametrization and its conjugate, which are determined by $f(z)$ and $g(z)$, are defined respectively by

$$x(u,v) = (x_1(u,v), x_2(u,v), x_3(u,v)) \quad \text{and} \quad y(u,v) = (y_1(u,v), y_2(u,v), y_3(u,v)).$$

THEOREM 5.19. *([**11**] Theorem 24.1.) Given an arbitrary analytic function $f(z)$ and an arbitrary meromorphic function $g(z)$, the Weierstrass associated local parametrization and its conjugate are both minimal and isothermal local parametrizations.*

COROLLARY 5.20. *([**11**] Corollary 24.2.) Let $f(z)$ and $g(z)$ meromorphic functions defined in a region U on the complex plane $\mathbb{C}$, and let $\overrightarrow{x}$ and $\overrightarrow{y}$ be the associated Weierstrass local parametrization and its conjugate respectively. Then*

$$z \mapsto (\overrightarrow{x} + \mathbf{i}\,\overrightarrow{y})(z)$$

is a minimal curve.

From the following lemma we can observe that the reciprocal is also true.

LEMMA 5.21. *([**11**] Lemma 24.3.) Let $\psi : U \longrightarrow \mathbb{C}^3$ be a minimal curve such that $\psi' = (\phi_1, \phi_2, \phi_3)$. Let us suppose that $\phi_1 - \mathbf{i}\phi_2$ is not identically zero. Let us define*

$$f = \phi_1 - \mathbf{i}\phi_2, \qquad g = \frac{\phi_3}{\phi_1 - \mathbf{i}\phi_2}. \tag{76}$$

Thus, f and g determine the Weierstrass representation of ψ, that is,

$$\psi' = (\frac{f}{2}(1-g^2), \frac{\mathbf{i}f}{2}(1+g^2), fg).$$

The Enneper surface, which is the only non-trivial minimal and polynomial surface of degree three up to affine reparametrizations and isometries on the space (see Example 5.1), is the Weierstrass local parametrization associated to a constant function f and to a degree one polynomial function g.

This matter was previously studied for rectangular Bézier surfaces in [**12**]. The authors considered the problem of determining all bicubical polynomial minimal surfaces bearing in mind the possible choices of functions f and g, in such a way that the Weierstrass parametrization is a polynomial of degree 3. They proved that: any bicubical polynomial minimal surface is, up to an affine transformation, a piece of Enneper's surface.

Therefore it is natural to study the properties that a cubical triangular control net must satisfy in order to be associated to a minimal surface. We will deduce those properties from the fact that the corresponding functions f and g must be as we have described previously: f a constant function and g a degree one complex polynomial.

3. Determining a cubical minimal surface given its vertices

In this section we will give a method to determine a minimal triangular Bézier cubical surface from its three corner points. Given the three vertices of a degree three control net, the associated minimal triangular Bézier surface with $(0, 0, 1)$ as normal unit[1] at its end can be determined because the complex functions f and g being a constant and a degree one polynomial respectively, characterize its control net.

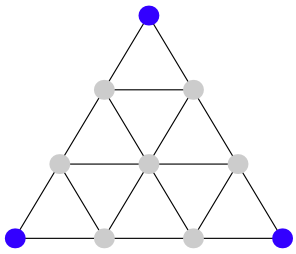

FIGURE 2. Given the three vertices, the other seven control points are determined in a minimal surface.

In order to characterize a minimal degree three control net $\mathcal{P} = \{P_I\}_{|I|=3}$ with $P_I = (a_I, b_I, c_I)$ given the three vertices, let us recall that, the only polynomial minimal surface for degree $n = 3$ is the Enneper surface, and that it is attained for

$$f(z) = k \qquad g(z) = r\, z + s. \tag{77}$$

Therefore, in order to be minimal, any degree three polynomial surface must be a local Weierstrass parametrization for f and g as above, Equation (77). That is,

[1]In the following section we will relate the Gauss map with the Weierstrass representation of a minimal surface, then we will explain why the normal vector at the infinity of the cubical minimal surface we consider here must be $(0, 0, 1)$.

$$\frac{\partial^{n+m} f(u,v)}{\partial u^n \partial v^m} = 0 \qquad \text{for} \quad m+n \geq 1 \tag{78}$$

$$\frac{\partial^{n+m} g(u,v)}{\partial u^n \partial v^m} = 0 \qquad \text{for} \quad m+n \geq 2.$$

If we bear in mind the complex derivative of a parametrization:

$$\frac{\partial \overrightarrow{x}}{\partial z} = \frac{1}{2}(\frac{\partial \overrightarrow{x}}{\partial u} - \mathbf{i}\frac{\partial \overrightarrow{x}}{\partial v})(u,v) = \frac{3}{2}\sum_{|I|=2}(\Delta^{1,0}P_I - \mathbf{i}\Delta^{0,1}P_I)B_I^2$$

$$=\frac{3}{2}(\sum_{|I|=2}(\Delta^{1,0}a_I - \mathbf{i}\Delta^{0,1}a_I)B_I^2, \sum_{|I|=2}(\Delta^{1,0}b_I - \mathbf{i}\Delta^{0,1}b_I)B_I^2, \sum_{|I|=2}(\Delta^{1,0}c_I - \mathbf{i}\Delta^{0,1}c_I)B_I^2) = (\phi_1, \phi_2, \phi_3),$$

then, the general expression of the functions f and g defined in Equation (76) in terms of $\mathcal{P}$ is given by:

$$f(z) = \phi_1 - \mathbf{i}\phi_2 = \frac{3}{2}(\sum_{|I|=2}(\Delta^{1,0}a_I - \mathbf{i}\Delta^{0,1}a_I)B_I^2 - \mathbf{i}\sum_{|I|=2}(\Delta^{1,0}b_I - \mathbf{i}\Delta^{0,1}b_I)B_I^2)$$

$$= \frac{3}{2}\sum_{|I|=2}((\Delta^{1,0}a_I - \Delta^{0,1}b_I) - \mathbf{i}(\Delta^{0,1}a_I + \Delta^{1,0}b_I))B_I^2,$$

$$g(z) = \frac{\phi_3}{\phi_1 - \mathbf{i}\phi_2} = \frac{\frac{3}{2}(\sum_{|I|=2}(\Delta^{1,0}c_I - \mathbf{i}\Delta^{0,1}c_I)\, B_I^2}{f(z)},$$

So let us compute the derivative of f:

$$\frac{\partial^{n+m} f}{\partial u^n \partial v^m} = \frac{\partial^{n+m}}{\partial u^n \partial v^m}(\frac{3}{2}\sum_{|I|=2}((\Delta^{1,0}a_I - \Delta^{0,1}b_I) - \mathbf{i}(\Delta^{0,1}a_I + \Delta^{1,0}b_I))B_I^2)$$

$$= \frac{3}{2}\sum_{|I|=2}((\Delta^{n+1,m}a_I - \Delta^{n,m+1}b_I) - \mathbf{i}(\Delta^{n,m+1}a_I + \Delta^{n+1,m}b_I))B_I^{2-(n+m)}.$$

Now to compute the derivative of g we will bear in mind that $f(z)$ is a constant function, so

$$g(z) = \frac{\frac{3}{2}(\sum_{|I|=2}(\Delta^{1,0}c_I - \mathbf{i}\Delta^{0,1}c_I)\, B_I^2}{f(0)},$$

and then, when we take derivatives, we get:

$$\frac{\partial^{n+m} g}{\partial u^n \partial v^m} = \frac{3}{2f(0)}\sum_{|I|=2}(\Delta^{n+1,m}c_I - \mathbf{i}\Delta^{n,m+1}c_I)B_I^{2-(n+m)}.$$

As we have said in Equation (78), the derivatives we have just computed must be zero for all $z = u + \mathbf{i}v$, then, at our convenience, we will evaluate these derivatives for $z = 0$. We

evaluate the Bernstein polynomials $B_I^{2-(n+m)}(u,v)$ and we get that

$$B^n_{(0,0,n)}(0,0) = 1 \quad \text{and} \quad B^n_{(i,j,n-i-j)}(0,0) = 0 \quad \text{if} \quad i,j \neq 0.$$

Therefore,

$$\begin{aligned}
\frac{\partial^{n+m} f}{\partial u^n \partial v^m}(0,0) &= \frac{3}{2}((\Delta^{n+1,m} a_{003} - \Delta^{n,m+1} b_{003}) - \mathbf{i}(\Delta^{n,m+1} a_{003} + \Delta^{n+1,m} b_{003})) \\
\frac{\partial^{n+m} g}{\partial u^n \partial v^m}(0,0) &= \frac{3}{2f(0)}(\Delta^{n+1,m} c_{003} - \mathbf{i}\Delta^{n,m+1} c_{003}).
\end{aligned}$$

Making these derivatives equal to zero we can relate the points in the control net by the following equations:

$$\left\{ \begin{array}{ll}
\Delta^{n+1,m} a_{003} - \Delta^{n,m+1} b_{003} = 0 & \text{for} \quad m+n \geq 1 \\
\Delta^{n,m+1} a_{003} + \Delta^{n+1,m} b_{003} = 0 & \text{for} \quad m+n \geq 1 \\
\Delta^{n,m} c_{003} = 0 & \text{for} \quad n+m = 3.
\end{array} \right. \tag{79}$$

On the other hand, the complex function $g(z)$ must satisfy another condition in order to be a complex polynomial of first degree ($g(z) = mz + n$), that is, $g(u + \mathbf{i}v) = mu + \mathbf{i}mv + n$. This condition can be written in the following way:

$$\mathbf{i}\frac{\partial g}{\partial u} = \frac{\partial g}{\partial v},$$

which evaluated at $z = 0$ gives:

$$\left\{ \begin{array}{c}
\mathbf{i}(\Delta^{2,0} c_{003} - \mathbf{i}\Delta^{1,1} c_{003}) = \Delta^{1,1} c_{003} - \mathbf{i}\Delta^{0,2} c_{003} \\
\Delta^{2,0} c_{003} + \Delta^{0,2} c_{003} = 0
\end{array} \right. \tag{80}$$

Equations (79) and (80) are linear so it is easy to determine five of the points of the control net:

$$\begin{cases} a_{012} = \frac{1}{6}(4a_{003} + 6a_{210} - 4a_{300} + 4b_{003} - b_{030} - 12b_{201} + 3b_{210} + 6b_{300}) \\ b_{012} = \frac{1}{6}(-4a_{003} + a_{030} + 12a_{201} - 3a_{210} - 6a_{300} + 4b_{003} + 6b_{210} - 4b_{300}) \\ c_{012} = \frac{1}{3}(3c_{003} + c_{030} - 3c_{201} + 2c_{300}) \end{cases}$$

$$\begin{cases} a_{021} = \frac{1}{3}(a_{030} + 3a_{201} + 3a_{210} - 4a_{300} + 2b_{003} - b_{030} - 6b_{201} + 3b_{210} + 2b_{300}) \\ b_{021} = \frac{1}{3}(-2a_{003} + a_{030} + 6a_{201} - 3a_{210} - 2a_{300} + b_{030} + 3b_{201} + 3b_{210} - 4b_{300}) \\ c_{021} = \frac{1}{3}(2c_{003} + 2c_{030} - 3c_{201} + 2c_{300}) \end{cases}$$

$$\begin{cases} a_{102} = \frac{1}{6}(2a_{003} + a_{030} + 6a_{201} - 3a_{210} - 2b_{003} + 6b_{201} - 4b_{300}) \\ b_{102} = \frac{1}{6}(2a_{003} - 6a_{201} + 4a_{300} + 2b_{003} + b_{030} + 6b_{201} - 3b_{210}) \\ c_{102} = \frac{1}{3}(c_{003} + 3c_{201} - c_{300}) \end{cases}$$

$$\begin{cases} a_{111} = \frac{1}{6}(4a_{003} + a_{030} - 6a_{201} + 3a_{210} + 4a_{300} + b_{030} - 3b_{210} + 2b_{300}) \\ b_{111} = \frac{1}{6}(-a_{030} + 3a_{210} - 2a_{300} + 4b_{003} + b_{030} - 6b_{201} + 3b_{210} + 4b_{300}) \\ c_{111} = \frac{1}{6}(2c_{003} + c_{030} + 3c_{210}) \end{cases}$$

$$\begin{cases} a_{120} = \frac{1}{3}(2a_{003} - 6a_{201} + 6a_{210} + a_{300} + 2b_{003} + b_{030} - 6b_{201} - 3b_{210} + 6b_{300}) \\ b_{120} = \frac{1}{3}(-2a_{003} - a_{030} + 6a_{201} + 3a_{210} - 6a_{300} + 2b_{003} - 6b_{201} + 6b_{210} + b_{300}) \\ c_{120} = \frac{1}{3}(c_{030} + 3c_{210} - c_{300}) \end{cases}$$

Note that, besides the three corners, P_{003}, P_{030} and P_{300}, there are two other control points, P_{210} and P_{201}, which are still unknown. They can be determined by asking for isothermality at the corners points.

$$P_{003} \quad P_{012} \quad P_{021} \quad P_{030}$$

$$P_{102} \quad P_{111} \quad P_{120}$$

$$P_{201} \quad P_{210}$$

$$P_{300}$$

The isothermality condition, given in Definition 5.1, at the three corner points, $\overrightarrow{x}(0,0)$, $\overrightarrow{x}(1,0)$ and $\overrightarrow{x}(0,1)$, translates into the following systems respectively.

$$\begin{cases} \Delta^{1,0}P_{003} \cdot \Delta^{1,0}P_{003} = \Delta^{0,1}P_{003} \cdot \Delta^{0,1}P_{003} \\ \Delta^{1,0}P_{003} \cdot \Delta^{0,1}P_{003} = 0 \end{cases}$$

$$\begin{cases} \Delta^{1,0}P_{201} \cdot \Delta^{1,0}P_{201} = \Delta^{0,1}P_{201} \cdot \Delta^{0,1}P_{201} \\ \Delta^{1,0}P_{201} \cdot \Delta^{0,1}P_{201} = 0 \end{cases}$$

$$\begin{cases} \Delta^{1,0}P_{021} \cdot \Delta^{1,0}P_{021} = \Delta^{0,1}P_{021} \cdot \Delta^{0,1}P_{021} \\ \Delta^{1,0}P_{021} \cdot \Delta^{0,1}P_{021} = 0. \end{cases}$$

Note that, since the isothermality conditions are non-linear, the previous is a quadratic system, with six equations and six unknowns that are the coordinates of the control points

P_{210} and P_{201}. Therefore, due to the difficulty involved in discussing it, we have solved it with the help of `Mathematica` in order to give some examples here.

The following figures are obtained by the method we have just described in this section. The characterization of a cubical control net associated to a polynomial minimal surface lets us to obtain the following surfaces with prescribed vertices.

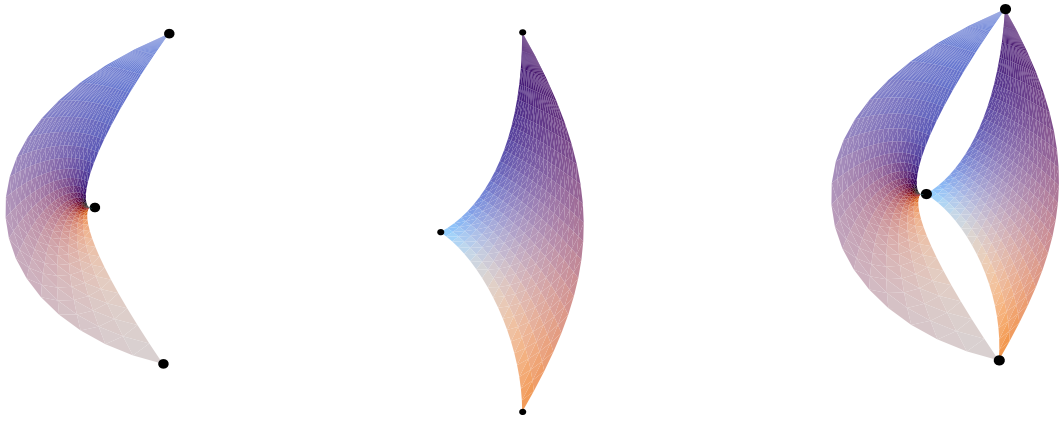

FIGURE 3. The quadratic system can sometimes have infinite solutions. For this example, with the vertices: $P_{003} = (0, 0, 0), P_{030} = (\frac{2}{3}, 0, -1)$ and $P_{300} = (0, \frac{2}{3}, 1)$, there is a family of solutions depending on one parameter, c_{210}. Therefore if we prescribe an arbitrary value for the parameter $c_{210} = \frac{2}{3}$, we find two solutions with different orientations.

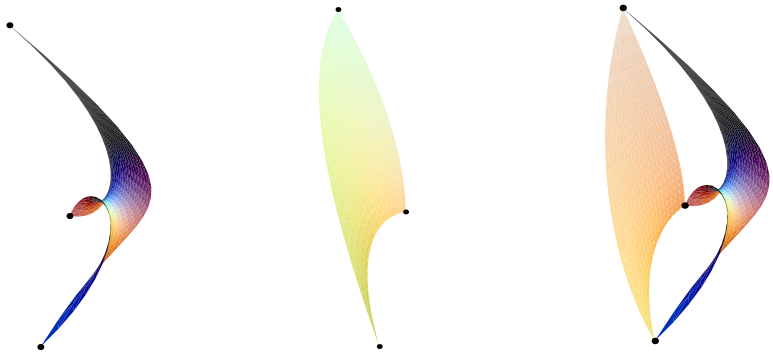

FIGURE 4. These surfaces correspond to the two orientations for the vertices $P_{003} = (0, \frac{2}{3}, 1), P_{030} = (\frac{5}{3}, \frac{5}{3}, 0)$ and $P_{300} = (0, \frac{-2}{3}, 4)$

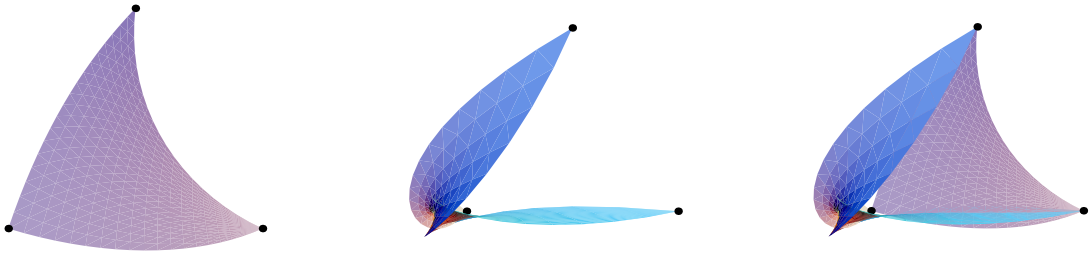

FIGURE 5. For this example we have chosen $P_{003} = (0,0,1), P_{030} = (0,1,0)$ and $P_{300} = (1,0,0)$ as vertices.

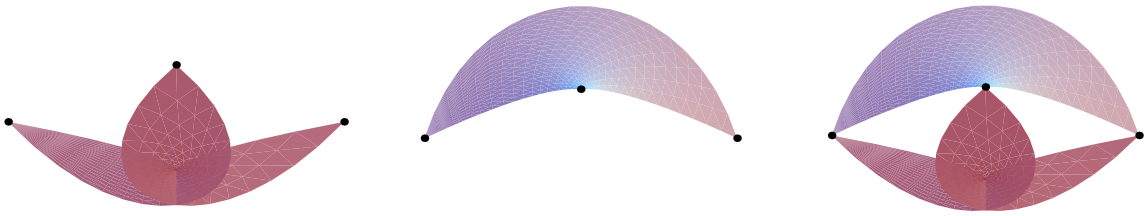

FIGURE 6. Here the vertices are $P_{003} = (\frac{-1}{2}, \frac{-1}{2}, \frac{\sqrt{2}}{2}), P_{030} = (1,-1,1)$ and $P_{300} = (-1,1,1)$. Let us recall that self-intersections may appear, as in fact, occurs with Enneper surface.

4. The Gauss map of minimal Bézier surfaces

In this section we give a method to obtain a minimal Bézier surface but, instead of just fixing the three vertices as we did for the cubical case in the previous section, we will also fix the tangent planes at the corner points.

We also give a similar method to obtain a minimal surface with prescribed tangent planes at the corner points, but now fixing a free set of points on the surface instead of only the three corners.

Any geometrical object related to a minimal surface can be written in terms of its Weierstrass representation. So, before introducing these new two methods, let us give an expression of the unit normal and discuss about the geometric interpretation of it.

From the definition of $\phi\left(\overrightarrow{x}\right) = \frac{d\overrightarrow{x}}{dz}$, given in Definition 5.6, we have that

$$\overrightarrow{x}_u \wedge \overrightarrow{x}_v = (2\mathrm{Re}\phi_1, 2\mathrm{Re}\phi_2, 2\mathrm{Re}\phi_3) \wedge (-2\mathrm{Im}\phi_1, -2\mathrm{Im}\phi_2, -2\mathrm{Im}\phi_3)\,,$$

where, see Lemma 5.21,

$$\phi = (\frac{f}{2}(1-g^2), \frac{\mathbf{i}f}{2}(1+g^2), fg)$$

with $f = f_1 + \mathbf{i}f_2$ and $g = g_1 + \mathbf{i}g_2$.

An easy computation allows us to express the unit normal vector of a surface in terms of its Weierstrass parametrization

$$N = \frac{2g_1}{1+|g|^2}\left(2g_1, 2g_2, |g|^2 - 1\right). \tag{81}$$

This expression gives us a geometric interpretation of the complex function g thanks to the stereographic projection of the sphere from the north pole. Let us recall the definition of stereographic projection.

DEFINITION 5.22. *Stereographic projection is defined as an application* $st : S^2(1) \longrightarrow \mathbb{C}$ *given by*

$$st(x, y, z) = \frac{x + \mathbf{i}y}{1 - z}.$$

It is easy to check that the complex function g is the stereographic projection of the normal unit.

LEMMA 5.23. *([**11**] Lemma 23.14.) Let* $\psi : U \longrightarrow \mathbb{C}^3$ *be a minimal curve such that* $\psi' = (\phi_1, \phi_2, \phi_3)$. *Let* N *be the unitary normal vector field of the local parametrization defined in Equation (75). Then*

$$st \circ N = \frac{\phi_3}{\phi_1 - \mathbf{i}\phi_2}.$$

At this point it is important to notice that if the complex function g is a polynomial, the limit at infinity of the normal unit we obtain that it is $(0, 0, 1)$, which means that the surface has a flat end. Moreover, since g is a non-identically zero polynomial it follows that the normal unit is $(0, 0, 1)$ only at infinity.

Now, if we consider the cubic case, the meromorphic function g must be of degree 1 at the most, then if g was a polynomial function the associated minimal surface would have a flat end, as we have just said, but let us consider in addition the rational case.

If $g = st \circ N$ was a rational function and it had a pole of order 1 in z_0, then, since $g(z_0) = st(N(u_0, v_0))$, the unit vector $N(u_0, v_0)$ must coincide with the north pole, $(0, 0, 1)$, which is the only singular value of the stereographic projection. Now let us consider a rotation of the surface in such a way that the singular value $(0, 0, 1)$ corresponds to the normal unit at infinity, then we can ensure that the associated function g has its pole at infinity, that is, it becomes a polynomial.

Now, let us show a property that the normal vectors at the corner points of a triangular piece of the Enneper surface satisfy.

LEMMA 5.24. *Let $\overrightarrow{x}$ be an isothermal parametrization of a piece of the Enneper's surface. Let N be the unitary normal vector field associated to the parametrization $\overrightarrow{x}$. Let us denote the normal vectors at the corner points, $\{N(\overrightarrow{x}(0,0)), N(\overrightarrow{x}(1,0)), N(\overrightarrow{x}(0,1))\}$, by $\{N_{003}, N_{300}, N_{030}\}$.*

Then

$$\{st(N_{003}), st(N_{300}), st(N_{030})\}$$

are the vertices of an isosceles right triangle.

Proof: Any isothermal parametrization of the Enneper surface with the same orientation can be seen as a Weierstrass representation with a degree one, $g(z) = mz+n$ where $m, n \in \mathbb{C}$, then

$$g(0) = n, \quad g(1) = m + n, \quad g(\mathbf{i}) = m\mathbf{i} + n,$$

are the vertices of an isosceles right triangle, and the length of its equal sides is given by m. ■

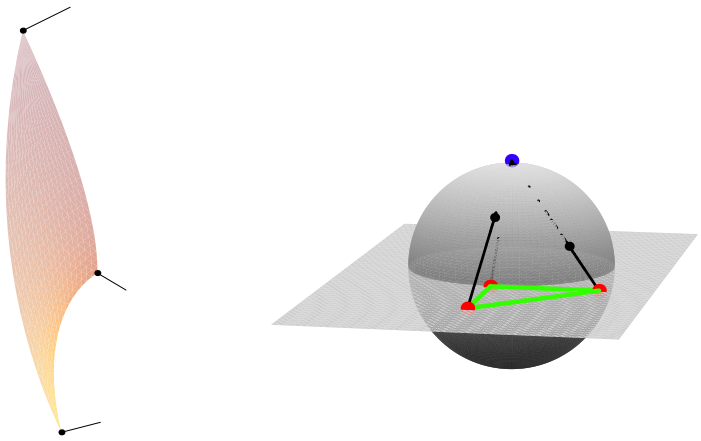

FIGURE 7. On the left a piece of Enneper's surface plotted as Triangular Bézier surface with its unit normal vectors at the corner points, on the right the normal unit vectors on a radius 1 sphere and the isosceles right triangle with the stereographic projection of the unit normal vectors as vertices.

The following proposition shows how a minimal and isothermal Bézier surface at least of degree six can be obtained if the corner points and the unitary normal vectors at these points are prescribed.

PROPOSITION 5.25. *Given the corner points $\{P_{003}, P_{300}, P_{030}\}$ and the unitary normal vectors at these points $\{N_{003}, N_{300}, N_{030}\}$, a minimal and isothermal Bézier surface of at least degree seven can be determined.*

Proof:

Let us recall what was said in Lemma 5.21, given a minimal curve, ψ, such that $\psi' = (\phi_1, \phi_2, \phi_3)$ and taking

$$f = \phi_1 - \mathbf{i}\phi_2, \qquad g = \frac{\phi_3}{\phi_1 - \mathbf{i}\phi_2}.$$

the Weierstrass representation of ψ is determined, that is,

$$\psi' = (\frac{f}{2}(1-g^2), \frac{\mathbf{i}f}{2}(1+g^2), fg),$$

and therefore the associated Weierstrass local parametrization is given by $\overrightarrow{x}(u,v) = Re\psi(u+\mathbf{i}v)$.

Moreover, from Theorem 5.19, we have that the Weierstrass local parametrization is minimal and isothermal by considering an analytic function $f(z)$ and an arbitrary meromorphic function $g(z)$.

On the other hand we can state from Lemma 5.23 that if ψ is a minimal curve as before, and N is the unitary normal vector field of the local parametrization $\overrightarrow{x}(u,v)$, then:

$$st \circ N = \frac{\phi_3}{\phi_1 - \mathbf{i}\phi_2}, \qquad \text{i.e.} \qquad st \circ N = g.$$

These previous results suggest us a method to build minimal surfaces through their Weierstrass local parametrization. We define the meromorphic functions g and f by:

$$g(z) = st(N_{003})\frac{(z-1)(z-\mathbf{i})}{\mathbf{i}} + st(N_{300})\frac{z(z-\mathbf{i})}{1-\mathbf{i}} + st(N_{030})\frac{z(z-1)}{\mathbf{i}(\mathbf{i}-1)}, \tag{82}$$

which is a kind of complex Lagrange polynomial, and we consider a quadratic complex polynomial

$$f(z) = b_0 + b_1 z + b_2 z^2$$

which enables us to consider the parametrization

$$\overrightarrow{x}(u,v) = Re\psi(u+\mathbf{i}v) = P_{003} + Re\int(\frac{f}{2}(1-g^2), \frac{\mathbf{i}f}{2}(1+g^2), fg)\,dz$$

involving the three complex parameters $b_j = Reb_j + \mathbf{i}Imb_j$ for $j = 0, 1, 2$.

Finally, we impose the conditions

$$\left.\begin{array}{l} \overrightarrow{x}(1,0) = P_{300} \\ \overrightarrow{x}(0,1) = P_{030}, \end{array}\right\}$$

which give a linear system of six equations that allow us to determine these three complex parameters. Therefore, a minimal surface is totally determined.

■

Let us comment that it can be found a related work in [**34**] , where the authors develop some methods to construct LN surfaces given three vertex points and its associated normal vectors.

REMARK 5.26. *Let us remark that the degree of the minimal surface is determined by the order of the polynomial functions $f(z)$ and $g(z)$. In the previous proposition, we chose two polynomials of order 2, and this implies that the minimal and isothermal parametrization is of degree seven in general.*

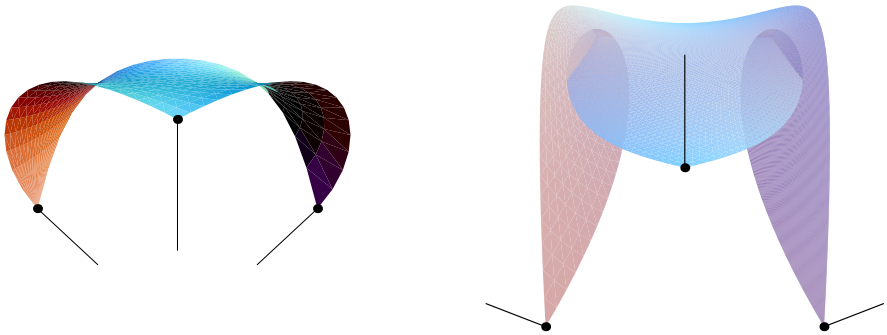

FIGURE 8. These two minimal surfaces of degree 7 are obtained by Proposition 5.25. The corner points and the unitary normal vectors at these points are prescribed.

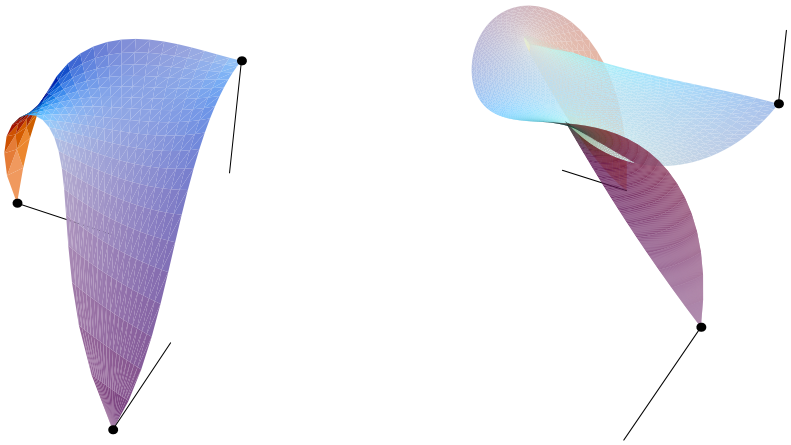

FIGURE 9. These two minimal surfaces of degree 7 are obtained by Proposition 5.25. The corner points and the unitary normal vectors at these points are prescribed.

Now, we give a new method, analogous to the one given in the previous proposition, which will enable us to fix some other points on the surface which is obtained. These points can be boundary points or not, they can be chosen freely.

The prescription of a larger set of points improves the control over the surface shape, but unfortunately implies an increase of degree.

PROPOSITION 5.27. *Given a set of points, $\{P_j\}_{j=0}^{m}$, and the three unitary vectors, $\{N_{003}, N_{300}, N_{030}\}$, a minimal and isothermal Bézier surface of at least degree $\frac{3m}{2}+4$ such that the given points belong to the surface and the vectors are the normal vectors at the three corner points can be determined.*

Proof:

This proof is analogous to the previous one. The choice of a meromorphic function $g(z)$ is again the one in Equation (82), but the chosen analytic function $f(z)$ increases its degree, we will consider a complex polynomial of order $\frac{3m}{2}-1$:

$$f(z) = \sum_{j=0}^{\frac{3m}{2}-1} b_j z^j.$$

Now if we consider, as before, the associated Weierstrass local parametrization,

$$\overrightarrow{x}(u,v) = Re\,\psi(u+\mathbf{i}v) = P_0 + Re\int (\frac{f}{2}(1-g^2), \frac{\mathbf{i}f}{2}(1+g^2), fg)\,dz,$$

we need to determine the set of $\frac{3m}{2}$ complex parameters $\{b_j\}_{j=0}^{\frac{3m}{2}-1}$ which are obtained thanks to the $3m$ linear equations:

$$P_j = \overrightarrow{x}(u_j, v_j) \qquad j = 1, ..., m$$

where $\{(u_j, v_j)\}_{j=0}^{m}$ is a sequence such that $(u_j, v_j) \in T$.

■

REMARK 5.28. *If $\frac{3m}{2}$ was not an integer we would consider the smallest integer greater than $\frac{3m}{2}$, that is, $\frac{3m+1}{2}$. Thus, the system of linear equations is underdetermined, with $3m$ equations and $3m+1$ unknowns.*

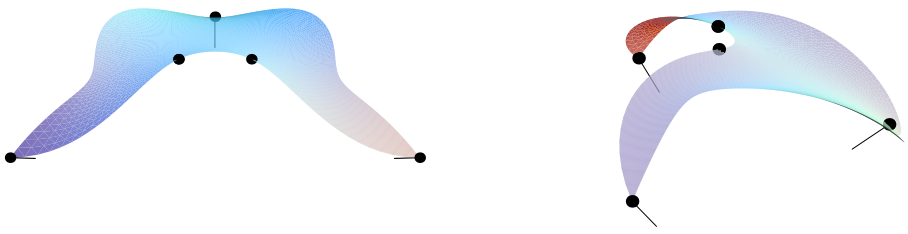

FIGURE 10. These are two views of a minimal surface of degree 10 obtained by Proposition 5.27. Five points and the unitary normal vectors at the corner points are prescribed.

5. Minimal Complex Bézier curves and minimal Bézier surfaces

In this section we will relate minimal complex Bézier curves with minimal Bézier surfaces. Let us recall the important result from the theory of minimal surfaces we gave in Lemma 5.10:

There is a one-to-one map between minimal curves and complex derivatives of minimal and isothermal local parametrizations.

Since we are interested in minimal Bézier surfaces it is natural to consider and study minimal regular complex Bézier curves.

In the first subsection we introduce complex Bézier curves in terms of the complex Bernstein polynomials and then, we provide a characterization of minimal complex Bézier curves in terms of their complex control points.

In the second subsection we characterize the derivative of the minimal Bézier curve associated to a minimal Bézier surface in terms of the control points of the surface.

In the third subsection we do the converse, we characterize minimal Bézier surfaces in terms of the complex control points of the associated minimal complex Bézier curve.

Finally in the last subsection, with the aim of reducing the set of initial data to the minimal set of data that determines a minimal surface, we give two methods that enable us to generate cubical minimal Bézier surfaces from two different sets of given parameters.

5.1. Minimal complex Bézier curves. First, let us define complex Bernstein polynomials and compute their derivatives.

Definition 5.29. *The complex Bernstein polynomials of degree n are defined by*

$$B_k^n(z) = \binom{n}{k} z^k (1-z)^{n-k}$$

where $z = u + \mathbf{i}v$.

The complex m-derivative of a complex Bernstein polynomial is analogous to the m-derivative of a real univariate Bernstein polynomial.

Definition 5.30. *The complex m-derivative of a complex Bernstein polynomial is given by*

$$\frac{d^m}{dz^m} B_k^n(z) = \frac{n!}{(n-m)!} \Delta^m B_k^{n-m}(z), \tag{83}$$

where the difference operators are defined by

$$\Delta^0 B_k^n(z) = B_k^n(z) \quad \textit{and} \quad \Delta^m B_k^n(z) = \Delta^{m-1}\left(B_{k-1}^{n-1}(z) - B_k^{n-1}(z)\right).$$

LEMMA 5.31. *The partial derivatives of a complex Bernstein polynomial of degree m are given by*

$$\frac{\partial^m}{\partial u^m} B_k^n(u+\mathbf{i}v) = \frac{n!}{(n-m)!}\Delta^m B_k^n(z)$$
$$\frac{\partial^m}{\partial v^m} B_k^n(u+\mathbf{i}v) = \frac{n!}{(n-m)!}\mathbf{i}^m\Delta^m B_k^n(z)$$

Now we can write a complex polynomial curve on the basis of complex Bernstein polynomials:

$$\psi(z) = \sum_{j=0}^{n} a_j B_j^n(z),$$

where $a_j \in \mathbb{C}^3$ are complex Bézier control points.

In the following proposition we characterize a minimal complex Bézier curve in terms of its complex control points.

PROPOSITION 5.32. *A complex Bézier curve* $\psi : \mathbb{C} \longrightarrow \mathbb{C}^3, z \mapsto \psi(z) = \sum_{j=0}^{n} a_j B_j^n(z)$, *is minimal if and only if*

$$\sum_{i=0}^{k} \binom{n-1}{i}\binom{n-1}{k-i} t_i \cdot t_{k-i} = 0, \tag{84}$$

where $t_i = \Delta a_i$.

Proof: From Definition 5.9, we have that a complex curve is minimal if and only if it is an analytic function which verifies the isothermality condition:

$$\psi'(z)\cdot\psi'(z) = 0 \quad \text{for all } z \in \mathbb{C}.$$

Since a complex Bézier curve is always an analytic function because it is a complex polynomial, we have only to rewrite condition $\psi'(z)\cdot\psi'(z) = 0$, in terms of complex control points.

The derivative of ψ is given by

$$\psi'(z) = n\sum_{j=0}^{n-1} B_j^{n-1}(z)(a_{j+1}-a_j) = n\sum_{j=0}^{n-1} B_j^{n-1}(z)\Delta a_j,$$

therefore

$$\psi'(z)\cdot\psi'(z) = n^2 \sum_{j=0,k=0}^{n-1} B_k^{n-1}(z)B_j^{n-1}(z)t_j\cdot t_k = n^2\sum_{k=0}^{2n-2}\sum_{i=0}^{k} \frac{\binom{n-1}{i}\binom{n-1}{k-i}}{\binom{2n-2}{k}} B_k^{2n-2}(z) t_i\cdot t_{k-i} = 0.$$

Then, due to the fact that the set of Bernstein polynomials of degree n is a basis of the vector space of polynomials of degree $\leq n$, we can state that $\psi' \cdot \psi' = 0$ iff

$$\sum_{i=0}^{k} \binom{n-1}{i}\binom{n-1}{k-i} t_i \cdot t_{k-i} = 0.$$

■

5.2. Minimal Bézier complex curve associated to a minimal Bézier surface. In this subsection we will describe the minimal Bézier complex curve associated to a minimal and isothermal Bézier chart, called its complexification. We will give the complex control points of the derivative of this minimal curve.

PROPOSITION 5.33. *Let $\{P_I\}_{|I|=n}$ be the control net of a minimal and isothermal triangular Bézier surface. Then the derivative of the associated minimal complex Bézier curve is given by*

$$\overrightarrow{x}'(z) = \sum_{j=0}^{n-1} t_j B_j^{n-1}(z)$$

where the control points $t_j \in \mathbb{C}^3$ are given by:

$$t_j = \frac{n}{2}\left(\Delta^{1,0}P_{0,j} - \mathbf{i}\Delta^{0,1}P_{0,j}\right).$$

Proof:
Given a minimal and isothermal Bézier chart, $\overrightarrow{x}$, let us compute its complex derivative:

$$\overrightarrow{x}'(z) = \frac{d\overrightarrow{x}}{dz}(u,v) = \phi(\overrightarrow{x})(u,v) = \frac{1}{2}\left(\overrightarrow{x}_u(u,v) - \mathbf{i}\,\overrightarrow{x}_v(u,v)\right).$$

The complex derivative of a minimal and isothermal chart can also be seen as the derivative of a minimal curve. Therefore it is an analytic function, so it must be a complex polynomial of degree $n-1$ in $z = u + \mathbf{i}v$, and, moreover, with the same coefficients as the polynomial in v: $\overrightarrow{x}'(0,v)$.

Bearing in mind the first derivative formulas, in Equation (8) and Equation (9), and also evaluating $B_I^{n-1}(0,v) = B_j^{n-1}(v)$, we get:

$$\overrightarrow{x}'(0,v) = \frac{n}{2}\sum_{j=0}^{n-1}(\Delta^{10}P_{0,j,n-j} - \mathbf{i}\Delta^{01}P_{0,j,n-j})B_j^{n-1}(v) = \sum_{j=0}^{n-1} t_j B_j^{n-1}(v) \qquad \text{where} \quad t_j \in \mathbb{C}^3.$$

Therefore we get the Bézier form of the derivative of the minimal complex curve associated to the minimal and isothermal chart, $\overrightarrow{x}$,

$$\overrightarrow{x}'(z) = \sum_{j=0}^{n-1} t_j B_j^{n-1}(z)$$

where the control points $t_j \in \mathbb{C}^3$ are given by :

$$t_j = \frac{n}{2}\left(\Delta^{1,0}P_{0,j} - i\Delta^{0,1}P_{0,j}\right).$$

These control points must satisfy the isothermality condition, given in Equation (84), since they belong to the derivative of a minimal curve.

■

5.3. Minimal chart associated to a minimal Bézier complex curve. In this subsection we follow the converse way of the previous one. We will obtain the harmonic and isothermal parametrization associated to a given minimal regular Bézier complex curve.

First we will give an expression of the complex Bernstein polynomials in terms of the real bivariate Bernstein polynomials.

PROPOSITION 5.34. *Any complex Bernstein polynomial of degree n, $B_k^n(z)$, can be written as:*

$$B_k^n(z) = \sum_{|I|=n} Q_I^k B_I^n(u,v),$$

where the $Q's$ can be recursively computed thanks to the formula

$$Q_{jm}^k = (-1)^m\, \mathbf{i}^m \Delta^{0,m}\delta_{jk-m} - \sum_{l=0}^{m-1}(-1)^{m-l}\binom{m}{l}Q_{jl}^k, \tag{85}$$

where we have denoted $Q_I^k = Q_{(j,l,n-l-j)}^k = Q_{jl}^k$, and δ_{jk} is the Kronecker delta, which is defined by

$$\delta_{jk} = \begin{cases} 1 & k = j, \\ 0 & k \neq j. \end{cases}$$

Proof:

The set of bivariate Bernstein polynomials of degree n is a basis of the space of bivariate polynomials of degree $\leq n$, so we can ensure the existence of a set of complex numbers $\{Q_I^k\}_{|I|=n}$ such that

$$B_k^n(z) = \sum_{|I|=n} Q_I^k B_I^n(u,v). \tag{86}$$

Then, if we evaluate the complex Bernstein polynomials $B_k^n(u+\mathbf{i}v)$ for $v=0$ we obtain

$$B_k^n(u) = \sum_{|I|=n} Q_I^k B_I^n(u,0) = \sum_{j=0}^{n} Q_{j0}^k B_j^n(u)$$

and therefore we deduce $Q_{j0}^k = \delta_{kj}$.

Now, we introduce an iterative process by taking derivatives repeatedly in Equation (86) and evaluating at $v = 0$.

In the first step, the first derivative,

$$\frac{\partial B_k^n(z)}{\partial v}\Big|_{v=0} = \frac{\partial}{\partial v}\Big|_{v=0} \left(\sum_{|I|=n} Q_I^k B_I^n(u,v) \right),$$

that is,

$$\mathbf{i}\left(B_{k-1}^{n-1}(u) - B_k^{n-1}(u)\right) = \sum_{j=0}^{n-1} \Delta^{01} Q_{j0}^k B_j^{n-1}(u).$$

Bearing in mind the definition of the Kronecker delta we can rewrite the previous equation,

$$\mathbf{i}\sum_{j=0}^{n-1}(\delta_{jk-1} - \delta_{jk})B_j^{n-1}(u) = \sum_{j=0}^{n-1}(Q_{j1}^k - Q_{j0}^k)B_j^{n-1}(u),$$

which implies

$$Q_{j1}^k = -\mathbf{i}\Delta^{0,1}\delta_{jk-1} + Q_{j0}^k.$$

Then, at the m-th step we deduce:

$$(-1)^m \mathbf{i}^m \Delta^{0,m}\delta_{jk-m} = \Delta^{0,m} Q_{j0}^k,$$

and that leads us to the desired result.

■

The following proposition will show how to obtain the minimal and isothermal parametrization associated to a given minimal Bézier complex curve.

PROPOSITION 5.35. *Given a minimal Bézier complex curve* $\psi(z) = \sum_{k=0}^n (a_k + \mathbf{i}b_k)B_k^n(z)$, *with* $a_k + \mathbf{i}b_k \in \mathbb{C}^3$, *the associated isothermal parametrization of the corresponding minimal surface is given by*

$$\overrightarrow{x}(u,v) = \sum_{|I|=n} P_I B_I^n(u,v) \quad \textit{where} \quad P_I = P_{j,r,n-j-r} = \sum_{k=0}^n a_k Re Q_{jr}^k - b_k\, Im Q_{jr}^k,$$

with the coefficients Q_{jr}^k *defined in Equation (85).*

Proof: A straightforward computation bearing in mind the previous proposition, Proposition 5.35, gives us the expression:

$$\psi(z) = \sum_{k=0}^{n}(a_k + \mathbf{i}b_k)B_k^n(z) = \sum_{k=0}^{n}(a_k + \mathbf{i}b_k)\sum_{|I|=n} Q_I^k B_I^n(u,v)$$
$$= \sum_{|I|=n}\left((a_k \mathrm{Re}Q_{jr}^k - b_k \mathrm{Im}Q_{jr}^k) + \mathbf{i}(b_k\,\mathrm{Re}Q_{jr}^k + a_k\,\mathrm{Im}Q_{jr}^k)\right)B_I^n(u,v),$$

which allows to state that

$$\overrightarrow{x}(u,v) = \mathrm{Re}\psi(u+\mathbf{i}v) = \sum_{|I|=n}\left(\sum_{k=0}^{n} a_k \mathrm{Re}Q_{jr}^k - b_k \mathrm{Im}Q_{jr}^k\right)B_I^n(u,v).$$

■

5.3.1. *Case n=3.* Here we will consider the general result obtained in Proposition 5.35 for the particular case $n = 3$. So, given a cubical minimal curve $\psi(z) = \sum_{k=0}^{3}(a_k+\mathbf{i}b_k)B_k^3(z)$, we will compute complex coefficients $\{Q_I^k\}_{|I|=3}$ such that $B_k^3(z) = \sum_{|I|=3} Q_I^k B_I^3(u,v)$, which will enable us to obtain the associated minimal and isothermal parametrization $\overrightarrow{x}(u,v) = \mathrm{Re}\,\psi(u+\mathbf{i}v)$ and its Bézier control points.

From Proposition 5.34 we have:

$$\begin{cases} Q_{j0}^k = \delta_{jk} \\ Q_{j1}^k = (1-\mathbf{i})\delta_{jk} + \mathbf{i}\delta_{jk-1} \\ Q_{j2}^k = -2\mathbf{i}\delta_{jk} + 2(\mathbf{i}+1)\delta_{jk-1} - \delta_{jk-2} \\ Q_{j3}^k = -(2+2\mathbf{i})\delta_{jk} + 6\delta_{jk-1} - (3-3\mathbf{i})\delta_{jk-2} - \mathbf{i}\delta_{jk-3}, \end{cases}$$

so we can compute $P_{jr} = \left(\sum_{k=0}^{3} a_k\,\mathrm{Re}Q_{jr}^k - b_k\,\mathrm{Im}Q_{jr}^k\right)$ in terms of the complex control points $(a_k + \mathbf{i}b_k)$:

$$\begin{cases} P_{j0} = a_j & j = 0,1,2,3 \\ P_{j1} = a_j - b_{j+1} + b_j & j = 0,1,2 \\ P_{j2} = 2a_{j+1} - a_{j+2} + 2b_j - 2b_{j+1} & j = 0,1 \\ P_{j3} = -3a_{j+2} + 6a_{j+1} - 2a_j + b_{j+3} - 3b_{j+2} + 2b_j & j = 0. \end{cases}$$

6. Building up cubical minimal Bézier surfaces

At this point we are able to obtain an isothermal parametrization of a cubical minimal surface, starting from the four complex control points of the associated minimal complex Bézier curve. In this section we will consider again the cubic case, we will give two methods to generate cubical minimal Bézier surfaces.

First, we will show the way to generate a minimal curve given a complex control point and three complex numbers, and then obtain a minimal Bézier surface as the real part of it.

In the second subsection we propose a method for generating cubical minimal surfaces from a given set of two real numbers. We will see that, for this method, the three control

points of a corner of the surface are prescribed with isothermality and the two real numbers are the third coordinates of two other control points.

6.1. Building up cubical minimal Bézier surfaces given a control point and three complex numbers. The following lemma will be needed in order to prove our next result.

LEMMA 5.36. *A complex point $z \in \mathbb{C}^3$ verifies $z \cdot z = 0$ if and only if it is given by*

$$z = a((1-b^2), \mathbf{i}(1+b^2), 2b),$$

for a pair of complex numbers $a, b \in \mathbb{C}$ or

$$z = a(-1, \mathbf{i}, 0)$$

for a complex number $a \in \mathbb{C}$.

As we said above, the following result states that given three complex numbers and a control point, it is possible to obtain the associated cubical isothermal and minimal Bézier parametrization with $(0,0,1)$ as normal vector at its end. This parametrization is obtained as the real part of a minimal Bézier curve.

THEOREM 5.37. *Any cubical, isothermal and minimal Bézier chart with $(0,0,1)$ as normal vector at its end verifies*

$$\overrightarrow{x}(u,v) = Re\left(\sum_{k=0}^{3} B_k^3(u+\mathbf{i}v)a_k\right),$$

where

$$\begin{aligned}
a_0 &= (a_x^0, a_y^0, a_z^0) \in \mathbb{C}^3,\\
a_1 &= a_0 + f_0((1-g_0^2), \mathbf{i}(1+g_0^2), 2g_0),\\
a_2 &= a_1 + f_0((1-g_0g_2), \mathbf{i}(1+g_0g_2), g_0+g_2),\\
a_3 &= a_2 + f_0((1-g_2^2), \mathbf{i}(1+g_2^2), 2g_2).
\end{aligned}$$

f_0, g_0, g_2 being complex numbers.

Proof: Equations (84) for the case n=3 are reduced to:

$$\left\{\begin{array}{l} t_0 \cdot t_0 = 0\\ t_0 \cdot t_1 = 0\\ 2t_1 \cdot t_1 + t_0 \cdot t_2 = 0\\ t_1 \cdot t_2 = 0\\ t_2 \cdot t_2 = 0 \end{array}\right. \tag{87}$$

where $t_j = \Delta a_j$.

From Lemma 5.36, we can suppose that

$$\begin{aligned} t_0 &= f_0((1-g_0^2), \mathbf{i}(1+g_0^2), 2g_0), \\ t_2 &= f_2((1-g_2^2), \mathbf{i}(1+g_2^2), 2g_2). \end{aligned} \tag{88}$$

Substituting Equation (88) in Equation (87), and writing $t_1 = (a, b, c) \in \mathbb{C}^3$, we have

$$\begin{cases} a(1-g_0^2) + b\mathbf{i}(1+g_0^2) + 2g_0 = 0 \\ a^2 + b^2 + c^2 = f_0 f_2 (g_0 - g_2)^2 \\ a(1-g_2^2) + b\mathbf{i}(1+g_2^2) + 2g_2 = 0. \end{cases} \tag{89}$$

From the first and the last equations we can obtain

$$a = c\,\frac{1-g_0g_2}{g_0+g_2} \quad b = c\,\mathbf{i}\frac{1+g_0g_2}{g_0+g_2}.$$

Substituting now in the second equation of the system in Equation (89), we arrive at $c = \sqrt{f_0 f_2}(g_0+g_2)$, so we can finally state that

$$t_1 = \sqrt{f_0 f_2}(1-g_0g_2, \mathbf{i}(1+g_0g_2), g_0+g_2).$$

Let us recall that if the normal vector at the end is (0,0,1), then the Weierstrass representation of the chart is given by $g(z)$ a complex polynomial of degree 1, and $f(z)$, a constant complex function.

Let us now compute $f(z)$. It is easy to see that

$$f(z) = 2f_0B_0^2(z) + 2\sqrt{f_0f_2}B_1^2(z) + 2f_2B_2^2(z).$$

Bearing in mind that $B_0^2(z) + B_1^2(z) + B_2^2(z) = 1$, then f will be a constant function if and only if $f_0 = \sqrt{f_0f_2} = f_2$.

Therefore

$$\begin{aligned} \Delta a_0 &= f_0((1-g_0^2), \mathbf{i}(1+g_0^2), 2g_0), \\ \Delta a_1 &= f_0((1-g_0g_2), \mathbf{i}(1+g_0g_2), g_0+g_2) \\ \Delta a_2 &= f_2((1-g_2^2), \mathbf{i}(1+g_2^2), 2g_2). \end{aligned}$$

■

Remark 5.38. *If we compute $g(z)$ we get*

$$g(z) = g_0(1-z) + g_2z = g_0B_0^1 + g_2B_1^1.$$

With such a function $g(0) = g_0$, $g(1) = g_2$ and $g(\mathbf{i}) = g_0 + \mathbf{i}(g_2 - g_0)$, so these three complex points, which are the the stereographic projection image of the normal vectors at the corner points of the Bézier surface, are located in the complex plane as vertices of an isosceles right triangle with length $|g_2 - g_0|$ on its equal sides.

REMARK 5.39. *The imaginary part of the complex control point a_0 has no influence on the minimal Bézier chart that we obtained. Hence, we can consider $a_0 \in \mathbb{R}^3$ and $f_0, g_0, g_2 \in \mathbb{C}$, and therefore there are $3 + 3 \cdot 2 = 9$ degrees of freedom to build up a cubical minimal and isothermal Bézier surface with $(0, 0, 1)$ as the normal vector at infinity.*

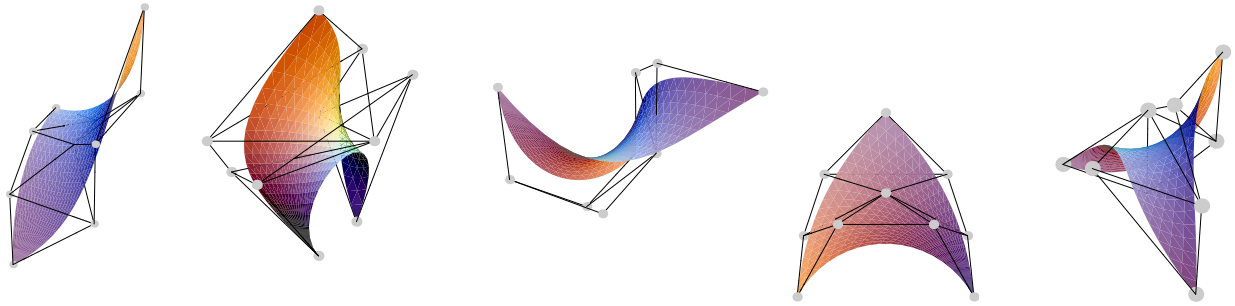

FIGURE 11. These minimal surfaces are obtained by Theorem 5.37, in particular these five examples are obtained respectively for the values

a_0	f_0	g_0	g_2
$(0,0,0)$	1	0	1
$(0,0,0)$	-1	$1-\mathbf{i}$	$1+\mathbf{i}$
$(0,0,0)$	1	1	$\mathbf{i}$
$(0,0,0)$	2	$1-\mathbf{i}$	1
$(1,0,1)$	$\mathbf{i}$	1	$\mathbf{i}$

.

6.2. Building up cubical minimal Bézier surfaces given a pair of real numbers. As we said in Remark 5.39, the surface generation method we have studied in the previous subsection leaves 9 degrees of freedom to build a cubical minimal surface with a flat end. In the following method we will only have two free parameters. We will prescribe the three control points of a corner of the surface

$$P_{000} = (0,0,0) \quad P_{012} = (1,0,0) \quad \text{and} \quad P_{102} = (0,1,0),$$

satisfying the isothermality condition, and we will give a method to obtain the associated cubical minimal and isothermal parametrization, with $(0, 0, 1)$ as the normal vector at its end, only the third coordinate of a pair of control points, P_{120} and the vertex P_{030} being kept free.

As we will see, in order to obtain the parametrization of this cubical minimal surface, we first determine the control points on the first two lines of the control net. After that we are able to determine the whole control net by Theorem 1.9 in Chapter 1, since we ask for harmonicity.

PROPOSITION 5.40. *Given the third coordinates, c_{021} and c_{030}, where we have denoted $P_I = (a_I, b_I, c_I)$, and prescribed the three control points at one corner in an isothermal way,*

$$P_{000} = (0,0,0) \quad P_{012} = (1,0,0) \quad \textit{and} \quad P_{102} = (0,1,0),$$

the isothermal parametrization of the cubical minimal surface, with a flat end associated to these control points, is given by

$$\begin{aligned}\overrightarrow{x}(u,v) = (&3v + (\frac{1}{3}c_{030}c_{120} - \frac{1}{9}c_{030}^2)u^3 + (\frac{1}{4}c_{030}^2 + \frac{1}{2}c_{030}c_{120} - \frac{3}{4}c_{120}^2)u^2v \\ &+(\frac{1}{3}c_{030}^2 - c_{030}c_{120})uv^2 + (\frac{1}{4}c_{120}^2 - \frac{1}{12}c_{030}^2 - \frac{1}{6}c_{030}c_{120})v^3, \\ &3u + (\frac{1}{4}c_{120}^2 - \frac{1}{12}c_{030}^2 - \frac{1}{6}c_{030}c_{120})u^3 + (c_{030}c_{120} - \frac{1}{3}c_{030}^2)u^2v \\ &+(\frac{1}{4}c_{030}^2 + \frac{1}{2}c_{030}c_{120} - \frac{3}{4}c_{120}^2)uv^2 + (\frac{1}{9}c_{030}^2 - \frac{1}{3}c_{030}c_{120})v^3, \\ &c_{030}v^2 + (3c_{120} - c_{030})uv - c_{030}u^2\big)\,.\end{aligned}$$

Proof:

In general in order to achive isothermality, the complex control points of a complex Bézier curve must satisfy the relations given in Equation (84). For the cubic case these relations are reduced to the equations given in (87), which as we have seen in Theorem 5.37, give us the solution:

$$\begin{cases} t_0 = f_0((1-g_0^2), \mathbf{i}(1+g_0^2), 2g_0), \\ t_1 = f_0(1-g_0g_2, \mathbf{i}(1+g_0g_2), g_0+g_2) \\ t_2 = f_0((1-g_2^2), \mathbf{i}(1+g_2^2), 2g_2), \end{cases}$$

which at our convenience, we will say is equivalent to:

$$\begin{cases} t_0 = \frac{n}{2} f_0((1-g_0^2), \mathbf{i}(1+g_0^2), 2g_0), \\ t_1 = \frac{n}{2} f_0(1-g_0g_2, \mathbf{i}(1+g_0g_2), g_0+g_2) \\ t_2 = \frac{n}{2} f_0((1-g_2^2), \mathbf{i}(1+g_2^2), 2g_2), \end{cases} \tag{90}$$

On the other hand, if we consider the analytic complex Bézier curve given by the complex derivative of a harmonic parametrization, we have that its control points are

$$t_j = \frac{n}{2}\left(\Delta^{1,0}P_{0,j} - \mathbf{i}\Delta^{0,1}P_{0,j}\right)$$

and therefore we can rewrite Equation (90) in terms of the real control points:

$$
\begin{aligned}
\left(\Delta^{10}P_{003} - \mathbf{i}\Delta^{012}P_{003}\right) &= f_0((1-g_0^2), \mathbf{i}(1+g_0^2), 2g_0),\\
\left(\Delta^{10}P_{012} - \mathbf{i}\Delta^{012}P_{012}\right) &= f_0((1-g_2^2), \mathbf{i}(1+g_2^2), 2g_2),\\
\left(\Delta^{10}P_{021} - \mathbf{i}\Delta^{012}P_{021}\right) &= f_0(1-g_0g_2, \mathbf{i}(1+g_0g_2), g_0+g_2).
\end{aligned} \tag{91}
$$

The first and the last equations give us the expression of f_0, g_0 and g_2 in terms of real control points, $P_I = (a_I, b_I, c_I)$,

$$
\begin{aligned}
f_0 &= \frac{1}{2}\left(\left(\Delta^{10}a_{003} - \mathbf{i}\Delta^{01}a_{003}\right) - \mathbf{i}\left(\Delta^{10}b_{003} - \mathbf{i}\Delta^{01}b_{003}\right)\right)\\
&= \frac{1}{2}((\mathbf{i}-1)a_{003} - \mathbf{i}a_{012} + a_{102} + (1+\mathbf{i})b_{003} - b_{012} - \mathbf{i}b_{102}),\\
g_0 &= \frac{1}{f_0}\left(\Delta^{10}c_{003} - \mathbf{i}\Delta^{01}c_{003}\right) = \frac{1}{f_0}(c_{102} - c_{003} - \mathbf{i}(c_{012} - c_{003})),\\
g_2 &= \frac{1}{f_0}\left(\Delta^{10}c_{021} - \mathbf{i}\Delta^{01}c_{021}\right) = \frac{1}{f_0}(c_{120} - c_{021} - \mathbf{i}(c_{030} - c_{021})).
\end{aligned}
$$

Now, bearing in mind that three control points in a corner are fixed with isothermality, that is,

$$P_{000} = (0,0,0) \quad P_{012} = (1,0,0) \quad \text{and} \quad P_{102} = (0,1,0),$$

we can see that f_0 and g_0 are totally determined.

Moreover, since the pair of coordinates c_{021} and c_{030} are given data, the second equation in (91) enables us to obtain:

$$
\begin{aligned}
P_{111} &= \left(1, 1, \frac{1}{6}(3c_{120} - c_{030})\right)\\
P_{021} &= (2, 0, \frac{1}{3}c_{030}).
\end{aligned}
$$

and from first and last equations in (91) we get:

$$
\begin{aligned}
a_{030} &= \frac{1}{12}(36 - c_{030}^2 - 2c_{030}c_{120} + 3c_{120}^2)\\
a_{120} &= \frac{1}{9}(18 + c_{030}^2 - 3c_{030}c_{120})\\
b_{030} &= \frac{1}{9}(c_{030}^2 - 3c_{030}c_{120})\\
b_{120} &= \frac{1}{12}(12 + c_{030}^2 + 2c_{030}c_{120} - 3c_{120}^2).
\end{aligned}
$$

Up till now, we have determined all the control points on the first two lines of the control net in terms of c_{030} and c_{120}. Therefore, the whole harmonic control net can be determined by Theorem 1.9.

The minimal and isothermal chart is given by:

$$\begin{aligned}\overrightarrow{x}(u,v) = (&3v + (\frac{1}{3}c_{030}c_{120} - \frac{1}{9}c_{030}^2)u^3 + (\frac{1}{4}c_{030}^2 + \frac{1}{2}c_{030}c_{120} - \frac{3}{4}c_{120}^2)u^2v \\ &+(\frac{1}{3}c_{030}^2 - c_{030}c_{120})uv^2 + (\frac{1}{4}c_{120}^2 - \frac{1}{12}c_{030}^2 - \frac{1}{6}c_{030}c_{120})v^3, \\ &3u + (\frac{1}{4}c_{120}^2 - \frac{1}{12}c_{030}^2 - \frac{1}{6}c_{030}c_{120})u^3 + (c_{030}c_{120} - \frac{1}{3}c_{030}^2)u^2v \\ &+(\frac{1}{4}c_{030}^2 + \frac{1}{2}c_{030}c_{120} - \frac{3}{4}c_{120}^2)uv^2 + (\frac{1}{9}c_{030}^2 - \frac{1}{3}c_{030}c_{120})v^3, \\ &c_{030}v^2 + (3c_{120} - c_{030})uv - c_{030}u^2\big)\,.\end{aligned}$$

■

Now we will show some examples of cubical minimal surfaces with isothermal chart, which are obtained thanks to Proposition 5.40. In each of the following figures there are three smaller black points which are the prescribed corners, the bigger black points are the control points with a free third coordinate, P_{120} and P_{003}. The other control points are in gray.

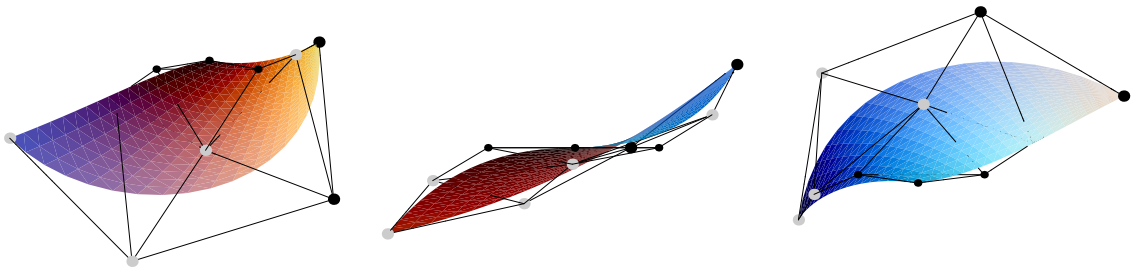

FIGURE 12. These minimal surfaces are obtained by Proposition 5.40 for $c_{003} = -1$ and for three different values of c_{120}, which are the following: $-2, 0, 2$.

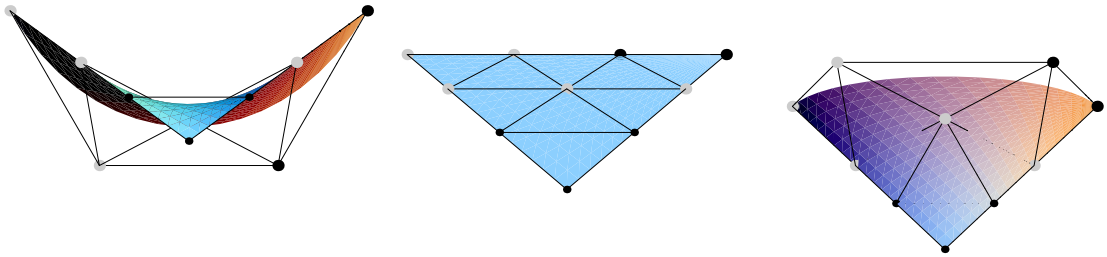

FIGURE 13. Analogously these three minimal surfaces have been obtained by Proposition 5.40 for $c_{003} = 0$ and for three different values of c_{120}, which are the following: $-2, 0, 2$. Note that when $c_{003} = c_{120} = 0$, the solution is a piece of a plane.

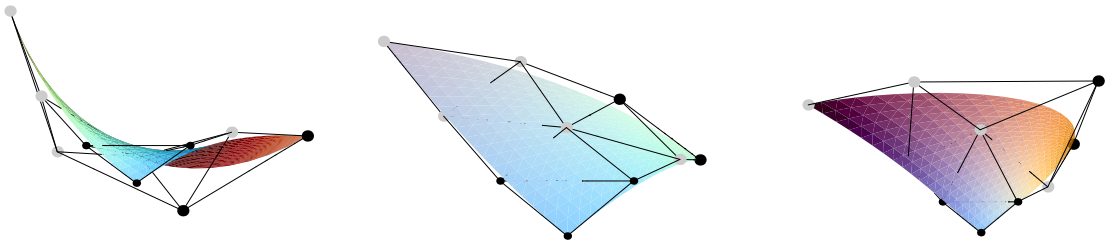

FIGURE 14. These are the figures given by Proposition 5.40 for $c_{003} = 1$ and again for the values of c_{120}: $-2, 0, 2$.

Let us remark that in this last section we have given two methods to generate cubical minimal surfaces with a flat end. Since the complex function g is considered to be a polynomial, we find, as we said before, that

$$\lim_{u,v\to\pm\infty} N(u,v) = (0,0,\pm 1).$$

If we impose this condition, that the normal vector at infinity be the North Pole, we find 9 degrees and 2 degrees of freedom, respectively, in the pair of methods we have presented. But, the minimal surface obtained could be rotated. Then, since such rotations are parametrized by two angles, we could consider that there are two more free parameters in order to build a surface with a non-planar end.

7. Conclusions

In this chapter we have given different methods to generate minimal surfaces with the prescription of some initial data.

We have described a method to generate a cubical minimal and isothermal triangular surface given its vertices, a second method to generate a degree seven minimal and isothermal triangular Bézier surface given, in addition to its three vertices, the tangent planes at those

points, and a third method, prescribing an arbitrary set of points on the surface and the tangent planes at the corner points, in order to generate a minimal and isothermal surface of a higher degree.

Moreover, here we have conducted a study relating minimal surfaces with minimal complex curves. We have deduced from this study two more methods to generate cubical minimal isothermal surfaces. With the aim of reducing the number of parameters that totally determine a minimal surface as much as possible, we have obtained two surface generation methods related with minimal curves, one with 9 degrees of freedom and another which only leaves 2 free parameters.

We find that, as soon as we reduce the size of the set of prescribed information, the use of minimal surfaces becomes too restrictive. Aesthetically we obtain good shapes for low degrees, such as pieces of the Enneper surface for the cubic case. But, we find that if the surface degree increases, the shapes obtained get too complicated.

Another of the consequences of this study is that we have realized that minimal surfaces are too rigid if we want to solve, for example, blending problems. The condition $H = 0$ imposes too many restrictions on a polynomial surface so that, given a prescribed border, we cannot expect to be able to find a minimal polynomial surface with that border.

CHAPTER 6

The Dirichlet functional results

In this chapter we address the problem of finding the triangular Bézier patch minimizing the area among all triangular Bézier surfaces with a prescribed boundary. As is well known, the border of a triangular Bézier surface is determined by the border control points. So, the problem can be reformulated as follows: Given the exterior points of a triangular control net, find the interior control points in such a way that the resulting triangular Bézier surface has minimal area among all the triangular Bézier surfaces with the same border. Let us call this problem the *triangular Bézier-Plateau problem.*

The theory of minimal surfaces shows that in order to prove the existence of minimal surfaces, one can replace the area functional (a highly non linear functional) by another functional, now linear, having the same extremals. The common substitute is the Dirichlet functional, as it is usually called in the mathematical literature, but which is known as the stretch functional in the CAGD literature, (see [**44**]).

The problem of minimizing the Dirichlet functional among all rectangular Bézier surfaces with a prescribed boundary was previously studied in [**29**] and [**30**]. The advantage of using the Dirichlet functional is that the determination of extremals becomes just a linear problem. Moreover, if a triangular Bézier patch is harmonic and isothermal it is the extremal of both the area and Dirichlet functionals. We have found that when the control net satisfies isothermality conditions at the three corner points then our method shows, in general, a significant improvement.

When isothermality is not satisfied at the three corner points, then considering the Dirichlet extremal as an approximation to the area extremal, presents an intrinsic error of the method error. In the last section of this chapter we propose an improvement on the approximation based on geometric principles which maintain the use of linear systems. Then, the triangular Bézier surfaces we obtain have a smaller area than the surfaces obtained by the other methods for the same border configurations.

The extremal for cubical triangular Bézier surfaces can be computed and the solution used as a mask for obtaining approximations at higher degrees. On the other hand, we can try to obtain the extremals of the Dirichlet functional at higher degrees directly. The use of masks is due to the fact that they make the system of linear equations easier to solve (since it is a sparse system) than the system deduced from the Dirichlet equations, which has no null coefficients.

The mask we have obtained, the Dirichlet mask, is an asymmetric mask, as expected, due to the asymmetry of triangular Bézier surfaces. But as we said in the Introduction, our asymmetric methods give good results. For example, for degree 3, it is possible to show that

fixing the border control points as the ones of an arbitrary triangular piece of the Enneper surface, our asymmetric mask gives always exactly the interior control point. It can even be shown that there are pieces of the Enneper surface for which the inner control point cannot be obtained by applying a symmetric mask to the exterior control points.

In this chapter we have also studied the biharmonic functional or bending energy functional, which is also known as thin plate energy. This functional can be chosen as a measure of the fairness of a surface. Here we have considered, in an analogous way to how we dealt the Dirichlet functional, the problem of finding a triangular Bézier surface which minimizes the biharmonic functional given a boundary.

1. The Dirichlet functional results

To solve the triangular Bézier-Plateau problem we have to try to minimize the functional area among all the triangular Bézier surfaces with a prescribed boundary which is determined by the exterior control points. Nevertheless, due to its high non-linearity, the problem of minimizing the area functional is hard to deal with, so we shall work instead with the Dirichlet functional:

$$\mathcal{D}(\mathcal{P}) = \frac{1}{2}\int_{\mathcal{T}} (\|\overrightarrow{x_u}\|^2 + \|\overrightarrow{x_v}\|^2) du\, dv.$$

There are two reasons for making such a substitution: the first one is given by the following fact relating the area and the Dirichlet functional:

$$(E\,G\, -\, F^2)^{\frac{1}{2}} \leq (E\,G)^{\frac{1}{2}} \leq \frac{E\, +\, G}{2}. \tag{92}$$

Therefore, for any triangular control net $\mathcal{P}$, $\mathcal{A}(\mathcal{P}) \leq D(\mathcal{P})$. Moreover, equality can occur only if $E = G$ and $F = 0$, i.e., for isothermal patches.

The second is related with the Euler-Lagrange equation associated to the Dirichlet functional, which is defined not on control nets, but on parametrizations

$$\overrightarrow{x} \to \frac{1}{2}\int_{\mathcal{T}} (\|\overrightarrow{x_u}\|^2 + \|\overrightarrow{x_v}\|^2) du\, dv.$$

This equation is just $\Delta\overrightarrow{x} = 0$. Therefore, if the extremal of the Dirichlet functional is an isothermal patch, it is automatically a harmonic patch, and hence the surface is minimal.

Nevertheless, we are not working with parametrizations. We are working instead with triangular control nets. So, our aim is to find the minimum of the real function $\mathcal{P} \to \mathcal{D}(\overrightarrow{x}_{\mathcal{P}})$, $\overrightarrow{x}_{\mathcal{P}}$ being the triangular Bézier patch associated to the control net $\mathcal{P}$. Both functionals, $\mathcal{A}$ and $\mathcal{D}$, have a minimum in the Bézier case due to the following facts: First, they can be considered as continuous real functions defined on $\mathbb{R}^{\frac{3(n-1)(n-2)}{2}}$, since there are $\frac{(n-1)(n-2)}{2}$ interior control points which belong to $\mathbb{R}^3$. Second, as a consequence of $E > 0$, $G > 0$, and $EG - F^2 > 0$, both functionals are bounded from below. Third, the infima are attained: when looking for a minimum, we can restrict both functions to a suitable compact subset. If a control point goes far away, then the same happens with a part of the surface and, therefore,

the area and the sum $E+G$ increase. So, a compact subset can be chosen such that, if one of the interior control points is outside it, then the area functional and also Dirichlet functional, are greater than some bound. Thus, if we restrict both continuous functions to a compact subset we can affirm that the infima exist and that they are attained.

NOTATION 6.1. *Throughout this chapter different subindexes, like J, K, etc. or I_n for some values of n will appear, then we will assume that in general*

$$J = \{J^1, J^2, J^3\}$$

and in particular for the indexes I_n and I we denote: $I = \{i, j, k\}$ and $I_n = \{I_n^1, I_n^2, I_n^3\}$.

The following result will allows us to compute the control net of an extremal of the Dirichlet by means of a system of linear equations.

PROPOSITION 6.2. *A triangular control net, $\mathcal{P} = \{P_I\}_{|I|=n}$, is an extremal of the Dirichlet functional among all triangular control nets with a prescribed boundary if and only if:*

$$0 = \sum_{|I|=n} \frac{\binom{n-1}{I}}{\binom{2n-2}{I+I_0}} (a_1 + a_2 + 2a_3 - b_{13} - b_{23})\ P_I \tag{93}$$

for all $|I_0| = n$ with $I_0^1, I_0^2, I_0^3 > 0$ and where:

$$a_r = \begin{cases} 0 & I^r = 0, \\ \frac{I_0^r I^r}{(I_0^r + I^r)(I_0^r + I^r - 1)} & I^r > 0 \end{cases} \qquad b_{rs} = \frac{I_0^r I^s + I_0^s I^r}{(I_0^r + I^r)\,(I_0^s + I^s)}. \tag{94}$$

Proof: Let us compute the gradient of the Dirichlet functional with respect to the coordinates of a control point $P_{I_0} = \left(x_{I_0}^1, x_{I_0}^2, x_{I_0}^3\right)$ where $I_0 = (I_0^1, I_0^2, I_0^3)$. For any $a \in \{1, 2, 3\}$, and any $|I_0| = n$, with $I_0^1, I_0^2, I_0^3 > 0$.

$$\begin{aligned} \frac{\partial \mathcal{D}(\mathcal{P})}{\partial x_{I_0}^a} =& \frac{1}{2} \int_{\mathcal{T}} \frac{\partial}{\partial x_{I_0}^a} (\|\overrightarrow{x_u}\|^2 + \|\overrightarrow{x_v}\|^2)\, du\, dv \\ =& \int_{\mathcal{T}} (< \frac{\partial \overrightarrow{x_u}}{\partial x_{I_0}^a}, \overrightarrow{x_u} > + < \frac{\partial \overrightarrow{x_v}}{\partial x_{I_0}^a}, \overrightarrow{x_v} >)\, du\, dv \end{aligned}$$

Let us now compute the partial derivatives

$$\frac{\partial \overrightarrow{x_u}}{\partial x_{I_0}^a} = \frac{\partial}{\partial x_{I_0}^a} \frac{\partial}{\partial u} \overrightarrow{x} = \frac{\partial}{\partial u} \frac{\partial}{\partial x_{I_0}^a} \overrightarrow{x} = \frac{\partial}{\partial u} B_{I_0}^n . e_a = n(B_{I_0 - e_1}^{n-1} - B_{I_0 - e_3}^{n-1})\, e_a \tag{95}$$

where e_a, $a \in \{1, 2, 3\}$, denotes the a-th vector of the canonical basis, that is, $e_1 = (1, 0, 0)$, $e_2 = (0, 1, 0)$ and $e_3 = (0, 0, 1)$.

Analogously

$$\frac{\partial \overrightarrow{x_v}}{\partial x_{I_0}^a} = n(B_{I_0 - e_2}^{n-1} - B_{I_0 - e_3}^{n-1})\, e_a. \tag{96}$$

Therefore

$$\frac{\partial \mathcal{D}(\mathcal{P})}{\partial x^a_{I_0}} = \int_{\mathcal{T}} n\left((B^{n-1}_{I_0-e_1} - B^{n-1}_{I_0-e_3}) < e_a, \overrightarrow{x_u} > + (B^{n-1}_{I_0-e_2} - B^{n-1}_{I_0-e_3}) < e_a, \overrightarrow{x_v} > \right) du\, dv$$

$$= \int_{\mathcal{T}} n \left((B^{n-1}_{I_0-e_1} - B^{n-1}_{I_0-e_3}) < e_a, \sum_{|I|=n} n\,(B^{n-1}_{I-e_1} - B^{n-1}_{I-e_3}) P_I > \right.$$

$$\left. + n\,(B^{n-1}_{I_0-e_2} - B^{n-1}_{I_0-e_3}) < e_a, \sum_{|I|=n} n\,(B^{n-1}_{I-e_2} - B^{n-1}_{I-e_3}) P_I > \right) du\, dv.$$

Multiplying the Bernstein polynomials, see Equation (2), and integrating while bearing in mind Equation (3): $\int_T B^n_I(u,v)\; dv\, du = \frac{1}{(n+1)(n+2)}$, we get

$$\begin{aligned}
\frac{\partial \mathcal{D}(\mathcal{P})}{\partial x^a_{I_0}} =& \frac{n^2}{2n(2n-1)} \sum_{|I|=n} \Big(\frac{\binom{n-1}{I_0-e_1}\binom{n-1}{I-e_1}}{\binom{2n-2}{I+I_0-2e_1}} + \frac{\binom{n-1}{I_0-e_2}\binom{n-1}{I-e_2}}{\binom{2n-2}{I+I_0-2e_2}} + 2\frac{\binom{n-1}{I_0-e_3}\binom{n-1}{I-e_3}}{\binom{2n-2}{I+I_0-2e_3}} \\
& - \frac{\binom{n-1}{I_0-e_1}\binom{n-1}{I-e_3} + \binom{n-1}{I_0-e_3}\binom{n-1}{I-e_1}}{\binom{2n-2}{I+I_0-e_1-e_3}} - \frac{\binom{n-1}{I_0-e_2}\binom{n-1}{I-e_3} + \binom{n-1}{I_0-e_3}\binom{n-1}{I-e_2}}{\binom{2n-2}{I+I_0-e_2-e_3}} \Big) < e_a, P_I > \\
=& \frac{n^2}{2n(2n-1)} \sum_{|I|=n} \frac{\binom{n-1}{I}\binom{n-1}{I_0}}{\binom{2n-2}{I+I_0}} (a_1 + a_2 + 2a_3 - b_{13} - b_{23}) \; < e_a, P_I >,
\end{aligned}$$

with a_r and b_r as they was defined in Equation (94).

■

Remark 6.3. *Equivalently,*

$$\frac{\partial \mathcal{D}(\mathcal{P})}{\partial x^a_{I_0}} = \sum_{|I|=n} \frac{\binom{n}{I}\binom{n}{I_0}}{\binom{2n}{I+I_0}} (a_1 + a_2 + 2a_3 - b_{13} - b_{23}) \; < e_a, P_I >,$$

since

$$\frac{2n(2n-1)}{n^2} \frac{\binom{n-1}{I}\binom{n-1}{I_0}}{\binom{2n-2}{I+I_0}} = \frac{\binom{n}{I}\binom{n}{I_0}}{\binom{2n}{I+I_0}}.$$

In particular we give the general result for the case $n = 3$.

Proposition 6.4. *A triangular Bézier surface of degree 3 is an extremal of the Dirichlet functional, $\mathcal{D}(\mathcal{P})$, among all Bézier surfaces with a prescribed boundary if and only if*

$$P_{111} = \frac{1}{4}\,(2\,P_{003} - P_{021} + P_{030} + P_{120} - P_{201} + P_{210} + P_{300}).$$

In the proposition that follows we give a formula to express the Dirichlet functional in terms of the control points, $P_I = (x^1_I, x^2_I, x^3_I)$, of a Bézier triangular patch.

PROPOSITION 6.5. *The Dirichlet functional, $\mathcal{D}(\overrightarrow{x})$, of a triangular Bézier surface can be expressed by the formula*

$$\mathcal{D}(\overrightarrow{x}) = \frac{1}{2}\sum_{a=1}^{3}\sum_{|I_0|=n}\sum_{|I_1|=n} C_{I_0I_1}x^a_{I_0}x^a_{I_1} \tag{97}$$

where

$$C_{I_0I_1} = \frac{\binom{n}{I_0}\binom{n}{I_1}}{\binom{2n}{I_0+I_1}}(a_1+a_2+2a_3-b_{13}-b_{23}) \tag{98}$$

and $a_1, a_2, a_3, b_{13}, b_{23}$ were defined in Equation (94).

Proof: The Dirichlet functional is a second-order functional that can be expressed by Equation (97), therefore we compute its second derivative in order to obtain the coefficients $C_{I_0I_1}$:

$$\frac{\partial^2\mathcal{D}(\overrightarrow{x})}{\partial x^a_{I_0}\partial x^a_{I_1}} = \frac{\partial^2}{\partial x^a_{I_0}\partial x^a_{I_1}}\frac{1}{2}\sum_{\bar{a}=1}^{3}\sum_{|I|=n}\sum_{|J|=n} C_{IJ}x^{\bar{a}}_I x^{\bar{a}}_J = \frac{\partial D}{\partial x^a_{I_1}}\frac{1}{2}\sum_{|J|=n} 2\,C_{I_0J}x^a_J = C_{I_0I_1}.$$

Now let us compute the first derivative

$$\frac{\partial\mathcal{D}(\overrightarrow{x})}{\partial x^a_{I_0}} = \frac{1}{2}\int_{\mathcal{T}}\frac{\partial}{\partial x^a_{I_0}}(\|\overrightarrow{x_u}\|^2+\|\overrightarrow{x_v}\|^2)\,du\,dv = \int_{\mathcal{T}}(<\frac{\partial\overrightarrow{x_u}}{\partial x^a_{I_0}},\overrightarrow{x_u}>+<\frac{\partial\overrightarrow{x_v}}{\partial x^a_{I_0}},\overrightarrow{x_v}>)\,du\,dv,$$

and the second derivative

$$\frac{\partial^2\mathcal{D}(\overrightarrow{x})}{\partial x^a_{I_0}\partial x^a_{I_1}} = \int_{\mathcal{T}}\frac{\partial}{\partial x^a_{I_1}}(<\left(B^n_{I_0}\right)_u e_a,\overrightarrow{x_u}>+<\left(B^n_{I_0}\right)_v e_a,\overrightarrow{x_v}>)\,du\,dv,$$

$$=\int_{\mathcal{T}}<\left(B^n_{I_0}\right)_u e_a,\left(B^n_{I_1}\right)_u e_a>\,dudv+\int_{\mathcal{T}}<\left(B^n_{I_0}\right)_v e_a,\left(B^n_{I_1}\right)_v e_a>\,dudv$$

$$=\int_{\mathcal{T}}\left(\left(B^n_{I_0}\right)_u\left(B^n_{I_1}\right)_u+\left(B^n_{I_0}\right)_v\left(B^n_{I_1}\right)_v\right)<e_a,e_a>\,dudv$$

$$=\int_{\mathcal{T}}\left((B^{n-1}_{I_0-e_1}-B^{n-1}_{I_0-e_3})(B^{n-1}_{I_1-e_1}-B^{n-1}_{I_1-e_3})+(B^{n-1}_{I_0-e_2}-B^{n-1}_{I_0-e_3})(B^{n-1}_{I_1-e_2}-B^{n-1}_{I_1-e_3})\right)\,dudv$$

$$=\frac{n^2}{2n(2n-1)}\frac{2n(2n-1)}{n^2}\frac{\binom{n}{I_0}\binom{n}{I_1}}{\binom{2n}{I+I_0}}(a_1+a_2+2a_3-b_{13}-b_{23}),$$

where we took into account the formula for the product of the Bernstein polynomials, given in Equation (2), and the value of a Bernstein polynomial integral given in Equation (3): $\int_T B^n_I(u,v)\;dv\,du = \frac{1}{(n+1)(n+2)}$.

Therefore

$$C_{I_0I_1} = \frac{\binom{n}{I_0}\binom{n}{I_1}}{\binom{2n}{I+I_0}}(a_1+a_2+2a_3-b_{13}-b_{23}),$$

where $a_1, a_2, a_3, b_{13}, b_{23}$ were defined in Equation (94).

■

Now, let us use this expression of the Dirichlet functional

$$\mathcal{D}(\overrightarrow{x}) = \frac{1}{2}\sum_{a=1}^{3}\sum_{|I|=n}\sum_{|J|=n} C_{IJ}x_I^a x_J^a$$

to compute, as we did in Proposition 6.2, the gradient of the functional with respect to the coordinates of a control point $P_{I_0} = \left(x^1_{I_0}, x^2_{I_0}, x^3_{I_0}\right)$ where $I_0 = (I_0^1, I_0^2, I_0^3)$:

$$\frac{\partial \mathcal{D}(\overrightarrow{x})}{\partial P_{I_0}} = \left(\sum_{|J|=n} C_{I_0J}x_J^1 \sum_{|J|=n} C_{I_0J}x_J^2, \sum_{|J|=n} C_{I_0J}x_J^3\right) = \sum_{|J|=n} C_{I_0J}P_J \tag{99}$$

Therefore, the condition

$$\sum_{|J|=n} C_{I_0J}P_J = 0 \quad \text{for all} \quad |I_0 = (I_0^1, I_0^2, I_0^3)| = n \quad \text{with} \quad I_0^1, I_0^2, I_0^3 > 0, \tag{100}$$

is equivalent to Equation (93), where it was given the characterization of a triangular control net with a prescribed boundary of an extremal of the Dirichlet functional, see Proposition 6.2.

2. Comparison with the Euler-Lagrange equation

Let us recall the Euler-Lagrange equation, for a Lagrangian. Given a second-order Lagrangian,

$$L\left(\overrightarrow{x}\right) = L\left(\overrightarrow{x}, \overrightarrow{x}_u, \overrightarrow{x}_v, \overrightarrow{x}_{uu}, \overrightarrow{x}_{uv}, \overrightarrow{x}_{vv}\right),$$

if it is considered the functional I to be,

$$I\left(\overrightarrow{x}\right) = \int_T L\left(\overrightarrow{x}\right)\, du\, dv,$$

then, the extremals of I satisfy the associated Euler-Lagrange differential equation, that is,

$$0 = \frac{\partial L}{\partial \overrightarrow{x}} - \frac{d}{du}\left(\frac{\partial L}{\partial \overrightarrow{x}_u}\right) - \frac{d}{dv}\left(\frac{\partial L}{\partial \overrightarrow{x}_v}\right) + \frac{d^2}{du^2}\left(\frac{\partial L}{\partial \overrightarrow{x}_{uu}}\right) + \frac{d^2}{dudv}\left(\frac{\partial L}{\partial \overrightarrow{x}_{uv}}\right) + \frac{d^2}{dv^2}\left(\frac{\partial L}{\partial \overrightarrow{x}_{vv}}\right).$$

Therefore problems in the calculus of variations can be studied by solution of the associated Euler-Lagrange equation.

Now, let us consider the Dirichlet functional,

$$\mathcal{D}(\overrightarrow{x}) = \frac{1}{2}\int_{\mathcal{T}} (\|\overrightarrow{x_u}\|^2 + \|\overrightarrow{x_v}\|^2)\, du\, dv.$$

Minimizing the functional $\mathcal{D}$, which is equivalent to requiring that the first variation of $\mathcal{D}$ is zero, gives rise to the corresponding Euler-Lagrange equation, in this case given by the harmonicity condition:

$$\Delta \overrightarrow{x} = 0. \tag{101}$$

Let us show this. First we will compute the first variation of the functional in order to obtain the sufficient and necessary condition that a patch must satisfy in order to be an extremal among all $\overrightarrow{x} \in \mathcal{C}^\infty(T)$ with a prescribed boundary. Afterwards, we will show how this condition changes when we look for an extremal among all polynomial patches, $\overrightarrow{x} \in \mathbb{R}_n[u,v]$. The condition for the restricted problem turns into a weak version of the Euler-Lagrange equation.

The patch $\overrightarrow{x}$ would be an extremal of the functional $\mathcal{D}(\overrightarrow{x})$ among all the patches with the same border if and only if for any $\overrightarrow{y} \in \mathcal{C}^\infty(T)$, null along the border of T, the following equality holds

$$0 = \frac{d}{dt}\Big|_{t=0} \mathcal{D}(\overrightarrow{x} + t\overrightarrow{y}) = \int_T < \overrightarrow{x}_u, \overrightarrow{y}_u > + < \overrightarrow{x}_v, \overrightarrow{y}_v > \, du\, dv.$$

Then, having in mind the integration by parts formula, it follows that

$$\begin{aligned}
\frac{d}{dt}\Big|_{t=0} \mathcal{D}(\overrightarrow{x} + t\overrightarrow{y}) &= \int_T < \overrightarrow{x}_u, \overrightarrow{y} >_u - < \overrightarrow{x}_{uu}, \overrightarrow{y} > + < \overrightarrow{x}_v, \overrightarrow{y} >_v - < \overrightarrow{x}_{vv}, \overrightarrow{y} > \, du\, dv \\
&= \int_T < -\Delta \overrightarrow{x}, \overrightarrow{y} > \, du\, dv + \int_T < \overrightarrow{x}_u, \overrightarrow{y} >_u + < \overrightarrow{x}_v, \overrightarrow{y} >_v \, du\, dv \\
&= \int_T - < \Delta \overrightarrow{x}, \overrightarrow{y} > \, du\, dv + \int_{\partial T} - < \overrightarrow{x}_v, \overrightarrow{y} > \, du + < \overrightarrow{x}_u, \overrightarrow{y} > \, dv.
\end{aligned}$$

Since $y\Big|_{\partial T} = 0$, a patch $\overrightarrow{x}$ is an extremal of the Dirichlet functional among all patches with a prescribed boundary if

$$0 = \frac{d}{dt}\Big|_{t=0} \mathcal{D}(\overrightarrow{x} + t\overrightarrow{y}) = \int_T - < \Delta \overrightarrow{x}, \overrightarrow{y} > \, du\, dv,$$

for any $\mathcal{C}^\infty(T)$, that is, if and only if it is a harmonic patch.

On the other hand, if we consider the Dirichlet functional restricted to polynomial patches, an extremal of the restricted problem is not necessarily harmonic. As before, a polynomial patch is an extremal of $\mathcal{D}$ among all polynomial patches with the same border if

$$0 = \frac{d}{dt}\Big|_{t=0} \mathcal{D}(\overrightarrow{x} + t\overrightarrow{y}) = \int_T < -\Delta \overrightarrow{x}, \overrightarrow{y} > \, du\, dv + \int_T < \overrightarrow{x}_u, \overrightarrow{y} >_u + < \overrightarrow{x}_v, \overrightarrow{y} >_v \, du\, dv,$$

for all $\overrightarrow{y} \in \mathbb{R}_n[u,v]$,

$$\overrightarrow{y}\,(u,v) = \sum_{|I|=n} Q_I B_I^n\,(u,v)\,, \quad |I| = |\{i,j,k\}| = n \quad \text{with} \quad i,j,k \neq 0,$$

null along the border of T. Equivalently, $\overrightarrow{x}$ would be an extremal if for all $|I| = |\{i,j,k\}| = n$ with $i,j,k \neq 0$,

$$0 = \int_T < -\Delta\overrightarrow{x}, B_I^n e_a > \, du\,dv + \int_T < \overrightarrow{x}_u, B_I^n\, e_a >_u + < \overrightarrow{x}_v, B_I^n\, e_a >_v \, du\,dv.$$

Moreover

$$\int_T < \overrightarrow{x}_u, B_I^n\, e_a >_u \, du\,dv = \int_0^1 < \overrightarrow{x}_u, B_I^n e_a > \Big]_0^{1-v} dv = 0,$$
$$\int_T < \overrightarrow{x}_v, B_I^n\, e_a >_v \, du\,dv = \int_0^1 < \overrightarrow{x}_v, B_I^n e_a > \Big]_0^{1-u} du = 0,$$

since $B_I^n(1-v,v) = B_I^n(0,v) = B_I^n(u,0) = B_I^n(u,1-u) = 0$ for $|I| = |\{i,j,k\}| = n$ with $i,j,k \neq 0$.

Therefore we can deduce that a polynomial patch $\overrightarrow{x}$ is an extremal of the Dirichlet functional $\mathcal{D}$ among all patches with a prescribed boundary if and only if

$$0 = -\int_{\mathcal{T}} < e_a, \Delta\overrightarrow{x} > \, B_I^n\, dudv, \quad \text{for all} \quad |I = (i,j,k)| = n \quad \text{with} \quad i,j,k > 0. \tag{102}$$

In fact, the computation of the gradient of the Dirichlet functional with respect to the coordinates of an interior control point $P_{I_0} = \left(x^1_{I_0}, x^2_{I_0}, x^3_{I_0}\right)$ gives rise to the previous equation

$$\begin{aligned}
\frac{\partial \mathcal{D}(\mathcal{P})}{\partial x^a_{I_0}} &= \int_{\mathcal{T}} (< \overrightarrow{x_u}, \left(B^n_{I_0}\right)_u\, e_a > + < \overrightarrow{x_v}, \left(B^n_{I_0}\right)_v\, e_a >)\, du\,dv \\
&= \int_T < \overrightarrow{x}_u, B^n_{I_0} >_u - < \overrightarrow{x}_{uu}, B^n_{I_0} > + < \overrightarrow{x}_v, B^n_{I_0} >_v - < \overrightarrow{x}_{vv}, B^n_{I_0} > \, du\,dv \\
&= -\int_{\mathcal{T}} < e_a, \Delta\overrightarrow{x} > \, B^n_{I_0}\, dudv.
\end{aligned}$$

REMARK 6.6. *Equation (102) is a kind of weak version of condition (101). Note that the Bernstein polynomials that appear multiplying the Laplacian operator in Equation (102) are only those with $i,j,k > 0$, that is, the Bernstein polynomials whose indexes correspond to border points are excluded. If these polynomials were included it would imply that $\Delta\overrightarrow{x} = 0$ from Lemma 3.12.*

Let us observe that the condition given in Equation (102) is equivalent to the other characterizations of the Dirichlet functional extremals we have given earlier in Equation (93) and in Equation (100).

3. Triangular permanence patches related with the Bézier-Plateau problem: The Dirichlet mask

As we said in Chapter 3, Farin and Hansford defined in [**14**] triangular permanence patches. Given a mask of the form

$$P_{i,j,k} = \begin{array}{ccccccc} & \alpha & & \beta & & \beta & & \alpha \\ & & \beta & & \star & & \beta & \\ & & & \beta & & \beta & & \\ & & & & \alpha & & & \end{array} \tag{103}$$

with $3\alpha + 6\beta = 1$, that is, $\alpha = \frac{1-6\beta}{3}$, the triangular patch formed with such a control net is called triangular permanence patch. Let us denote this mask by M_α.

The mask M_0 is the discrete form of the Laplacian operator when the control net is considered as a discretization of the Bézier surface. Such a mask is used in the cited reference to obtain control nets resembling minimal surfaces that fit between given boundary polygons.

Other important masks are: $M_{\frac{1}{9}}$ which can be deduced by asking the quadrilaterals associated to the inner edges of the triangular patch to be as close as possible to parallelograms, and mask $M_{\frac{1}{3}}$, which is the dual of M_0 in the sense that for $\alpha = \frac{1}{3}$ we have $\beta = 0$.

From the condition obtained in Proposition 6.4, and given the exterior control points, we can try to generate the whole triangular net by solving a linear system where the equations are:

$$\begin{aligned} 4P_{i,j,k} = {} & 2\,P_{i+2,j-1,k-1} - P_{i,j-1,k+1} - P_{i,j+1,k-1} + P_{i-1,j+2,k-1} \\ & + P_{i-1,j+1,k} + P_{i-1,j,k+1} + P_{i-1,j-1,k+2}, \end{aligned}$$

$P_{i,j,k}$ being a interior control point. This equation can be expressed as the following mask, which will be called the *Dirichlet mask :*

$$\frac{1}{4} \times \begin{array}{ccccccc} & 1 & & 1 & & 1 & & 1 \\ & & -1 & & \star & & -1 & \\ & & & 0 & & 0 & & \\ & & & & 2 & & & \end{array}$$

As we can see, the Dirichlet mask is not a mask like Farin-Hansford's mask because it is not symmetric. The asymmetry of the Dirichlet mask is due to the fact that the triangle on which we define the Bernstein polynomials is not an equilateral triangle. By applying a symmetrization process to the Dirichlet mask, we obtain one of the masks worked in [**14**], more specifically the one with $\alpha = \frac{1}{3}$.

4. The Biharmonic functional results

In interactive surface modeling, the biharmonic functional or bending energy functional, which is also called thin plate energy, is always chosen as a measure of the fairness of a

surface and mesh. In this section we will study the problem of finding a triangular Bézier surface which minimizes the biharmonic functional,

$$\mathcal{B}(\overrightarrow{x}) = \frac{1}{2}\int_T \|\overrightarrow{x_{uu}}\|^2 + 2\|\overrightarrow{x_{uv}}\|^2 + \|\overrightarrow{x_{vv}}\|^2\, du\, dv, \tag{104}$$

defined in the triangle, T, among all polynomial patches with the same boundary.

This problem was discussed in a similar way in [**28**]. The authors gave a characterization of the control net for both rectangular and triangular Bézier extremals of the bending energy functional with given boundary curves. Their methods were based on the results of the Dirichlet functional for rectangular and triangular Bézier surfaces, in [**29**], [**30**] and [**3**]. Derived from this characterization of extremals they deduced a mask for the generation of rectangular and triangular patches. Later in this section will also show this mask.

In the following proposition we give a formula to express the biharmonic functional, $\mathcal{B}$, of a Bézier triangular patch in terms of the control points, $P_I = (x_I^1, x_I^2, x_I^3)$.

PROPOSITION 6.7. *The functional, $\mathcal{B}(\overrightarrow{x})$, of a triangular Bézier surface can be expressed by the formula*

$$\mathcal{B}(\overrightarrow{x}) = \frac{1}{2}\sum_{a=1}^{3}\sum_{|I_0|=n}\sum_{|I_1|=n} C_{I_0I_1}x^a_{I_0}x^a_{I_1} \tag{105}$$

with

$$\begin{aligned} C_{I_0I_1} = 2n\,(2n-1)\,\frac{\binom{n}{I_0}\binom{n}{I_1}}{\binom{2n}{I_0+I_1}}\Big(&\frac{1}{2}(b_{11}^{11}+b_{22}^{22}+4b_{33}^{33}) + b_{33}^{11} + b_{33}^{22} + b_{12}^{12} - 2(b_{11}^{13}+b_{12}^{23}+b_{12}^{13} \\ &+b_{22}^{23} - b_{33}^{12} - b_{23}^{13}) + 3(b_{13}^{13}+b_{23}^{23}) - 4(b_{13}^{33}+b_{23}^{33})\Big) \end{aligned} \tag{106}$$

where the coefficients b_{rs}^{tl} satisfy the symmetry relation $b_{rs}^{tl} = b_{sr}^{tl} = b_{rs}^{lt} = b_{sr}^{lt}$, and are defined in Equation (36).

Proof: The functional is a second-order functional and, therefore, similarly to Proposition 6.5, in order to compute the coefficients $C_{I_0I_1}$ we can compute its second derivative.

We compute the first derivative

$$\begin{aligned} \frac{\partial\mathcal{B}(\overrightarrow{x})}{\partial x^a_{I_0}} =& \frac{1}{2}\int_{\mathcal{T}} < \frac{\partial\overrightarrow{x}_{uu}}{\partial x^a_{I_0}}, \overrightarrow{x}_{uu} > +2 < \frac{\partial\overrightarrow{x}_{uv}}{\partial x^a_{I_0}}, \overrightarrow{x}_{uv} > + < \frac{\partial\overrightarrow{x}_{vv}}{\partial x^a_{I_0}}, \overrightarrow{x}_{vv} > du\, dv \\ =& \frac{1}{2}\int_{\mathcal{T}} < (B^n_{I_0})_{uu}, \overrightarrow{x}_{uu} > +2 < (B^n_{I_0})_{uv}, \overrightarrow{x}_{uv} > + < (B^n_{I_0})_{vv}, \overrightarrow{x}_{vv} > du\, dv, \end{aligned}$$

and the second

$$\frac{\partial^2\mathcal{B}(\overrightarrow{x})}{\partial x^a_{I_0}\partial x^a_{I_1}} = \int_{\mathcal{T}} < (B^n_{I_0})_{uu}, (B^n_{I_1})_{uu} > +2 < (B^n_{I_0})_{uv}, (B^n_{I_1})_{uv} > + < (B^n_{I_0})_{vv}, (B^n_{I_1})_{vv} > du\, dv.$$

Then bearing in mind the derivatives

$$(B_I^n)_{uu} = n\,(n-1)\left(B_{I-2e_1}^{n-2} - 2B_{I-e_1-e_3}^{n-2} + B_{I-2e_3}^{n-2}\right)$$
$$(B_I^n)_{uv} = n\,(n-1)\left(B_{I-e_1-e_2}^{n-2} - B_{I-e_1-e_3}^{n-2} - B_{I-e_2-e_3}^{n-2} + B_{I-2e_3}^{n-2}\right)$$
$$(B_I^n)_{vv} = n\,(n-1)\left(B_{I-2e_2}^{n-2} - 2B_{I-e_2-e_3}^{n-2} + B_{I-2e_3}^{n-2}\right)$$

we compute the integral of the Bernstein polynomials

$$\int_{\mathcal{T}} B_{I_0+I_1}^{2n-4}(u,v)\;dudv = \frac{1}{(3n-2)(3n-3)}$$

and we perform some simplifications like the following:

$$\int_{\mathcal{T}} B_{I_0-2e_1}^{n-2} B_{I_1-2e_3}^{n-2}\,dudv =$$
$$= \int_{\mathcal{T}} \frac{\binom{n-2}{I_0-2e_1}\binom{n-2}{I_1-2e_3} + \binom{n-2}{I_0-2e_3}\binom{n-2}{I_1-2e_1}}{\binom{2n-4}{I_0+I_1-2e_1-2e_3}} B_{I_0+I_1-2e_1-2e_3}^{2n-4}\,dudv$$
$$= \frac{2n\,(2n-1)}{n^2(n-1)^2}\frac{\binom{n}{I_0}\binom{n}{I_1}}{\binom{2n}{I_0+I_1}}\frac{I_0^1(I_0^1-1)I_1^3(I_1^3-1) + I_0^3(I_0^3-1)I_1^1(I_1^1-1)}{(I_0^1+I_1^1)(I_0^3+I_1^3)(I_0^1+I_1^1-1)(I_0^3+I_1^3-1)}$$
$$= \frac{2n\,(2n-1)}{n^2(n-1)^2}\frac{\binom{n}{I_0}\binom{n}{I_1}}{\binom{2n}{I_0+I_1}} b_{11}^{33}.$$

Therefore

$$\frac{\partial^2 \mathcal{B}(\overrightarrow{x})}{\partial x_{I_0}^a \partial x_{I_1}^a} = 2n\,(2n-1)\,\frac{\binom{n}{I_0}\binom{n}{I_1}}{\binom{2n}{I_0+I_1}}\Big(\frac{1}{2}(b_{11}^{11} + b_{22}^{22} + 4b_{33}^{33}) + b_{33}^{11} + b_{33}^{22} + b_{12}^{12} - 2(b_{11}^{13} + b_{12}^{23} + b_{12}^{13}$$
$$+ b_{22}^{23} - b_{33}^{12} - b_{23}^{13}) + 3(b_{13}^{13} + b_{23}^{23}) - 4(b_{13}^{33} + b_{23}^{33})\Big) = C_{I_0 I_1},$$

with b_{rs}^{tl} defined in Equation (36).

■

In the previous proposition, as we did just before for the Dirichlet functional and for the functional $\mathcal{F}$ in chapter 3, we have given a formula, in Equation (105), of the functional in terms of the control points

$$\mathcal{B}(\overrightarrow{x}) = \frac{1}{2}\sum_{a=1}^{3}\sum_{|I_0|=n}\sum_{|I_1|=n} C_{I_0 I_1} x_{I_0}^a x_{I_1}^a.$$

In the following proposition we compute the gradient of the functional with respect to the coordinates of a control point $P_{I_0} = \left(x_{I_0}^1, x_{I_0}^2, x_{I_0}^3\right)$. Then we will characterize the extremal of the functional among all Bézier surfaces with the same border as a solution of a linear system.

PROPOSITION 6.8. *A triangular control net, $\mathcal{P} = \{P_I\}_{|I|=n}$, is an extremal of the functional, $\mathcal{B}$, among all triangular control nets with a prescribed boundary if and only if*

$$\sum_{|J|=n} C_{I_0 J} P_J = 0 \quad \textit{for all} \quad |I_0 = (I_0^1, I_0^2, I_0^3)| = n \quad \textit{with} \quad I_0^1, I_0^2, I_0^3 \neq 0, \tag{107}$$

with C_{IJ} defined in Equation (106).

Proof: The gradient of the functional with respect to the coordinates of an interior control point $P_{I_0} = \left(x_{I_0}^1, x_{I_0}^2, x_{I_0}^3\right)$ is given by

$$\frac{\partial \mathcal{B}(\overrightarrow{x})}{\partial P_{I_0}} = \left(\sum_{|J|=n} C_{I_0 J} x_J^1, \sum_{|J|=n} C_{I_0 J} x_J^2, \sum_{|J|=n} C_{I_0 J} x_J^3 \right) = \sum_{|J|=n} C_{I_0 J} P_J.$$

■

Equivalently, a triangular control net, $\mathcal{P} = \{P_I\}_{|I|=n}$, is an extremal among all control nets with prescribed border control points if and only if

$$\begin{aligned} 0 = \sum_{|I|=n} \frac{\binom{n}{I}}{\binom{2n}{I_0+I}} \Big(\frac{1}{2}(b_{11}^{11} + b_{22}^{22} + 4b_{33}^{33}) + b_{33}^{11} + b_{33}^{22} + b_{12}^{12} - 2(b_{11}^{13} + b_{12}^{23} + b_{12}^{13} \\ + b_{22}^{23} - b_{33}^{12} - b_{23}^{13}) + 3(b_{13}^{13} + b_{23}^{23}) - 4(b_{13}^{33} + b_{23}^{33})) \, P_I \end{aligned}$$

for all $|I_0 = (I_0^1, I_0^2, I_0^3)| = n$ with $I_0^1, I_0^2, I_0^3 \neq 0$, where b_{rs}^{tl} were defined in Equation (36).

In particular we give the general result for the case $n = 3$.

PROPOSITION 6.9. *A triangular control net of degree 3, $\mathcal{P} = \{P_I\}_{|I|=3}$, is an extremal of the functional, $\mathcal{B}(\mathcal{P})$, among all triangular control nets with a prescribed boundary if and only if*

$$P_{111} = \frac{1}{12} \left(2P_{003} + 3P_{012} - 3P_{021} + P_{030} + 3P_{102} + 4P_{120} - 3P_{201} + 4P_{210} + P_{300}\right).$$

From the condition obtained in Proposition 6.9 we can generate, given the exterior control points, the whole triangular net by solving a linear system where the equations are:

$$\begin{aligned} 12P_{i,j,k} = 2P_{i-1,j-1,k+2} + 3P_{i-1,j,k+1} - 3P_{i-1,j+1,k} + P_{i-1,j+2,k-1} + 3P_{i,j-1,k+1} + 4P_{i,j+1,k-1} \\ - 3P_{i+1,j-1,k} + 4P_{i+1,j,k-1} + P_{i+2,j-1,k-1} \end{aligned}$$

$P_{i,j,k}$ being an interior control point. This equation can be expressed by the following mask:

$$P_{i,j,k} = \frac{1}{12} \times \begin{array}{ccccc} & 2 & & 3 & & -3 & & 1 \\ & & 3 & & \star & & 4 & \\ & & & -3 & & 4 & & \\ & & & & 1 & & & \end{array} \tag{108}$$

which was also considered in [**28**], where it was called the bending energy mask.

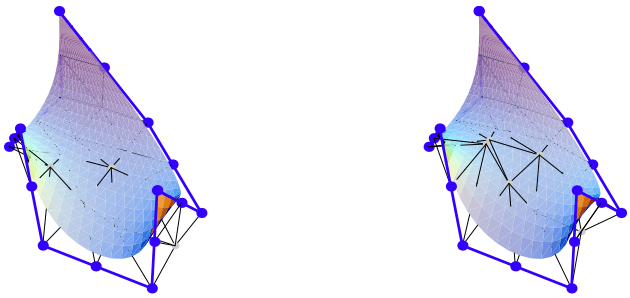

FIGURE 1. Two Bézier surfaces with the same border, the one on the left is a Bézier extremal of the functional $\mathcal{B}$ and the figure on the right is obtained by means of the mask in Equation (108).

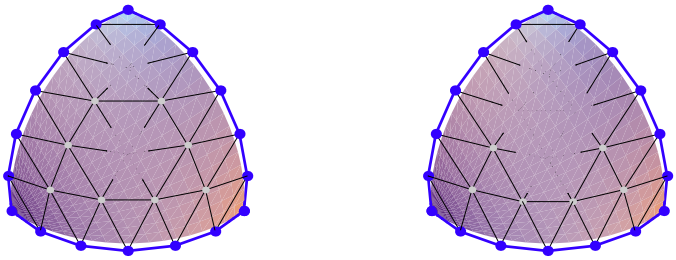

FIGURE 2. Two more examples of Bézier triangles, a Bézier extremal of $\mathcal{B}$ on the left and a Bézier surface built with the mask (108).

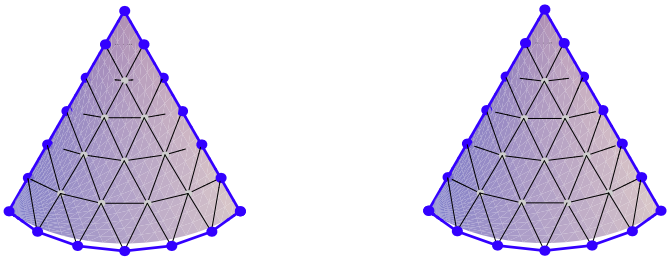

FIGURE 3. As before, a polynomial extremal of $\mathcal{B}$ on the left and on the right another surface with the same boundary but obtained thanks to the associated mask.

From the figures above it can be seen that the shapes of surfaces and control nets obtained by means of the mask, in Equation (108), are almost as good as those derived from the extremal of the functional $\mathcal{B}$. Nevertheless, as is natural, the bending energy is smaller for the polynomial extremals than for the surfaces generated with the bending energy mask.

5. Comparison between masks

The question that naturally arises regarding which mask is the best and, more generally, whether there is a better mask, has a negative answer. This depends on the boundary conditions.

In this section we will show some examples with simple boundary curves.

5.1. *Case $n = 3$.* Let us start the comparison by studying some examples in the cubic case. We fix the three boundary curves with their control points and we construct the triangular Bézier surface by computing the interior control point using the masks M_α, the Dirichlet mask and the Biharmonic mask defined in Equation (108).

We have chosen some examples with their border control points: along the border of a piece of the Enneper's surface in the first example; along two straight lines and a circle of radius 1 in NI1; along three circles of radius 1 in NI2; the boundary of Is is built in such a way that at the corner points any associated patch would be isothermal. Finally, border HNI is such that the isothermality conditions at its corners are far from being fulfilled. The following figures show the borders and the triangular Bézier surfaces constructed by means of the Dirichlet mask.

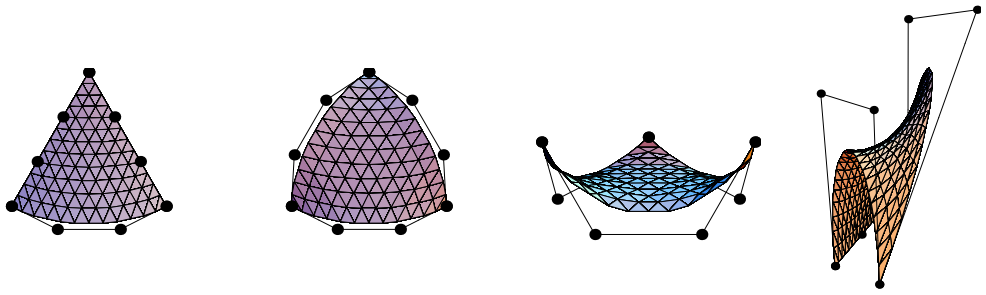

FIGURE 4. Surfaces NI1, NI2, Is and HNI are Dirichlet extremals for given boundaries.

The following table shows the areas of the corresponding triangular Bézier surfaces:

Method	Enneper	NI1	NI2	Is	HNI
M_0	4.67858	0.99685	1.21350	2.99046	13.22692
$M_{\frac{1}{9}}$	4.67835	0.99631	1.20844	2.88558	12.66618
$M_{\frac{1}{3}}$	4.67899	0.99563	1.20275	2.76656	11.67948
Dirichlet mask	4.67778	0.99793	1.20277	2.76957	12.22934
Dirichlet Correction	4.67778	0.99546	1.20216	2.75167	11.36520
Biharmonic Mask	4.67814	0.99931	1.20845	2.89077	13.24778

Table I: Comparison between different masks for triangular Bézier surfaces of degree 3.

As we will introduce the method that we have called Dirichlet correction later in this work, let us first analyze the results for the M_α masks, the Dirichlet mask and the Biharmonic mask. We can find that for these cubical examples the lesser areas are obtained by the $M_{\frac{1}{3}}$

mask with the exception of the Enneper case, which we will study in a later section. Let us recall that the Farin-Hansford mask, $M_{\frac{1}{3}}$, can also be obtained after a symmetrizing of the Dirichlet mask.

5.2. *Case* $n = 10$. Let us see in this section how things change with more degrees of freedom. The following examples, for the case $n = 10$, are similar to the cubical examples NI2, Is and HNI. In NI2 we have chosen equally spaced border control points along the circles described before. In the other cases the choice of the borders was made with the same configuration as before but with a slight modification in order to ensure isothermality at the corners in Is and non-isothermality in HNI.

The following table shows the areas of the corresponding triangular Bézier surfaces by using the M_α masks, the Dirichlet mask and the area of the Dirichlet extremal, which is the area of the triangular Bézier surface whose interior control points are obtained by applying the Dirichlet equations in Proposition 6.2. Moreover we show the area of the Biharmonic extremal, that is the extremal of the Biharmonic functional for these boundaries, and the area of the surface obtained by means of the Biharmonic mask.

Method	NI2	Is	HNI
M_0 mask	1.34247	3.54592	12.61296
$M_{\frac{1}{9}}$ mask	1.34009	3.49978	12.53044
$M_{\frac{1}{3}}$ mask	1.33864	3.47307	12.47569
Dirichlet mask	1.33961	3.43799	12.68629
Dirichlet extremal	1.33963	3.43659	12.68513
Dirichlet Correction	1.33623	3.41091	12.42494
Second step	1.33625	3.37410	12.25581
Biharmonic extremal	1.34809	3.63199	13.27275
Biharmonic mask	1.34149	3.45068	12.87336

Table II: Different masks, the Biharmonic functional extremal and the Dirichlet extremal areas for $n = 10$.

In the NI2 and the HNI cases the best area is the one obtained using the $M_{\frac{1}{3}}$ mask, but now when we have isothermality at the corners, as in case Is, the Dirichlet extremal is the one that gives us the lesser area, and even the use of the Dirichlet mask represents a significant improvement. An explanation of why the Dirichlet extremal has less area in Is will be given in section 7.

The following figures show the control nets of the triangular Bézier surfaces of degree 10 obtained, for the Is example, by means of the mask M_0 and the Dirichlet mask.

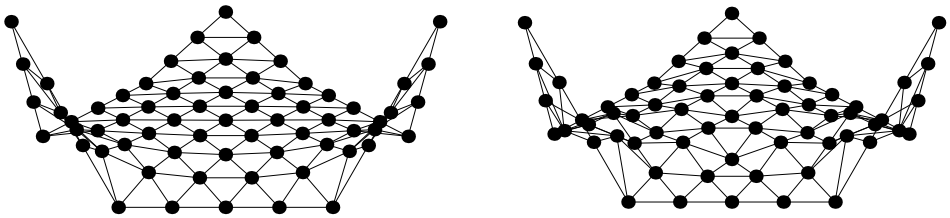

FIGURE 5. A pair of degree 10 control nets with the boundary Is. The net in the left is obtained by means of the mask M_0 and in the net in the right is obtained by means of the Dirichlet mask.

Note the non-regular shape of the control net in the figure on the right, that is, the one obtained using the Dirichlet mask for degree 10, in comparison with the figure on the left, which is the one obtained by using the M_0 mask, which is the mask for the discrete form of the Laplacian operator. The control net is not regular, but the associated Bézier surface is a better approximation to the minimal surface. Recall that we are looking for triangular Bézier surfaces minimizing some functional related with the surface, and not for triangular control nets minimizing some functional related with the net. The same fact also happens for rectangular Bézier surfaces.

6. The Enneper's surface as a testing model

The first non-trivial example of minimal surface with polynomial coordinate functions is Enneper's surface (see [**19**] or [**12**] for some plots of this surface), $\overrightarrow{x} : \mathbb{R}^2 \longrightarrow \mathbb{R}^3$ defined by

$$\overrightarrow{x}(u,v) := (u - \frac{u^3}{3} + uv^2, v - \frac{v^3}{3} + vu^2, u^2 - v^2). \tag{109}$$

Therefore, it can be used to test the masks we have used. Moreover, as the parametrization (109) is isothermal, then it is an extremal not only of the area functional, but also of the Dirichlet functional. This means that, if we take a triangular piece of the Enneper's surface, we determine its control net, and we look for the extremal of the Dirichlet functional with those border control points, then the interior control point P_{111} is always given by the formula in Proposition 6.4.

Nevertheless, there are cases where all symmetric masks fail to reobtain the interior control points. For example, let us consider the patch

$$\overrightarrow{y}(u,v) = \overrightarrow{x}(u+1,v), \qquad (u,v) \in T.$$

This is again an isothermal and harmonic patch, and so it is a patch of a minimal triangular surface and the area of this triangular Bézier surface is 4.67778.

The control net is

$$\begin{array}{ccccccc} (\frac{2}{3},0,1) & & (\frac{2}{3},\frac{2}{3},1) & & (1,\frac{4}{3},\frac{2}{3}) & & (\frac{5}{3},\frac{5}{3},0) \\ & (\frac{2}{3},0,\frac{5}{3}) & & (\frac{2}{3},1,\frac{5}{3}) & & (\frac{4}{3},2,\frac{4}{3}) & \\ & & (\frac{1}{3},0,\frac{8}{3}) & & (\frac{1}{3},\frac{5}{3},\frac{8}{3}) & & \\ & & & (-\frac{2}{3},0,4) & & & \end{array}$$

It is easy to confirm that this control net verifies the formula in Proposition 6.4. So, the interior control point P_{111} can be reobtained using the corresponding asymmetric mask.

Nevertheless, for a symmetric mask, M_α, the computation of the interior control points gives

$$P^\alpha_{111} = (\frac{13-9\alpha}{18}, \frac{17-21\alpha}{18}, \frac{5}{3}),$$

and there is no value for α such that $P_{111} = (\frac{2}{3}, 1, \frac{5}{3})$.

Moreover, the minimum of the area of the associated triangular Bézier surface with interior control point P^α_{111} is attained at $\alpha = 0.12833$ and its value is 4.67834.

7. Correction of the Dirichlet extremal

Obtaining an approximation of the minimal Bézier surface according to the Dirichlet functional minimization method has a serious drawback.

The first fundamental form at the corners of any triangular Bézier surface with prescribed border is determined by the border control points. For example, at the point $\overrightarrow{x}(0,0)$ the three coefficients of the first fundamental form are determined by the control points $P_{0,0,n}, P_{0,1,n-1}$ and $P_{1,0,n-1}$. And analogously for the other three vertices.

Therefore, since the three points are border control points, the coefficients E, F and G at $\overrightarrow{x}(0,0)$ of any triangular Bézier patch with prescribed boundary will always be the same, even for the Dirichlet extremal, no matter what interior control points we have.

Let us recall that the Dirichlet method is based on substituting the area functional by the Dirichlet one, so it will cause a negligible error. Both functionals only agree for isothermal patches. If the configuration of the border control points is such that the patch is always non-isothermal at the corner points, then the inequalities in Equation (92) are strict. The non-isothermality at the corner points will produce an error when substituting the area functional by the Dirichlet one. At points other than the corner points, the configuration of the Dirichlet extremal tends toward isothermality of the patch. But at the corner points, isothermality or not is fixed by the border control points and it cannot be modified. This is why the Dirichlet extremal does not improve the results obtained with other methods in some cases.

Throughout this section we will propose a method to obtain, from the Dirichlet extremal as a first approximation to the minimal Bézier surface, a new and better approximation that attempts to avoid this problem but maintaining the fact that the new approximation is computed thanks to a system of linear equations.

Let us recall the following fact about the Dirichlet functional. The Euler-Lagrange equation of the Dirichlet functional defined on the set of all differentiable patches with prescribed border is

$$\Delta \overrightarrow{x} = 0,$$

where Δ is the usual Laplacian operator. This equation is related to minimal surfaces thanks to Proposition 5.5. But there is another main result that does not mention the isothermality condition.

PROPOSITION 6.10. *A patch $\overrightarrow{x}$ is minimal iff $\Delta^g \overrightarrow{x} = 0$ where g represents the first fundamental form of $\overrightarrow{x}$ and Δ^g is the associated Laplacian operator for a function f:*

$$\Delta f = \left(\frac{f_u G - f_v F}{\sqrt{EG - F^2}} \right)_u + \left(\frac{-f_u F + f_v E}{\sqrt{EG - F^2}} \right)_v.$$

It is easy to confirm that, for a given metric, g, with coefficients E, F and G, the equation $\Delta^g \overrightarrow{x} = 0$ is the Euler-Lagrange equation of the functional

$$\mathcal{D}^g(\overrightarrow{x}) = \int_{\mathcal{T}} \left(\frac{||\overrightarrow{x}_u||^2 G - 2 < \overrightarrow{x}_u, \overrightarrow{x}_v > F + ||\overrightarrow{x}_v||^2 E}{\sqrt{EG - F^2}} \right) dudv = \int_{\mathcal{T}} g^{-1}(d\overrightarrow{x}, d\overrightarrow{x}) \mu_g,$$

where $\mu_g = \sqrt{EG - F^2} dudv$ is the metric volume element.

Note that for a given g, the extremal of the functional $\mathcal{D}^g$ is a patch that can be computed thanks to a linear system.

Therefore, the correction of the Dirichlet method is the following: let $\overrightarrow{x}_0$ be the Dirichlet extremal and let g_0 be its first fundamental form. The new approximation is the extremal of the functional $\mathcal{D}^{g_0}$, that is, using the Dirichlet extremal as the fixed metric. Note that the functional $\overrightarrow{x} \to \mathcal{D}^{g_0}(\overrightarrow{x})$ is quadratic in $\overrightarrow{x}$. Therefore the equations that the extremal must satisfy are linear.

PROPOSITION 6.11. *A triangular control net, $\mathcal{P} = \{P_I\}_{|I|=n}$, is an extremal of the functional $\mathcal{D}^{g_0}$ among all triangular control nets with prescribed border if and only if:*

$$\begin{aligned} 0 = \sum_{|I|=n} \frac{\binom{n-1}{I}}{\binom{2n-2}{I+I_0}} \Big(& \int_{\mathcal{T}} \frac{G_0}{\mu_{g_0}} a_1 \, B^{2n-2}_{I_0+I-2e_1} + \int_{\mathcal{T}} \frac{E_0}{\mu_{g_0}} a_2 \, B^{2n-2}_{I_0+I-2e_2} \\ & + \int_{\mathcal{T}} \frac{G_0 - 2F_0 + E_0}{\mu_{g_0}} a_3 \, B^{2n-2}_{I_0+I-2e_3} - \int_{\mathcal{T}} \frac{G_0 - F_0}{\mu_{g_0}} b_{13} \, B^{2n-2}_{I_0+I-e_1-e_3} \\ & - \int_{\mathcal{T}} \frac{F_0}{\mu_{g_0}} b_{12} \, B^{2n-2}_{I_0+I-e_1-e_2} - \int_{\mathcal{T}} \frac{E_0 - F_0}{\mu_{g_0}} b_{23} \, B^{2n-2}_{I_0+I-e_2-e_3} \Big) \, P_I \end{aligned}$$

for all $|I_0 = (I_0^1, I_0^2, I_0^3)| = n$ with $I_0^1, I_0^2, I_0^3 > 0$ and where a_s and b_{rs} were defined in Proposition 6.2.

Proof: Let us compute the gradient of the functional $\mathcal{D}^{g_0}$ with respect to the coordinates of a control point $P_I = (x^1_{I_0}, x^2_{I_0}, x^3_{I_0})$. For any $a \in \{1,2,3\}$ and any I_0 such that $|I_0| = n$ with $I^1_0, I^2_0, I^3_0 > 0$.

$$\frac{\partial \mathcal{D}^{g_0}(\mathcal{P})}{\partial x^a_{I_0}} = \int_T 2\frac{G_0}{\mu_0} < \frac{\partial \overrightarrow{x_u}}{\partial x^a_{I_0}}, \overrightarrow{x_u} > du\,dv + \int_T 2\frac{E_0}{\mu_0} < \frac{\partial \overrightarrow{x_v}}{\partial x^a_{I_0}}, \overrightarrow{x_v} > du\,dv$$
$$- \int_T 2\frac{F_0}{\mu_0}\left(< \frac{\partial \overrightarrow{x_u}}{\partial x^a_{I_0}}, \overrightarrow{x_v} > + < \frac{\partial \overrightarrow{x_v}}{\partial x^a_{I_0}}, \overrightarrow{x_u} > \right) du\,dv.$$

Using the value of the partial derivatives, given in Equations (95) and (96), we have that:

$$\frac{\partial \mathcal{D}^{g_0}(\mathcal{P})}{\partial x^a_{I_0}} = 2n^2 \int_T (\frac{G_0}{\mu_0}(B^{n-1}_{I_0-e_1} - B^{n-1}_{I_0-e_3}) < e_a, \sum_{|I|=n}(B^{n-1}_{I-e_1} - B^{n-1}_{I-e_3})P_I >)\, du\,dv$$
$$+ 2n^2 \int_T (\frac{E_0}{\mu_0}(B^{n-1}_{I_0-e_2} - B^{n-1}_{I_0-e_3}) < e_a, \sum_{|I|=n}(B^{n-1}_{I-e_2} - B^{n-1}_{I-e_3})P_I >)\, du\,dv$$
$$- 2n^2 \int_T (\frac{F_0}{\mu_0}(B^{n-1}_{I_0-e_1} - B^{n-1}_{I_0-e_3}) < e_a, \sum_{|I|=n}(B^{n-1}_{I-e_2} - B^{n-1}_{I-e_3})P_I >)\, du\,dv$$
$$- 2n^2 \int_T (\frac{F_0}{\mu_0}(B^{n-1}_{I_0-e_2} - B^{n-1}_{I_0-e_3}) < e_a, \sum_{|I|=n}(B^{n-1}_{I-e_1} - B^{n-1}_{I-e_3})P_I >)\, du\,dv.$$

Now, taking into account the formula given in Lemma 1.2 and using a_r and b_{rs} defined in Proposition 6.2 we have that a triangular control net is an extremal of the functional $\mathcal{D}^{g_0}$ if and only if for any $|I_0| = n$ with $I^1_0, I^2_0, I^3_0 > 0$, the following expression vanishes:

$$\frac{\partial \mathcal{D}^{g_0}(\overrightarrow{x})}{\partial x^a_{I_0}} = \sum_{|I|=n} \frac{\binom{n-1}{I}}{\binom{2n-2}{I+I_0}} (\int_{\mathcal{T}} \frac{G_0}{\mu_{g_0}} a_1\, B^{2n-2}_{I_0+I-2e_1} + \int_{\mathcal{T}} \frac{E_0}{\mu_{g_0}} a_2\, B^{2n-2}_{I_0+I-2e_2}$$
$$+ \int_{\mathcal{T}} \frac{G_0 - 2F_0 + E_0}{\mu_{g_0}} a_3\, B^{2n-2}_{I_0+I-2e_3} - \int_{\mathcal{T}} \frac{G_0 - F_0}{\mu_{g_0}} b_{13}\, B^{2n-2}_{I_0+I-e_1-e_3}$$
$$- \int_{\mathcal{T}} \frac{F_0}{\mu_{g_0}} b_{12}\, B^{2n-2}_{I_0+I-e_1-e_2} - \int_{\mathcal{T}} \frac{E_0 - F_0}{\mu_{g_0}} b_{23}\, B^{2n-2}_{I_0+I-e_2-e_3})\ P_I.$$

■

The formulas obtained in the last proposition give us a system of linear equations for the interior points of the triangular net given its border. Now if we have a look to the corresponding values in Table I and Table II, we can see that this method improves the results obtained through all the other methods, and moreover we get this improvement for all the examples, even when we deal with non-isothermal patches.

Finally, we have gone one step forward. If $\overrightarrow{x}_1$ is the Dirichlet extremal of the functional $\mathcal{D}^{g_0}$ and g_1 is its first fundamental form the new approximation is the extremal of the functional $\mathcal{D}^{g_1}$. The results obtained from this last method are shown in the Second step row in Table II, and from them we conjecture that, especially for highly non-isothermal patches, the improvement given by the correction method can be further enhanced by repeating the process.

8. Conclusions

In this chapter we have deduced and compared different methods to generate surfaces with prescribed boundary. They can be polynomial extremals of the Dirichlet functional, polynomial extremals of the biharmonic functional, or they can also be obtained by means of masks.

The surfaces obtained by minimizing the Dirichlet functional are polynomial approximations to minimal surfaces with prescribed boundary. Since we have compared the area of the surfaces obtained by this method with the surfaces obtained with the use of different masks, we can ensure that they are good approximations to minimal surfaces that can also be improved with the Dirichlet correction method. Nevertheless, the approximations obtained by means of the Dirichlet mask, or any of the other masks we have considered, they can be obtained with a smaller computational cost, despite having a bigger area. This is due to the fact that they are obtained as a solution of a linear sparse system while the linear system of the control points associated to the Dirichlet functional has no null coefficients.

The shapes of the triangular Bézier surfaces, which are extremals of the Dirichlet functional among all polynomial patches with a given boundary, have a stable behavior according to the boundary information. This method is a good way of generating surfaces because, in addition to obtaining a patch fitted to the boundary, it allows us to minimize the area since a polynomial approximation to a minimal surface is obtained.

On the other hand, concerning our study of the biharmonic functional, we can say that the shapes of the surfaces and control nets obtained by means of the biharmonic mask are almost as good as those obtained for the extremals of the biharmonic functional. Nevertheless, the bending energy is smaller for the polynomial extremals than for the surfaces generated with the bending energy mask, as it could be expected.

CHAPTER 7

Triangular Bézier approximations to Constant Mean Curvature surfaces

Minimal surfaces are characterized by the vanishing of the mean curvature. A generalization of this condition is to ask for constant mean curvature. Surfaces with constant mean curvature (CMC-surfaces) are the mathematical abstraction of physical soap films and soap bubbles, so they correspond to real situations. From a variational point of view CMC-surfaces can be seen as the critical points of area for those variations that left the enclosed volume invariable . In general, the characterization of "area minimizing under volume constraint" is no longer true from a global point of view, since they could have self-intersections and extend to infinity. But locally, every small neighborhood of a point is still area minimizing while fixing the volume which is enclosed by the cone defined by the neighborhood's boundary and the origin.

An exhaustive discussion of the existence of surfaces of prescribed constant mean curvature spanning a Jordan curve in $\mathbb{R}^3$ can be found in [**40**]. In this chapter we will show these results in order to discuss the existence of triangular Bézier extremals of the functional $\mathcal{D}_H$, which is defined as follows. Given $H \in \mathbb{R}$

$$\begin{aligned}\mathcal{D}_H(\overrightarrow{x}) =& \mathcal{D}(\overrightarrow{x}) + 2HV(\overrightarrow{x}) \\ =& \frac{1}{2}\int_{\mathcal{T}} (\|\overrightarrow{x}_u\|^2 + \|\overrightarrow{x}_v\|^2)\, dudv + 2\frac{H}{3}\int_{\mathcal{T}} < \overrightarrow{x}_u \wedge \overrightarrow{x}_v, \overrightarrow{x} > \, dudv.\end{aligned}$$

If an isothermal patch is an extremal of the functional $\mathcal{D}_H$, then it is a CMC-surface. The "volume" term, $V(\overrightarrow{x})$, measures the algebraic volume enclosed in the cone segment consisting of all lines joining points $\overrightarrow{x}\,(u,v)$ on the surface with the origin. The first term $\mathcal{D}(\overrightarrow{x})$ is the Dirichlet functional.

We will give some examples of Bézier extremals of prescribed boundary curves for different prescribed constant mean curvatures.

1. Existence of triangular Bézier surfaces of prescribed constant mean curvature

A simple argument can be used to see that the function assigning the value $V(\overrightarrow{x}^{\mathcal{P}})$ to each control net, $\mathcal{P}$, with fixed boundary control points, has no global minimum.

Let us suppose that a minimum exists. Since spatial translations do not affect the curvature of the surface, we can suppose that the origin is located far enough away from the surface so that the control net is enclosed in a half-space passing through the origin. Let us move an interior control point, P_{I_0}, toward the origin. Then, a well-known property

of Bézier surfaces states that all the points of $\overrightarrow{x}(u,v)$ change in a parallel direction with intensity $B_I^n(u,v)$. Then, since the new cone segment is totally included in the initial one, its volume decreases.

Now, let us consider the CMC-functional,

$$\mathcal{D}_H(\overrightarrow{x}) = \mathcal{D}(\overrightarrow{x}) + 2HV(\overrightarrow{x}).$$

As we said in chapter seven, the function, $\mathcal{P} \to \mathcal{D}(\overrightarrow{x}^{\mathcal{P}})$, for control nets with fixed boundary always has a minimum and, as we have just seen, the function $\mathcal{P} \to V(\overrightarrow{x}^{\mathcal{P}})$, never has a minimum. Therefore, by using the constant H to balance both functions we can say that the function, $\mathcal{P} \to \mathcal{D}_H(\overrightarrow{x}^{\mathcal{P}})$, will have a minimum only for $H \in [a,-a]$ for some constant $a \in \mathbb{R}$. It should be noted that when $H=0$, $\mathcal{D}_H$ is reduced to $\mathcal{D}$ and then there is a minimum, whereas when H is too big, the main term in $\mathcal{D}_H$ is V, and therefore the minimum does not exist.

The symmetry of the interval, $[a,-a]$, is a consequence of the fact that reversing the orientation of a surface means a change in the sign of the mean curvature.

The value of a depends on the boundary control points. Let us denote Γ the prescribed boundary. According to the results in [**40**] about "small" solutions, if there is a radius R such that $\Gamma \subset B_R(0)$, and $|H| \leq \frac{1}{R}$ there always exists a surface of constant mean curvature H.

Moreover, there is another result, called the Heinz' non-existence result, which illustrates the need for the previous smallness condition: There exists another constant M defined through an integral along the boundary curve, such that, when $|H| > M$ there is no surface of constant mean curvature H. So, there are some values of the curvature, $\frac{1}{R} < |H| \leq M$, for which the existence of a solution for curvatures within this interval, cannot be ensured.

A solution to the problem of finding extremals of the functional $\mathcal{D}_H$ among all surfaces with prescribed border and constant mean curvature H can only be obtained with certainty if $|H| \leq \frac{1}{R}$.

Let us illustrate by means of an example why the possibility of finding an extremal of the CMC-functional only exists if the prescribed mean curvature, H, belongs to a symmetric interval $[-a,a]$.

EXAMPLE 7.2. *Let us consider a triangular control net of degree 4 and prescribe the border control points along a planar equilateral triangle. Moreover, in order to reduce the number of variables in this example we will use a symmetric configuration for the three interior control points. These three interior control points, that is nine degrees of freedom, are reduced to a pair by the following symmetric restriction on them:*

$$P_{112} = \left(a\cos\frac{4\pi}{3}, a\sin\frac{4\pi}{3}, b\right) \quad P_{121} = \left(a\cos\frac{2\pi}{3}, a\sin\frac{2\pi}{3}, b\right) \quad P_{211} = (a,0,b).$$

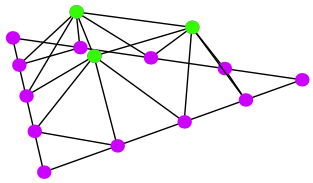

FIGURE 1. A symmetric configuration of the control net will simplify the computation of an extremal of D_H.

The associated Bézier surface is

$$\overrightarrow{x}(u,v) = \Bigg(-\frac{1}{2}(-1+3u)(-1+3(4a-1)u^2v+3(4a-1)u(v-1)v),$$
$$-\frac{\sqrt{3}}{2}(u+2v-1)(-1+3(4a-1)u^2v+3(4a-1)u(v-1)v), -12buv(u+v-1)\Bigg),$$

and the functional is reduced to a function $f_H(a,b)$

$$\mathcal{D}_H(\overrightarrow{x}) = f_H(a,b) = \frac{1}{30800}\Big(46585+24640b^2+8598\sqrt{3}bH+16a^2(385+18\sqrt{3}bH)$$
$$+8a(-385+312\sqrt{3}bH)\Big).$$

Then, to find the critical points of $f_H(a,b)$ *we have to solve the system*

$$\frac{\partial f_H(a,b)}{\partial a} = \frac{\partial f_H(a,b)}{\partial b} = 0,$$

that is,

$$\begin{cases} 385 = 1540a + 312\sqrt{3}bH + 72\sqrt{3}abH \\ 0 = 24640b + 3\sqrt{3}(1433+416a+48a^2)H. \end{cases}$$

From the second equation we get

$$b = \frac{-1}{24640}(3(1433\sqrt{3}H + 416\sqrt{3}aH + 48\sqrt{3}a^2H))$$

and substituting in the first equation we obtain the following third-order equation

$$-1185800 + 4743200a - 502983H^2 - 262089aH^2 - 50544a^2H^2 - 3888a^3H^2 = 0.$$

Cardano's formula would give us the solution of this cubic equation and it has the following discriminant

$$\frac{-166375}{14693280768H^6}(-641395994624000+92020318790400H^2-158618386080H^4+480048687H^6).$$

The real solutions of

$$0 = -641395994624000 + 92020318790400H^2 - 158618386080H^4 + 480048687H^6$$

are ± 2.65596*, which implies that the discriminant is greater than or equal to 0 if and only if* $H \in [-2.65596, 2.65596]$*. Therefore the existence of an extremal of the CMC-functional can be ensured if the prescribed mean curvature,* H*, belongs to a symmetric interval* $[-2.65596, 2.65596]$*.*

Here we have the plot of the extremal of $\mathcal{D}_H$ *for different mean curvatures:*

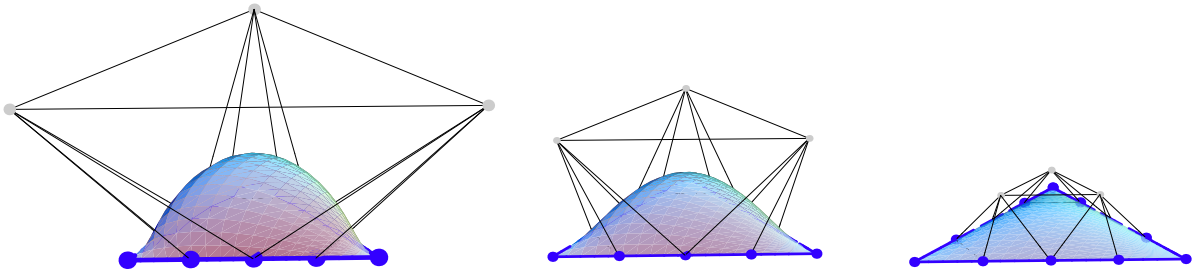

FIGURE 2. These surfaces are symmetric approximations to CMC-surfaces with curvatures $H = -2.5$, $H = -2$ and $H = -1$ respectively.

2. The CMC-functional results

The following proposition, which can be found in [**40**], gives a condition that involves the Laplacian operator in order to characterize an isothermal CMC-surface. Let us recall that an analogous characterization of isothermal minimal surfaces was given in Proposition 5.5.

PROPOSITION 7.1. *Let* $\overrightarrow{x}$ *be an isothermal patch. It is a constant mean curvature surface (CMC-surface) if and only if*

$$\Delta \overrightarrow{x} = 2H \overrightarrow{x}_u \wedge \overrightarrow{x}_v. \tag{110}$$

Expression (110) is the Euler-Lagrange equation of the functional $\mathcal{D}_H$

$$\mathcal{D}_H(\overrightarrow{x}) = \mathcal{D}(\overrightarrow{x}) + 2HV(\overrightarrow{x}). \tag{111}$$

Moreover, an isothermal patch satisfies the PDE in (110) if and only if it is an extremal of $\mathcal{D}_H$.

There are two qualitative differences between the Dirichlet functional and the CMC-functional: whereas for the Dirichlet functional the extremal always exists and it is the solution of a linear system, now, the existence of the extremal can only be ensured with

certainty when $|H| \leq m$, for a certain constant, $m = \frac{1}{R}$, depending on the boundary configuration, and they are computed as solutions of a quadratic system.

Moreover, since the Euler-Lagrange equation of the functional $\mathcal{D}_H$, in Equation (110), is not linear we cannot determine a Bézier solution as a solution of a linear system of equations in terms of the control points. In comparison, in the first and the second chapters we saw that, given some control points as initial data, the harmonic equation and hence the biharmonic equation, allow us to determine the associated PDE surface as a solution of a linear system. Analogously, in the fourth chapter, we prescribed the boundary curves and we were able to compute the associated PDE surface by the third-order method while also solving a linear system.

Here we will give an expression of the CMC-functional in terms of the control points of a triangular Bézier surface, which implies that the restriction of the functional to the Bézier case can be seen as a function instead of as a functional. Afterwards, we will give the condition that a triangular control net must fulfill in order to be an extremal of the CMC-functional among all Bézier triangles with a prescribed boundary.

The following result will simplify the way to obtain the formula in terms of control points of the functional $\mathcal{D}_H$. First, we will work the volume term of the CMC-functional. It can also be written as a polynomial in terms of the coordinates of the control points, $\mathcal{P} = \{P_I\}_{|I|=n}$, of the Bézier triangular surface, $\overrightarrow{x}$. Therefore the restriction of the functional, $V(\overrightarrow{x})$, to the Bézier case is also reduced to a real function by assigning the value $V(\overrightarrow{x}^{\mathcal{P}})$ to each control net, $\mathcal{P} = \{P_I\}_{|I|=n}$.

PROPOSITION 7.2. *Let $\overrightarrow{x}$ be the triangular Bézier surface associated to the control net, $\mathcal{P} = \{P_I\}_{|I|=n}$, then the volume*

$$V(\overrightarrow{x}) = \frac{1}{3}\int_{\mathcal{T}} < \overrightarrow{x}_u \wedge \overrightarrow{x}_v, \overrightarrow{x} > dudv,$$

can be expressed in terms of the control points, $P_I = (x_I^1, x_I^2, x_I^3)$, with $|I| = |\{I^1, I^2, I^3\}| = n$, by the formula

$$V(\overrightarrow{x}) = \sum_{|I_0|=|I_1|=|I_2|=n} C_{I_0I_1I_2} x_{I_0}^1 x_{I_1}^2 x_{I_2}^3$$

where

$$C_{I_0I_1I_2} = \frac{\binom{n}{I_0}\binom{n}{I_1}\binom{n}{I_2}}{\binom{3n}{I_0+I_1+I_2}}(d_{12}^{I_0I_1I_2} + d_{23}^{I_0I_1I_2} + d_{13}^{I_0I_1I_2}) \tag{112}$$

with

$$d_{rs}^{IJK} = \frac{I^rJ^s - J^rI^s}{(I^r + J^r + K^r)(I^s + J^s + K^s)}.$$

Proof: The volume of a Bézier surface,

$$V(\overrightarrow{x}) = \frac{1}{3}\int_{\mathcal{T}} < \overrightarrow{x}_u \wedge \overrightarrow{x}_v, \overrightarrow{x} > dudv = \sum_{|I_0|=n}\sum_{|I_1|=n}\sum_{|I_2|=n} C_{I_0I_1I_2} x^1_{I_0} x^2_{I_1} x^3_{I_2},$$

is a cubical polynomial of the control points, so in order to compute the coefficients $C_{I_0I_1I_2}$ we will compute its third derivative. We will then have

$$\frac{\partial^3 V(\overrightarrow{x})}{\partial x^1_{I_0}\partial x^2_{I_1}\partial x^3_{I_2}} = C_{I_0I_1I_2}.$$

First of all we compute the derivative with respect to a first coordinate $x^1_{I_0}$ of an arbitrary interior point $P_{I_0} = \{x^1_{I_0}, x^2_{I_0}, x^3_{I_0}\}$, where $|I_0| = n$ and $I^1_0, I^2_0, I^3_0 \neq 0$.

$$\begin{aligned}
\frac{\partial V(\overrightarrow{x})}{\partial x^1_{I_0}} =& \frac{1}{3}\int_{\mathcal{T}} (\ < \left(B^n_{I_0}\right)_u e^1 \wedge \overrightarrow{x}_v, \overrightarrow{x} > + < \overrightarrow{x}_u \wedge \left(B^n_{I_0}\right)_v e^1, \overrightarrow{x} > \\
&+ < \overrightarrow{x}_u \wedge \overrightarrow{x}_v, \left(B^n_{I_0}\right) e^1 > \ )\, du\, dv \\
=& \int_{\mathcal{T}} < B^n_{I_0} e^1 \wedge \overrightarrow{x}_v, \overrightarrow{x} >_u - < B^n_{I_0} e^1 \wedge \overrightarrow{x}_{vu}, \overrightarrow{x} > + < \overrightarrow{x}_u \wedge B^n_{I_0} e^1, \overrightarrow{x} >_v \ du\, dv \\
&- \int_{\mathcal{T}} < \overrightarrow{x}_{uv} \wedge B^n_{I_0} e^1, \overrightarrow{x} > + < \overrightarrow{x}_u \wedge \overrightarrow{x}_v, B^n_{I_0} e^1 > \ du\, dv.
\end{aligned}$$

After computing the derivative with respect to an arbitrary first coordinate, we applied the integration by parts formula. Now, bearing in mind that

$$\begin{aligned}
\int_{\mathcal{T}} < B^n_{I_0} e^1 \wedge \overrightarrow{x}_v, \overrightarrow{x} >_u &= \int_0^1 < B^n_{I_0} e^1 \wedge \overrightarrow{x}_v, \overrightarrow{x} > \Big]_0^{1-v} dv = 0, \\
\int_{\mathcal{T}} < \overrightarrow{x}_u \wedge B^n_{I_0} e^1, \overrightarrow{x} >_v &= \int_0^1 < \overrightarrow{x}_u \wedge B^n_{I_0} e^1, \overrightarrow{x} > \Big]_0^{1-u} du = 0,
\end{aligned}$$

since $B^n_{I_0}(1-v, v) = B^n_{I_0}(0, v) = B^n_{I_0}(u, 0) = B^n_{I_0}(u, 1-u) = 0$ for $|I_0| = n$ with $I^1_0, I^2_0, I^3_0 \neq 0$, and the properties of the cross and the scalar triple product:

$$\begin{aligned}
a \wedge b &= -b \wedge a \\
< a \wedge b, c > &= < b \wedge c, a > = < c \wedge a, b >,
\end{aligned}$$

we obtain that

$$\frac{\partial V(\overrightarrow{x})}{\partial x^1_{I_0}} = \frac{1}{3}\int_{\mathcal{T}} < \overrightarrow{x}_u \wedge \overrightarrow{x}_v, B^n_{I_0} e^1 > . \tag{113}$$

Now we must compute the derivative with respect to a second coordinate, $x^2_{I_1}$, of an arbitrary interior point, such that, as before, $|I_1| = n$ with $I^1_1, I^2_1, I^3_1 \neq 0$.

We will do this in an analogous way to the previous computation of $\frac{\partial V(\overrightarrow{x})}{\partial x^1_{I_0}}$:

$$\begin{aligned}\frac{\partial^2 V(\overrightarrow{x})}{\partial x^1_{I_0}\partial x^2_{I_1}} =&\frac{1}{3}\int_{\mathcal{T}} \frac{\partial}{\partial x^2_{I_1}} < \overrightarrow{x}_u \wedge \overrightarrow{x}_v, B^n_{I_0} e^1 > \, du\, dv\\ =&\frac{1}{3}\int_{\mathcal{T}} < \left(B^n_{I_1}\right)_u e^2 \wedge \overrightarrow{x}_v, B^n_{I_0} e^1 > + < \overrightarrow{x}_u \wedge \left(B^n_{I_1}\right)_v e^2, B^n_{I_0} e^1 > \, du\, dv\\ =&\frac{1}{3}\int_{\mathcal{T}} < B^n_{I_0} e^1 \wedge \left(B^n_{I_1}\right)_u e^2, \overrightarrow{x}_v > - < B^n_{I_0} e^1 \wedge \left(B^n_{I_1}\right)_v e^2, \overrightarrow{x}_u > \, du\, dv\\ =&\frac{1}{3}\int_{\mathcal{T}} \big(< B^n_{I_0} e^1 \wedge \left(B^n_{I_1}\right)_u e^2, \overrightarrow{x} >_v - < \left(B^n_{I_0}\right)_v e^1 \wedge \left(B^n_{I_1}\right)_u e^2, \overrightarrow{x} >\\ &- < B^n_{I_0} e^1 \wedge \left(B^n_{I_1}\right)_v e^2, \overrightarrow{x} >_u + < \left(B^n_{I_0}\right)_u e^1 \wedge \left(B^n_{I_1}\right)_v e^2, \overrightarrow{x} > \big)\, dudv.\end{aligned}$$

As before, the following integrals are null

$$\int_{\mathcal{T}} < B^n_{I_0} e^1 \wedge \left(B^n_{I_1}\right)_u e^2, \overrightarrow{x} >_v \, dudv = \int_0^1 < B^n_{I_0} e^1 \wedge \left(B^n_{I_1}\right)_u e^2, \overrightarrow{x} > \Big]_0^{1-u} du = 0$$
$$\int_{\mathcal{T}} < B^n_{I_0} e^1 \wedge \left(B^n_{I_1}\right)_v e^2, \overrightarrow{x} >_u \, dudv = \int_0^1 < B^n_{I_0} e^1 \wedge \left(B^n_{I_1}\right)_v e^2, \overrightarrow{x} > \Big]_0^{1-v} dv = 0,$$

therefore

$$\frac{\partial^2 V(\overrightarrow{x})}{\partial x^1_{I_0}\partial x^2_{I_1}} = \int_{\mathcal{T}} \left(\left(B^n_{I_0}\right)_u \left(B^n_{I_1}\right)_v - \left(B^n_{I_0}\right)_v \left(B^n_{I_1}\right)_u\right) < e^1 \wedge e^2, \overrightarrow{x} > \, du\, dv.$$

Finally we compute the derivative with respect to an arbitrary third coordinate $x^3_{I_2}$ with $|I_2| = n$ and such that $I^1_2, I^2_2, I^3_2 \neq 0$:

$$\begin{aligned}\frac{\partial^2 V(\overrightarrow{x})}{\partial x^1_{I_0}\partial x^2_{I_1}\partial x^3_{I_2}} &= \int_{\mathcal{T}} \frac{\partial}{\partial x^3_{I_2}} ((B^n_{I_0})_u (B^n_{I_1})_v - (B^n_{I_0})_v (B^n_{I_1})_u) < e^1 \wedge e^2, \overrightarrow{x} > \, dudv\\ &= \int_{\mathcal{T}} ((B^n_{I_0})_u (B^n_{I_1})_v - (B^n_{I_0})_v (B^n_{I_1})_u) B^n_{I_2} < e^1 \wedge e^2, e^3 > \, dudv\\ &= \int_{\mathcal{T}} ((B^n_{I_0})_u (B^n_{I_1})_v - (B^n_{I_0})_v (B^n_{I_1})_u) B^n_{I_2}\, du\, dv.\end{aligned}$$

Therefore

$$C_{x^1_{I_0}x^2_{I_1}x^3_{I_2}} = \int_{\mathcal{T}} ((B^n_{I_0})_u (B^n_{I_1})_v - (B^n_{I_0})_v (B^n_{I_1})_u)\, B^n_{I_2}\, dudv$$

$$= n^2 \int_{\mathcal{T}} ((B^{n-1}_{I_0-e_1} - B^{n-1}_{I_0-e_3})(B^{n-1}_{I_1-e_2} - B^{n-1}_{I_1-e_3}) - (B^{n-1}_{I_0-e_2} - B^{n-1}_{I_0-e_3})(B^{n-1}_{I_1-e_1} - B^{n-1}_{I_1-e_3}))B^n_{I_2}\, dudv$$

$$= \frac{\binom{n}{I_0}\binom{n}{I_1}\binom{n}{I_2}}{\binom{3n}{I_0+I_1+I_2}} \Big(\frac{I^1_0 I^2_1 - I^1_1 I^2_0}{(I^1_0+I^1_1+I^1_2)(I^2_0+I^2_1+I^2_2)} + \frac{I^2_0 I^3_1 - I^2_1 I^3_0}{(I^2_0+I^2_1+I^2_2)(I^3_0+I^3_1+I^3_2)}$$

$$+ \frac{I^3_0 I^1_1 - I^3_1 I^1_0}{(I^3_0+I^3_1+I^3_2)(I^1_0+I^1_1+I^1_2)} \Big),$$

where we have achieved the last formula after computing the integral of the Bernstein polynomials, given in Equation (3),

$$\int_{\mathcal{T}} B^{3n-2}_I (u,v)\, dudv = \frac{1}{3n(3n-1)}$$

and performing some simplifications like the following:

$$\int_{\mathcal{T}} B^{n-1}_{I_0-e_1} B^{n-1}_{I_1-e_2} B^n_{I_2}\, dudv = \int_{\mathcal{T}} \frac{\binom{n-1}{I_0-e_1}\binom{n-1}{I_1-e_2}\binom{n}{I_2}}{\binom{3n-2}{I_0+I_1+I_2-e_1-e_2}} B^{3n-2}_{I_0+I_1+I_2-e_1-e_2}\, dudv$$

$$= \frac{\binom{n}{I_0}\binom{n}{I_1}\binom{n}{I_2}}{\binom{3n}{I_0+I_1+I_2}} \frac{3n(3n-1)}{n^2} \frac{I^1_0 I^2_1}{(I^1_0+I^1_1+I^1_2)(I^2_0+I^2_1+I^2_2)}$$

$$= \frac{\binom{n}{I_0}\binom{n}{I_1}\binom{n}{I_2}}{\binom{3n}{I_0+I_1+I_2}} \frac{3n(3n-1)}{n^2}\, d^{I_0 I_1 I_2}_{12}.$$

■

REMARK 7.3. *The coefficients d's verify the following symmetry relation:*

$$d^{IJK}_{rs} = -d^{JIK}_{rs},$$

which is immediate from its definition in Proposition 7.2, since:

$$d^{JIK}_{rs} = \frac{J^r I^s - I^r J^s}{(I^r + J^r + K^r)(I^s + J^s + K^s)}.$$

LEMMA 7.4. *The coefficients C_{IJK} verify the following symmetry relations*

$$C_{IJK} = -C_{JIK} = C_{JKI}.$$

Proof: The symmetry of the coefficients C's is a direct consequence of the symmetry of d's shown in the previous remark.

■

In the following proposition we give a formula for the CMC-functional, $\mathcal{D}_H(\overrightarrow{x})$ in terms of the control net, $\mathcal{P} = \{P_I\}_{|I|=n}$, of the Bézier triangular surface, $\overrightarrow{x}$. As we said before, this lets us to see the functional as a real function assigning the value $\mathcal{D}_H(\overrightarrow{x}^{\mathcal{P}})$ to each control net, $\mathcal{P} = \{P_I\}_{|I|=n}$.

PROPOSITION 7.5. *Let $\overrightarrow{x}$ be the triangular Bézier surface associated to the control net, $\mathcal{P} = \{P_I\}_{|I|=n}$, then let us write $P_I = (a_I, b_I, c_I)$ and establish the subindex $I_n = \{I_n^1, I_n^2, I_n^3\}$, then the CMC-functional, $\mathcal{D}_H$, can be expressed by the formula*

$$\mathcal{D}_H(\overrightarrow{x}) = \frac{1}{2}\sum_{a=1}^{3}\sum_{|I_0|=n}\sum_{|I_1|=n} C_{I_0I_1}x^a_{I_0}x^a_{I_1} + 2H\sum_{|I_0|=|I_1|=|I_2|=n} C_{I_0I_1I_2}x^1_{I_0}x^2_{I_1}x^3_{I_2}$$

where

$$C_{I_0I_1} = \frac{\binom{n}{I_0}\binom{n}{I_1}}{\binom{2n}{I_0+I_1}}(a_1 + a_2 + 2a_3 - b_{13} - b_{23}) \quad \textit{with} \quad a_r \textit{ and } b_{rs} \textit{ defined in Equation (94) and}$$

$$C_{I_0I_1I_2} = \frac{\binom{n}{I_0}\binom{n}{I_1}\binom{n}{I_2}}{\binom{3n}{I_0+I_1+I_2}}(d_{12}^{I_0I_1I_2} + d_{23}^{I_0I_1I_2} + d_{13}^{I_0I_1I_2}) \quad \textit{with} \quad d_{rs}^{IJK} \textit{ defined in Equation (112).}$$

We have just seen in Proposition 7.5 that the CMC-functional, $\mathcal{D}_H(\overrightarrow{x})$, is a function of the control points, so let us now compute its gradient with respect to the coordinates of an arbitrary control point. We will then be able to give a characterization of the control net of the triangular Bézier extremals of $\mathcal{D}_H$.

The gradient of the first addend, corresponding to the Dirichlet functional, was computed in the previous chapter, see Equation (99). So, let us consider the volume expression

$$V(\overrightarrow{x}) = \sum_{|I|,|J|,|K|=n} C_{IJK}x^1_I x^2_J x^3_K,$$

in order to compute its the gradient with respect to the coordinates of a control point $P_{I_0} = \left(x^1_{I_0}, x^2_{I_0}, x^3_{I_0}\right)$ where $I_0 = (I_0^1, I_0^2, I_0^3)$.

$$\begin{aligned}\frac{\partial V(\overrightarrow{x})}{\partial P_{I_0}} &= \left(\sum_{|J|,|K|=n} C_{I_0JK}x^2_J x^3_K, \sum_{|I|,|K|=n} C_{II_0K}x^1_I x^3_K, \sum_{|I|,|J|=n} C_{IJI_0}x^1_I x^2_J\right)\\ &= \sum_{|J|,|K|=n} C_{I_0JK}(x^2_J x^3_K, -x^1_J x^3_K, x^1_J x^2_K) \qquad (114)\\ &= \sum_{|J|,|K|=n} \frac{C_{I_0JK} - C_{I_0KJ}}{2}(x^2_J x^3_K, -x^1_J x^3_K, x^1_J x^2_K) =\end{aligned}$$

$$= \frac{1}{2} \sum_{|J|,|K|=n} C_{I_0JK}(x_J^2 x_K^3, -x_J^1 x_K^3, x_J^1 x_K^2) + \frac{1}{2} \sum_{|J|,|K|=n} C_{I_0JK}(-x_J^2 x_K^3, x_J^1 x_K^3, -x_J^1 x_K^2)$$

$$= \frac{1}{2} \sum_{|J|,|K|=n} C_{I_0JK}(x_J^2 x_K^3 - x_K^2 x_J^3, x_K^1 x_J^3 - x_J^1 x_K^3, x_J^1 x_K^2 - x_K^1 x_J^2)$$

$$= \frac{1}{2} \sum_{|J|,|K|=n} C_{I_0JK}\, P_J \wedge P_K.$$

Now we can characterize the triangular control net of an extremal of the CMC-functional among all triangular Bézier patches constrained by a given boundary.

PROPOSITION 7.6. *A triangular control net, $\mathcal{P} = \{P_I\}_{|I|=n}$, is an extremal of the CMC-functional, $\mathcal{D}_H$, among all triangular control nets with a prescribed boundary if and only if:*

$$0 = \sum_{|J|=n} C_{I_0J} P_J + H \sum_{|J|,|K|=n} C_{I_0JK}\, P_J \wedge P_K \tag{115}$$

for all $|I_0 = (I_0^1, I_0^2, I_0^3)| = n$ with $I_0^1, I_0^2, I_0^3 > 0$, where the coefficients C_{I_0J} and C_{I_0JK} are defined in Equation (98) and Equation (112) respectively.

Proof: The gradient of the functional with respect to the coordinates of an interior control point:

$$\frac{\partial \mathcal{D}_H(\overrightarrow{x})}{\partial P_{I_0}} = \frac{\partial \mathcal{D}(\overrightarrow{x})}{\partial P_{I_0}} + 2H \frac{\partial V(\overrightarrow{x})}{\partial P_{I_0}}$$

is determined by the gradient of $\mathcal{D}(\overrightarrow{x})$ and $V(\overrightarrow{x})$, computed respectively in Equation (99) and Equation (114).

■

Let us remark that in comparison to our analog results for the Dirichlet and the biharmonic functional, where a polynomial extremal could be computed as a solution of a linear system, here the system defined in Equation (115) is a quadratic system in terms of the control points. This quadratic system has no solution for some values of the curvature, H, as we explained in the first section of this chapter.

In addition, since we compute solutions to a restricted problem, that is, we find extremals of the functional $\mathcal{D}_H$ among all polynomial patches with prescribed border, we obtain Bézier approximations to CMC-surfaces.

Now, let us recall Proposition 7.1, where it was said that an isothermal patch is a constant mean curvature surface, that is, it is an extremal of the functional $\mathcal{D}_H$, if and only if

$$\Delta \overrightarrow{x} = 2H \overrightarrow{x}_u \wedge \overrightarrow{x}_v.$$

Therefore our aim is to remark that, if we consider the restricted problem, $\overrightarrow{x}$ is an extremal of the functional $\mathcal{D}_H$ among all triangular Bézier patches with a prescribed boundary if and

only if a weak version of the above condition is fulfilled. This weak condition is given in the following proposition.

PROPOSITION 7.7. *A triangular Bézier patch* $\overrightarrow{x}$ *is an extremal of the CMC-functional,* $\mathcal{D}_H$*, among all patches with a prescribed boundary if and only if:*

$$0 = \int_{\mathcal{T}} (\Delta \overrightarrow{x} - 2H \overrightarrow{x}_u \wedge \overrightarrow{x}_v)\, B^n_{I_0}\, dudv \quad \textit{for all} \quad |I_0 = (I_0^1, I_0^2, I_0^3)| = n \tag{116}$$

with $I_0^1, I_0^2, I_0^3 > 0$.

Proof: We simply compute the gradient of the CMC-functional with respect to an arbitrary control point bearing in mind Equations (102) and (113), where the gradients of the Dirichlet functional and the gradient of the volume term were computed respectively. ■

The following surfaces have the same prescribed boundary as in Example 2: the border control points are placed along a planar equilateral triangle. But, now we have obtained different approximations to CMC-surfaces without asking for the symmetric configuration for the three interior control points that we considered in Example 2 in order to simplify our computations.

These figures show approximations to CMC-surfaces obtained as a solution of the quadratic system of the control points in Equation (115). They are polynomial extremals of the CMC-functional.

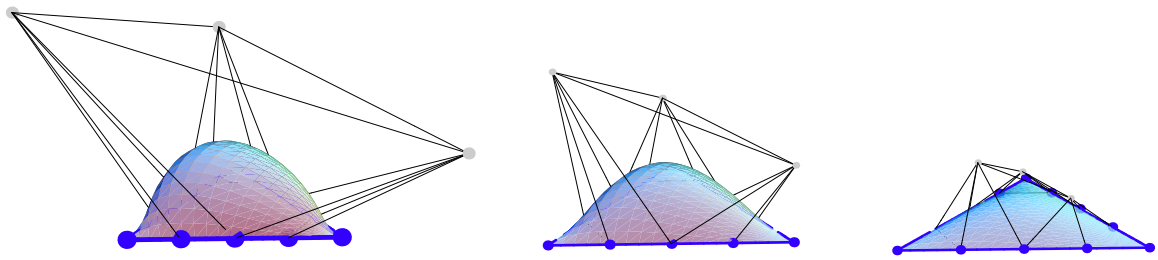

FIGURE 3. Approximations to CMC-surfaces with curvatures $H = -2.5$, $H = -2$ and $H = -1$ respectively.

The boundary curves of our following example describe an approximation to a circle. Therefore we will obtain approximations to spheres. As in our previous example, we can obtain an approximation to a CMC-surface as a solution to the quadratic system in Equation (115). In addition, we could generate a different approximation to a CMC-surface also as an extremal of the functional $\mathcal{D}_H$, but asking for some symmetry property of interior control points, as we did in Example 2. These figures show two different points of view of three different approximations to CMC-surfaces with curvatures $H = -1.5$, $H = -1$ and $H = -0.5$ respectively. Here we have asked the interior control points to fulfill a symmetry condition.

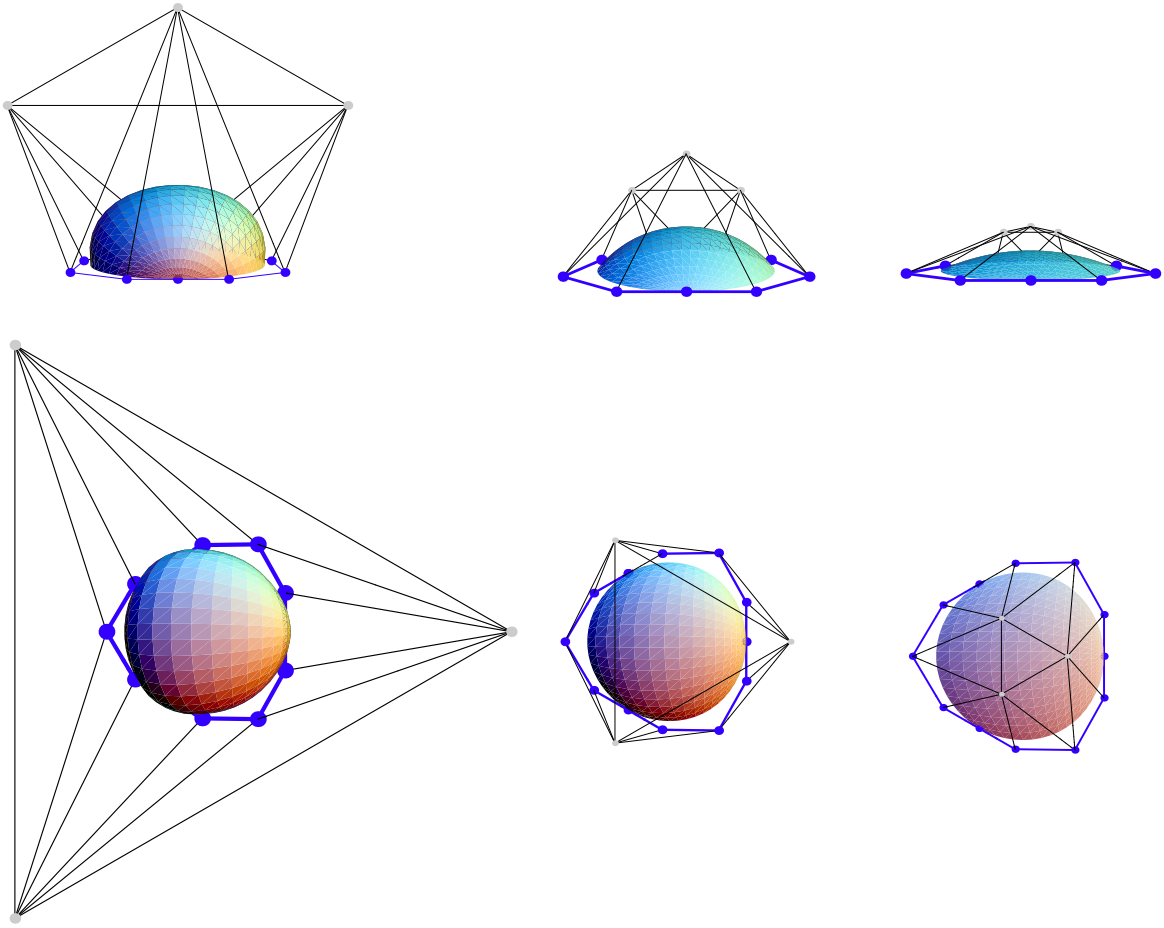

FIGURE 4. These surfaces are approximations to CMC-surfaces with curvatures $H = -1.5$, $H = -1$ and $H = -0.5$ respectively. The interior control points are in a symmetric position.

The following figures are obtained as a solution of the system of quadratic equations described in Equation (115). Here we don't ask for any kind of symmetry.

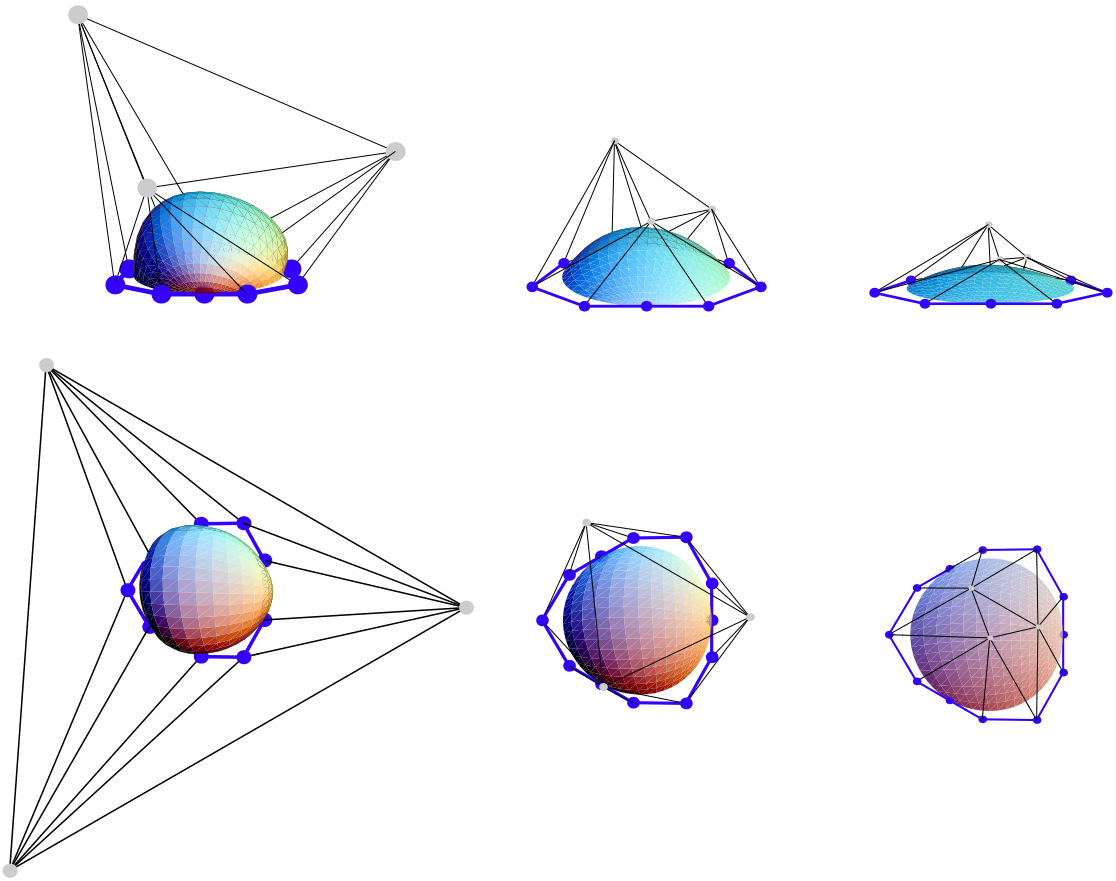

FIGURE 5. These surfaces are approximations to CMC-surfaces with curvatures $H = -1.5$, $H = -1$ and $H = -0.5$ respectively.

Finally we present some more examples of approximations to CMC-surfaces obtained by solving the quadratic system in Equation (115). We prescribe two different boundaries.

The boundary curves in the first example are built in such a way that any associated patch would be isothermal at the corner points.

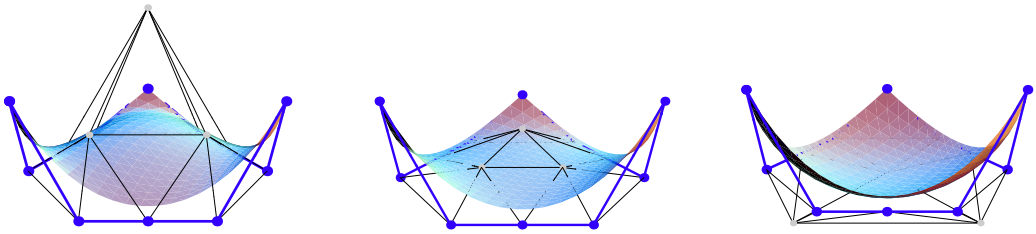

FIGURE 6. These surfaces are approximations to CMC-surfaces with curvatures $H = -1$, $H = 0$ and $H = 1$ respectively.

The following six figures show two points of view of three surfaces approximating CMC-surfaces with mean curvatures $H = -2$, $H = -1.5$ and $H = -1$. The prescribed boundary curves are approximations to three circular arcs, and therefore our results look like pieces of a sphere.

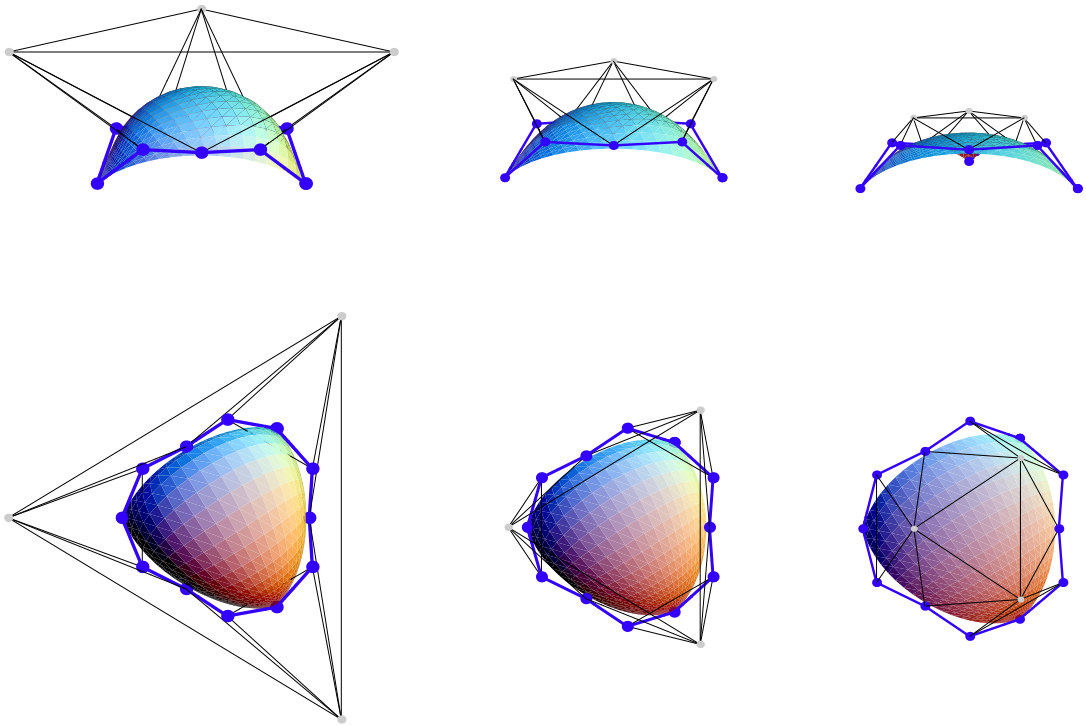

FIGURE 7. These surfaces are approximations to CMC-surfaces with curvatures $H = -2$, $H = -1.5$ and $H = -1$ respectively.

The resulting plots are pleasant and moreover they can be continuously deformed by the parameter H, thus allowing the designer to choose of the shape which best fits the objective. We maintain the good shapes we got with the Dirichlet results but now the choice of the curvature gives the designer another degree of freedom, although the surfaces are obtained as a solution of a quadratic system of the control points.

3. The $\mathcal{C}^1$ problem

In this section we will consider the prescription of not only the boundary but also the tangent planes along the boundary curves, the $\mathcal{C}^1$ problem. Now, the boundary and the next to the boundary control points are fixed, but again the extremals of the CMC-functional, where the other interior control points are considered as variables, can also be computed.

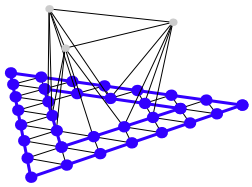

FIGURE 8. The border control points and their neighboring lines of control points are prescribed.

Here we show an example. Again, we consider the same prescribed boundary as in Example 2: the border control points are placed along a planar equilateral triangle. But, now we also prescribe three more lines of control points. These control points are placed along a smaller planar equilateral triangle inside the boundary triangle.

The following figures show approximations to CMC-surfaces obtained as a solution of the quadratic system of the control points in Equation (115), but now for all $|I_0 = (I_0^1, I_0^2, I_0^3)| = n$ with $I_0^1, I_0^2, I_0^3 > 1$. The free points are the interior control points outside the boundary and its next line of control points.

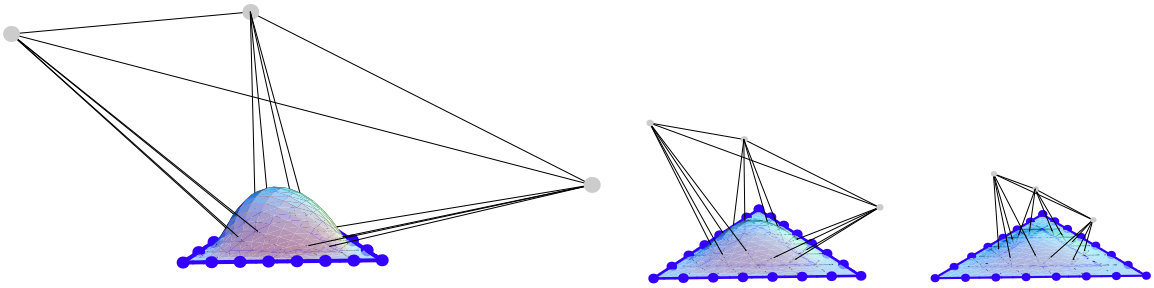

FIGURE 9. These surfaces are approximations to CMC-surfaces with curvatures $H = -2$, $H = -1.5$ and $H = -1$ respectively.

4. Conclusions

In this chapter we have given a method to obtain polynomial approximations to constant mean curvature surfaces. An isothermal patch has constant mean curvature H if and only if it is an extremal of the functional

$$\mathcal{D}_H(\overrightarrow{x}) = \mathcal{D}(\overrightarrow{x}) + 2HV(\overrightarrow{x}).$$

Here we have generated approximations to CMC-surfaces, since we have considered the problem of minimizing this functional restricted to the space of polynomials. We have obtained an expression of the CMC-functional in terms of the control points of a triangular Bézier surface. After that, we deduced the condition that a triangular control net must fulfill in order to be an extremal of the CMC-functional among all Bézier triangles with a prescribed boundary. This characterization of the Bézier extremals of $\mathcal{D}_H$ allowed us to

compute them as a solution of a quadratic system of the control points. The surfaces that are obtained have regular shapes and have the advantage of allowing prescription of the desired curvature in addition to the boundary. This makes it possible to ensure, for a given boundary, the existence of a family of polynomial approximations to CMC-surfaces with this boundary and curvatures within a particular interval. Therefore, the prescription of the curvature in this method can be seen as another degree of freedom in comparison with the Dirichlet surface generation method.

Finally, in the last section, we consider the $\mathcal{C}^1$ problem, that is, once the boundary curves and the tangent planes along them have been prescribed we give a way to generate a polynomial approximation to CMC-surface associated to this initial information.

Bibliography

[1] U. Abel, Z. Li, *A new proof of an identity of Jetter and Stöckler for multivariate Bernstein polynomials*, Computer Aided Geometric Design **23**, 297-301, (2006).

[2] M. Abramowitz, I. A. Stegun, (Eds.), *Handbook of Mathematical Functions with Formulas, Graphs, and Mathematical Tables*, New York: Dover, (1972).

[3] A. Arnal, A. Lluch, J. Monterde, *Triangular Bézier surfaces of minimal area*, Proceedings of the International Workshop on Computer Graphics and Geometric Modeling 2003, Montreal, Lecture Notes in Computer Science **2669**, 366-375, Springer-Verlag, (2003).

[4] R. E. Barnhill, G. Birkhoff, W. Gordon. *Smooth interpolation in triangles*, Journal of Approximation Theory **8**, 114-128, (1973).

[5] R. E. Barnhill, J. A. Gregory, *Polynomial interpolation to boundary data on triangles*, Mathematics of Computation **29**, 726-735, (1975).

[6] J. V. Beltran, J. Monterde, *Bézier solutions of the wave equation*, Proceedings of the Second Technical Session on Computer Graphics and Geometric Modeling, TSCG'2004, Assisi, Lecture Notes in Computer Science **3044**, 631-640, Springer-Verlag, (2004).

[7] M. I. G. Bloor, M. J. Wilson, *Using partial differential equations to generate freeform surfaces*, Computer Aided Design **22**, 202-212, (1990).

[8] M. I. G. Bloor, M. J. Wilson, *Generating blend surfaces using partial differential equations*, Computer Aided Design **21**, 165 - 171, (1989).

[9] M. I. G. Bloor, M. J. Wilson, *Using partial differential equations to generate freeform surfaces*, Computer Aided Design **22**, 202-212, (1990).

[10] S. A. Coons, *Surfaces for computer aided design of space forms*, MIT, MAC-TR-41, (1967).

[11] L. A. Cordero, M. Fernández, A. Gray, *Geometría diferencial de curvas y superficies con Mathematica*, Addison-Wesley Iberoamericana, Wilmington, United States, (1995).

[12] C. Cosín, J. Monterde, *Bézier surfaces of minimal area*, Proceedings of the International Conference of Computational Science, ICCS'2002, Amsterdam, Sloot, Kenneth Tan, Dongarra and Hoekstra, (Eds.), Lecture Notes in Computer Science **2330**, 72-81, Springer-Verlag, (2002).

[13] G. Farin, *Triangular Bernstein-Bézier patches*, Computer Aided Geometric Design **3**, 83-127, (1986).

[14] G. Farin, D. Hansford, *Discrete Coons patches*, Computer Aided Geometric Design **16**, 691-700, (1999).

[15] G. Farin, J. Hoschek, M.-S. Kim, (Eds.), *Handbook of CAGD*, Elsevier, (2002).

[16] R. T. Farouki, *Legendre-Bernstein basis transformations*, Journal of Computational and Applied Mathematics, **119**, 145-160, (2000).

[17] R. T. Farouki, T. N. T. Goodman, T. Sauer, *Construction of orthogonal bases for polynomials in Bernstein form on triangular and simplex domains*, Computer Aided Geometric Design **20**, 209-230, (2003).

[18] M. S. Floater, M. Reimers, *Meshless parameterization and surface reconstruction*, Computer Aided Geometric Design **18**, 77-92, (2001).

[19] J. Gallier, *Curves and surfaces in Geometric Modeling*, Morgan Kaufmann Publishers, S. Francisco, California, (2000).

[20] G. Greiner, *Variational design and fairing of spline surfaces*, M. Daehlen, L. Kjelldahl, (Eds.), Blackwell Publishers **13**, Eurographics, (1994).

[21] J. Hoscheck, D. Lasser, *Fundamentals of Computer Aided Geometric Design*, A. K. Peters, Wellesley, (1993).

[22] K. Jetter, J. Stöckler, *An identity for multivariate Bernstein polynomials*, Computer Aided Geometric Design **20**, 563-577, (2003).

[23] B. Jüttler, *The dual basis functions for the Bernstein polynomials*, Advances in Computational Mathematics **8**, 345-352, (1998).

[24] B. Jüttler, M. Oberneder, A. Sinwel, *On the existence of biharmonic tensor-product Bézier surface patches*, Computer Aided Geometric Design **23**, 612-615, (2006).

[25] B. Kim, J. Rossignac, *Localized bi-Laplacian solver on a triangle mesh and its applications*, Georgia Institute of Technology, GVU Technical Report Number: GIT-GVU-04-12, (2004).

[26] T. Lyche, K. Scherer, *On the p-norm Condition Number of the Multivariate Triangular Bernstein Basis*, Journal of Computational and Applied Mathematics **119**, 259-273, (2000).

[27] V. V. Meleshko, *Biharmonic problem in a rectangle*, In: Fascination of Fluid Dynamics, Applied Scientific Research **58**, 217-249, A. Biesheuvel, G. J. F van Heist (Eds.), (1998).

[28] Y. Miao, H. Shou, J. Feng, Q. Peng, A. R. Forrest, *Bézier surfaces of minimal internal energy*, In: H. Bez, M. Sabin, R. R. Martin (Eds.), Mathematics of Surfaces 2005. In: Lecture Notes in Computer Science **3604**, Springer, Berlin, 318-335, (2005).

[29] J. Monterde, *The Plateau-Bézier problem*, In: Mathematics of Surfaces X. Lecture Notes in Computer Science **2768**, M. J. Wilson, R. R. Martin, (Eds.), Springer, Berlin, 262-273, (2003).

[30] J. Monterde, *Bézier surfaces of minimal area: The Dirichlet approach*, Computer Aided Geometric Design **21**, 117-136, (2004).

[31] J. Monterde, H. Ugail, *On harmonic and biharmonic Bézier surfaces*, Computer Aided Geometric Design **21**, 697-715, (2004).

[32] G. M. Nielson, D. Thomas, J. Wixom, *Boundary data interpolation on triangular domains*, Technical Report GMR-2834, General Motors Research Laboratories.

[33] G. M. Nielson, D. Holliday, T. Roxborough, *Cracking the cracking problem with Coons patches*, Proceedings of the conference on Visualization '99, San Francisco, California, United States, 285 - 290, (1999).

[34] M. L. Sampoli, M. Peternell, B. Jüttler, *Rational surfaces with linear normals and their convolutions with rational surfaces*, Computer Aided Geometric Design **23**, 179-192, (2006).

[35] J. Sánchez-Reyes, *The Symmetric Analogue of the Polynomial Power Basis*, ACM Trans. Graph., **16**, 319-357, (1997).

[36] J. Sánchez-Reyes, *Algebraic manipulation in the Bernstein form made simple via convolutions*, Computer Aided Design **35**, 959-967, (2003).

[37] T. Sauer, *Jacobi polynomials in Bérnstein form*, preprint, (2004).

[38] R. Schneider, L. Kobbelt, *Geometric fairing of irregular meshes for free-form surface design*, Computer Aided Geometric Design **18**, 359-379, (2001).

[39] R. Schneider, L. Kobbelt, H. P. Seidel, *Improved bi-Laplacian mesh fairing*, In: Innovations In Applied Mathematics Series. Mathematical Methods for Curves and Surfaces, Oslo 2000, T. Lyche, L. L. Schumaker, (Eds.), Vanderbilt Univ. Press, 445-454, (2001).

[40] M. Struwe, *Plateau's problem and the calculus of variations*, Mathematical notes, Princeton University press, Princeton, (1988).

[41] R. A. Sweet, *A Recursive relation for the Determinant of a Pentadiagonal Matrix*, Communications of the ACM **12**, 330-332, (1969).

[42] H. Ugail, *On the Spine of a PDE Surface*, Mathematics of Surfaces X, M. J. Wilson, R. R. Martin, (Eds.), Springer, 366-376, (2003).

[43] H. Ugail, M. I. G. Bloor, M. J. Wilson, *Techniques for Interactive Design Using the PDE Method*, ACM Transactions on Graphics **18**, 195-212, (1999).

[44] R. C. Veltkamp, W. Wesselink, *Variational Modeling of triangular Bézier Surfaces*, `url: citeseer.ist.psu.edu/387772.html`.